

Whole building model predictive control with optimization for HVAC systems utilizing
surface level weather forecasts

by

Trent Hilliard

Submitted in partial fulfilment of the requirements
for the degree of Doctor of Philosophy

at

Dalhousie University
Halifax, Nova Scotia
August 2017

© Copyright by Trent Hilliard, 2017

To my wife, Ainsley MacLeod Hilliard, whose love and support have made this all possible.

Table of Contents

Table of Contents.....	iii
List of Tables	vii
List of Figures	x
Abstract	xv
List of Abbreviations and Symbols Used.....	xvi
Acknowledgments.....	xx
Chapter 1 Introduction	1
1.1 Research Contributions	8
Chapter 2 Background Information	12
2.1 Model Predictive Control Overview.....	12
2.2 Building Physics.....	17
2.3 Occupant Comfort	20
Chapter 3 Literature Review	26
3.1 Component/Subsystem Level Studies	34
3.2 Single Zone Studies	40
3.3 Whole Building Studies	45
3.4 Analysis and Discussion	53
3.5 Building Parameters for Model Predictive Control.....	60
3.6 Conclusions from the Literature	64
Chapter 4 Building Energy Model	66
4.1 Introduction	68
4.2 Thermal Envelope and Zones.....	70
4.3 HVAC System.....	74
4.4 Control Review.....	82
4.4.1 Strategy	82
4.4.2 Software	83
4.5 Occupancy, Equipment, and Lighting	84
4.6 Calibration and Verification	87
4.6.1 Weather	88

4.6.2 Steam Consumption.....	90
4.6.3 Electricity Consumption.....	92
4.6.4 Electricity Demand.....	93
4.6.5 Temperature Performance.....	94
4.7 Energy Model Results.....	95
4.7.1 Daily Profile Plots.....	95
4.7.2 Electricity by End Use.....	100
4.8 Conclusions of Building Energy Modelling.....	102
Chapter 5 Zone Operative Temperature.....	103
5.1 Zone Mean Radiant Temperature Analysis of Characteristic Zones.....	104
5.1.1 Interior Zone 2C.....	104
5.1.2 Exterior Zone with Large Windows 2N.....	105
5.1.3 Exterior Zone Small Windows 2SW.....	108
5.1.4 Zone Radiant Temperature Difference from Zone Air Temperature Compared to Outdoor Ambient Air Temperature and Solar Radiation.....	111
5.1.5 Zone Radiant Temperature Difference from Zone Temperature Compared to Outdoor Ambient Air Temperature and Solar Radiation With 180 Degree Building Rotation.....	113
5.2 Mean Radiant Temperature Differential from Zone Temperature Approximation Method.....	116
5.2.1 Exterior Zone Large Windows 2N Occupied Only Mode Filter.....	117
5.2.2 Exterior Zone Large Windows 2N Occupied Cooling Mode Filter.....	119
5.2.3 Exterior Zone Large Windows 2N Occupied Heating Mode Filter.....	122
5.2.4 Exterior Zone Large Windows 2N Comparison of Filters.....	124
5.2.5 Exterior Zone Small Windows 2SW.....	125
5.2.6 Summary of Zone and Mode Filters.....	125
5.2.7 Surface Level Forecasting – Total Solar Radiation.....	126
5.2.8 Direct and Diffuse Solar Forecasting.....	130
5.3 Conclusions of Zone Operative Temperature Analysis.....	137
Chapter 6 Model Predictive Control Methodology.....	138
6.1 Research Tool Use.....	141
6.2 Whole Building Model Predictive Control Modeling Method.....	144
6.3 Building Response Model.....	145
6.4 Objective Function.....	152
6.5 Optimization.....	155

6.5.1 Morning Start	155
6.5.2 Occupied	156
6.5.3 Unoccupied	158
6.6 Occupant Feedback	159
6.7 Zone Operative Temperature Comfort.....	161
6.8 Forecasts	164
6.9 Emulated Model Predictive Control Method.....	165
6.10 Model Predictive Control Modifications for Experimental Implementation.....	169
Chapter 7 Model Predictive Control Simulation Results	171
7.1 Fixed Energy Prices	171
7.1.1 Rule Based Control.....	171
7.1.2 Model Predictive Control with Energy Optimization	176
7.1.3 Model Predictive Control with Total Cost Minimization.....	182
7.1.4 Addition of a Switching Penalty to Total Cost Minimization	188
7.1.5 Results Comparison for Fixed Energy Pricing.....	195
7.2 Electricity Demand Mitigation Only.....	198
7.3 Time of Use Electricity Pricing	202
7.3.1 Rule Based Control.....	203
7.3.2 Total Cost Minimization with a Switching Penalty of 1.....	205
7.3.3 Results Comparison for Time of Use Electricity Pricing	209
7.4 Comparison of Time of Use Electricity Pricing to Constant Pricing	212
7.5 Conclusions of Model Predictive Control Simulations.....	218
Chapter 8 Emulated Model Predictive Control Simulations	220
8.1 Results of Emulated Model Predictive Control.....	221
8.2 Conclusions from Emulated Model Predictive Control Simulations.....	230
Chapter 9 Experimental Results.....	232
9.1 Introduction	232
9.2 Building Response Model	233
9.3 Energy Savings	236
9.4 Zone Operative Temperature Adjustment	244
9.5 User Feedback.....	245
9.6 Conclusions of Experimental Implementation	246
Chapter 10 Conclusions and Future Work	248
10.1 Conclusions	248

10.2 Recommendations	252
References	255
Appendix A – Taylor and Francis Publishing Agreement	265
Appendix B – Reprint of Figures/Tables Licences	266

List of Tables

Table 2.1	Nonlinear optimization techniques [41]	14
Table 2.2	MPC objectives and constraints for buildings	15
Table 2.3	PMV/PPD variables.....	21
Table 2.4	Thermal comfort standard comparison	22
Table 2.5	PMV/PPD sensitivity analysis	25
Table 3.1	Models and optimization techniques.....	28
Table 3.2	System information for models and optimization	30
Table 3.3	Strengths and weaknesses of the research (experimentally studies in boldface).....	32
Table 3.4	Building envelope variations [56].....	41
Table 3.5	HVAC and other controllable systems, “x” indicates it is in use [56]	42
Table 3.6	Building envelope characteristics.....	62
Table 3.7	Desirable traits for MPC	63
Table 4.1	Exterior surfaces and layer properties	73
Table 4.2	Hot water loop parameters.....	76
Table 4.3	Common HP loop setpoints.....	78
Table 4.4	Common HP loop actuators	79
Table 4.5	Common HP loop pumps.....	79
Table 4.6	AHU serviced zones	79
Table 4.7	HVAC air loop setpoints.....	81
Table 4.8	Primary control strategies	82
Table 4.9	Occupied Period	83
Table 4.10	Peak occupant, equipment, and light loads as a function of space type	84
Table 4.11	Zone types	85
Table 4.12	Occupancy schedules (fraction of peak)	86
Table 5.1	Exterior zone large windows occupied only mode linear regression coefficients	117
Table 5.2	Exterior zone large windows occupied cooling mode linear regression coefficients	120
Table 5.3	Exterior zone large windows occupied heating mode linear regression coefficients	122
Table 5.4	Comparison of zone 2N large exterior windows	125
Table 5.5	Exterior zone small windows linear regression coefficients	125
Table 5.6	Comparison of north and south facing correlation coefficients for occupied mode	126

Table 5.7	HRF coefficients and r^2 compared to global level forecasts.....	127
Table 5.8	Comparison of total HRF to component (direct, diffuse) HRF forecasts.....	131
Table 5.9	Mona Campbell coefficients.....	135
Table 6.1	Model inputs and outputs.....	149
Table 6.2	Annualized BRM fit statistics to E+ input data.....	151
Table 6.3	Morning start optimization heating setpoints ($^{\circ}\text{C}$) at 06:00.....	156
Table 6.4	Occupied period setpoint options ($^{\circ}\text{C}$).....	157
Table 7.1	Monthly RBC energy consumption and costs with fixed energy prices.....	175
Table 7.2	Energy minimization MPC energy consumption and costs with fixed energy prices.....	180
Table 7.3	Energy minimization MPC vs RBC monthly cost comparison with fixed energy prices.....	181
Table 7.4	Total cost minimization MPC energy consumption and costs with fixed energy prices.....	186
Table 7.5	Total cost minimization MPC vs RBC monthly cost comparison with fixed energy prices.....	187
Table 7.6	Decay penalty = 1 monthly costs and energy consumption with fixed energy prices.....	192
Table 7.7	Decay penalty = 2 monthly costs and energy consumption with fixed energy prices.....	193
Table 7.8	Decay penalty = 5 monthly costs and energy consumption with fixed energy prices.....	194
Table 7.9	Decay penalty cost comparison with fixed energy prices.....	197
Table 7.10	August 5 th at 14:00 predictions (kW for power, $^{\circ}\text{C}$ for temperature).....	199
Table 7.11	Summer start electricity demand predictions (kW).....	200
Table 7.12	Winter start electricity demand predictions (kW).....	200
Table 7.13	Comparison of electricity demand mitigation only costs (all units in \$).....	201
Table 7.14	RBC monthly energy consumption and costs.....	204
Table 7.15	Decay penalty = 1 energy consumption and costs.....	208
Table 7.16	Time of use electricity price cost comparison.....	211
Table 7.17	Cost and savings comparison between constant and time of use electricity pricing (\$).....	217
Table 8.1	Monthly comparison of total costs for emulated MPC scenarios (\$).....	226
Table 8.2	Monthly comparison of electricity demand costs for emulated MPC scenarios (\$).....	227
Table 8.3	Monthly comparison of electricity energy costs for emulated MPC scenarios (\$).....	228

Table 8.4	Monthly comparison of steam energy costs for emulated MPC scenarios (\$)	229
Table 9.1	BRM model fit to measured site data	235
Table 9.2	Regression model statistics	241
Table 9.3	Monthly electricity consumption (kWh), MPC savings in bold	243
Table 9.4	Monthly steam consumption (kWh), MPC savings in bold	243

List of Figures

Figure 1.1	MPC system diagram.....	2
Figure 1.2	Optimized start time	3
Figure 1.3	Measured summer zone air temperatures within the Mona Campbell building.....	7
Figure 1.4	Prediction forecast horizon and timestep.....	8
Figure 2.1	Major energy flows in a building based on [44]	18
Figure 2.2	Wall nodes for conduction	18
Figure 2.3	Heat flux time lag [45]	19
Figure 2.4	Clothing insulation as a function of outdoor air dry-bulb temperature at 06:00 [48]	24
Figure 3.1	RC model diagram [84].....	46
Figure 3.2	Simulation software distribution.....	55
Figure 3.3	Distribution of reviewed MPC optimization techniques.....	56
Figure 3.4	Distribution of MPC forecast horizon.....	57
Figure 3.5	Distribution of MPC simulation timestep.....	58
Figure 4.1	Mona Campbell Building	69
Figure 4.2	Mona Campbell Building – 3D rendering with shading surfaces	70
Figure 4.3	External building dimensions (left – footprint; right – floor levels).....	70
Figure 4.4	Floor subdivision into thermal zones (bottom: basement; middle: occupied space; top: penthouse)	72
Figure 4.5	Combined HVAC system diagram as installed.....	75
Figure 4.6	Hot water (HW) loop as modelled.....	77
Figure 4.7	Common heat pump (HP) Loop.....	78
Figure 4.8	HVAC air loop	80
Figure 4.9	Monthly ambient temperature comparison	89
Figure 4.10	Monthly solar radiation.....	89
Figure 4.11	Steam use comparison	91
Figure 4.12	Electricity use comparison	92
Figure 4.13	Electrical demand comparison	93
Figure 4.14	Temperature histogram	94
Figure 4.15	Energy consumption sources for February, hourly profile	96
Figure 4.16	Winter zonal temperatures	97
Figure 4.17	Energy consumption sources for August, hourly profile.....	98
Figure 4.18	Summer zonal temperatures.....	99
Figure 4.19	Annual electricity by end use	100

Figure 4.20	Monthly electricity by end use - simulated	101
Figure 5.1	Scatter plot of ZOT versus ZAT for an interior zone	105
Figure 5.2	Exterior zone large windows winter day (January 8 2013)	106
Figure 5.3	Exterior zone large windows summer day (August 8 2013).....	107
Figure 5.4	Exterior zone large windows spring day (April 6 2013).....	107
Figure 5.5	Distribution of variations between ZRT and ZAT for an exterior north- facing zone with large windows	108
Figure 5.6	Exterior zone small windows winter day (January 8 2013).....	109
Figure 5.7	Exterior zone small windows summer day (August 8 2013)	109
Figure 5.8	Exterior zone small windows spring day (April 6 2013)	110
Figure 5.9	Distribution of variations between ZRT and ZAT for an exterior south- facing zone with small windows.....	110
Figure 5.10	Difference of ZRT and ZAT vs outdoor ambient air temperature	111
Figure 5.11	Difference between ZRT and ZAT vs solar radiation	112
Figure 5.12	Difference between ZRT and ZAT vs outdoor temperature with the 180- degree rotation	114
Figure 5.13	Difference between ZRT and ZAT vs solar radiation with the 180-degree rotation.....	115
Figure 5.14	Exterior zone large windows occupied only mode approximation error vs time of day.....	118
Figure 5.15	Exterior zone large windows occupied only mode approximation error vs temperature difference.....	118
Figure 5.16	Exterior zone large windows occupied only mode approximation error distribution	119
Figure 5.17	Exterior zone large windows occupied cooling mode approximation error vs time of day	120
Figure 5.18	Exterior zone large windows occupied cooling mode approximation error vs temperature difference	121
Figure 5.19	Exterior zone large windows occupied cooling mode approximation error distribution	121
Figure 5.20	Exterior zone large windows occupied heating mode approximation error vs time of day	122
Figure 5.21	Exterior zone large windows occupied heating mode approximation error vs temperature difference	123
Figure 5.22	Exterior zone large windows occupied heating mode approximation error distribution	123
Figure 5.23	Comparison of filter error distribution.....	124
Figure 5.24	2N HRF approximation error vs ZRT-ZAT.....	128

Figure 5.25	2N HRF ZRT-ZAT approximation error distribution	129
Figure 5.26	2SW HRF approximation error of ZRT-ZAT vs ZRT-ZAT	129
Figure 5.27	2SW HRF ZRT-ZAT approximation error distribution	130
Figure 5.28	2N Direct and Diffuse ZRT-ZAT approximation error vs ZRT-ZAT	131
Figure 5.29	2N Direct and Diffuse ZRT-ZAT approximation error distribution	132
Figure 5.30	2SW Direct and Diffuse ZRT-ZAT approximation error vs ZRT-ZAT	132
Figure 5.31	2SW Direct and Diffuse ZRT-ZAT approximation error distribution.....	133
Figure 5.32	Comparison of direct and diffuse coefficients on the basis of zone orientation.....	136
Figure 5.33	Comparison of the ambient air and offset coefficients on the basis of zone orientation	136
Figure 6.1	MPC optimization loop.....	138
Figure 6.2	Flow diagram of MPC implementation	140
Figure 6.3	BCVTB Interface between E+ and R.....	142
Figure 6.4	Co-simulation process	144
Figure 6.5	Sample training setpoint profile.....	146
Figure 6.6	Example classification tree for electricity prediction	147
Figure 6.7	Winter BRM performance	150
Figure 6.8	Summer BRM Performance.....	151
Figure 6.9	ASHRAE Standard 55 graphical comfort chart	153
Figure 6.10	Brute force iterative methodology.....	158
Figure 6.11	Client feedback portal	160
Figure 6.12	Example of ZOT based nudging for thermal comfort.....	162
Figure 6.13	Nine unique sets for delayed morning start-up, with zone heating/cooling temperature setpoints (solid) and AHU state control (dashed).....	166
Figure 6.14	Example of nine start-up heating/cooling temperature setpoint scenarios (solid) and the resultant average zone operative temperature (dashed).....	167
Figure 6.15	Sample of varying emulated MPC start times.....	168
Figure 6.16	Operational MPC workflow	169
Figure 7.1	RBC monthly costs by source with constant energy prices.....	172
Figure 7.2	RBC winter temperature (top), energy consumption (middle), and costs (bottom) with constant energy prices.....	173
Figure 7.3	RBC summer temperatures (top), energy consumption (middle), and costs (bottom) with constant energy prices.....	174
Figure 7.4	Cost comparison of MPC energy minimization vs RBC by source	177
Figure 7.5	Comparison of MPC energy minimization vs RBC winter temperature (top), energy consumption (middle), and costs (bottom).....	178

Figure 7.6	Comparison of MPC energy minimization vs RBC summer temperature (top), energy consumption (middle), and costs (bottom).....	179
Figure 7.7	Cost comparison of MPC total cost minimization vs RBC by source	183
Figure 7.8	Comparison of MPC total cost minimization vs RBC winter temperature (top), energy consumption (middle), and costs (bottom).....	184
Figure 7.9	Comparison of MPC total cost minimization vs RBC summer temperatures (top), energy consumption (middle), and costs (bottom).....	185
Figure 7.10	Comparison of decay penalty values in winter temperature (top), energy consumption (middle), and cost (bottom)	190
Figure 7.11	Comparison of decay penalty values in summer temperature (top), energy consumption (middle), and cost (bottom)	191
Figure 7.12	Decay penalty monthly cost comparison by source.....	196
Figure 7.13	August 5th temperature profile (top) and energy consumption (bottom)...	199
Figure 7.14	Time of use electricity profiles	202
Figure 7.15	RBC monthly costs comparison by source	203
Figure 7.16	Decay penalty = 1 monthly costs by source	205
Figure 7.17	Decay penalty = 1 vs RBC sample winter temperatures (top), energy consumption (middle), and costs (bottom).....	206
Figure 7.18	Decay penalty = 1 vs RBC sample summer temperatures (top), energy consumption (middle), and costs (bottom).....	207
Figure 7.19	Time of use electricity pricing monthly cost comparisons.....	210
Figure 7.20	Monthly cost comparison of time of use and constant price electricity for MPC with penalty = 1	213
Figure 7.21	Annual cost comparison between constant and time of use electricity pricing MPC with penalty = 1	214
Figure 7.22	Penalty = 1 MPC comparison between time of use and constant electricity pricing winter temperature (top), energy consumption (middle) and cost (bottom)	215
Figure 7.23	Penalty = 1 MPC comparison between time of use and constant electricity pricing summer temperature (top), energy consumption (middle) and cost (bottom)	216
Figure 8.1	Emulated MPC monthly cost comparison	223
Figure 8.2	Emulated MPC winter comparison.....	224
Figure 8.3	Emulated MPC summer comparison.....	225
Figure 9.1	Comparison of measured data to BRM predictions in summer.....	234
Figure 9.2	Comparison of measured data to BRM predictions in winter.....	235
Figure 9.3	Historical HVAC electricity usage	237
Figure 9.4	Historical steam consumption.....	238

Figure 9.5	Historical ambient condition trends as defined by HDD and CDD	238
Figure 9.6	Comparison prior to (week 31 – solid) and after (week 33 – dashed) MPC integration electricity, steam, and temperature.....	240
Figure 9.7	Weather comparison prior to (week 31 – solid) and after (week 33 - dashed) MPC integration.....	240
Figure 9.8	Comparison between measured data and regression model for electricity	242
Figure 9.9	Comparison between measured and regression model for steam.....	242
Figure 9.10	ZOT based thermal comfort adjustments – first floor west.....	244

Abstract

The commercial and institutional sector of the building stock present a significant portion of energy consumption within Canada, and of that the majority is used for space conditioning. In order to meet reduction in greenhouse gas emission targets to combat climate change as outlined in the Paris Agreement, a reduction in energy use is required. Due to the expectations of a comfortable workspace and employee salaries outweighing operational costs of a building, technological changes are needed to reduce energy consumption, as dissatisfaction with environmental conditions impacts employee output. While many new technologies being developed are more efficient than existing HVAC solutions, they are often costly to retrofit into the existing building stock. One solution is to use the existing equipment in the building more efficiently through the use of advanced control algorithms that account for upcoming conditions, such as weather and occupancy. This form of predictive control can realize savings that are not possible when using reactive, or rule based control that is the current industry norm.

This dissertation creates a new model predictive control (MPC) method for application to an institutional building using advanced surface level weather forecasts and multi-tiered implementation strategy. A simulation platform was created to test and evaluate various control strategies, followed by an experimental implementation at the operating building. A whole building optimization was conducted, with the surface level climatic forecasts used to ensure occupant comfort was maintained, via zone operative temperature, throughout the building zones. The simulation results show a reduction in total energy use of 2-3% (5-6% HVAC energy) annually, while the experimental results show a HVAC savings of 30% (29% for HVAC electricity and 63% for steam). Experimental results outperform the simulation results due to real building inefficiencies not captured in the simulation model benchmark assumptions and differing baseline control strategy.

The research contributions of this dissertation include: i) the implementation of zone operative temperature as a whole building comfort variable ii) the usage of various models and objective functions to achieve improved energy and cost performance, iii) the introduction of emulated model predictive control for both model validation and for the morning start optimization of MPC, iv) the usage of surface level weather forecasts for predictive control, and v) the use of a *randomForest* regression model for buildings.

List of Abbreviations and Symbols Used

Acronyms

2C	2 nd floor core zone
2N	2 nd floor north zone
2SW	2 nd floor southwest zone
ACEnet	Atlantic Computational Excellence Network
AHU	Air handling unit
AMY	Actual meteorological year
ANN	Artificial neural network
AQR	Affine Quadratic Regulator
BCVTB	Building Controls Virtual Test Bed
BRM	Building response model
C&I	Commercial and institutional
CDD	Cooling Degree Days
CO ₂	Carbon dioxide
COP	Coefficient of performance
CV(RMSE)	Coefficient of variance of the root mean square error
DHW	Domestic hot water
ECCC	Environment and Climate Change Canada
GLM	Generalized linear models
GPL	Green Power Labs
HDD	Heating Degree Days
HRF	High resolution forecast

HVAC	Heating, Ventilation and Air Conditioning
HW	Hot water
IAQ	Indoor air quality
MPC	Model predictive control
NMBE	Normalized mean bias error
NSP	Nova Scotia Power
PID	Proportional-Integral-Derivative
PMV	Predicted mean vote
PPD	Predicted percentage of dissatisfied
PSO	Particle swarm optimization
r^2	Coefficient of determination
RBC	Rule based control
RC	Resistive capacitive
RMSE	Root mean square error
SQP	Sequential Quadratic Programming
ToU	Time of use
VAV	Variable air volume
VFD	Variable frequency drive
WAHP	Water to air heat pump
ZAT	Zone air temperature
ZOT	Zone operative temperature
ZRT	Zone mean radiant temperature

Symbols

α	Constant
β	Constant
Δ	Difference between ZRT and ZAT
ρ	Constant
$A, B, C, D,$ and F	State space matrices
a, b, c, d	Regression constants
f_{cl}	Clothing factor
h_c	Convective heat transfer coefficient
I_{cl}	Clothing insulation in clo
J	Objective/cost function
M	Metabolic rate in W/m^2
N, n	Horizon length
n_{change}	Timesteps since last setpoint change
O	Variable weighting matrix
p_a	Vapor pressure of air in kPa
Q	Setpoint fluctuation penalty
R_{cl}	Clothing insulation level
r	Fuel sources
T	Temperature
t_a	Air temperature in $^{\circ}C$
t_{cl}	Clothing surface temperature in $^{\circ}C$
t_i	Timestep interval

t_r	Mean radiant temperature in °C
u	Control input
Δu	Rate of input change
V	Air velocity in m/s
W	External work in W (typically 0)
w	System disturbance
x	System state
y	System output

Acknowledgments

I'd like to first thank my supervisor, Dr. Lukas Swan, for his guidance and support throughout this endeavour. His knowledge and guidance in both this research and in life have proved to be invaluable. His leadership and positivity inspire and provide confidence. His knowledge of building performance simulation, and connections within both academics and industry have allowed this research to be successful.

The next group of people to thank are my industry research partners at Green Power Labs. First to Alexandre Pavlovski and Marlene Moore for providing me with the opportunity to work with the team. Some heartfelt thanks also go out to Jim Fletcher and Aaron Caldwell, the technical leads of building services, as well as Martin Vander Baaren for his project management to keep the research on schedule and providing resources when necessary. The work would not have been possible to complete without the efforts of Zheng Qin, Simon DeWolfe, and Victor Wei in development of the communication protocol with Metasys, as well as the database setup for collection of real-time data from the site and integration for control. A big thanks to the forecasting team at Green Power Labs for developing the high-resolution forecasts used during the experimental phase. This includes the work of Dustin Ott and Andrey Kostylev in generating the geometry and development of the high-resolution forecast, as well as the work of Philip Shott and Michael Palmer in setting up the forecasting for the site. Finally, the assistance of Pawan Lingras and his research team at St. Mary's University in conjunction with Zheng who aided in developing the building response model and final framework for experimental implementation, including the genetic algorithm and clustering methodology for real-time application.

The second group of people to thank are the staff of Dalhousie University in both the sustainability office and facilities management. Glen MacDougall was an instrumental link to obtaining historical operating data for the building, organizing site visits to both the Mona Campbell and steam exchangers in Howe Hall, and providing contact information within facilities management. Rochelle Owen was instrumental in getting approval from facilities management to allow for the experimental testing, as well as providing the building diagrams for the construction of the EnergyPlus model. Mark Power in facilities

management for providing his in-depth knowledge of the facility and of the Metasys software, and Dean Harnish for his Metasys knowledge and support during the experimental phase.

Chapter 1 INTRODUCTION

Due to rising energy costs [1], the threat of climate change [2], and regulatory policies (such as the Paris Agreement [3]) to reduce greenhouse gas emissions, a need to improve the way energy is consumed exists. One potential area for energy reduction measures is the building stock. Commercial and institutional (C&I) buildings in Canada consumed 1,057.3 PJ of energy in 2010 [4], which accounts for 12.5% of all energy consumed in Canada. Of that, 50% of the energy was used for space heating and space cooling [5]. Worldwide an existing trend of increasing energy consumption by buildings exists [6], and has been exponentially growing as population has grown. This disparity is driven by emerging economies that are forecasted to continue their growth and demand for energy in all sectors [6]. Due to the large amount of energy involved in space conditioning of C&I buildings through HVAC systems, new methods for cost effective energy efficient HVAC technologies are being studied by researchers and industry (e.g. [7], Johnson Controls¹). Some of the physical technologies include heat pumps [8], energy storage [9], phase change materials [10] [11] [12], combined heat and power [13], liquid desiccant air conditioning [14], liquid to air membrane energy exchangers [15]. While these technologies are more efficient than existing systems in buildings, they can be expensive or physically difficult to retrofit into existing buildings and incur significant payback periods. An alternative technological branch is control, where changes to how the existing equipment is used can lead to reductions in energy consumption. There are two main methods this can be done: reducing the conditioning needs of a space (via zone temperature setpoints) [16] [17], or through optimization of the system (through system setpoints such as hot water temperature [18], or dual duct air temperatures [19]). The advantage of a control based strategy is they can be implemented as a software layer that integrates with existing building automation systems (BAS), and thus at a much lower cost.

¹<http://www.johnsoncontrols.com/content/us/en/news.html?newsitem=http%3A%2F%2Fjohnsoncontrols.mediareom.com%2Findex.php%3Fs%3D113%26item%3D3396>

The research objective of this dissertation is to develop an advanced HVAC control utilizing model predictive control (MPC) to maintain or improve occupant thermal comfort while reducing energy usage, demand, and/or operating costs. Conventional building control is both reactionary (waits for conditions to be outside of range to respond) and scheduled, causing HVAC equipment to operate unnecessarily or inefficiently. MPC is a low capital cost technology as it is an add-on software layer that utilizes forecast data of building operations, climate. Thus minimal or no additional hardware is required. MPC uses a building system model and forecasts of internal and external conditions (climate, occupancy, equipment), and a set of HVAC control options (such as thermal zone setpoints) to reduce energy usage and/or operating costs based on a desired objective function (cost, energy, demand, greenhouse gases). A sample system diagram is found in Figure 1.1 that highlights the information flow paths.

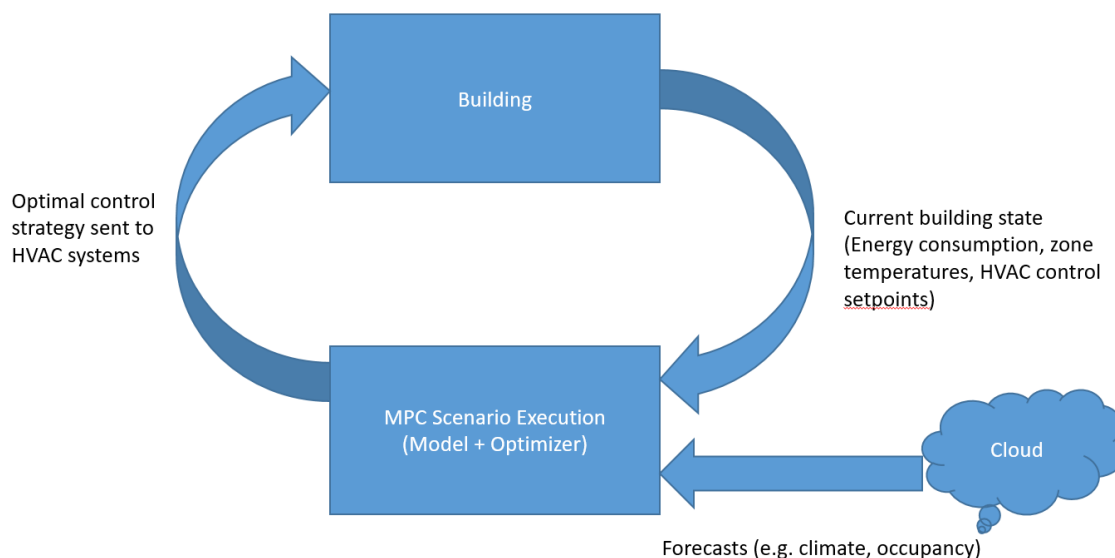


Figure 1.1 MPC system diagram

MPC strategies can reduce energy use and/or operational costs compared to conventional controls through the following methods:

- Optimized start time – By forecasting climatic and occupancy conditions, the optimal start time can be determined to reduce energy consumption from

conventional rule based controls (RBC). An example of this can be found in Figure 1.2, where the objective of achieving thermal comfort by 08:00 is met by MPC with a delayed start reducing thermal losses during a heating period for the building in comparison to RBC. A final option is that of a ramp based input, which would lead to a lower peak demand, but an increase in energy consumption compared to the MPC case.

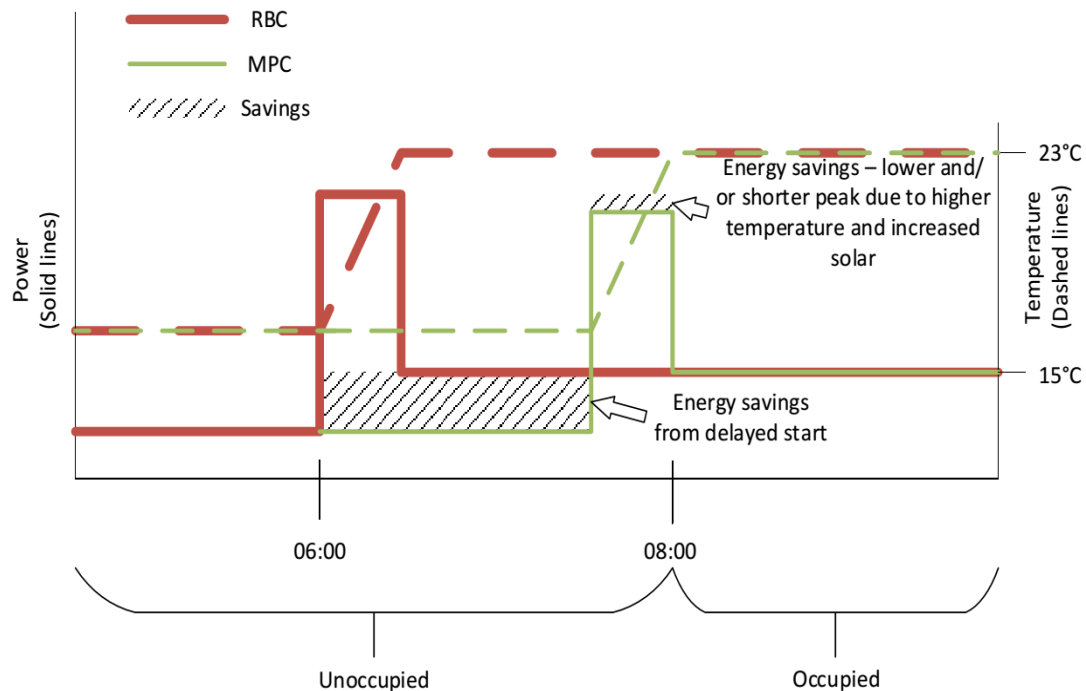


Figure 1.2 Optimized start time

- Optimized shutdown – Similar to the optimized start time, predictions for occupancy and climatic conditions can determine the optimal time to turn off the HVAC system that allows the building thermal dynamics to maintain comfort. Indoor air quality requirements may limit the feasibility of this approach by mandating fresh air.
- Free cooling – Free cooling refers to the use of building ventilation fans to circulate outdoor air through the building to chill the space overnight without the use of

compression based systems. Current systems typically used a dry-bulb temperature differential or enthalpy differential to turn on the fans. An MPC approach can improve upon this by calculating the optimal start time that minimizes fan runtime (fan use increases energy consumption) by using the forecast conditions as opposed to a fixed differential.

- Demand limiting – Many C&I customers pay for energy based on both consumption and peak demand during the billing period. MPC can be used to predict future energy consumption levels and find a control solution that limits the peak demand by initiating conditioning systems earlier and at a lower peak power level.
- Time-of-use pricing – with knowledge of future conditions and energy pricing, MPC can find a control solution that minimizes the total operating cost of a building while still maintaining thermal comfort. An example would be to pre-cool a building in the summer to the lower limit of thermal comfort prior to the high energy price period, and allow for the thermal dynamics of the building to carry the building through the high price period.
- Part-load efficiency – Many HVAC systems have a design operating scenario where efficiency is at its highest, and should be operated around these points as often as possible. Traditional reactive control does not account for these efficiencies and often will run equipment at non-ideal part-load on efficiency curves. Predictive controls can anticipate the efficiency response of the HVAC equipment and turn on pre-emptively or later to maintain higher efficiency.

The above objectives can be achieved by exploiting the building as a source of thermal storage, and the typical oversized HVAC system power that exists in buildings.

Some of the technological barriers to using MPC for buildings have been addressed in recent years. These include:

- Advances in computing – Increased computational capability has enabled a broader range of control scenarios to be examined within a reasonable period for application, including computationally expensive options such as MPC.
- Acquisition and storage of building data through measurement and verification – With increased data storage of building conditions, more information is now available to allow for the development of building process models and to evaluate the performance gains when new control strategies are implemented.
- Conditions forecasting - With more advanced occupancy models [20] [21] and forecasting methods [22] and/or improved weather forecasting (accuracy and/or resolution) [23] the performance of the MPC strategies improves.
- Artificial intelligence - The ability to integrate artificial intelligence into building models so the model can learn/evolve based on recorded measurements and real-time data from the building, leading to more accurate models that can adapt to equipment or operational changes over time [24]. While initially discussed in the early 1990s [25], advancements are still on-going due to high degree of complexity in buildings and advancements in machine learning.

This dissertation outlines the design and implementation of a new MPC control strategy for HVAC in a commercial building. The principal research thrust was to use MPC to optimize all of the modelled thermal zones within the building to minimize energy and/or cost while maintaining thermal comfort according to standardized metrics within a building. Depending on the HVAC system and thermal comfort metrics employed, energy can be transferred from high thermal loads (such as South facing zones with large glazing area²) to lower thermal load zones (such as North facing zones). This was done by utilizing surface level (i.e. walls and windows) forecasting for ambient environmental conditions (solar radiation, temperature, humidity, wind) provided by a collaborating industry

² In the northern hemisphere

research partner, Green Power Labs Inc. (GPL). Surface level forecasting refers to forecasting the conditions on each zone exterior surface, as GPL produces forecasts on a square meter basis³. The advancement to surface level forecasts is a key catalyst for the research, as it can better predict the solar based loads for each thermal zone and account for factors such as surface/zone orientation (North vs South) and shading, which is critical in highly glazed C&I buildings. The individual zone level control can then adjust setpoints for each zone to maintain comfort based on forecast conditions, while minimizing energy/cost. No research has been found in the literature to indicate the use of whole building MPC utilizing individual surface level forecasts for individual zone optimization through the use of a whole building solution then being modified at the zone level. Figure 1.3 shows the potential value for individual zone optimization, as some zones will run at or near cooling setpoint (central zones, high occupancy zones, high solar gain zones) while others operate at or near the heating setpoint (basement zones, north facing zones). Factors such as large predictable and unavoidable thermal loads (e.g. sun through windows), dynamic or time-of-use energy pricing, and ability to store thermal energy are integral for the value of the research.

³ <https://greenpowerlabs.com/>

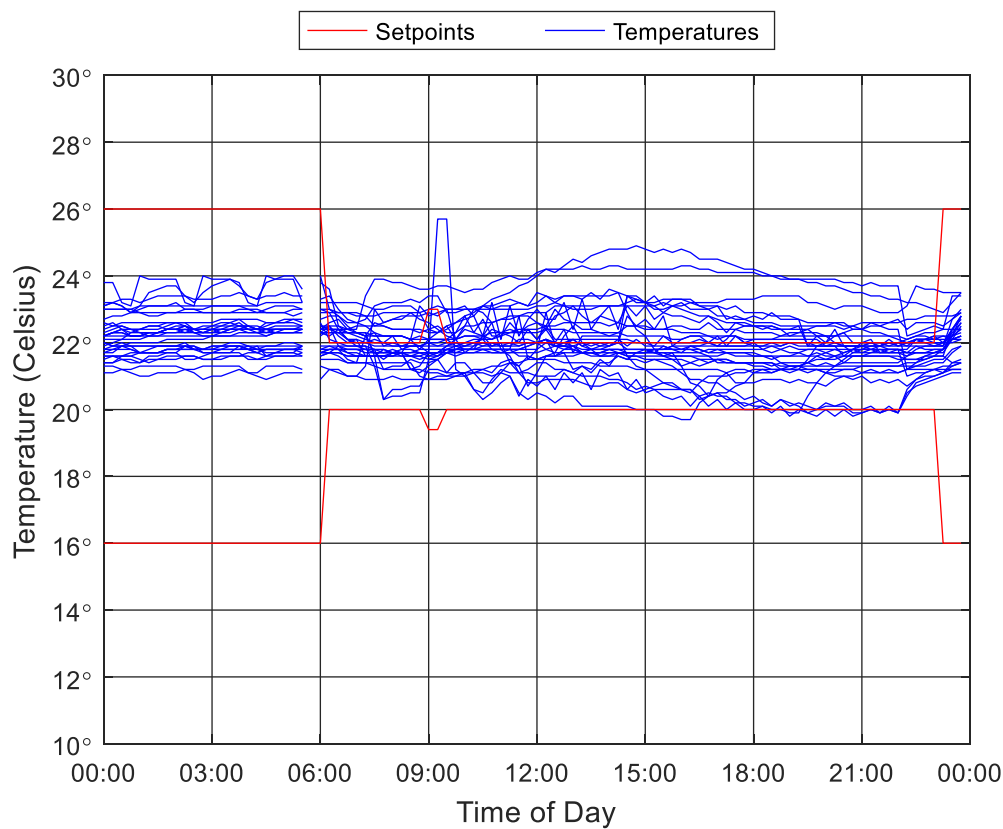


Figure 1.3 Measured summer zone air temperatures within the Mona Campbell building

A second area of research within the zone level optimization of an entire building is the proper selection of MPC parameters, namely the forecast horizon length and update frequency (or timestep) as demonstrated in Figure 1.4 (e.g. a five minute timestep and eight hour forecast horizon). While MPC research indicates it to be a function of the forecast accuracy (such as occupant behavior in individual offices discussed in [26]) and system time constant with respect to control inputs, there has been little work completed in the field of whole building MPC to identify the ideal parameters as a function of building type. The challenge for buildings is that the time constants are a function the envelope materials, interior materials, usage, and HVAC systems installed within the building; the ideal parameter values are building specific.

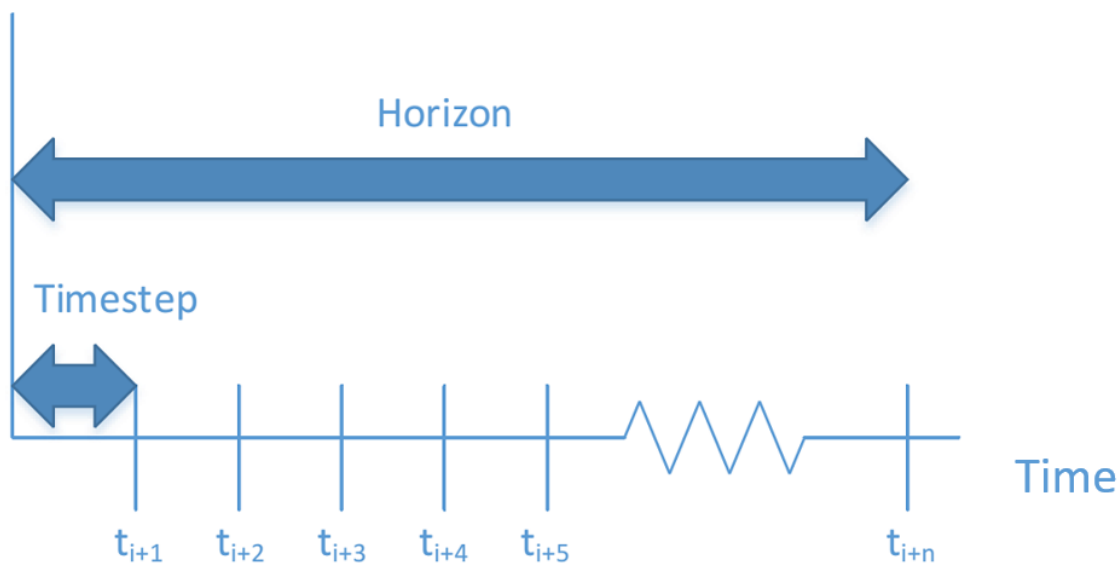


Figure 1.4 Prediction forecast horizon and timestep

A final consideration that is of critical importance is thermal comfort, as it is the primary function of the building. Dry bulb air temperature in a zone is a common feedback tool as it is the industry standard measurement and used by zone level HVAC controllers. In contrast, many standards use either the operative temperature, or other comfort models such as predicted mean vote or predicted percentage dissatisfied (discussed in detail in Chapter 2.3), which rely on advanced measurements such as mean radiant temperature that are not common in buildings. For a new technology to be widely adapted, seamless integration with existing building systems is paramount. A method of utilizing existing building measurements and solar forecast information to estimate operative temperature is provided in Chapter 5, and is a key development. A drawback of the method is that a detailed building model is currently required to generate the necessary data for creating the estimation.

1.1 Research Contributions

The main contributions to the literature during the completion of the thesis are as follows:

1. The use of surface level weather forecasts to allow for a single whole building optimization (computationally efficient) to be modified to ensure thermal comfort throughout the building. This is done through the usage of zone operative temperature (ZOT), as opposed to zone air temperature (ZAT), which accounts for the radiant effects of solar radiation on the building exterior. While the usage of ZOT is not a new aspect in terms of thermal comfort for a space [27] [28] [29], it is typically not used in experimental whole building MPC work due to the lack of measurement in most buildings. Due to ZAT being used as the feedback mechanism in HVAC equipment, it is commonly measured and used for control in experimental work. By using ZOT as a comfort control after the whole building MPC is run, a computationally efficient solution is achieved as opposed to running a much larger optimization problem where each zone is optimized simultaneously.
2. To support operative temperature in number one above, a linear regression model for estimating the difference between zone mean radiant temperature (ZRT) and ZAT was developed to estimate ZOT. While researchers have developed methods for predicting either ZRT or ZOT in detail [30] [31] [32] [33] [34], no work has shown the use of a simplified prediction method used in conjunction with ZAT measurements for whole building MPC.
3. A multi-layered, multi-model MPC was developed and tested experimentally for energy savings, and showed a reduction of HVAC electricity of 29% and steam of 63% compared to the same period the previous year. The multi-layered approach is based on the initial whole building optimization where a single setpoint pair is used during optimization, and then adjusted across zones to maintain thermal comfort based on outdoor conditions for each zone. A layer of occupant feedback is also included to enhance thermal comfort, and to allow for collection of data of occupant satisfaction. The multi-model approach stems from the use of the *randomForest* model for daytime optimization (08:00 to 22:00) of comfort, while a detailed EnergyPlus model was used for morning start optimization (06:00 to 08:00). This

differs from current published work where a single model and single objective function are used for all portions of the day.

4. A new method of evaluating simplified building prediction model performance and to allow the use of detailed models for some specific MPC tasks was developed. The method emulates MPC for simple optimizations that occur once a day and have a convergence period after, such as morning start optimization with constant daytime performance afterwards. The emulated MPC method simulates all possible scenarios, parses each day for the optimal choice, and stitches together these individual days to create a new optimal year. This method relies on the convergence of results prior to the next optimization to allow for the method to work. The results can then be used directly as was done in the experimental work, and also to evaluate the performance of a simplified model trained using data from the advanced model. The difference in MPC performance from emulated MPC shows the losses incurred by the simplified prediction model.
5. A study on the impact of forecast horizon length was conducted utilizing the emulated MPC method for time-of-use pricing with demand mitigation. The results were contrasted to a pure energy minimization algorithm, and found that a 1-day total cost minimization saves less money a month than pure energy minimization. The difference is due to the competing nature between consumption and demand. More energy is consumed to maintain a lower demand early in a month, but an unavoidable increase later in the month renders the excess energy used to maintain the previously lower demand as waste. By forecasting the whole month as opposed a single day, the proper demand peak can be used and prevent the waste of energy.
6. The use of the *randomForest* regression tree modeling technique to generate a building response model for use within MPC. While other researchers have used other statistical/black box models (such as neural networks [35] [36] [37]), the use of *randomForest* has not been attempted. During MPC model selection it was shown to have better performance than neural networks for the same training and

test data. The downside to the models are they can become quite large, and require a large amount of training data. Both of these challenges are being overcome due to advances in computing and storage minimizing the impacts of model size, while buildings are capturing more data at a higher frequency, allowing for increased amounts of training data from a building itself. Alternatively, an advanced modeling tool (such as EnergyPlus) can be used to generate the needed data for model training.

Chapter 2 BACKGROUND INFORMATION

This chapter provides additional background information on the areas of MPC, building physics and how its operation can be advantaged by MPC, and how occupant comfort can be used within MPC.

2.1 Model Predictive Control Overview

MPC is a branch of control theory that utilizes a model of a system or process that is subject to constraints, and attempts to find an optimal solution based on current and forecast values. The optimal solution is typically found by solving an objective function (typically a cost minimization), with constraints that limit the range of output control values. A prediction horizon is used, along with a specified timestep to allow the optimizer to simulate into the future and consider complex, interrelated dynamic effects so that an optimal solution is found over the entire forecast, not just the current timestep. If optimization of only the current timestep is considered, the solution may lead to a less optimal solution over entire forecast, and its ability to address rate of change limitations is impaired. Because MPC considers future effects, it is an ideal control strategy for systems with large time constants (hours), such as buildings [38]. The anticipatory nature of MPC is a strategic advantage compared with reactionary rule-based-controls (e.g. PID⁴).

MPC can account for constraints of the optimization setup and model definition uncertainties such as system identification errors [39]. As an example, assume a linear state space system of the form in Equation 2.1, where x is the system state, u is the control vector, y is the system output, w the system disturbance, and A , B , C , D , and F are constant state space matrices that can have minor uncertainties.

⁴ Proportional, integral, differential type controller use past and present values to control buildings and achieve setpoints.

$$\dot{x}(t) = Ax(t) + Bu(t) + Fw(t) \quad 2.1$$

$$y(t) = Cx(t) + Du(t)$$

From the above system, it is common (but not necessary) to minimize the control input u , while ensuring the output y tracks a reference signal y_r . An example objective cost function is constructed along with constraints given in the form of Equation 2.2, where α and β are weighting factors for the two competing components, and u_{min} and u_{max} represent the constrained space of solutions with a Δu rate of change limitation at maximum value of ρ (constant). The solution is summed over the prediction horizon of length N , with i representing the timestep interval. Only the result for the current timestep is implemented, and the optimization over the horizon period is then carried out at each subsequent timestep. The optimization is redone each timestep to account for model inaccuracies, change in forecasts, and changes in climatic conditions. It is not necessary to limit the cost function to quadratic terms, as any form of function can be implemented, with varying methods (linear, quadratic, non-linear, particle swarm) to find the optimal solution.

$$J(t) = \sum_{i=1}^N (\alpha(y(t_i) - y_r(t_i))^2 + \beta u(t_i)^2)$$

$$u_{min} \leq u \leq u_{max} \quad 2.2$$

$$\Delta u \leq \rho$$

Optimization is a technique used to find the scenario which best achieves an objective function. The objective usually consists of a desired element to be minimized/maximized within hard and/or soft constraints. An example for buildings would be an objective function that minimizes energy consumption/cost within the hard limits of the mechanical systems (i.e. heating/cooling) and the soft limit of thermal zone condition for occupancy comfort. The latter soft limit may incur a penalty if it is exceeded. An issue arises when multiple minima exist for a single cost function, as the global minimum is desired (the truly optimal solution) as opposed to a local minimum.

One method of ensuring a global minimum is to structure the cost function in a linear or quadratic form, to insure only one exists. Thus, the simplest forms of optimization are

linear methods with a single, global minimum. However, certain systems (such as air conditioning [40]) experience highly nonlinear dynamics, and consequently must be modelled using nonlinear techniques which may experience multiple minima. There are several methods of nonlinear optimization, each with specific advantages and disadvantages. Table 2.1 from [41] summarizes some common nonlinear optimization techniques. It is important to recognize that optimization results are dependent of the horizon forecast range, timestep used, and the accuracy of the predictions [39] [42]. Several nonlinear optimization approaches for MPC are explored in detail in [42].

Table 2.1 Nonlinear optimization techniques [41]⁵

Techniques	Strength	Weakness	Application Examples	
Nonlinear Local Techniques	Direct search	Simple and easy to be understood and implemented. No derivatives are required.	Often fails to obtain an optimal solution. It is less computationally efficient.	Wright and Hanby 1987; Sreedharan and Haves 2001; Braun and Chaturvedi 2002; etc.
	Sequential quadratic programming	Can efficiently handle a large number of inequality constraints.	Has to start from initial guesses and its convergence speed is affected by its initial guesses.	Olson and Liebman 1990; House and Smith 1995; Kota et al. 1996; Sun and Reddy 2005; etc.
	Lagrange method	Easy to be implemented since Lagrange formula does not depend on the order in which the nodes are arranged.	The convergence is not always guaranteed.	Hach and Katoh 2003; Chang 2004; etc.
	Conjugate gradient method	Overall computational cost is small for large number of decision variables.	Less efficient and robust compared to other technique, i.e., quasi-Newton method.	Nizet et al. 1984; etc.
Nonlinear Global Techniques	Univariate search	Simple and easy to be implemented.	The convergence speed is quite slow and it can not find the optimum values at some cases.	Hanby and Angelov 2000; Bassily and Colver 2005; etc.
	Branch and bound (B&B)	Can provide a good and/or a subgood solution. It is easy to incorporate any constraint into this method.	High computational cost is always required and it is possible to miss the globally optimum solution.	Sousa et al. 1997; Chang et al. 2005; etc.
	Simulated annealing	Relatively easy to be implemented and has strong ability to provide reasonably good solutions.	High computational cost and memory demand are always required.	Koeppel et al. 1995; Flake 1998; Chang et al. 2006; etc.
	Evolutionary algorithms and genetic algorithm	With high generalities and flexibilities, and there are also robust to find the global minimum.	Extensive computational cost and memory demand are always required due to high number of fitness evaluations.	Huang and Lam 1997; Wang and Jin 2000; Nassif et al. 2005; Lu et al. 2004, 2005b; Fong et al. 2006; etc.

Table 2.2 summarizes a set of typical objectives and constraints when applying control strategies to buildings. A principal objective is typically the reduction of energy used by

⁵ Reprinted from HVAC&R, Vol 14, Iss 1, Wang & Ma, Supervisory and Optimal Control of Building HVAC: A Review, 3-32, Copyright 2008, with permission from Taylor and Francis

the building. This may be accomplished by reducing “energy requirement” or “energy consumption”:

- *Energy requirements* of the building can be reduced by altering the necessary heating/cooling in the thermally conditioned zone. In the control sense this is not accomplished by energy efficiency retrofits (e.g. adding insulation), but rather by changing the thermal zone operating setpoints. For example, if strong sunlight is forecast for the next several hours, the blinds should be closed to reduce the necessary zone cooling requirements (air conditioning).
- *Energy consumption* of the building can be reduced by operating the HVAC systems more efficiently. This may be accomplished by increasing part-load efficiency, decreasing cycling, or by sequencing of certain equipment. For example, if strong sunlight is only forecast for one hour, a multi-sequence cooling system should be started early and run continuously for two hours instead of all systems starting for only half an hour. It should be noted that a reduction in *energy requirements* often leads to a reduction in *energy consumption*, although this is not always the case (e.g. reduced lighting may necessitate increased inefficient space heating).

Table 2.2 MPC objectives and constraints for buildings

Objectives	Constraints
Energy minimization	Thermal comfort range
Cost minimization	Equipment limits range
Greenhouse gas emissions minimization	Thermodynamic limits
Thermal comfort maximization	

While reducing energy used by the building is often a principal objective, this may be motivated by an objective to reduce operational cost and/or greenhouse gas emissions.

These objectives are typically strongly linked when considering single energy sources (e.g. natural gas) and fixed rate energy billing. However, energy source switching, demand or time-based billing, or principal objective hierarchy may cause this to not be the case. For example:

- Switching from natural gas (fluctuating price) to electricity during certain periods may save both energy (more efficient system) and cost, but may increase greenhouse gas emissions in coal-fired electricity jurisdictions.
- The use of thermal storage may dramatically decrease electricity demand costs and also energy costs through time-of-use billing periods, but may increase energy consumption due to storage system inefficiency.
- An objective of reduced greenhouse gas emissions may lead an organization to opt for a program such as Bullfrog Power⁶, thus paying increased costs for electricity.

As shown in Table 2.2, thermal comfort is often the principal constraint in building operations. It is of most importance to operations of commercial and institutional buildings, as occupant discomfort impairs the building in carrying out its principal services. The thermal comfort constraint may consist of a range of suitable temperatures, with weighted penalties for excursions beyond a certain value. Additional constraints include equipment limits and thermodynamic limits. Equipment limits are typically the magnitude of operation of the HVAC system (e.g. heating and cooling power), but also include the sequencing and rate-of-change of equipment. Thermodynamic constraints inform the optimizer so that it does not attempt to breach the practical operation when searching for a solution. For example, a thermodynamic constraint on a liquid water loop would restrict the operating temperature range from 5 to 95 °C. Another example is a large decrease in temperature in a humid environment can cause condensation buildup, leading to damage and increased maintenance costs.

⁶ <https://www.bullfrogpower.com/>

2.2 Building Physics

In order to develop a suitable prediction model, calibrate a detailed energy model, and understand the value of advanced forecast information for a building, a solid understanding of the heat transfer mechanisms through the building envelope and within the building is required. Figure 2.1 highlights these flows which can be broken down into four main categories: conduction, convection, short wave radiation, and long wave radiation. Conduction occurs through the building envelope, both with the external environment and between adjacent zones. Within building simulation programs, there are two main methods for solving the conduction problem: conduction transfer functions and numerical methods. The text by Clarke [43] is a good resource on the differences of the methods. Both methods use a nodal discretization of the materials as shown in Figure 2.2, where the number of nodes depend on the material properties and material thickness. Convection occurs between the air point (typically the point to be controlled) and all internal surfaces (walls, windows, people, equipment) to add/remove energy from the air point. In many buildings, the primary heating and cooling is supplied via air from the air handling unit (AHU) system which introduces forced convection energy loads to the air point. Infiltration through the building envelope (such as gaps around windows/doors) also introduce convective loads to the air point. Convection also occurs between the building fabric and the environment which alters surface temperatures and conduction rates through the building envelope. Short wave solar radiation from the sun is absorbed by building surfaces (both external and internal through window transmittance) where it can then be released to the air point through convection across the heated surfaces. Long wave radiation effects occur between surfaces within a zone, and can ultimately lead to convective transfer to the air point. Long wave radiation effects also occur between the building fabric and external surfaces such as the ground, adjacent buildings, and the sky.

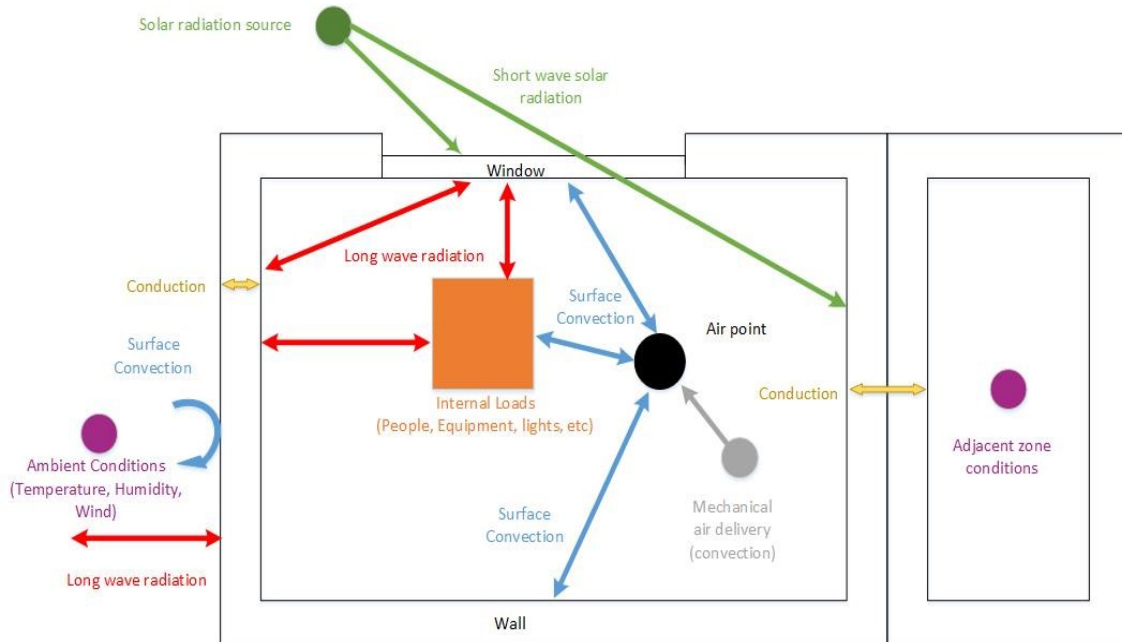


Figure 2.1 Major energy flows in a building based on [44]

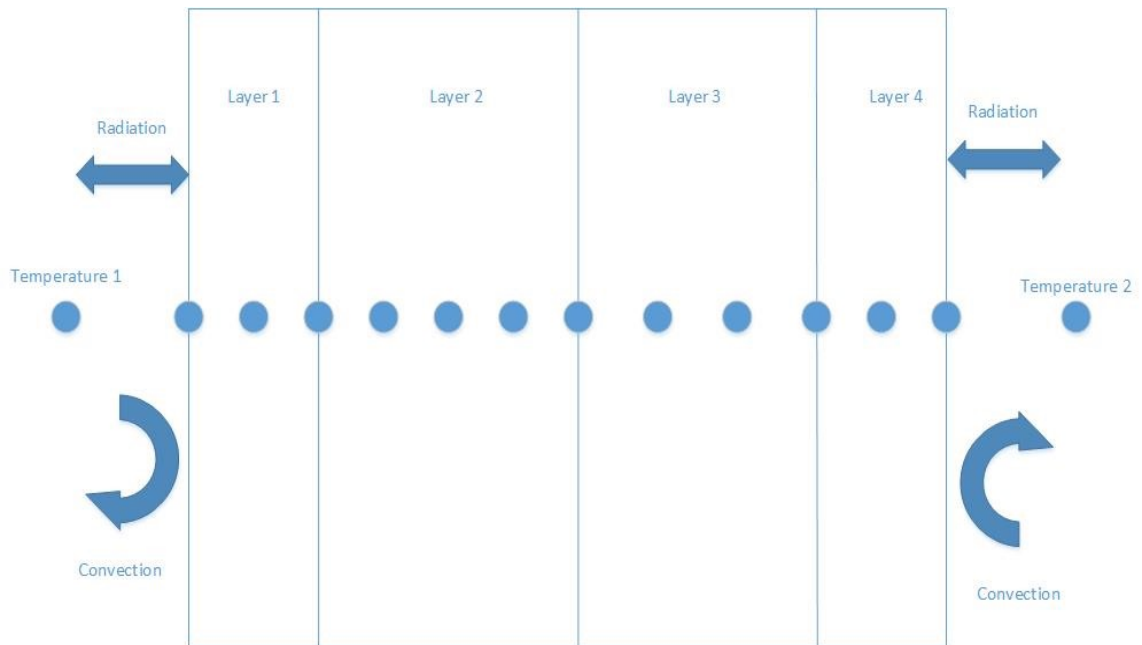


Figure 2.2 Wall nodes for conduction

It is also important to consider the energy storage effects of the building envelope, interior materials, and air. The storage effects offer a time-lag between peak outdoor conditions and indoor conditions [45], which offer another opportunity for MPC, by being able to

predict the time lag and magnitude shift correctly to minimize energy consumption. An example is shown in Figure 2.3.

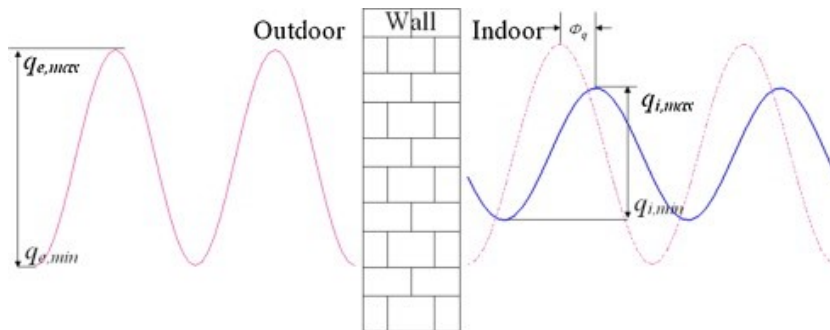


Figure 2.3 Heat flux time lag [45]⁷

⁷ Energy and Buildings, Volume 47, Jin, Zhang, Cao, & Wang, Thermal performance evaluation of the wall using heat flux time lag and decrement factor, 369-374, Copyright 2012, with permission from Elsevier

2.3 Occupant Comfort

Occupant comfort is an expansive research topic that has been and is still being studied extensively. While it is necessary to maintain a comfortable space (due to occupant salaries outweighing operational costs for most commercial buildings [46], [47]), it is not the direct goals of the research to develop new metrics. Thus, existing models/techniques for occupant thermal comfort have been implemented. When considering thermal comfort there are three typical metrics employed: thermal zone temperature (both air and operative), predicted percentage dissatisfied (PPD), and predicted mean vote (PMV) [48]. The latter metrics were introduced by [49] as static models to describe thermal comfort based on human body heat balance consisting of air temperature, mean radiant temperature, relative humidity, air velocity, clothing levels, and people activity rates. The PMV model is based on a scale of -3 (cold) to +3 (hot) with comfort defined as the range from -0.5 to +0.5. Based on this definition, minimizing the absolute value of PMV is a valid comfort criteria for an objective function term. The challenge with such a technique is that not all the parameters used in the calculation are measured by a building energy management system and require additional sensors or approximations for the variable. For reference, the equations for PMV and PPD are as follows (Equations 2.3 - 2.8):

$$PMV = [0.303e^{-0.036M} + 0.028]\{(M - W) - 3.96E^{-8}f_{cl}[(t_{cl} + 273)^4 - (t_r + 273)^4] - f_{cl}h_c(t_{cl} - t_a) - 3.05[5.75 - 0.007(M - W) - p_a] - 0.42[(M - W) - 58.15] - 0.0173M(5.87 - p_a) - 0.0014M(34 - t_a)\} \quad 2.3$$

$$PPD = 100 - 95e^{[-(0.3353PMV^4 + 0.2179PMV^2)]} \quad 2.4$$

$$f_{cl} = 1.0 + 0.2I_{cl} \text{ or } 1.05 + 0.1I_{cl} \quad 2.5$$

$$t_{cl} = 35.7 - 0.0275(M - W) - R_{cl}\{(M - W) - 3.05[5.75 - 0.007(M - W) - p_a] - 0.42[(M - W) - 58.15] - 0.0173M(5.87 - p_a) - 0.0014M(34 - t_a)\} \quad 2.6$$

$$R_{cl} = 0.155I_{cl} \quad 2.7$$

$$h_c = 12.1(V)^{\frac{1}{2}} \quad 2.8$$

Where the variables are outlined in Table 2.3.

Table 2.3 PMV/PPD variables

Variable	Description	Easily Measured
f_{cl}	Clothing factor	No
h_c	Convective heat transfer coefficient	No
I_{cl}	Clothing insulation in clo	No
M	Metabolic rate in W/m^2	No
p_a	Vapor pressure of air in kPa	Indirectly
R_{cl}	Clothing insulation level	No
t_a	Air temperature in °C	Yes
t_{cl}	Clothing surface temperature in °C	Yes, limited
t_r	Mean radiant temperature in °C	Yes, limited
V	Air velocity in m/s	Indirectly
W	External work in W (typically 0)	No

It is also important to note that while occupant comfort is often thought in terms of thermal comfort, other factors exist. The main factor is indoor air quality, which can be impacted by factors such as pollution, material off gassing, CO₂ buildup from lack of ventilation, and other irritants. These issues can lead to “sick building syndrome” [50]. Thus it is necessary to ensure that changes to the thermal comfort controls maintain existing flow rates, or that overrides for factors such as CO₂ accumulation (ASHRAE Standard 62 [51] suggest between 1000-1200 ppm) exist to maintain a healthy and comfortable environment. A study done in [52] examines other indoor air quality pollutants including carbon monoxide, nitrogen dioxide, and formaldehyde. While outside the scope of the research, forecasts for environmental conditions can be used in regions where outdoor air pollution can become a concern to adjust the fresh air system behavior to enhance indoor air quality.

An analysis of the standards produced by ASHRAE [48], ISO [53], and BS-EN [54] that relate to thermal comfort in the built environment is shown in Table 2.4. The standards are typically based on PMV or PPD.

Table 2.4 Thermal comfort standard comparison

Standard	Mechanical Systems	Natural Ventilation
ASHRAE 55:2013	PMV/PPD based, either graphical with assumptions or calculation for PPD < 10 Zone operative temperature from psychometric chart for typical indoor conditions Local thermal discomfort (i.e. draught, radiant asymmetry)	Based on outdoor air temperature
ISO 7730:2015	PMV/PPD based, either graphical with assumptions or calculation with 3 categories of PPD (A < 6, B < 10, C < 15) Local thermal discomfort (i.e. draught, radiant asymmetry) Provides design level tables based on space types	Not listed
BS-EN 15251:2007	PMV/PPD based on ISO 7730	Based on outdoor air temperature

While Table 2.3 states which variables are measurable inputs and which are dependent variables to be calculated, several of the inputs are difficult to measure.

- Zone air temperature (ZAT, dry bulb) is the easiest measurement as almost all zones contain a thermometer as part of the thermostat.

- Water vapor partial pressure can be calculated from relative humidity measurements, which are often taken at the main AHU level.
- Air velocity is indirectly calculated by variables such as variable air volume damper positions and AHU fan rate.
- Zone mean radiant temperature (ZRT) in a space is measured using a black globe thermometer. However, it is a point measurement and they are not typically installed/connected to conventional building management systems.
- Metabolic rate can be approximated by the common activity with a thermal zone, but can fluctuate when abnormal activity occurs in a space.
- Clothing level is more challenging to approximate, as each individual person in a space likely is wearing different levels of clothing, which typically changes seasonally. [48] has an approximation chart for clothing levels based on outdoor air temperature and can be found in Figure 2.4.

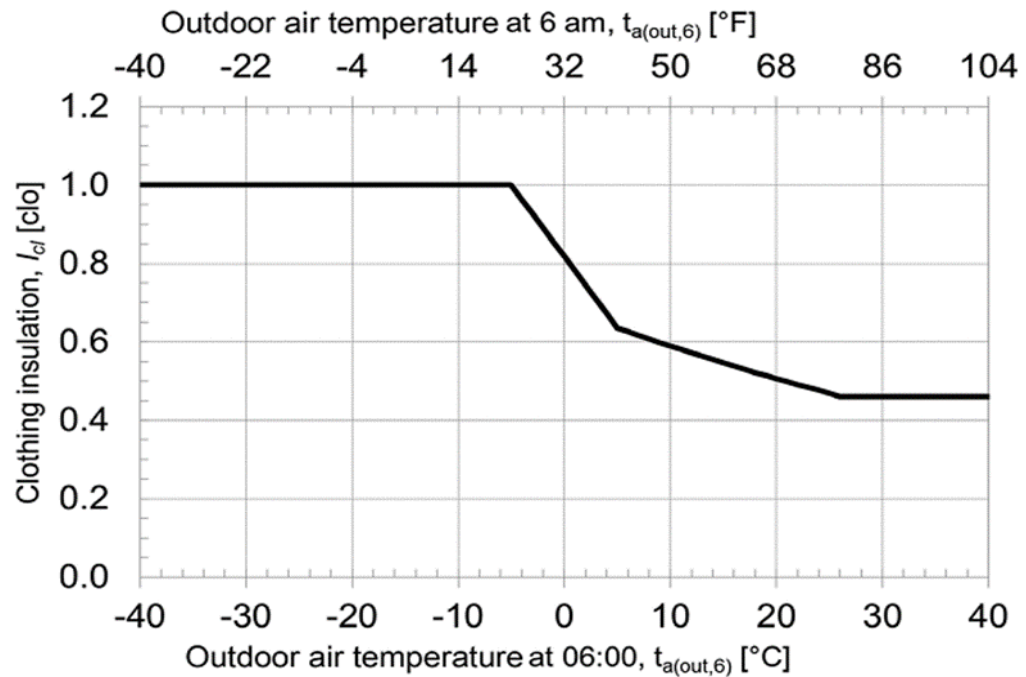


Figure 2.4 Clothing insulation as a function of outdoor air dry-bulb temperature at 06:00 [48]⁸

A PMV sensitivity analysis was conducted with results tabulated in Table 2.5. An initial base case is used to compare the impact of changing individual components of the PMV/PPD calculation. The changed variable in each case is highlighted in yellow, with the corresponding change in PMV and PPD located at the bottom of the table. The variables with the largest impact are clothing and metabolic rate, both of which are not easily measured.

⁸ ASHRAE standard by AMERICAN SOCIETY OF HEATING, REFRIGERATING AND AIR
 Reproduced with permission of THE SOCIETY, in the format Republish in a thesis/dissertation via
 Copyright Clearance Center.

Table 2.5 PMV/PPD sensitivity analysis

Variable	Reference Case	Case 2	Case 3	Case 4	Case 5	Case 6	Case 7	Case 8	Case 9	Case 10	Case 11	Case 12	Case 13	Case 14
Air Temperature	24	20	22	26	28	24	24	24	24	24	24	24	24	24
Radiant Temperature	24	24	24	24	24	20	28	24	24	24	24	24	24	24
Air Speed	0.1	0.1	0.1	0.1	0.1	0.1	0.1	0.15	0.1	0.1	0.1	0.1	0.1	0.1
Humidity	50	50	50	50	50	50	50	50	20	35	65	80	50	50
Metabolic Rate	1.1	1.1	1.1	1.1	1.1	1.1	1.1	1.1	1.1	1.1	1.1	1.1	1.5	1.1
Clothing Level	0.5	0.5	0.5	0.5	0.5	0.5	0.5	0.5	0.5	0.5	0.5	0.5	0.5	1.0
PMV	-0.46	-1.24	-0.83	-0.12	0.23	-1.07	0.18	-0.51	-0.68	-0.57	-0.35	-0.24	0.31	0.39
PPD	9%	37%	20%	5%	6%	29%	6%	11%	15%	12%	8%	6%	7%	8%
PMV change from Case 1	N/A	-170%	-80%	74%	150%	-133%	139%	-11%	-48%	-24%	24%	58%	167%	165%

Chapter 3 LITERATURE REVIEW

Portions of this chapter have been published in the following article:

Hilliard, T., Kavgic M., & Swan L. (2015). Model predictive control for commercial buildings: trends and opportunities. *Advances in Building Energy Research*. 10:2, 172-190 doi:10.1080/17512549.2015.1079240 [55]

And have been reproduced under Taylor and Francis licensing agreement section 4 vii (see Appendix A).

Trent Hilliard is the principal researcher and author of the article. He conducted the research as part of his PhD. Thus, while he received supervision and guidance from his supervisor Dr. Lukas Swan and post-doctoral fellow Dr. Miroslava Kavgic, he carried out the work, wrote the article, and communicated with the editor of the journal. Minor grammatical and content changes have been made to integrate the article within this dissertation, and incorporate the latest literature.

This chapter examines recently published literature of MPC (2010 to 2017) and its application to buildings. The initial search included all levels of MPC applications (i.e. equipment specific and single zone), with latter reviews focused on whole building implementations with experimental validation. The following information for each work is noted (where given by the authors):

- building or space type
- space conditioning HVAC system
- model type and detail
- simulation software
- simulation timestep
- required sensors
- optimization (variables, type, and horizon)
- constraints placed on the optimization

- control variables
- results

The details of the studies are found in a series of tables that capture the salient points and allow for comparison, with a brief description of each study located thereafter. The studies are organized by their MPC scope and then chronologically. Table 3.1 lists the type of model used to represent the building, also known as a building response model. The type of models include resistive-capacitive (RC) networks ([56], [18]), neural networks ([57], [36]), or other black (or grey) box statistical methods ([58], [17]), and advanced building simulation engine models. Research has shown there is no one ‘best’ model for predictive controls, as discussed in [59], [60], [61].

Table 3.2 lists the modeling and simulation software packages used to implement both the building prediction model and MPC optimization, followed by the type of optimization algorithm used to solve the MPC problem. It concludes with a description of the area/equipment that the MPC is attempting to optimize and control. Table 3.2 contains the information needed for the MPC controller. Typically, the optimization is calculated at each timestep for the forecast horizon. Table 3.2 also lists the measurements required for the model portion of the MPC, and concludes by defining the control outputs. Table 3.3 outlines the strengths and weaknesses of each work, with the savings noted in each case. Boldface is used to identify studies in which experimental validation occurred, thus emphasis should be placed on these results. Given the early stage of MPC research for buildings, validation is crucial to give confidence in research results.

The research is classified into three sub-categories based on the control scope as listed in Table 3.1: component/subsystem level, zone level, and whole building.

Table 3.1 Models and optimization techniques

	Study	Response model type	Simulation software	Optimization method	Control scope
Component / subsystem level	[62]	Linearized state space	Matlab and Simulink	Linear	Single zone electric heater
	[58]	Black box state space	Scilab	Weighted square sum (quadratic)	Building heating system
	[18]	RC based linear state space	Scilab	Quadratic and linear terms	Building heating system
	[63]	Discrete time RC	Matlab	Quadratic with linear constraints	Single zone AC
	[9]	Mixed model, RC and physics	Matlab	Linear	Cooling storage tank
	[64]	Physics based	TRNSYS	Exhaustive search	Condenser
	[65]	Hammerstein-Wiener	Matlab	Weighted square sum (quadratic)	Home AC heat pump
	[66] case II	EnergyPlus	EnergyPlus, GenOpt	Hookes-Jeeves algorithm in GenOpt	Radiant cooling slab
	[66] case III	TRNSYS physics based	TRNSYS, GenOpt	GenOpt Hookes-Jeeves Multi-Start	Cogeneration plant for electric reduction
	[67]	12 dimension linear state space	TRNSYS, Matlab	AQR, SQP	Variable flow AHU cooling system
Zone level	[68]	Bilinear state space	Matlab	Linear	Single zone
	[66] case I	Physics based	Modelica, GenOpt, SimCon	Hookes-Jeeves algorithm in GenOpt	Single zone with shading and natural ventilation
	[69]	EnergyPlus based regression statistical model	EnergyPlus, OpenStudio	Linear	Cooling system with real time pricing, ideal loads
	[56]	12th order RC	TRNSYS	Linear and quadratic	Single zone
Whole building	[70]	1 st order time delay with uncertainties, statespace	Matlab	Quadratic	AHU with VAV
	[71]	EnergyPlus based regression model	EnergyPlus, Matlab, BCVTB	Linear	Entire building with only cooling
	[72]	Generalized linear models	EnergyPlus, Matlab	Particle swarm	Whole building with natural and mechanical ventilation
	[73]	Linearized state space with RC	Matlab	Linear programming	Single zone building

	Study	Response model type	Simulation software	Optimization method	Control scope
Whole building	[74]	EnergyPlus	EnergyPlus, Matlab	Particle swarm	Multiple scenarios, whole building
	[75]	EnergyPlus	EnergyPlus, Matlab, MLE+	Exhaustive search (Brute force)	Entire building HVAC system
	[19]	3R2C with EKF	Matlab, Ipopt	Interior point nonlinear programming	Multi-zone building
	[17]	Gray box model	OptiCOOL	Linear and quadratic terms	Whole building
	[76]	3R2C with ANN	Matlab	Linear programming	Multiple zones within airport
	[77]	RC based regression	TRNSYS	Linear programming	Multi-zone office space
	[78]	Bi-linear RC physics	Matlab	Linear	Multi-zone office building
	[79]	Physics based	Modelica	Multiple layers	Multi-zone building
	[80]	Physics based state space	N/A	Linear	Air handling unit level
	[81]	RC circuit model	Matlab & EnergyPlus	Quadratic	Multi-zone house
	[82]	RC circuit model	Matlab	Quadratic	Multi-zone house

Table 3.2 System information for models and optimization

	Study	Forecast horizon	Simulation timestep	Input sensors	Control outputs
Component/subsystem level	[62]	5 hours	10 minutes	Zone T, ambient T, electric power	Electric power
	[58]	Not given	Not given	Supply T, return T, zone T, max and min ambient T	Supply water temperature
	[18]	2 days	20 minutes	Room capacitance, wall resistance, zone T, ambient T, return T, supply T	Supply water temperature
	[63]	5 hours	15 minutes	Zone T, AC power	AC state (on/off)
	[9]	1 day	1 hour	Return T, ambient T, tank T, stratification height	Cooling tower T, chilled water T, chiller run time
	[64]	N/A	N/A	Ambient T, inlet T, outlet T, cooling demand	Outlet T
	[65]	1 day	15 minutes	Zone T, ambient T, AC power	AC state (of/off)
	[66] case II	24 hours	Not given	EnergyPlus model	Cooling slab charge
	[66] case III	Not given	Not given	Heating and cooling loads, electricity demand and cost	Amount of time to operate cogeneration plant
	[67]	AQR–1 day SQP–6 hours	10 minutes for both	Zone T, mean radiant T, wall T, GSR, ambient T, ambient RH, supply air T, supply air flow	Rate of heat addition/removal
Zone level	[68]	6 days	1 hour	Occupancy, zone T, zone RH, luminance, ambient T, ambient RH, GSR	Multiple configurations
	[66] case I	Not given	Not given	Zone T, ambient T, internal loads, GSR	Shades and ventilation rate
	[69]	8 hours	1 hour	Zone T, ambient T, occupancy	Zone setpoint
	[56]	6 days	1 hour	Occupancy, zone T, zone RH, luminance, ambient T, ambient RH, GSR	Multiple configurations
Whole building	[70]	N/A	6 seconds	Air Temperature, water temperature	Air flow
	[71]	End of day	25 minutes	Zone setpoints, Zone T	Zone setpoints
	[72]	24 hours	1 hour	EnergyPlus model	Window state (open/closed)
	[73]	N/A	N/A	Room T, ambient T, solar radiation	Radiator water T

	Study	Forecast horizon	Simulation timestep	Input sensors	Control outputs
Whole building	[74]	7 days	1 hour	EnergyPlus model	Room setpoint temperature
	[75]	24 hours	1 hour	EnergyPlus model	Zone setpoints
	[19]	3 hours	15 minutes	CO2, occupancy, zone T, zone RH, ambient T, ambient RH	Stream temperatures and air volume flow
	[17]	End of day	5 minutes	Ambient T, zone T, occupancy, HVAC power	Zone setpoints
	[76]	1 day	10 minutes	Supply air T, supply air flow rate, neighbor zone T, CO2, ambient T	Zone temperature
	[77]	1 day	15 minutes	Supply T, return T, water flow rate, ambient T, solar radiation	Zone temperature
	[78]	58 hours	15 minutes	Average room T, heat flux, air flow, internal gains, ambient T, solar radiation	Water temperature and flow rate
	[79]	6 hours	15 minutes	Heat flux, room T, solar radiation, ambient T	Water temperature
	[80]	125 seconds	1 second	Incoming T and humidity, heat transfer coefficients	Water temperature and flow
	[81]	N/A	N/A	Room humidity, room T, ambient T, ground T, solar radiation	HVAC power and flow
	[82]	N/A	N/A	Room humidity, room T, ambient temperature, ground temperature, solar radiation	Heater power

Table 3.3 Strengths and weaknesses of the research (experimentally studies in boldface)

	Study	Strengths	Weaknesses
Component/subsystem level	[62]	Unique aspect to thermal comfort, 37% thermal improvement with 14% savings	Extremely simple, no solar aspects
	[58]	Experimental validation with back simulation, 17-29% savings	No forecast information given, limited disturbances (no solar)
	[18]	Experimental validation, savings of 15-28%	Questionable implementation of HDD
	[63]	Simple, minimal inputs required, up to 70% savings, experimental validation	Cooling only, not transferrable
	[9]	Mixed model for building and tank system, 75% savings, experimental validation	Weak baseline setup, cooling only
	[64]	Includes fault detection and correction. Savings of 5% with all features included.	Specific to condenser behavior, only simulation based results.
	[65]	Simplified model, uses variable electricity pricing, 13% savings	Cooling only, minimal savings due to low thermal capacitance
	[66] case II	EnergyPlus model, weather forecasting, 10% PPD reduction	Assumes interpolation exists
	[66] case III	Advanced method of subdividing optimization, 11% savings	Assumes interpolation exists
	[67]	Simplified model validated to TRNSYS, AQR has 26% savings	Cooling only, SQP increased cost by 54%, low off peak pricing
Zone level	[68]	Considers forecast uncertainty, 25% savings in theory	Only 10% savings actually achieved with weather uncertainty
	[66] case I	Offline optimization table, 57% savings	Assumes interpolation exists, weak baseline controller
	[69]	Linear regression from EnergyPlus for model, 1-5% savings	Need to remake model for any changes, minimal thermal comfort
	[56]	Simplified model verified to TRNSYS, advanced building, 16% savings	Single zone with adiabatic walls, no mention of IAQ
Whole building	[70]	Simple models, common HVAC systems, deals with model uncertainties	Plant based optimization, focus on signal tracking
	[71]	Multizone building, 25% energy savings	Cooling only, model specific results

	Study	Strengths	Weaknesses
Whole building	[72]	GLM to extract from EnergyPlus MPC, GLM results 70-90% of MPC	PSO algorithm doesn't guarantee a solution
	[73]	Developed cost function to go from traditional MPC mechanics to practical building control.	Single zone building with only heating explored.
	[74]	PSO allows for nonlinear functions, use high fidelity models	PSO algorithm doesn't guarantee a solution, no discussion on implementation
	[75]	Multizone building, 20% energy savings, both heating and cooling	Attempts to rewind EnergyPlus, requires EnergyPlus models
	[19]	Experimental validation, whole building analysis, 19-32% savings	No optimization on weekends, gray box model requires lots of training
	[17]	Whole building, simplified model validated to measured data, experimental results, 65% savings	Experimental results have different weather, inherently inefficient base system
	[76]	Multi-zonal study with both simulation and experimental results. Savings of 13% cost in experiment	No accounting of solar radiation on the highly glazed building
	[77]	Multi-zonal study with both simulation and experimental results. Improvement in thermal comfort compared to traditional TABS control	Negligible energy savings, no discussion on fresh air impact
	[78]	Whole building study with simulation and experimental results. Simulation showed energy savings of 17%.	No energy discussion of experiment, only focus on occupant comfort.
	[79]	Whole building study. Able to handle uncertainty in the system. Provides a pareto front of savings vs comfort.	Savings levels appear minimal, but does enhance comfort.
	[80]	Experimental validation with reduced settling time and smoother system response to step changes.	Strictly system optimization, no assessment of comfort. No assessment of energy savings.
	[81]	Detailed analysis of model simplification method and simulated savings of 34%.	Complex base models, lots of data required for heat and moisture
	[82]	Experimental simulations with 43% savings from base case.	Quarter size models in environmental chambers.

3.1 Component/Subsystem Level Studies

The work of [63] was focused on the cooling of a university computer lab using a single stage air conditioning heat pump. The system was modelled using a discrete time model based on RC circuit methods. The only sensors required by the system are room temperature and the power consumed by the air conditioner along with an occupancy schedule. The occupancy schedule is also used to modify the equipment schedule, as a base load is assumed, with increases in load occurring when the room is occupied. The optimization is done using Matlab with the objective of minimizing energy use while maintaining a room temperature of $22^{\circ}\text{C} \pm 2^{\circ}\text{C}$ as a hard constraint, with $\pm 1^{\circ}\text{C}$ incorporated as a penalty within the cost function for even better temperature control. The only control variable is whether the air conditioner is on or off, and by using MPC the cooling lag can be incorporated for when the power is turned off but cooling is still being done by the air conditioner. A prediction forecast of five hours is used, with a 15 minute timestep. Experimental testing show a reduction of electricity use by 30-70% from traditional two stage (on/off) control. The model is very simple with minimal sensors required and has experimental verification, but the transferability to other scenarios may be limited due to the single control variable and the on/off nature of it. Also of concern is how the authors treated the disturbances as a temperature, which is due to the decision to focus solely on convective heat transfer. While it simplifies the modelling greatly, other effects such as radiation seem to be neglected. Also the work focuses on a single zone, and coupling effects from adjacent zones are not considered and can play a large role if a temperature differential exists.

[67] looked at an AHU cooling system with a variable flow cooling coil used to extract heat from a space. The system was modelled as a 12-dimension discrete time linearized and reduced order state space model based on the work of [83]. The work of [83] developed a reduced order model with validation to an advanced TRNSYS model. While the model is a reduced order linear model, a large amount of sensors are required which include:

- zone air temperature

- mean radiant temperature
- wall temperatures
- solar radiation
- ground radiation
- ambient temperature
- ambient relative humidity
- supply air temperature
- supply air flow rate

The optimization was done based on cost, where a thermal penalty converted to dollars (based on salaries of employees) is used to ensure comfort. The room setpoint was set to 26°C when occupied, and allowed to float otherwise. Two different optimization solvers were used in Matlab: an Affine Quadratic Regulator (AQR) with a one day horizon and a Sequential Quadratic Programming (SQP) using a six hour prediction horizon and both methods use a ten minute timestep. The AQR approach requires that all terms in the cost function be quadratic, while the SQP approach is more relaxed in that it requires the cost function to be twice continuously differentiable. The SQP then approximates the system as quadratic for solving the problem. The results from the study show a cost savings of 26% using the AQR solver, while the SQP increased cost of 54%, mainly due to thermal discomfort penalties (due to a different cost function and solution method). While the system reports savings, some concerning factors were an extremely low electricity price (0.01\$/kWh off peak), the AHU power for only fresh air was neglected, and that the predictors were working with a perfect forecast, something not available in practice.

The work of [65] analyzed dynamic load control using real time electricity pricing for a home air conditioning heat pump. The system model is a first order linear differential equation, and is modelled in Matlab using the Hammerstein-Wiener system model. The information required by the model is the ambient air temperature, indoor air temperature,

and the power consumed by the air conditioner, while the optimizer requires the day ahead electricity pricing at a 15 minute interval. The optimizer is focused on cost reduction under two cases, with the first case of holding a temperature of 25.5°C , while the second case lets the temperature float from 25°C to 26°C , while using a 24 hour horizon and 15 minute timestep. The optimization uses a weighted square sum so that an optimal solution will always exist, while the control variable is the state of the air conditioner (on or off). When using the fixed temperature, a cost savings of 5% are realized, while a floating temperature range improves savings to 13%. The work is experimentally validated, but without a large mass to store energy, the only gains are by exploiting day ahead pricing and the dynamics of the air conditioner where it still provides cooling after being turned off (0.25°C). The work is restricted to cooling only, and solar effects are not considered. By incorporating solar loads, a better estimation of external loads can be done and a potentially larger savings could be realized with better thermal performance. Also, the addition of thermal mass that can be precooled would allow for even more savings.

[62] proposed a distributed MPC scheme for thermal regulation of a space during the heating season. The HVAC system consists solely of an electric heater, with no consideration for IAQ. A linearized state space model is used where the inputs required for the system are only temperatures (zones and outdoor) and the electric heating power. The optimization is done with energy as the focus and a penalty term used to ensure thermal comfort. A ten minute timestep is used with a five hour prediction horizon, and a constraint on temperature of 20°C . Three different control strategies are utilized – decentralized, centralized, and distributed. The decentralized controller is the simplest controller but does not account for temperature effects of neighboring zones, producing a suboptimal result. Centralized control can provide the optimal result, but the processing time required due to the large decision space would exceed the 10 minute timestep if implemented in real time. Distributed control allows the individual zone controllers to pass information amongst each other and allow for similar performance to a centralized controller while not exceeding the time period. The decentralized controller resulted in a lower energy usage, but also decreased thermal comfort due to the lack thermal coupling between zones. Centralized and distributed control experienced a 37% thermal improvement with a 14% energy

savings. An interesting feature by the authors is to not penalize temperature in unoccupied periods and heavily penalize it when occupied so that the controller focuses on occupied periods when doing its forecasting. However, the model is extremely simple, and does not account for solar radiation effects and is incapable of any cooling.

The work of [58] and [18] look at the heating system in a university building in the Czech Republic. [58] developed a linear time invariant discrete time state space model using subspace identification from thermal response data for the test building. This amounts into a black box style formulation, where the state space matrices do not have any physical meaning. The HVAC system is a Crittal style ceiling system that uses radiant in ceiling tubing for water to be used for heating and cooling. The control variable for the system is the supply water temperature, as water is circulated by a constant volume pump. The system tries to follow a reference schedule of 22°C while occupied and 19°C when unoccupied for the heating season. The hot water that circulates in the system is limited to the range of 20 to 55°C, with a rate of change of no more than 20°C per minute. The optimization and modeling were carried out using the Scilab⁹ software (open source software for numerical computation), and the following information was needed for the model: supply water temperature, return water temperature, maximum and minimum temperature forecast, and indoor room temperature. Optimization was done to minimize energy while having a quadratic error tracking term to enforce temperature compliance. As with most work reviewed, the optimization algorithm can find the single optimal solution, which showed a 17-29% reduction in energy use. The authors recognized that they are limited by only considering the outdoor air temperature as a disturbance, and that the inclusion of effects such as solar radiation would further improve the performance. It would have been helpful if the authors had provided their forecast ranges and timestep information as other studies have concluded these factors can greatly affect performance.

⁹ <http://www.scilab.org/>

[18] conducted a research project using the same building as [58] which means they were subjected to the same HVAC system, control variables, and measurements. However, they used a discrete time linear state-space RC based model as opposed to the black box model used by [58]. A second difference noted is that the optimization was quadratic in nature for both energy and setpoint tracking, where a 20 minute timestep was specified with a two day horizon. The results demonstrated a 15-28% reduction when experimentally implemented on the test building, as the building had sister towers with one using the existing rules based control and the other using the MPC controller. Some concerns from the work were the calculation and usage of heating degree days (HDD) based on the desired indoor temperature, which means that any internal gains are ignored, as HDD are normally calculated to 18°C to account for internal heat gain. However, the results of the study also show a reduction in peak power (drop in supply to return temperature difference of 30 °C), which can result in significant cost savings for commercial customers.

The work in [9] focus on using MPC for the control a cooling plant for a building with a stratified storage tank for the cooled water. The modelling for the work consists of a mixed model with an RC model for the building, while the stratified storage tank is modelled using physics based equations. The MPC work is focused on the optimization of the tank storage, not the thermal characteristics of the building. The building model is used to determine the loads needed to be supplied by the tank, so the assumption is that any changes made to the cooling system will not affect the thermal capabilities of the building. The system consists of the water storage tank, an electric chiller, a cooling tower on a condenser loop for the chiller, and several demand loops for chilled water from the tank/chiller. The sensors required for the model of the tank are the chilled water return temperature, the ambient outdoor temperature, the temperatures in the tank, and the height of the stratification point in the tank. The system is constrained in that it must be able to meet the daily cooling loads, and that the water flow rate variable within a specific range and the size of the tank is fixed. The controller is responsible for determining the cooling tower outlet temperature, chilled water flow rate, chilled water temperature, and how long the chiller runs. The optimization is done to minimize costs and increase the coefficient of performance (COP) of the system with a one hour sampling time and a one day prediction

horizon. Experimental results indicate a reduction of energy cost by 75% while improving the COP by 20%, mainly due to running the system at more efficient periods of the day (such as at night). While the work shows how MPC can be used for building subsystems, it may be challenging to implement to a building automation system without thermal storage as the controller is making better use of the stratified storage tank.

[64] developed an MPC scheme with a focus on fault detection and tolerance for a building condenser. While minimal details of how the MPC portion of the problem was solved were given, the ability to detect faults and compensate for them are a unique feature of the work. Results indicate that 5% savings can be achieved using the MPC scheme when faults are detected and corrected.

3.2 Single Zone Studies

The OptiControl¹⁰ project was a joint project between researchers at the Swiss Federal Institute of Technology, Siemens, Gruner, and SwissElectric with a focus of predictive technology for building control. In their published final report [7], they detail their methodology used. For the models used, they started with an EnergyPlus (*E+*) detailed model of the test building, and then minimized to a high order RC circuit model. They then further reduced to the complexity of the high order RC model to a lower order RC model that was then implemented for real time control. They concluded that while models showed savings, a mismatch in savings and energy use between the building and simulation existed, and noted that models were good for long term savings and as a starting point for control, but to expect to have changes once the new control is implemented. The project only implemented high level control on the test building (a six story office in Basel), with Matlab being the software used for MPC. The primary heating and cooling for the building was provided by in-floor radiant heating/cooling pipes. Constant fresh air ventilation was only supplied during occupied hours, and the same water system used to heat/cool the building was used to condition the air heading to the zones in the building. The final report indicated that MPC had a reduction of energy use for HVAC by 25% compared to the original installed control strategy. Simulation results from this work is included in [56] and [68].

The work of [56] focuses on a single zone modelled with a 12th order RC circuit network that is calibrated to a TRNSYS model of the system to within $\pm 0.5^{\circ}\text{C}$, and was part of the OptiControl project. Thirty-two different building envelope scenarios were tested and are outlined in Table 3.4. Likewise, five different setups of HVAC and other controllable systems (such as automated blinds) configurations were considered, with the variations outlined in Table 3.5. Individual linear or bilinear models were used for all the HVAC and other controllable systems. Measurements required by the model are occupancy, zone temperature and relative humidity, zone luminance, ambient temperature, ambient relative humidity and global solar radiation. The optimization is to minimize energy use while

¹⁰ <http://www.opticontrol.ethz.ch/>

maintaining thermal comfort between 21-25°C or 22-27°C depending upon the outdoor air temperature to represent heating and cooling seasons. Only linear and quadratic optimization functions were considered due to their simplicity, with a six day forecast horizon and an hourly timestep. The authors also assume that the predictions for weather are perfect, and thus present a theoretical maximum savings achievable by their work. The indoor air quality (IAQ) was not directly controlled, but the ventilation rate was based on the occupancy schedule to try to meet IAQ requirements. The results show a reduction of 16% of energy for advanced buildings in the climate region considered (Zurich, Switzerland). The positive aspects include that work focussed on an advanced test building (should have limited room for improvements) and simplified the system to all linear and bilinear components while maintaining accuracy to the original TRNSYS model ($\pm 0.5^\circ\text{C}$). The simplifications are aimed at portability by limiting the amount of information needed by the model. Some negative aspects include that the controller is designed for a single zone and currently does not account for thermal effects from adjacent zones (assumes adiabatic walls), and there is no mention in changes of airflow or impact on the IAQ in the results presented.

Table 3.4 Building envelope variations [56]¹¹

Attribute	Value	Identifier	Remarks ^a
Façade orientation	North	N	Middle office
	South	S	Middle office
	South + East	SE	Corner office
	South + West	SW	Corner office
Construction type	Heavyweight	h	$c_{\text{dyn}} \approx 80 \text{ Wh/m}^2 \text{ K}^{\text{b}}$
	Lightweight	l	$c_{\text{dyn}} \approx 36 \text{ Wh/m}^2 \text{ K}$
Building standard	Swiss average	sa	$U_{\text{op}} \approx 0.6 \text{ W/m}^2 \text{ K}^{\text{c}}$
	Passive house	pa	$U_{\text{op}} \approx 0.1 \text{ W/m}^2 \text{ K}$
Window area fraction	Low	wl	30% window area per façade
	High	wh	80% -

^a Reference for c_{dyn} and U -values is the floor area.

^b c_{dyn} : internal dynamic heat capacity of the room.

^c U_{op} : overall heat transfer coefficient of opaque façade parts.

^d U_{win} : overall heat transfer coefficient of windows including frame.

$U_{\text{win}} = 2.8 \text{ W/m}^2 \text{ K}^{\text{d}}$
 $U_{\text{win}} = 0.7 \text{ W/m}^2 \text{ K}$

¹¹ Reprinted from Energy and Buildings, Vol 58, Lehmann, Gyalistras, Gwerder, Wirth, & Carl, Intermediate complexity model for Model Predictive Control of Integrated Room Automation, 250-262, Copyright 2013, with permission from Elsevier

Table 3.5 HVAC and other controllable systems, “x” indicates it is in use [56]¹²

Automated subsystems	Building system				
	S1	S2	S3	S4	S5
Blinds (<i>bPos</i>)	x	x	x	x	x
Electric lighting (<i>eLighting</i>)	x	x	x	x	x
Mechanical ventilation with heating, cooling and energy recovery (<i>nMev0</i> , <i>hPowMev</i> , <i>cPowMev</i> , <i>nMevE</i>)	-	x	x	x	x
Natural ventilation heating/cooling (night-time only) (<i>nNav</i>)	-	-	-	x	-
Cooling ceiling (capillary tube system) acting through cooling ceiling or TABS (<i>cPowSlab</i>)	x	x	-	-	-
Free cooling with wet cooling tower (<i>fcUsqFact</i>)	x	x	-	-	x
Radiator heating (<i>hPowRad</i>)	x	x	-	-	-
Floor heating (<i>hPowSlab</i>)	-	-	-	x	-
Thermally activated building systems (TABS) for heating/cooling (<i>hPowSlab</i>), (<i>cPowSlab</i>)	-	-	-	-	x

A second OptiControl project was undertaken by [68]. The model used in the work is a bilinear state space model that uses sequential linear programming at each timestep. The same five HVAC systems outlined in Table 3.5 are considered in the work. A differentiating feature from the work of [56] is the consideration of the forecast uncertainty, creating a stochastic problem. The system is programmed in Matlab, with an optimizer that implements a linear cost function to reduce non-renewable energy usage. An hourly timestep is used with a forecast period of six days. The work also computes what they term the performance bound, or the theoretical improvements that can be achieved with perfect weather knowledge. The sensors required for the system are the indoor air temperature, the outdoor dry-bulb and wet-bulb temperatures, zone luminance, and the incoming solar radiation. The system is constrained to maintain the temperature between 21 and 27 °C. Similar to [56], the controls are blind positions, windows, fresh air and heating/cooling rate. From their studies, a performance bound of 25% savings exist, while the stochastic controller achieves a minimum savings of 10%. All the simulations were validated against TRNSYS simulations to ensure the simplified model was not the source of performance

¹² Reprinted from Energy and Buildings, Vol 58, Lehmann, Gyalistras, Gwerder, Wirth, & Carl, Intermediate complexity model for Model Predictive Control of Integrated Room Automation, 250-262, Copyright 2013, with permission from Elsevier

improvements. The results vary from the work of [56] due to the inclusion of weather forecast error, as the choice of cost function varies to account for the forecast error.

In the work of [74], two case studies are examined for MPC with application to commercial buildings. For both cases, a high fidelity *E+* model is used of the building for predictions while being coupled with Matlab to perform the optimization. For both cases, a particle swarm optimization (PSO) technique is used. The PSO requires a set of seed values to be implemented to algorithm that migrate around and converge on the optimal solution by communicating with one another. Issues arise however when poor seeds are chosen, as the algorithm is not guaranteed to converge, and can be slow to converge. Due to the slow nature of *E+* simulations and potential for long run times with the PSO, the authors chose to have the algorithm run once per day with a seven day forecast and hourly timestep, and to generate the optimal setpoints throughout the day. For the first study case, the control variable adjusted was the setpoint room temperature, and it was limited to a band of 22-24 °C during occupied hours, and 16-32 °C when unoccupied. A variable electricity price scheme was employed for the system which consisted of a variable air volume (VAV) system with heating and cooling water coils. By using their MPC strategy, a savings of 5.3% in cost are achieved. As the system was only simulated, no discussion on the required sensor information was given, nor was any discussion given on the nature of the forecast used. It is expected that exact weather data would be known and that an existing weather file for *E+* is used for forecasting. The other limitation to the first case study is that only results for the cooling season were shown. In the second case study a 100% outdoor air system is employed that uses a low temperature radiant in floor heating and cooling system connected to a ground source heat pump with a bypass installed to allow for free cooling. The setpoint range for the system was a function of the outdoor air temperature, where if the outdoor air was cooler at 15°C, the setpoints were between 20-24°C, otherwise the setpoint range was between 23-26°C. The supply water temperature to the radiant system was limited to 16-28°C. The results of the MPC indicate a 54% energy savings, a vast improvement from the first case. The authors attribute this to the slower dynamics of the system, where predictive control is more impactful than in the faster dynamics of the first case. Similar to the first case, no discussion of sensors is given, and the forecast is assumed

to be perfect. While the results of these studies are done using validated software, the lack of discussion on practical implementation should be noted.

In the studies of [69], a summertime cooling system with real time electricity pricing is considered for using MPC. The model is developed using an *E+* input file and a linear regression statistical model to create a reduced order model from the *E+* base model. The OpenStudio platform (particularly the software development kit) is used to create the baseline model and testing using *E+*, as it has tools such as RunManager to execute several *E+* simulations automatically in an iterative nature. The system is modelled using ideal air loads, where it is assumed the electrical use scales with the cooling power needed in a linear fashion. For the simplified model, the parameters used are the temperature setpoint and occupancy, while all other disturbances are lumped into a single term. The authors note that the other disturbances such as ambient temperature and solar radiation can be separated if desired, but were lumped for simplicity. Optimization is done to minimize cost, while maintaining the system between 22-24°C when occupied, and 19-28°C when the space is unoccupied. A timestep of one hour is used, with a forecast horizon of eight hours. The only manipulated variable in the system is the temperature setpoint, and the MPC is shown to have 1-5% cost savings in the face of variable electricity pricing. The results are rather small, as the ideal air loads assume the HVAC can respond to any change necessary in a fast manner, which limits the effectiveness of predictive control, which has better performance for slower systems that can't react to all the changes in the system. While the results are independent of the HVAC system as presented, changing the HVAC system would change the system dynamics, and a new linear regression model would need to be developed. Also, the system is specific to cooling, but could be ported over to heating with fuel pricing information and a relationship between heating required and fuel consumption. Also, the authors assume that staying within the temperature range given satisfies thermal comfort.

3.3 Whole Building Studies

The work of [70] utilized a white box first order plus time delay model of an AHU system, and applied robust MPC approach for VAV AHUs. The system was simulated using MATLAB. One factor considered in the work that was neglected by many others was valve and system component wear, and the cost was computed by analyzing the changes in control input. While presented as a whole building study, the primary focus of the paper is on the optimization of the HVAC unit that does the conditioning of the building. Due to this focus, the impacts on thermal comfort are not explored, however they are assumed to be improved due to the improved response times of the HVAC system. Also, due to a much smaller time constant when only considering AHU dynamics, a simulation timestep of six seconds was used, with no mention of the forecast horizon.

The work of [19] is based on a five zone building model, with each zone modelled as a 3R2C model (see Figure 3.1) with an extended Kalman filter dynamic temperature model, developed by [84]. The model assumes the zones airpoint are well mixed and long range radiation is ignored. Static models for HVAC equipment were used to relate power consumption to the heating/cooling provided to the room. The HVAC system in the test building was a dual air duct system, with hot water from a boiler used for heating, and chilled water from an electric chiller is used for cooling. A variable air volume (VAV) fan is used with individual dampers for each zone to mix the hot and cold streams of air. The control strategy objective is to adjust the air stream temperatures (hot and cold) and to adjust the air delivery volume to zones to maintain a maximum of 900 ppm of carbon dioxide (CO₂), while maintaining zone temperatures. The work does not consider humidity at all. The information required for the model and optimizer is CO₂ readings, occupancy estimation, zone air temperature and relative humidity, and outdoor air temperature and relative humidity. The optimization is done only for operating cost, with a 15 minute timestep and three hour forecast horizon, and the cost function and constraints are nonlinear and solved using the interior-point nonlinear programming solver Ipopt¹³, which is

¹³ <https://projects.coin-or.org/Ipopt>

implemented in Matlab. A key constraint is that the tracking error from the reference signal must be within $\pm 1^\circ\text{F}$. Results show a reduction of 65% energy consumption and 25% in peak power demand. The values are derived from experimental testing during back to back periods, which are influenced by the weather. During the testing the weather was more favorable for the MPC case than baseline. Ideally the controller would have also been back simulated through software such as *E+* to further validate the results, and eliminate any bias introduced by weather variations. The energy reduction is significant, and that can be partially attributed to the inherent energy inefficiency in a dual air duct system, where streams of air are heated and cooled, and then mixed to generate the desired temperature in the end. The study was also only conducted during the heating season, and it would be beneficial to see performance during other periods, whether it be in the form of simulation or experimental testing.

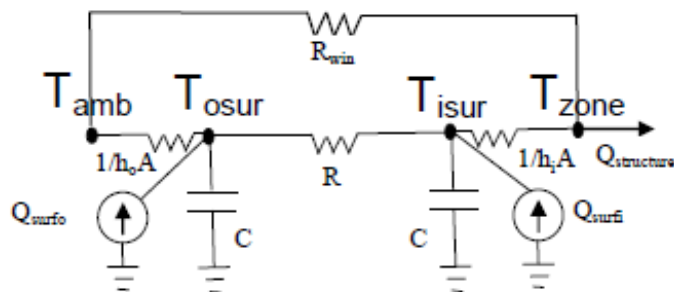


Figure 3.1 RC model diagram [84]

Researchers in [72] developed an advanced model predictive controller, but due to its extensive run time, derived a set of lookup tables to approximate the performance of the MPC based controller. For their work, they used an *E+* model of the target building and generalized linear models (GLM) to extract the set of rules to be used in the lookup table. The building considered was a mixed mode building, which has both natural and mechanical ventilation. The natural ventilation is controlled by automated windows while a VAV system is used to supplement the natural ventilation, or when it is inappropriate to use natural ventilation. Similar to [74], a PSO technique in Matlab is used to perform the optimization to reduce energy use with a strong penalty term to maintain thermal comfort. The optimization is run once per day, with 24 hour horizon and one hour timestep. The

control variable was the window position, and it was limited to being fully open or closed. The VAV system would then respond to ensure that all thermal comfort constraints are maintained. The GLM results compare favorably to the MPC results, where the GLM achieves approximately 70% of the MPC performance in the first study (9.3% reduction compared to 13% reduction). In the second study the MPC showed a 46% energy savings while the GML showed 43% savings, with the GLM capturing over 90% of the potential savings. By using a GLM strategy, the optimization can be done offline and the results uploaded and used in the real time environment. The results are also promising in that they work for both heating and cooling and account for all weather factors, not just temperature.

In a similar strain of work as [72], the work of [66] focuses on offline lookup table generation for MPC using existing building simulation tools. In his work, the author looks at three distinct cases and different tools to implement MPC with offline optimization. For the first case study, a physics based equation model is developed and implemented into Modelica¹⁴. It is assumed that ideal loads are used to condition the space (i.e. the HVAC system has no limitations), while the controller adjusts automated shades and the ventilation rate. The sensor information required is the ambient temperature, zone temperature, internal loads, and solar radiation as direct and diffuse components. The optimization is designed to minimize energy while maintaining comfort, and is performed using GenOpt¹⁵. The software SimCon¹⁶ is used to link GenOpt with Modelica. The MPC results are then discretized into a series of grid points based on the disturbances, creating a lookup table of values for the online controller to work with and interpolate between. The results of the study show that full MPC can generate 57% energy savings, while the lookup table approximation achieves 50% savings. It should be noted that a weak baseline

¹⁴ <https://www.modelica.org/>

¹⁵ <http://simulationresearch.lbl.gov/GO/>

¹⁶ <http://www.simconglobal.com/company.html>

controller was used for comparison, but that the lookup table still achieves 88% of the savings that MPC generates.

The second scenario considered by [66] was a radiant cooling slab system for a building. The restrictions were that the slab could only be charged overnight, and the controller was required to determine when to start charging and for what duration. For this case, the model was run using *E+*, while the optimization was again performed using GenOpt to minimize predicted percentage dissatisfied (PPD). The optimization is run for a 24 hour period using a 48 hour forecast, with no timestep information given. The system is dependent on the zone temperature, maximum ambient temperature, and the slab temperature. The results show that the lookup table captures 59% of the maximum savings. However, an issue occurs with the start up conditions of *E+* as they cannot be manually set. Instead, the program runs for a set number of days prior to starting the desired simulation to reach a convergence temperature. To overcome this, careful selection of warm up length is needed to ensure to convergence value for each new timestep matches the previous timestep result. Results of testing show only 1% discrepancy in PPD reduction from using the default horizon compared to a forced seven day horizon. Secondly the simplifications used in the weather forecasting method of determining the minimum and maximum values and fitting a diurnal curve can lead to errors as not all days follow the diurnal pattern. The focus of this study was on parameterization of the weather forecasting (finding the minimum, maximum and fitting the curve) and how it affects results, and shows that on MPC the effect is minimal as 94% of the PPD reduction is captured compared to using the true forecast.

The final case covered by [66] looks at problem decomposition of MPC, with a focus on reducing peak demand for a combined heat and power system. The idea behind problem decomposition is that the MPC can be broken down into a main high level problem that can be optimized offline, with a simpler, faster to execute problem to be run in real time. For the case study, the high level problem determines the peak electric power for the month, while the lower level problem determines when to run the plant and the best use of the heat generated by the system, as an absorption chiller is capable of turning waste heat into

cooling. A model for the system was developed using TRNSYS, with inputs of the heating demand, cooling demand, electricity demand, electric peak demand, electricity cost (fluctuates hourly, peak in summer), and fuel cost (no information on fluctuation). The minimization is first done to reduce the electric demand from the grid, along with an optimization to minimize total cost. The results of the study show that when installing a cogeneration system, the payback period is reduced by 5% with the implementation of MPC compared to traditional rule-based-control. The installation of a cogeneration plant would reduce annual energy costs by 11.6%.

Researchers in [17] developed a gray box based model for MPC and then implemented their controller on two test buildings in Australia. The gray box models developed were multiple input linear time invariant models based on assumed physical relationships, and then empirically correlated to measured data to derive the needed coefficients. The model is based on the ambient temperature, indoor temperature, occupancy loads (as a function of temperature), and HVAC power consumption. The optimization is done every five minutes with the forecast period being until the end of the current business day (hence a moving horizon), and the optimization is done using OptiCOOL¹⁷ software. The optimization seeks to minimize power consumption and costs while maintaining a PPD of less than 20%, and is of a quadratic form. The controller manipulates zone setpoints to maintain the constraints and reduce energy consumption. The results of experimental testing show a 19-32% energy use reduction, and the work considers an entire building layout, not just a single zone. The choice of prediction horizon is interesting, in that it leaves the system approximately 7 hours of warm up in the morning, and the weekend control is limited to the last setpoint of Friday evening.

The work of [71] implemented MPC for a VAV air system for a five zone building with only cooling, using Matlab connected with *E+* via the Building Controls Virtual Test Bed (BCVTB). An autoregressive exogenous model for use in Matlab was developed from the

¹⁷ <http://www.csiro.au/en/Organisation-Structure/Flagships/Energy-Flagship/Opticool.aspx>

results of the $E+$ model. The optimization horizon was daily with a shrinking window, while a 15 minute timestep was used. The constraint on the system was the range of temperature setpoints, which is also how thermal comfort was ensured (no other metrics were used). The results showed a 25% energy reduction with the implementation of their MPC strategy. The work considers multiple thermal zones and their interactions, however the work is limited to strictly cooling.

A second study with a focus on linking $E+$ and Matlab was conducted by [75]. A differentiating difference from [71] is the use of $MLE+$ as the connection software compared to BCVTB. A brute force method of optimization is used to test all possible scenarios and select the one with the greatest savings. The model uses a predicted mean vote (PMV) methodology to determine thermal comfort. No simplified model is used in the work. Instead, a special weather file is created which holds the weather constant for several timesteps to allow the brute force algorithm to find the optimal solution. However, the building conditions and states will change during this period, and it is not possible to reset $E+$ to the original states, leading to error. The forecast horizon for the MPC is 24 hours, with an hourly timestep, with a piecewise objective function to first meet thermal comfort, and then reduce energy consumption. The simulation results indicate a 20% energy savings, but these should be questioned based on the $E+$ simulation approach previously discussed. However, the approach is valid for multiple zone systems, and incorporates both heating and cooling.

Published in [76] is a study where a hybrid RC/artificial neural network (ANN) system modeled in Matlab is used to model the AHUs and uncertainties. The study uses a 10 minute timestep and one day ahead forecast horizon. The results are experimentally validated on an airport in Australia with a cost savings of 13% realized for the similar temperature conditions. However, no mention of solar radiation was given and may have been a contributing factor, as images of the airport show large windows.

In [77], a thermo-active building system is explored, with the system being modeled as a RC network. A two-zone building is simulated, with a similar setup used within an

environmental chamber as an experimental system. Simulation results show a decrease in pump runtime and improvements in thermal comfort, while using more energy. The experimental setup explored the ability for the algorithm to handle a change in internal loads, where when the loads were cut in half, the system still maintained a target setpoint temperature. While the results of the work are promising, they are limited to thermo-active building systems, and used a large number of sensors.

In [78], MPC was run on a swiss office building that utilized a combination of AHU and radiant infloor heating/cooling. The system was modelled as a bilinear physics based system modelled in MATLAB. Comfort was managed using the building air temperature, with season shifts (22-25 °C in winter, 22-27 °C in summer). The actuated variables were AHU air temperature and flow, as well as the infloor water temperature and flow. For the experimental portion, the comfort control was measured in kelvin hours of discomfort. Thermal loads were controlled via automated blinds, where measurements above 200 W/m² activated the blinds to close to prevent glare.

In [79], a non-linear physics based model using 16 states were developed using Modelica for use within MPC. The HVAC system consisted of AHUs to provide fresh air, and an infloor radiant heating/cooling system with a thermal storage tank. The MPC controlled the flow of water and supply temperature. Multiple modules are used to simplify the problem for computational feasibility by controlling the heat flux of the system, and concurrently the level of thermal storage. Thermal comfort is controlled by monitoring the air temperature and reported as total Kelvin-hours of discomfort.

The authors of [80] implemented a multi-input multi-output control of an AHU with the heating and cooling coils modelled as third order systems. The output variables were the temperature and humidity of the conditioned air, with the control variables being the flow through the coils. The objective was to track a reference temperature and humidity, with comparison to an industry standard PI controller. The MPC controller showed improved tracking performance with lower overshoot and a shorter settling time.

The work of [81] explores the development of a hygrothermal effects model of heat and moisture transfer within a building in Matlab. The model is a state-space model with a basis on a 3R2C network, and assumes 1-direction heat and moisture flow. The states of the model are wall and indoor air temperature and relative humidity, with the inputs split into uncontrolled components such as weather conditions (temperature, humidity, radiation, wind), and controlled components such as HVAC system power. A simulation based study is presented with a cost function related to the error of temperature and humidity from a reference value compared to the cost of running the HVAC system (measured as system power). The target buildings used were residential buildings, with an energy savings potential of 37% compared to the baseline of constant temperature. A second paper, [82], explores the experimental setup using an environmental chamber and quarter-scale models of the building and HVAC system. Experimental savings of 43% are realized for the controlled environment, however several environmental factors (solar, wind) were not present in the chamber, and only heating was considered. While the results show good agreement with the simulation work, the large savings can be partially attributed to a poor base case, as a rule based setback control achieved 38% of the savings from the constant temperature base case.

As has been shown by the previous studies analyzed, a large emphasis has been placed on finding accurate lower order models that can be used for real time control application. [85] developed an ANN model that accounts for thermal bridging between zones in a building. To build the model, first a physics based model was developed and had sensitivity analysis performed on it to determine the key input variables needed for the ANN. Once the inputs were identified, the model was built and trained using measured data from the building. Based on the sensitivity analysis, they only consider temperature as an input (both ambient and zone) and do not consider the effects of humidity and solar radiation. While currently many RC models exist and are common reduction method used, ANN models can provide better results as long as sufficient training data is available for the ANN. The authors also considered multi-zone buildings and the effects of thermal coupling, and show that prediction accuracy increased by up to 1°C when using neighboring zone temperature, with most improvement when the change in temperature is highest.

3.4 Analysis and Discussion

In short, of the papers reviewed, 9 of them focused on the control of a single component or subsystem. These component studies were split evenly between heating and cooling applications. Some examples include:

- Air conditioners [63], [67], [65]
- Cooling plants [9]
- Heating system or cooling system only [62], [58], [18], [71]

Four studies analysed single zone systems, with two of the works derived from OptiControl. A key factor in zone level studies is that more than one piece of equipment is operating to maintain thermal comfort, and the MPC takes a coordinated approach. An example is automated window coverings combined with HVAC [68] [56], or natural ventilation in conjunction with mechanical ventilation [66]. The whole zone approach is a step up from single components as there are often multiple systems to control, and typically more information is required such as occupancy periods, solar gains, and other disturbances not pertinent to single component control.

The final category of MPC research in buildings is the optimization of entire buildings, which are covered by the remaining 16 studies. Multizonal optimization for systems with both heating and cooling represents the most advanced systems and challenging control scenario in buildings. Such scope is advantageous because inter-zonal transfers of energy may be predicted. While they may not impact overall building energy use, they can be used to impact estimate the thermal losses and impact on comfort due to varying boundary conditions. The additional challenges that arise are the increased size of the solution space (more equipment and/or zones to control), along with the interactions between zones (shared thermal boundaries). These challenges require more advanced models to capture the thermal coupling and more advanced methods to deal with the expanded search space.

While the number of studies is an insufficient number to conduct a thorough statistical investigation and draw confident conclusions, it does permit a trends analysis. These

resultant trends inform as to the direction that MPC research is headed, and what deficiencies may exist that need to be addressed.

While a detailed description of the reviewed research has been presented in tables, it is important to analyse the methodologies for trends and reasoning as to why certain decisions or selections were made by researchers. From Table 3.1, the first noticeable trend of the research reviewed is the use of simplified models to represent the thermal dynamics of the building, whether it be RC models, linearized state space models, or black/gray box models. The main factor driving this decision is the computational time required for advanced simulation models such as *E+* being prohibitively long, where the simulation of the range of control setpoints over the forecast horizon could potentially exceed the desired timestep resolution (10 or 15 minutes). While *E+* can do a yearlong simulation for a single control strategy in approximately 15 minutes for a single control strategy, a MPC approach attempts many possible control strategies per timestep and would require *E+* to reinitialize repeated, causing a large amount of runtime. A second factor for the use of reduced order models is the lesser amount of information needed to run the model. Advanced platforms such as *E+* require great details about the building and how the HVAC system works, where an RC model requires only thermal resistivity, capacitances, and heat fluxes. The method of model reduction is dependent on measured data available to the modeller from the building. The more measured data that is available, the more likely that a gray or black box model was employed to generate a model to match the physics of the space. It is critical an accurate predictions model is used to ensure proper control decisions are made [86] [87] [88] [89] [90].

Table 3.1 also give the simulation software tool, and this has been shown proportionally by type in Figure 3.2. Matlab is the principal software for executing models (36%), and *E+* is the most commonly used advanced simulation engine. Matlab is a common choice as it has in-built toolboxes for tasks such as system identification and optimization. *E+* is a freely-available high-resolution advanced building simulation engine. It is considered the industry standard and has been extensively validated. It should be noted that Figure 3.2 is an aggregate of the entire software count, not on a per study basis.

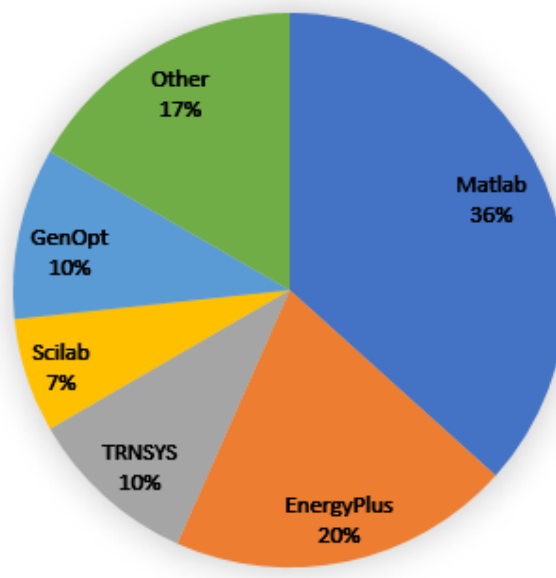


Figure 3.2 Simulation software distribution

In terms of optimization, Table 3.1 shows most of the reviewed papers used linear or quadratic optimization techniques, due to their simplicity and ability to guarantee to find the global minimum. Some studies used other methods such as particle swarms [74] [72] or other nonlinear methods [19]. All of the reviewed papers show only a single controller on the system, but some of the research was done by groups using the same test building and show different results [58] [18]. This highlights the fact that the MPC optimization method will influence results. Figure 3.3 illustrates the proportions of optimization technique use. Linear and quadratic optimization constitute over two-thirds of the optimizers reviewed. Non-linear and particle swarm solving techniques are advantageous in that they allow for unique cost function structures, as they do not require derivatives and/or continuity. The tradeoff to using these techniques is that they can be slow, computationally expensive, and may not find the optimal solution if the problem is too complex ([41], [42]). Because of this, it appears to date that they are of less interest.

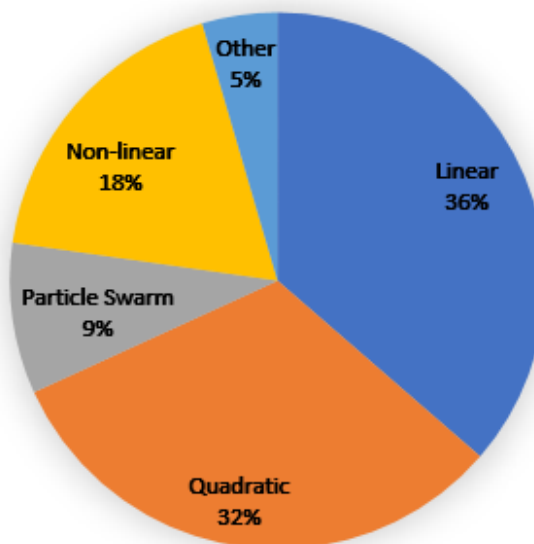


Figure 3.3 Distribution of reviewed MPC optimization techniques

Table 3.2 notes the variety of forecast horizons that are used, and these range widely from three hours or less to seven days. Most authors offer only limited justification for their selection, although it is assumed that the selected value is based on the building system time constant, fundamental weather periods (forecast horizon and diurnal weather trends), or to ensure optimization can be completed in the objective function timestep. Figure 3.4 illustrates selections of horizon sorted by MPC scope; this differentiation in scope was given because time constants of components, zones, and buildings differ. It shows that a 24 hour horizon is most widely used among the studies reviewed, which appears in building frequency responses due to it matching the diurnal temperature cycle. Also frequently used is a 12 hour forecast horizon, presumably to key on the alternating occupancy of a building from occupied (daytime) to unoccupied (night time). Longer forecast horizons may have been chosen to match other disturbance loads such workday/weekend (168 hours equals seven days), or based on using the maximum amount of information possible from forecasts (weather forecasts are typically one week ahead [91] [92]. Table 3.2 also gives simulation timestep, and the proportions of these are shown in Figure 3.5, again separated by MPC scope. Sixty minutes appears to be extensively used and is likely because climate data and forecasting is typically given on an one hour basis. A 60 minute period is

considerably longer than the time constant of conventional HVAC equipment, and is also longer than the minimum cycling time. As a consequence a control strategy using such a timestep for component level simulations is disadvantaged. This may be the reason that many component level MPCs use shorter timestep periods, while zones and buildings do use a 60 minute timestep. Shorter timesteps range from five to 25 minutes. These shorter values can be attributed to either the computational time to solve the MPC problem or to the minimum cycling time of the equipment being controlled. The ideal timestep is expected to be a function of the speed of the MPC execution, and the nature of the equipment being controlled.

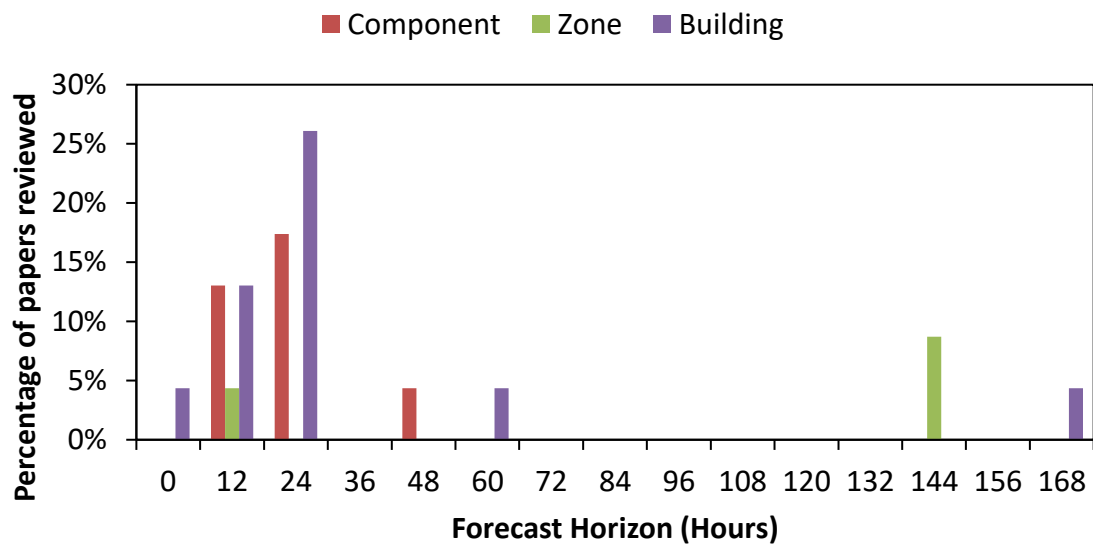


Figure 3.4 Distribution of MPC forecast horizon

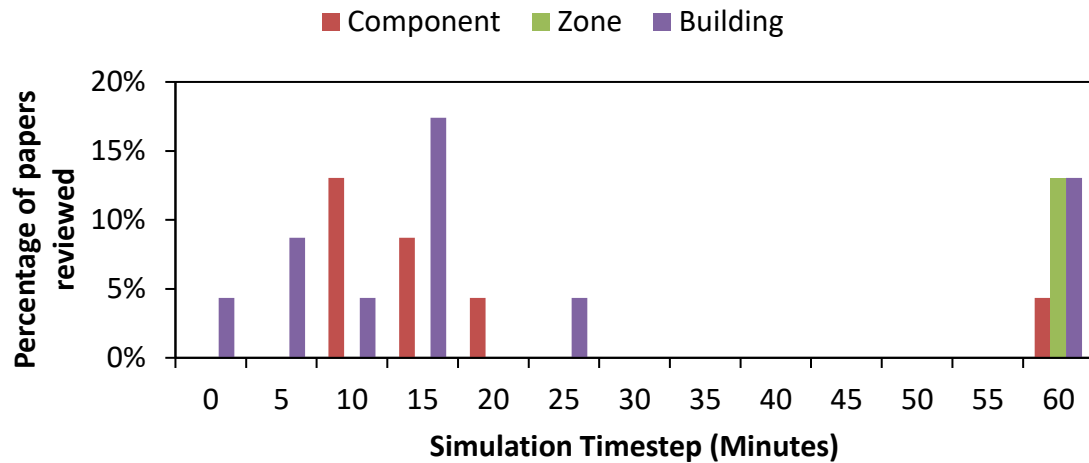


Figure 3.5 Distribution of MPC simulation timestep

Forecast accuracy for items such as climate and occupancy was examined as it may help drive the choice of timestep and horizon. Only the works of [68] and [66] explicitly consider the effects of climate forecast error, where they conclude the results can vary by upwards of 50% for energy consumption, but still use less energy than traditional rule-based-control. More work in this area is needed as most researchers use forecasts from sites such as NOAA (<http://www.noaa.gov/>) without considerations for its error, thus assuming a perfect forecast.

Table 3.3 outlines strengths and potential weaknesses of each study reviewed. Energy savings range from a minimum of 5% to a maximum of 75%. The minimum savings case in [69] is for a building with little thermal mass and idealized air loads which means the HVAC system is sufficiently sized to match any load required. Due to the quick response of such a system and assumed 100% efficiency, little room for improvement exists. In contrast, 65% energy savings were achieved using a dual air duct system [19]. These systems are inherently inefficient, as one stream of air is heated while a second stream is cooled, and then subsequently mixed at each zone to provide the desired temperature. The savings were gained by lowering the hot air stream temperature and increasing the low air stream temperature to match the maximum and minimum desired zone temperatures. This contrasts to the static air temperatures previously employed that would significantly

overheat and overcool the air streams. A second study on a cooling system using a cooling tower and water storage tank [9] show significant cost savings (75%) by choosing to charge the tank during colder periods, such as overnight when the system efficiency is higher due to colder ambient temperatures.

Modelling and simulation attempt to estimate and represent the performance of a building that might be reasonable expected to occur in reality. Confidence in building performance simulation continues to increase as additional experience is gained, however, modelling of new technologies still requires experimental verification. Table 3.3 notes in boldface if the results were experimentally verified. There is no distinction in energy savings between experiments or simulation verified models, so a broad range of performance results have indeed been verified. Ideally all the studies should have experimental verification, and a greater emphasis should be placed on the results containing experimental verification.

While most researchers used an objective function aimed at minimizing energy use or cost, a constraint of occupant thermal comfort conditions was imposed. The way that various researchers approached thermal comfort varied immensely, with some authors putting a hard constraint on the air temperature band, while others only looked at error from the reference or desired setpoint, and others using comfort parameters such as PPD and PMV to determine comfort. In the study by [17], complaints to the building operator of discomfort were monitored and used as a measure to see if any changes in thermal comfort occurred when switching from the original control to MPC. It is impractical to consider occupancy comfort a hard constraint for most buildings as it is not directly measurable (only air temperature is typically measured and is only part of comfort), so weighted penalty based PPD and PMV methods likely represent the most appropriate for informing MPC.

3.5 Building Parameters for Model Predictive Control

Based on the results of the reviewed papers, characteristics which are desirable for buildings utilizing MPC are as follows:

- Heavy walls and floors
- Thermal storage (both passive and active)
- Large predictable loads (solar, occupancy, weather)
- Broad thermal comfort/indoor air quality range
- Slow HVAC systems
- Low infiltration
- High insulation

These characteristics benefit MPC because they provide a building which has both thermal inertia and an internal environment which can be precisely controlled over a range of operating conditions. Heavy walls and floors substantially increased the thermal mass of the building and are used to store energy provided by sunlight and the HVAC system [93]. This allows for load shifting and peak demand mitigation. MPC can thus alter control strategies and take advantage of forecast information, or take advantage of time-of-day energy prices. The same characteristics and theory for heavy walls and floors applies to both active and passive thermal storage systems.

Large predictable loads are valuable to MPC as the controller can take advantage of these to aid in providing the heating necessary to a space, or to counteract their effects. An example of this would be if there is a forecast for high solar radiation on a building to not heat all the way to the initial setpoint, but close to it and let the solar radiation finalize the heating process. This reduces the heating energy, but also prevents the need for cooling

that would arise if the space was already fully heated to an upper temperature and then exposed to the radiation.

The idea of a broader thermal comfort or indoor air quality [94] range also allows for more potentially viable solutions to the MPC problem, which can lead to higher savings than in cases of strict environmental conditions. An example of a broad setpoint building would be an office building, in which the goal is to prevent thermal discomfort. In contrast, a hospital has strict thermal comfort and indoor air quality requirements in order to treat patients and prevent the spread of disease.

Fast acting HVAC systems (e.g. electric baseboards) can quickly respond to a wide range of operational or climatic disturbances applied to the system. While MPC may still improve performance by exploiting the building thermal characteristics, a fast acting HVAC system does not present a good MPC opportunity due to the limited potential for savings. In contrast, smaller and slower response HVAC systems (e.g. in-floor radiant heat) are beneficial with MPC because it can make use of forecast information to insure the space is adequately conditioned at respective points in time. MPC prevents overheating and overcooling that rudimentary control algorithms experience with slower response systems.

Low infiltration and high insulation levels help minimize the impact of outdoor conditions on the interior space [95], allowing for an environment that is easier to control. While infiltration loads can be linked with wind speeds, they are difficult to model and measure. They can be considered as negative disturbances to be minimized. Similarly for insulation levels, higher values prevents energy losses/gains through the envelope which are also negative disturbances that should be minimized.

After analysing the results of the previous studies, it was determined that while consensus has been reached on the general characteristics of a building suitable for MPC, the terms are often “soft” and non-numeric. An example would be a “tight, heavy” building. Thus, a method of categorizing building characteristics numerically is important. Table 3.6 outlines building thermal envelope characteristics and categorizes these based upon numeric ranges. These numeric values are representative of North American commercial and institutional

building types and climates. Values will differ for other locations and building types of the world. External walls are categorized as either heavy or light based on their thermal capacitance in accordance with ASHRAE Standard 90.1-2004. The infiltration rate is categorized by air changes per hour (ACH) at 75 Pa, based on studies by [96], [97], [98], and [99]. The other parameters for Table 3.6 are derived from the US Department of Energy commercial reference buildings [100]. The characteristics for each building was analysed, with binning for the different levels of parameters based on range of values encountered. In Table 3.6, labels of “tight” and “high” are most suitable for MPC.

Table 3.6 Building envelope characteristics

<i>External wall type</i>		<i>Infiltration (L/s/m² @ 75 Pa)</i>			<i>External wall insulation levels (m²K/W)</i>			<i>Windows (m²K/W)</i>			<i>Solar radiation (window to wall ratio)</i>		
Value	Category	Min	Max	Label	Min	Max	Label	Min	Max	Label	Min	Max	Label
> 102 kJ/m ² ·°C	Heavy	0	1	Tight	0	1	Low	0	0.33	Low	0	0.1	Low
< 102 kJ/m ² ·°C	Light	1	2	Avg.	1	2	Avg.	0.33	0.38	Avg.	0.1	0.2	Avg.
		2		Loose	2		High	0.38		High	0.2		High

The internal loads and systems in a building also affect MPC and these are presented in Table 3.7. The values were again derived by analysing the commercial reference buildings developed by the US Department of Energy. Large predictable fluctuations in the internal loads are desirable for MPC as the controller can allow them to meet the HVAC loads. As load fluctuations are beneficial, buildings that experience variable occupancy are a better candidate than buildings that are always occupied. An example of a building with variable occupancy would be an office, which experiences high loads during business hours, and no loads overnight. Meanwhile, a constantly occupied building such as hospital or manufacturing facility would experience fewer fluctuations. As the commercial reference database does not provide specific information about HVAC system response, further literature by [101] and [102] was examined to considered typical HVAC component response times, combined with experience to determine the categorization for HVAC

systems. In Table 3.7, labels of “high” and “slow” are most suitable for MPC. The HVAC time constant refers to the time it takes to achieve 67% of a step change.

Table 3.7 Desirable traits for MPC

<i>Lights (W/m²)</i>			<i>Electric equipment (W/m²)</i>			<i>People (m²/per)</i>			<i>HVAC Time Constant (min)</i>		
Min	Max	Label	Min	Max	Label	Min	Max	Label	Min	Max	Label
	10	Low		10	Low		10	High		15	Fast
10	20	Avg.	11	20	Avg.	10	20	Avg.	15	90	Avg.
20		High	20		High	20		Low	90		Slow

3.6 Conclusions from the Literature

Based on the results of the literature review several conclusions and recommendations can be drawn. The first is that the field of applying MPC to buildings is growing, with a greater emphasis being placed on experimental validation. Experimental validation is challenging in that along with developing a control algorithm, practical issues such as connecting to a building automation system exist, and often require software/coding expertise. A second trend is that many solutions are building specific, in that they optimize the HVAC system within the building. While providing energy savings, further savings could be achieved by also optimizing the space temperature within a building, as this is what creates the demand for energy.

As shown and noted in other research, there is appears to be no single best choice for parameters for within MPC. Examples include the wide variety of modeling techniques and tools used, the various forms of objective functions employed, the solution technique of the objective function, and the MPC parameters of timestep and forecast horizon. It is expected that the objective function is tailored to the desired goal of MPC (i.e. energy reduction, cost savings), where factors such as energy pricing structure or carbon intensity can dictate terms included in the objective function. For example, a cost based MPC would include an electricity demand charge (used in most jurisdictions), where as an energy based minimization would not include such a term.

Other parameters that are influenced by the MPC goal are the MPC system timestep and forecast horizon. The ideal scenario is the usage of the smallest timestep possible with the longest forecast horizon, but computational demand and forecast constraints place limits on these parameters. An example of objective function imposing limits are the potential need to forecast for the entire billing period for when doing demand charge mitigation, as only the peak power draw in the billing period is considered. This also imposes a minimum timestep, as hourly timesteps would be insufficient to capture a 15 minute demand peak event. Other factors such as the building and HVAC system time constants should be considered when choosing the MPC timestep and horizon, as to ensure those effects are

adequately captured (i.e. if your building has a one hour time constant, the forecast horizon should exceed it).

Several design choices can be made based on the results of the literature review. The first is that an efficient method to solve the MPC problem is needed, as it appears computational time is a constraint on the system. Ideally an efficient whole building problem is solved, with an additional layer to translate results to the zone level. A second guiding factor is the choice of a 15 minute timestep, as it is in line with research norms for whole building studies, and can be used to capture demand charge effects. The time horizon should be chosen based off the building dynamics, objective function goals, and forecast reliability.

Chapter 4 BUILDING ENERGY MODEL

As part of the advanced MPC work explored in this dissertation, a building energy model was required. The model serves the purpose of a virtual building during simulation testing, in that it acts and behaves similar to how a real building would during experimental testing. Thus, it is used only to provide sensor feedback information to the prediction model to make MPC decisions. The detailed energy model is also used as a source of data to train a simplified prediction model for MPC, as limited measured timestep data was available. The Mona Campbell Building at Dalhousie University Studley Campus in Halifax, NS, Canada is used for all subsequent work and validation, as it provides a benchmark of performance with both energy and demand data. Access was granted to both the building automation system (BAS) and system operator to provide their insights and experiences with the building and allowance for control of the building for experiments. The BAS contains a great deal of information, and provided additional information than what is typically available, providing extra information on system behavior not available with other buildings.

For the development of the detailed energy model, the building performance and simulation package EnergyPlus ($E+$) was chosen. It is a software package designed specifically for building energy and physics analysis, and has been used extensively in industry and academia. $E+$ models the heat transfers modes as described in section 2.2 using an analytical solution for heat balance, TARP for inside surface convection, DOE-2 for outside surface convection, and conduction transfer functions. Detailed models for HVAC equipment components such as heat pumps, boilers, fans, coils are employed. Control and loads are defined using schedules that define equipment run time, operational setpoints, occupancy, equipment, and lights.

While $E+$ is an accurate and validated building performance simulation software, it has some limitations that inhibits its ability for use with MPC in its native form. For reference, MPC relies on the use of a model and forecasts of internal and external conditions (e.g. climate) to determine the optimal control strategy to minimize the cost of a desired

objective function. For real-time applications, this requires iteration and a model that can be executed in a short manner, and for a variety of initial conditions. The limitations for $E+$ are:

- It does not allow for user specified initial conditions [103] - Instead, $E+$ takes the user specified setpoints and runs a number of warm-up days (minimum of five typically) to allow for the system to converge to the correct value. This limits the ability to use exact conditions from one timestep to the next when performing iterative solutions.
- Runtime of $E+$ is relatively long in comparison to simpler models – Due to the complex and physics based nature of $E+$, it has drastically increased runtime from simpler models (seconds compared to milliseconds), which would limit the number of options that could be calculated within a timestep for a real-time application.
- Limitations on control logic within $E+$ [103] – Due to the inability to set initial conditions or “rewind” simulation timesteps, control logic that only is executed for the current timestep can be supported by the in-built Energy Management System.

While $E+$ cannot be used directly as the prediction model for MPC, it can be used to generate data to train a prediction model to supplement the existing measured data (if there is any at a fine enough resolution) and can be used to test the outcome of an MPC decision.

4.1 Introduction

The Mona Campbell Building, shown in Figure 4.1, is a large education building owned and operated by Dalhousie University in Halifax, NS, Canada. It is LEED¹⁸ Gold certified and operates year round. The building consists of four occupied floors, as well as a basement and penthouse for mechanical systems. It has an approximate 2,000 m² footprint, for a total of 10,000 m² of floor area. The main floors provide space for classrooms, open space, atriums, offices, and a cafeteria. The Mona Campbell building is serviced by hot water from Howe Hall (located across the street) that is produced from steam (with condensate return) from Dalhousie Central Services via Facilities Management. Electricity service is provided by Nova Scotia Power (NSP) on a dedicated pad mount transformer.

Building designs and specifications were obtained from site surveys, detailed engineering design documents, and discussion with Glen MacDougall (embedded Efficiency Nova Scotia representative for Dalhousie). A three-dimensional model of the building was created using drafting program Google SketchUp. This was then imported using OpenStudio to the building energy performance simulator package *E+* (version 8.2).

The thermal envelope characteristics are derived from the building drawings, the HVAC system has been simplified to a two AHU system: one with heat pump reheat, and one with hot water (HW) coil reheat. Major assumptions of the model include occupancy, hot water loop system losses, building infiltration, building insulation, and domestic hot water (DHW) usage.

¹⁸ www.cagbc.org/leed



Figure 4.1 Mona Campbell Building

4.2 Thermal Envelope and Zones

The model was developed in several stages, starting with defining the building envelope. The physical building envelope was modelled using Google SketchUp, with dimensions provided from the Mona Campbell Building drawings as shown in Figure 4.2 and Figure 4.3.

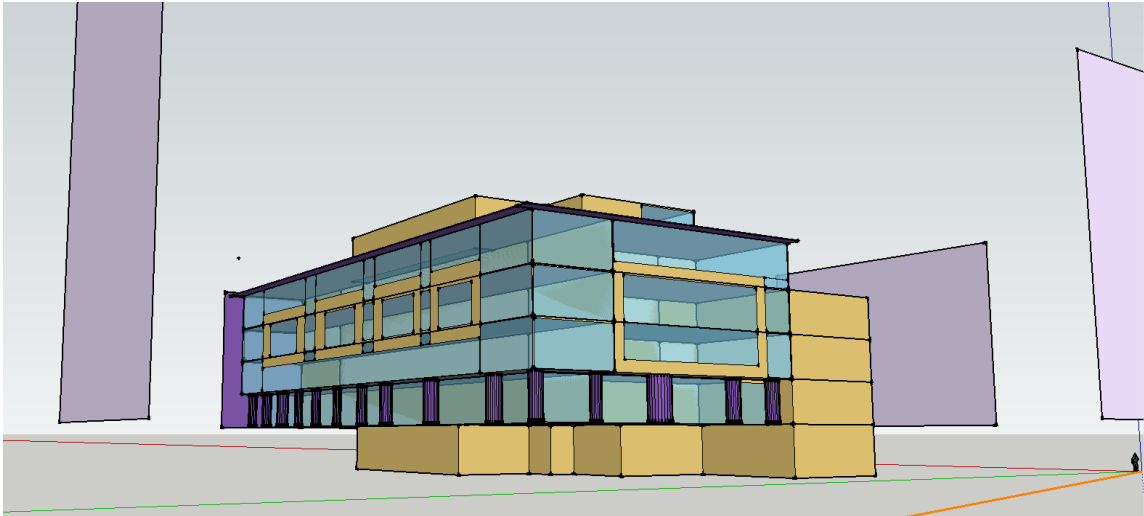


Figure 4.2 Mona Campbell Building – 3D rendering with shading surfaces

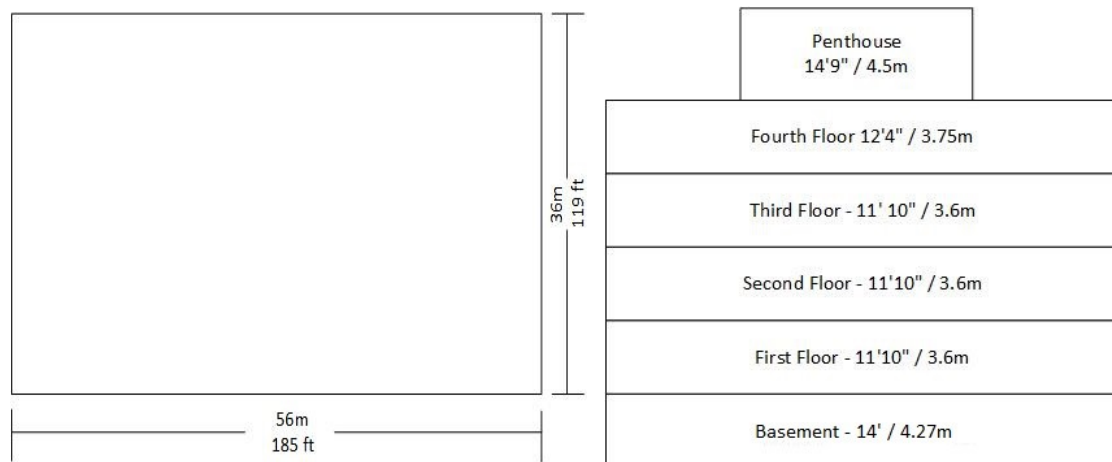


Figure 4.3 External building dimensions (left – footprint; right – floor levels)

Each of the six floors is subdivided into thermal zones, as shown in Figure 4.4. Actual spaces were amalgamating into thermal zones on the basis of location in the building, AHU service, and end use. Each zone is numbered as XY, where X is the floor number, and Y is the direction the primary exterior walls face, C is used for the core zone, and A for where the atrium resides (e.g. 2E would represent the exterior zone on the second floor where the primary wall faces east). The only zone on the 5th floor is a penthouse for HVAC equipment and it is labelled as Penthouse. It should be noted that most HVAC equipment resides in either the penthouse or basement, but that some components may be found on other floors (such as heat pumps).

After defining the physical dimensions using SketchUp, the program OpenStudio was used to set the various constructions of the building. The provided design drawing suite was used to create constructions for the interior and exterior building elements, with the properties outlined in Table 4.1.

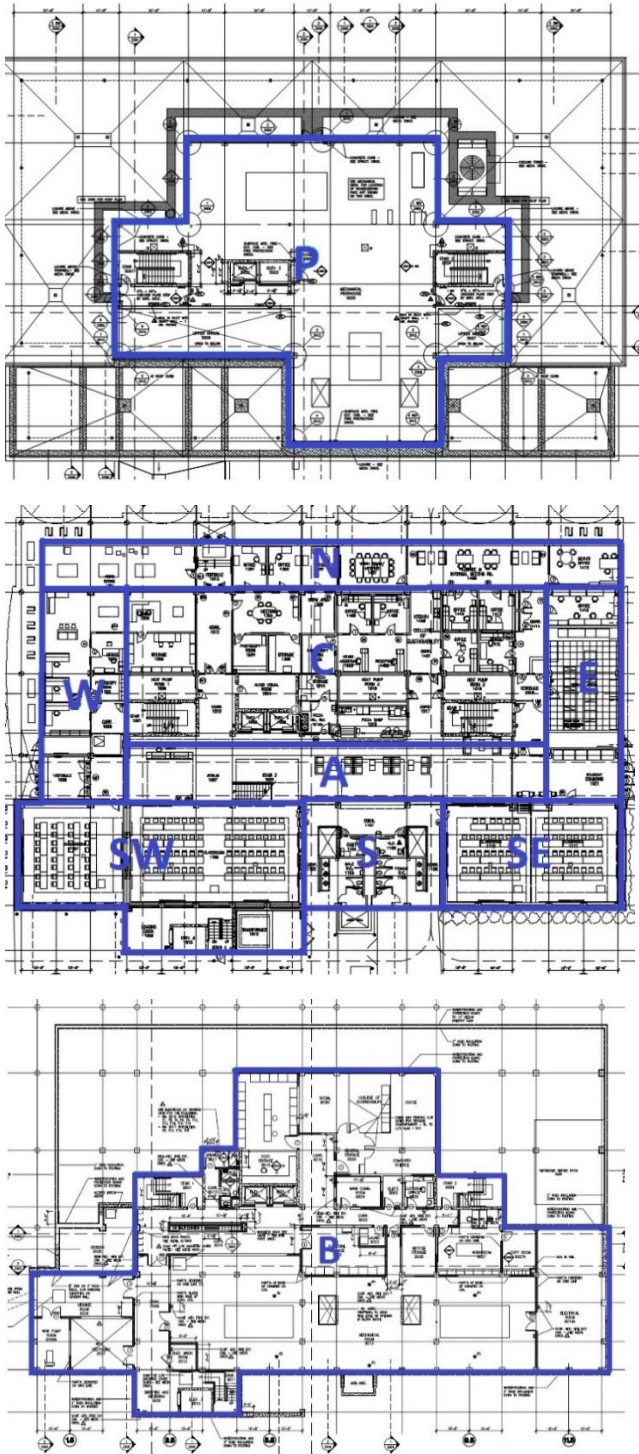


Figure 4.4 Floor subdivision into thermal zones (bottom: basement; middle: occupied space; top: penthouse)

Table 4.1 Exterior surfaces and layer properties

Surface	Layer	Thickness (mm)	Thm. Conductivity (Wm-1K-1)	Emissivity (-)
Foundation Wall	Insulation	50.8	0.03	
	Concrete	203.3	1.73	
Foundation Floor	Concrete	152.4	1.73	
Exterior Walls	Simulated Stone	88.9	0.04	
	Vapour barrier and air	N/A	6.66 (Wm-2K-1)	
	Spray Foam	88.9	0.032	
	Insulated Steel Frame	152.4	0.1	
	Gypsum board	15.9	0.16	
Exterior Windows	Outer glass	6	0.9	0.84
	Argon gap	13	0.016	
	Low-E inner glass	6	0.9	0.2
Exterior Door	Outer glass	6	0.9	0.84
	Argon gap	13	0.016	
	Low-E inner glass	6	0.9	0.2
Roof	Membrane	9.5	0.16	
	Insulation	100	0.033	
	Concrete	279.4	1.73	
Interior Walls	Gypsum board	15.9	0.16	
	Insulated Steel Frame	152.4	0.1	
	Gypsum board	15.9	0.16	
Interior Ceiling/Floor	Concrete	279.4	0.53	
	Air	N/A	5.55 (Wm-2K-1)	
	Acoustic tile	19	0.06	

4.3 HVAC System

The HVAC system for the Mona Campbell Building consists of four main components:

- Common heat pump (HP) water loop which links the heat pumps servicing the AHU and zone level heat pumps to the hot water loop and cooling tower.
- Hot water loop which provides heat to the common HP loop, DHW, VAV reheat coils, and radiant heating panels. The hot water loop is heated from a steam converter located in Howe Hall.
- Main air loop which provides supply and return air to the zones. The system consists of three AHUs with AHU 1 and 2 servicing classrooms and study areas while AHU 3 services offices. The system includes fresh air and a return air mixing box. There are water to air heat pumps (WAHP) integral to the AHUs to condition incoming air.
- Zone level WAHP which transfer heat between the main water loop and the zone air.

Figure 4.5 shows how the systems are interconnected. The hot water loop is used as the heating source for the common HP loop, DHW, VAV reheat terminals and the radiant heating panels. The common HP loop feeds the zone level heat pumps and the AHU heat pumps which are connected to the air stream. The main air loop heats/cool the incoming fresh air to the building before it is delivered to the various zones. There are three AHUs in the system, with AHUs 1 and 2 servicing the classrooms and common areas, while AHU 3 services the offices. Only the offices are equipped with heat pumps, while all other areas use the VAV reheat and radiant heating panels for temperature regulation. Cooling is provided by the use of 16 °C AHU air delivery. The zone level heat pumps, VAV reheat coils and radiant heating panels provide the final conditioning to the zones, and will work to make up any deficits in heating/cooling from the main air loop.

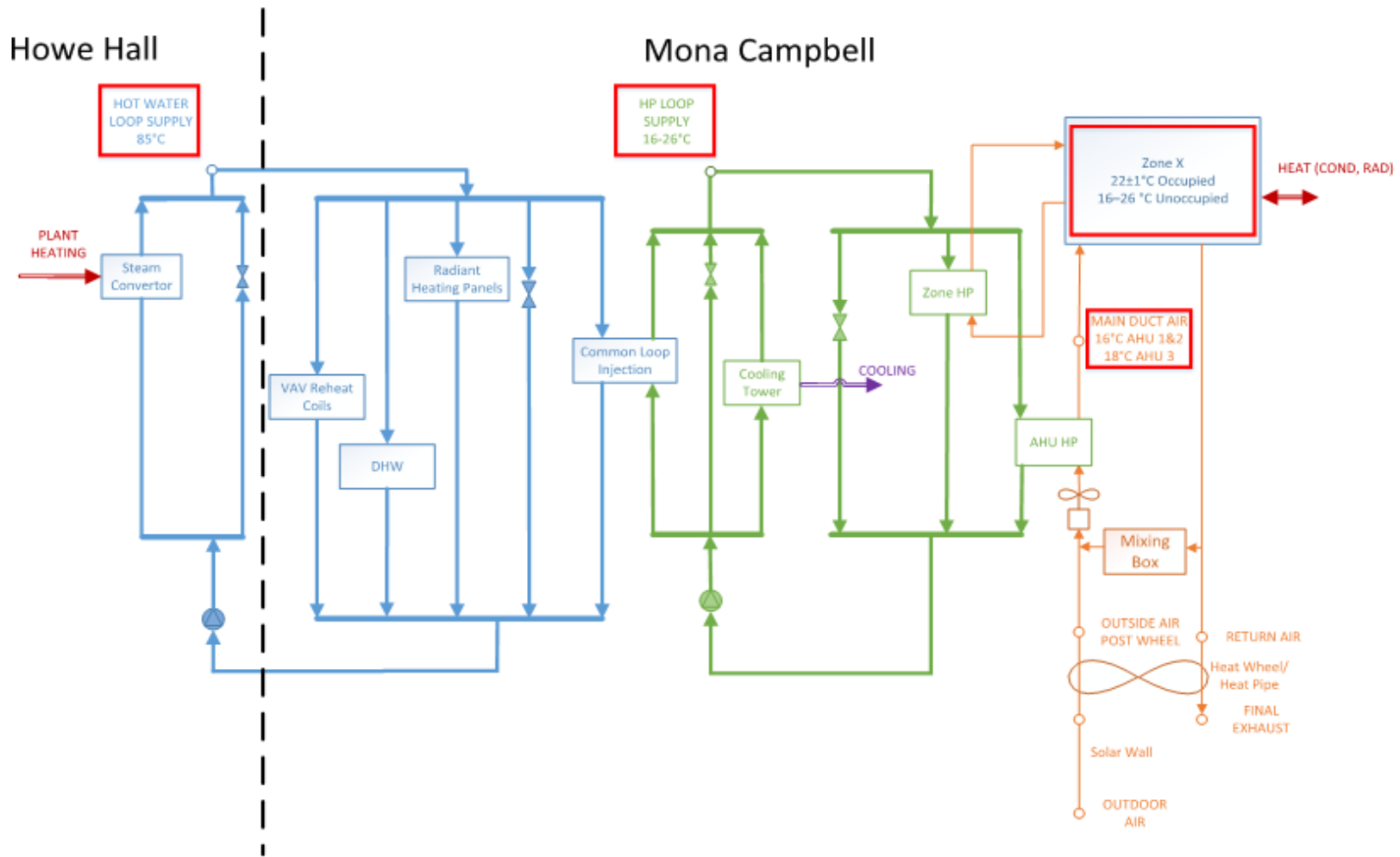


Figure 4.5 Combined HVAC system diagram as installed

The hot water loop is used for 3 purposes: space heating via reheat coils in VAV boxes and radiant heating panels, heating of DHW, and as a heat source for the common HP loop. The radiant heating panels are not modelled, as their effects can be incorporated into the VAV reheat coils due to the small load of the panels. Pipe heat losses to the building and the ground in the transport from Howe Hall heat exchangers (used solely for the Mona Campbell building) are modelled using a nominal six inch pipe diameter with one inch of insulation of a length of 150 m. A diagram of the system as modelled is in Figure 4.6, with system parameters outlined in Table 4.2.

Table 4.2 Hot water loop parameters

Sensor Location	Setpoint Temperature	Peak Flow Rate (l/s)
HOT WATER LOOP SUPPLY	85 °C	7.57

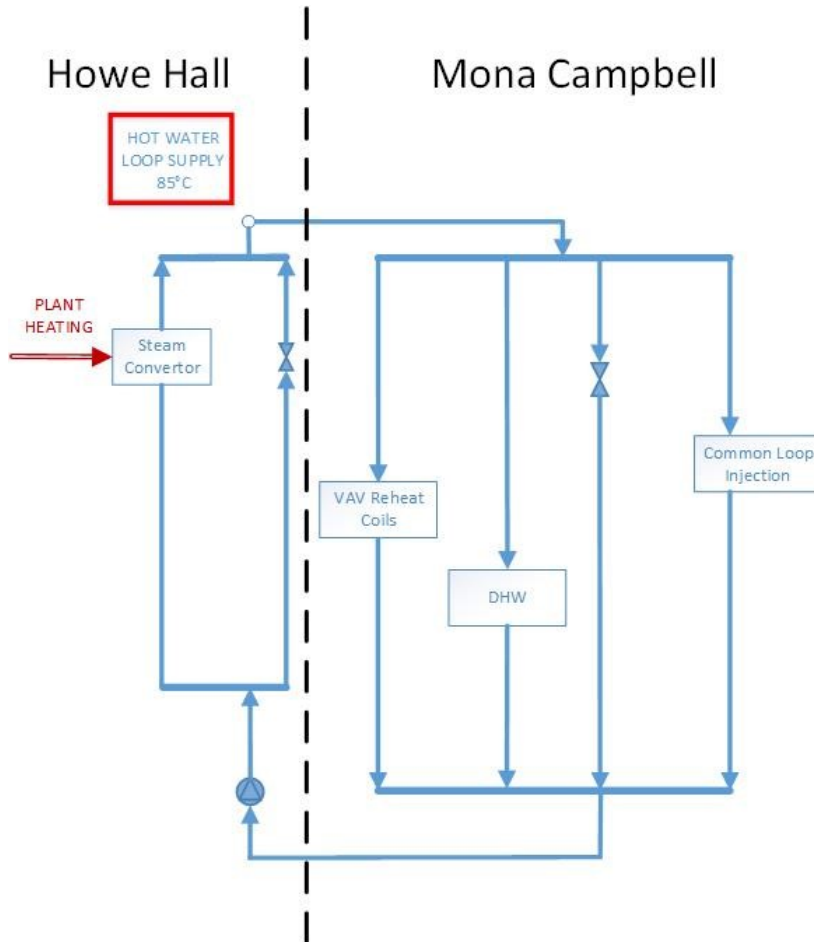


Figure 4.6 Hot water (HW) loop as modelled

The common HP loop is used to connect the hot water loop and cooling tower to the WAHPs in both the zones and AHUs. It is important to keep a stable loop temperature to provide ideal operating conditions for the heat pumps and minimize electricity consumption. In order to maintain a stable temperature, direct injection from the hot water loop is used to provide heat to the loop, while a cooling tower is used to dissipate heat from the loop. The layout of the loop and what items run in parallel are in Figure 4.7. The hot water injection is modelled as a heat exchanger (working fluid of water on both sides) with a large surface area to mimic the effects of direct hot water injection.

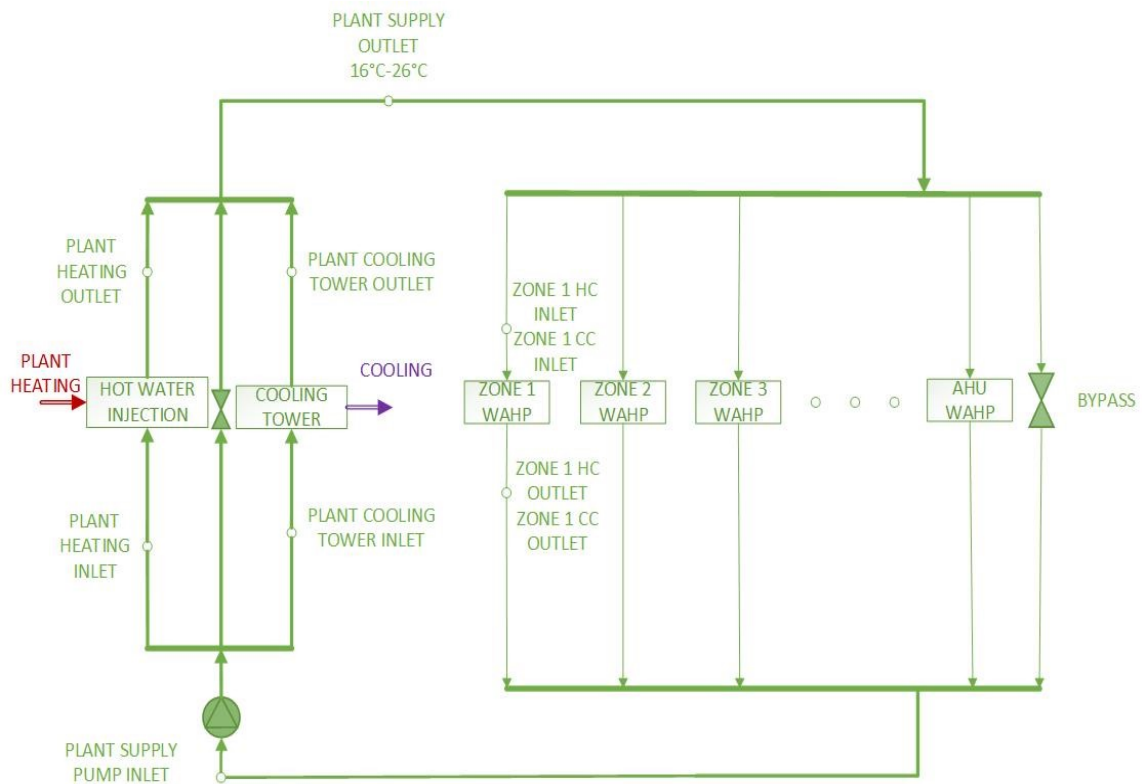


Figure 4.7 Common heat pump (HP) Loop

A temperature sensor is located at the common HP loop supply to monitor the temperature of the loop and determine if heating or cooling is required. Table 4.3 outlines the heating and cooling setpoints for the system. Table 4.4 outlines the actuators available to the loop and their effects. The loop is powered by a main circulating pumps that flows water at a variable speed up to 66.2 L/s. The cooling tower has a peak flow rate of 66.2 L/s, while the hot water injector has a maximum water flow rate of 1.58 L/s. These values are outlined in Table 4.5.

Table 4.3 Common HP loop setpoints

Sensor	Heating setpoint	Cooling setpoint
Plant Supply Outlet	16 °C	26 °C

Table 4.4 Common HP loop actuators

Actuator	Effect
Hot Water Flow Rate	Adds heat to loop
Cooling Tower Flow Rate	Removes heat from the loop

Table 4.5 Common HP loop pumps

Location	Flowrate (L/s)
Main pumps	66.2
Hot water injection	1.58
Cooling tower	66.2

For simplicity, the three AHUs are currently modelled as a 2 AHU loops, with AHU 1/2 combined for classrooms and common areas, and AHU 3 for the office side of the building. Figure 4.8 is a sample system diagram, where AHU 3 does not have a mixing box (100% fresh air) and AHU 1/2 does not have heat pumps for reheat, but instead HW reheat coils in the VAV boxes. Table 4.6 outlines which zones are serviced by each AHU, where the penthouse and basement are conditioned solely by zone level heat pumps.

Table 4.6 AHU serviced zones

AHU	Zones Serviced
1/2	1A, 1S, 1SE, 1SW, 2A, 2S, 2SE, 2SW, 3A, 3S, 3SE, 3SW, 4A, 4S
3	1C, 1E, 1N, 1W, 2C, 2E, 2N, 2W, 3C, 3E, 3N, 3W, 4C, 4E, 4N, 4W

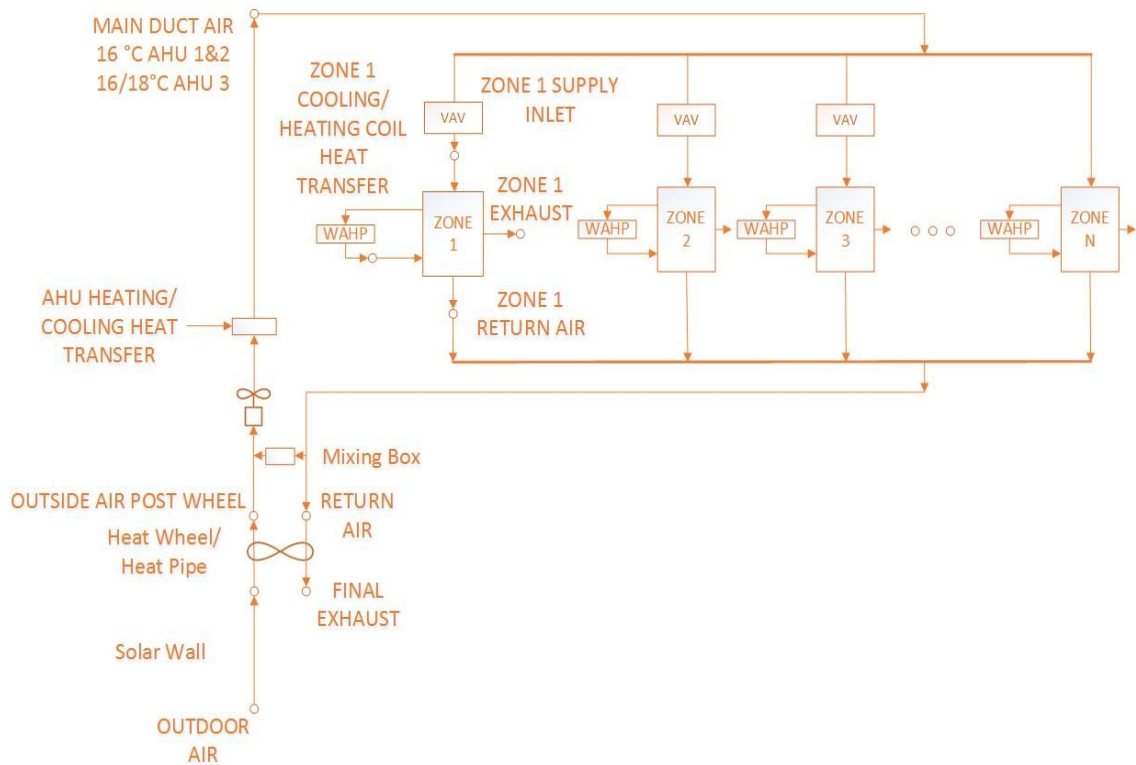


Figure 4.8 HVAC air loop

The main air loop consists of a set of variable frequency drive fans (VFD) that are actuated based on 3 variables: occupancy, temperature regulation, and indoor air quality. A minimum amount of air flow is specified when a space is deemed occupied (based on room located occupancy sensors), and the system then ramps up based on high levels of CO₂ or a need to provide additional cooling as the AHUs are the air conditioning source for all areas except offices. The AHUs have different setpoints based on service area outlined in Table 4.7, with WAHPs in each AHU to meet the setpoint. AHUs 1 and 2 are equipped with a heat pipe to recover energy from exhaust air, while AHU 3 has a heat wheel to perform the same function. The energy recovery systems have an economizer mode to prevent overheating/overcooling. A solar wall is also used to preheat incoming air to the AHUs. The heat wheels are tuned by increasing sensible heat gain in attempt to account for the solar wall effects, as it is not modelled.

Table 4.7 HVAC air loop setpoints

Sensor	AHU 1 & 2	AHU 3
MAIN DUCT AIR	16 °C	16/18 °C based on outdoor air temperature

All of the components within these systems are modelled in *E+*. Most equipment is specified based on operating conditions (such as max heat transfer, flow rates, and COP) that are taken from manufacturer specifications for the equipment within the building. The only exception is the steam convertor, where a district heating element is used, and then converted to steam amounts based on the steam conditions on site. For reference, steam is provided by Dalhousie at 862 kPa gauge and it is assumed that the devices convert the steam to pure condensate.

4.4 Control Review

4.4.1 Strategy

The control strategy at the Mona Campbell Building has four operating scenarios as outlined in Table 4.8. There are two strategies based on building occupancy (based on zone sensor feedback) for the classrooms and common areas, and four strategies for the office section. Each strategy has a unique palate of setpoints as outlined, while the type of control is listed under “Note”. All of the setpoints are coded into *E+* and used by the algorithms within the software. The classrooms and common areas work on schedules 3 and 4. The occupied period is defined in Table 4.9. The AHUs are always available and their output is determined by if the space is occupied or not.

Table 4.8 Primary control strategies

Operating scenarios	1	2	3	4	Note
Season	Heating	Heating	Cooling	Cooling	
Occupancy	Occupied	Unoccupied	Occupied	Unoccupied	
AHU	On	On	On	On	VFD present
Supply air setpoint	18 °C	18 °C	16 °C	16 °C	Modulated
Room thermostat setpoints	22±1 °C	16-26 °C	22±1 °C	16-26 °C	HP, Flow Rate, VAV Reheat
Water loop return setpoint	16-26 °C	16-26 °C	16-26 °C	16-26 °C	Modulated

Table 4.9 Occupied Period

Period	Days	Start Time	End Time
Occupied	Monday-Friday	06:00	22:00

4.4.2 Software

The Mona Campbell BAS is the Metasys software package produced by Johnson Controls¹⁹ and used for the majority of buildings at Dalhousie University. A Java based web application can be used to view the current building state, as well as information for the past 12 hours for most variables.

¹⁹ <http://www.johnsoncontrols.com/>

4.5 Occupancy, Equipment, and Lighting

The thermal comfort and space heating/cooling of a building energy simulation is affected by the presence and schedule of internal loads such as occupants (people), equipment, and lighting. “Equipment” includes technology, refrigeration, and vending, but also includes plug loads such as computers, and table lamps. Table 4.10 outlines the peak values of these loads for typical zone types of offices, classrooms, and cafeteria used in the simulation. These values were derived from the sub metered data and split evenly across all zones based on floor area. It should be noted that “occupant” loads are heat released by occupants which manifest itself as heat within the building (65% sensible, 35% latent). Loads of “equipment” and “lights” consume electricity and manifest as heat within the building (100% sensible convective loads).

The Mona Campbell Building has been modelled to accommodate the various zone types. The specific zone classifications and corresponding zone numbers of the model are given in Table 4.11.

Table 4.10 Peak occupant, equipment, and light loads as a function of space type

Zone Type	Occupants (W/m ²)	Equipment (W/m ²)	Lights (W/m ²)
Office	6	7	7.3
Classroom	6	4.7	10
Cafeteria	6	10	7.3
Server Room	0	20	3

Table 4.11 Zone types

Zone type	Zone label
Office	1C, 1N, 1S, 1E, 2A, 2C, 2E, 2N, 2S, 2W, 3A, 3C, 3E, 3N, 3S, 3W, 4A, 4C, 4E, 4N, 4S, 4W, B, P
Classroom	1SE, 1SW, 2SE, 2SW, 3SE, 3SW
Cafeteria	1A
Server Room	1E

Table 4.12 defines the typical schedules for the building. The values are based on sub metered data for lighting and equipment provided from the Mona Campbell Building. The server room has an additional 80 kW constant load, while the cafeteria as has an additional peak load of 9 kW that follow the occupancy schedule.

Table 4.12 Occupancy schedules (fraction of peak)

Hour	Workday			Saturday			Sunday/Holiday		
	Occupancy	Equipment	Lights	Occupancy	Equipment	Lights	Occupancy	Equipment	Lights
0	0%	50%	20%	0%	50%	20%	0%	50%	20%
1	0%	50%	20%	0%	50%	20%	0%	50%	20%
2	0%	50%	20%	0%	50%	20%	0%	50%	20%
3	0%	50%	20%	0%	50%	20%	0%	50%	20%
4	0%	50%	20%	0%	50%	20%	0%	50%	20%
5	0%	50%	30%	0%	50%	30%	0%	50%	20%
6	10%	50%	30%	10%	50%	30%	0%	50%	20%
7	20%	50%	52%	10%	50%	52%	0%	50%	20%
8	85%	90%	75%	40%	50%	75%	0%	50%	20%
9	85%	90%	75%	40%	50%	75%	0%	50%	20%
10	85%	90%	75%	40%	50%	75%	0%	50%	20%
11	85%	90%	75%	40%	50%	75%	0%	50%	20%
12	50%	80%	75%	40%	50%	75%	0%	50%	20%
13	85%	90%	75%	40%	50%	75%	0%	50%	20%
14	85%	90%	75%	40%	50%	75%	0%	50%	20%
15	85%	90%	75%	40%	50%	75%	0%	50%	20%
16	85%	90%	75%	40%	50%	75%	0%	50%	20%
17	70%	80%	55%	40%	50%	55%	0%	50%	20%
18	40%	60%	50%	40%	50%	50%	0%	50%	20%
19	40%	60%	50%	40%	50%	50%	0%	50%	20%
20	10%	50%	47%	10%	50%	47%	0%	50%	20%
21	10%	50%	47%	10%	50%	47%	0%	50%	20%
22	0%	50%	40%	0%	50%	40%	0%	50%	20%
23	0%	50%	30%	0%	50%	30%	0%	50%	20%

4.6 Calibration and Verification

It is necessary to calibrate and verify that the detailed model is predicting correctly in comparison to actual building thermal performance (internal temperatures) and energy consumption (electricity and steam). To do this several metrics are compared for the 2013 calendar year.

ASHRAE Guideline 14-2014 [104] addresses accuracy requirements of building performance simulation for energy savings. It requires that the simulated results (\hat{y}_t) agree with measured energy data (or billing data) (y_t) to the following extent:

- Normalized mean bias error (NMBE) of $\pm 5\%$ on an annual basis for monthly measurements (Equation 4.1).

$$NMBE = \frac{\sum_{t=1}^n (\hat{y}_t - y_t)}{\sum_{t=1}^n y_t} \quad 4.1$$

- Coefficient of variation of the root mean square error “CV(RMSE)” of 15% for monthly measured data (Equations 4.2 and 4.3, with \bar{y} mean consumption).

$$RMSE = \sqrt{\frac{\sum_{t=1}^n (\hat{y}_t - y_t)^2}{n}} \quad 4.2$$

$$CV(RMSE) = \frac{RMSE}{\bar{y}} \quad 4.3$$

The parameters to be adjusted for calibration are the internal loads (occupants, equipment, and lighting), infiltration, insulation, DHW, pipe losses, and equipment efficiencies. Plug loads and lighting were set based on provided sub metered data, while occupancy was set from ASHRAE standard 189.1-2009 [105] values with the peak values listed in section 4.5 while the schedules for each (based on fraction of peak) were sourced from the sub metered data, with occupancy assumed to track similar to lighting.

The following subsections examine and compare the model estimates with the site specific measured data.

4.6.1 Weather

To create a calibrated model, climatic data for the actual meteorological year (AMY) at the site is required. An AMY file was purchased from Weather Analytics²⁰ corresponding to a lat/long of 44.488, -63.750, the nearest available Weather Analytics weather location according to their online tool was used. The lat/long correspond to a point southwest from the site by 21 km. To confirm the climate file, the environmental conditions for 2013 at Shearwater, NS (lat/long 44.617, -63.500) were downloaded from Environment and Climate Change Canada (ECCC). The data from ECCC is limited to temperature, dew point, relative humidity, wind speed, wind direction and station pressure. The key limitation is that no solar information is provided. For comparative purposes, Figure 4.9 shows the monthly average temperature for both sources, and while they have similar trends, the AMY file tends to be warmer in the winter and cooler in the summer than the ECCC data. Figure 4.10 plots the monthly total horizontal solar radiation at the site, separated into direct and diffuse components, from the Weather Analytics AMY file.

²⁰ <http://www.weatheranalytics.com/wa/company/how-we-do-it/>

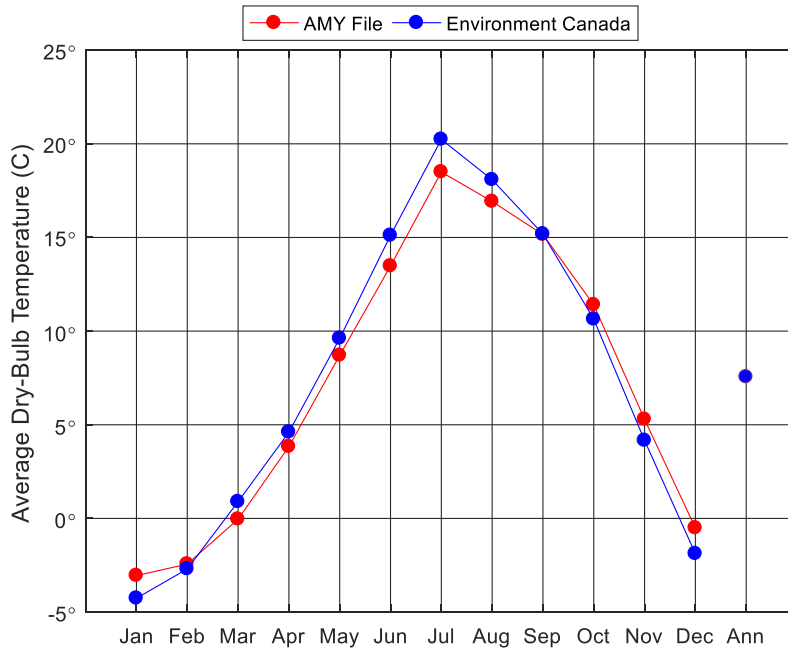


Figure 4.9 Monthly ambient temperature comparison

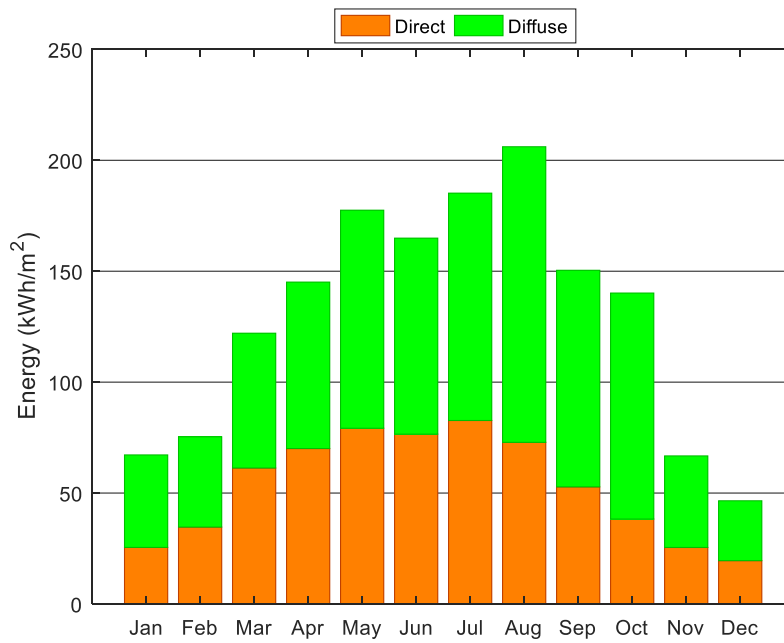


Figure 4.10 Monthly solar radiation

4.6.2 Steam Consumption

Monthly total steam consumption values of the steam converters that service the Mona Campbell Building were provided. These represent total steam use for the building and include both space heating and domestic hot water. It should be noted that changes were made between March-April and October-November to account for an early reading in March, and a late reading in October. For this modeling exercise, an assumed hot water profile was needed as to account for the steam usage. It was assumed that the hot water usage would follow the same schedule as the occupancy, with an assumed load of 0.0001 m³/s during occupied periods. This equals to approximately 1,000 m³ annually, which is 20% of the total potable water usage as outlined in the measurement and verification report by CBCL [106]. This is a reasonable assumption for the building as it is a large office space building with minimal hot water needs (washrooms and small cafeteria vendor). Losses from the hot water loop to environment have also been modelled, with an averaged pipe diameter of six inches, with one inch of insulation on the pipes. The large steam usage in summer is due to the loop being held at a higher temperature than necessary (85 °C vs 60 °C), leading to system losses that are the cause of larger than expected summer steam usage.

A direct comparison of simulation results to measured steam use for the Mona Campbell Building is show in Figure 4.11. It should be noted that monthly values are normalized by the number of days in a period, so that they can be directly compared, as well as compared to an “Ann” annual average value. The NMBE of 0% is realized for the year, with a winter (Nov-Apr) value of 6% and a summer (May-Oct) value of -9%. The CV(RMSE) of 11% for the year is realized, with a winter value of 9% and summer value of 13%, which meets ASHRAE Guideline 14 [104] for annual monthly measurements. A Pearson coefficient of 0.97 confirms a positive correlation between the measured and simulated data.

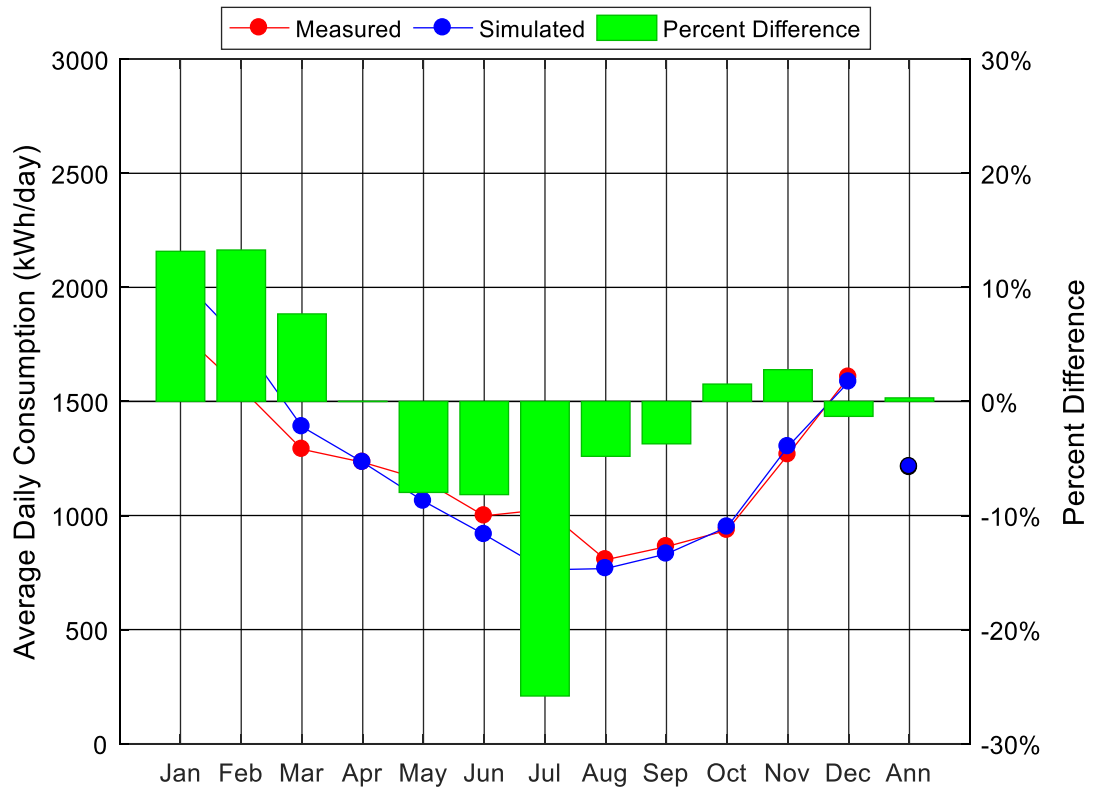


Figure 4.11 Steam use comparison

4.6.3 Electricity Consumption

For calibration of electricity consumption, internal sub metered electricity data from the building was provided by Schneider Electric²¹ ION meters. Figure 4.12 displays a comparison of total monthly electricity consumption. The data shows that while the initial winter months consume additional energy, the overall trending and annual consumption numbers match. The NMBE of -1% is achieved annually, with a winter NMBE of -1% and summer NMBE of -1%. The CV(RMSE) for annual data of 4% is realized, with winter having 2% and summer 5%, which meets ASHRAE Guideline 14 [104]. The data has a Pearson coefficient of 0.93 for the monthly measured totals, which confirms a strong correlation.

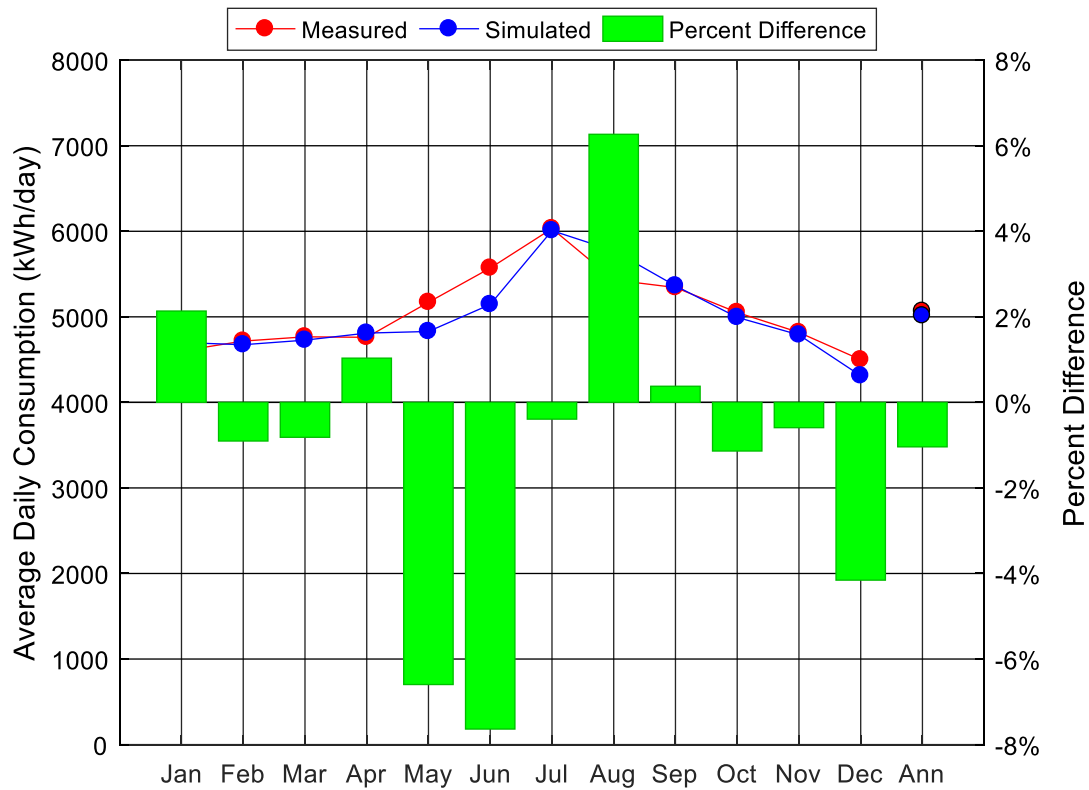


Figure 4.12 Electricity use comparison

²¹ <http://www.schneider-electric.ca/en/>

4.6.4 Electricity Demand

An electricity demand analysis was conducted on the building to determine if the magnitudes of load are of the correct size, and the peaking occurs during the correct month. As peak electric demand occurs for a single 15 minute period, it is challenging to model exactly as special events outside of normal operation (such as an open house) can create the measured peak demand. The data is plotted in Figure 4.13, which shows a strong correlation in magnitude between measured and simulated data. The NMBE of -11% is seen, with a CV(RMSE) of 14% and a Pearson coefficient of 0.90, indicating a strong correlation between the data sets. It is not necessary for these values to meet ASHRAE Guideline 14 as they are peak values, not energy usage measurements.

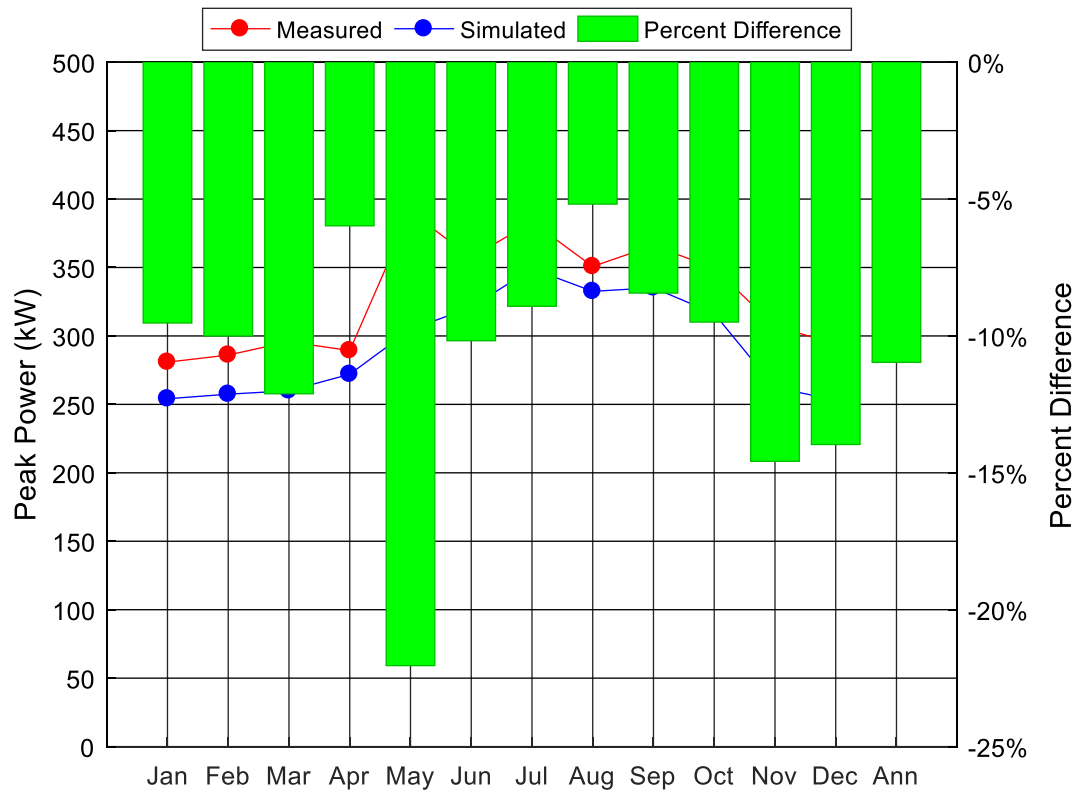


Figure 4.13 Electrical demand comparison

4.6.5 Temperature Performance

It is important to analyze the building temperature performance to ensure that the building is performing the desired function of maintaining occupancy comfort, due to the initial lack of measured data for comparison. Figure 4.14 displays the frequency of each average building temperature encountered during the simulation, along with highlighting the values that occur during the primary occupancy period from 08:00 to 20:00. As shown, the building does not go below the lowest heating setpoint of 16 °C, above the highest cooling setpoint of 26 °C, and the occupied temperatures lie between 21 and 23 °C, the occupied setpoint temperatures.

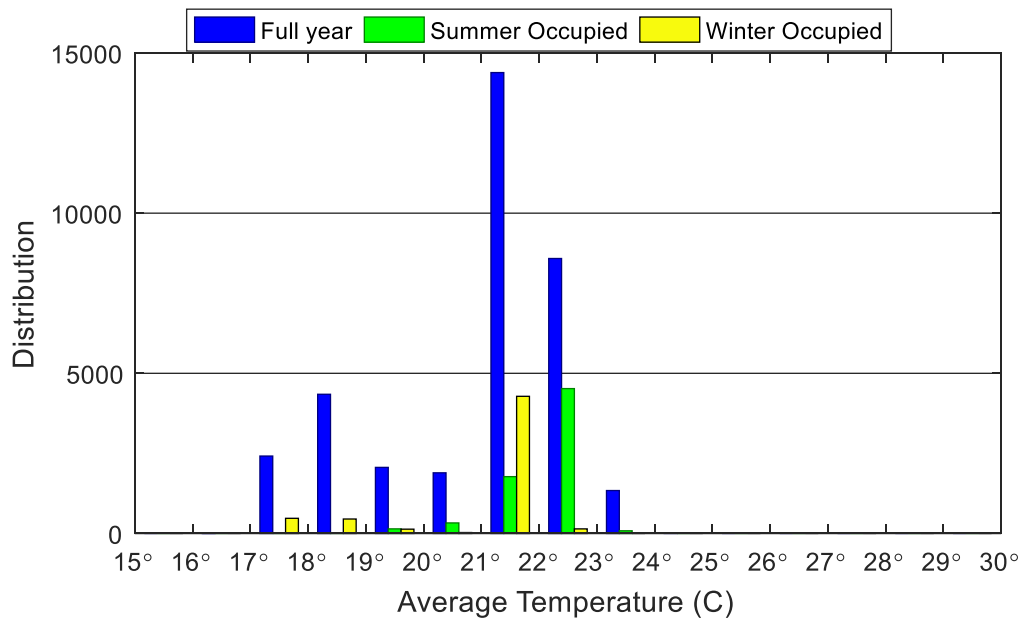


Figure 4.14 Temperature histogram

4.7 Energy Model Results

4.7.1 Daily Profile Plots

To better highlight how the system behaves, simulation time of day plots for energy consumption for steam thermal energy and electricity loads are given in Figure 4.15 for February 6th, and Figure 4.17 for August 6th. The plots highlight the increased HVAC electrical demand load during the summer cooling season, and the morning HVAC steam peak in the winter that does not exist in the summer. The winter season shows a morning HVAC spike in electricity and steam, with steam use occurring later in the day as some of the zones require heating as they are below the average temperature. This effect is shown in the top plot of Figure 4.16, where the red lines correspond to the setpoints and the other coloured lines to individual zone temperatures. The chosen day is one of the coldest of the year hence most temperatures at the heating setpoint. The same plots for the summer period can be found in Figure 4.18 for one of the warmest days of the year, hence some overheating in some zones during peak temperature and solar radiation points. Also of note is that the server room (Zone 1E) is not plotted and not part of the average temperature as it has an independent control strategy due to it not being an occupied space.

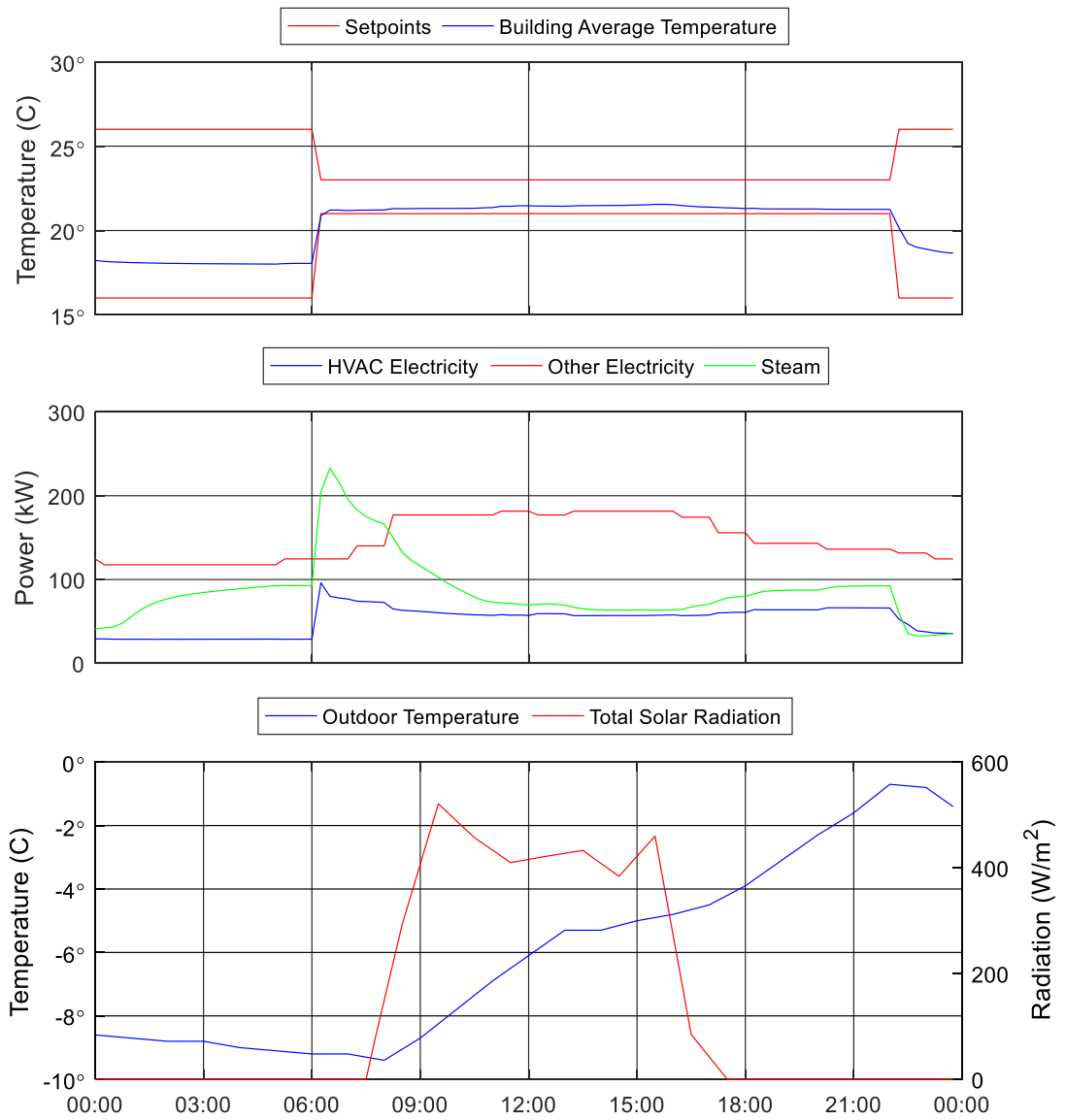


Figure 4.15 Energy consumption sources for February, hourly profile

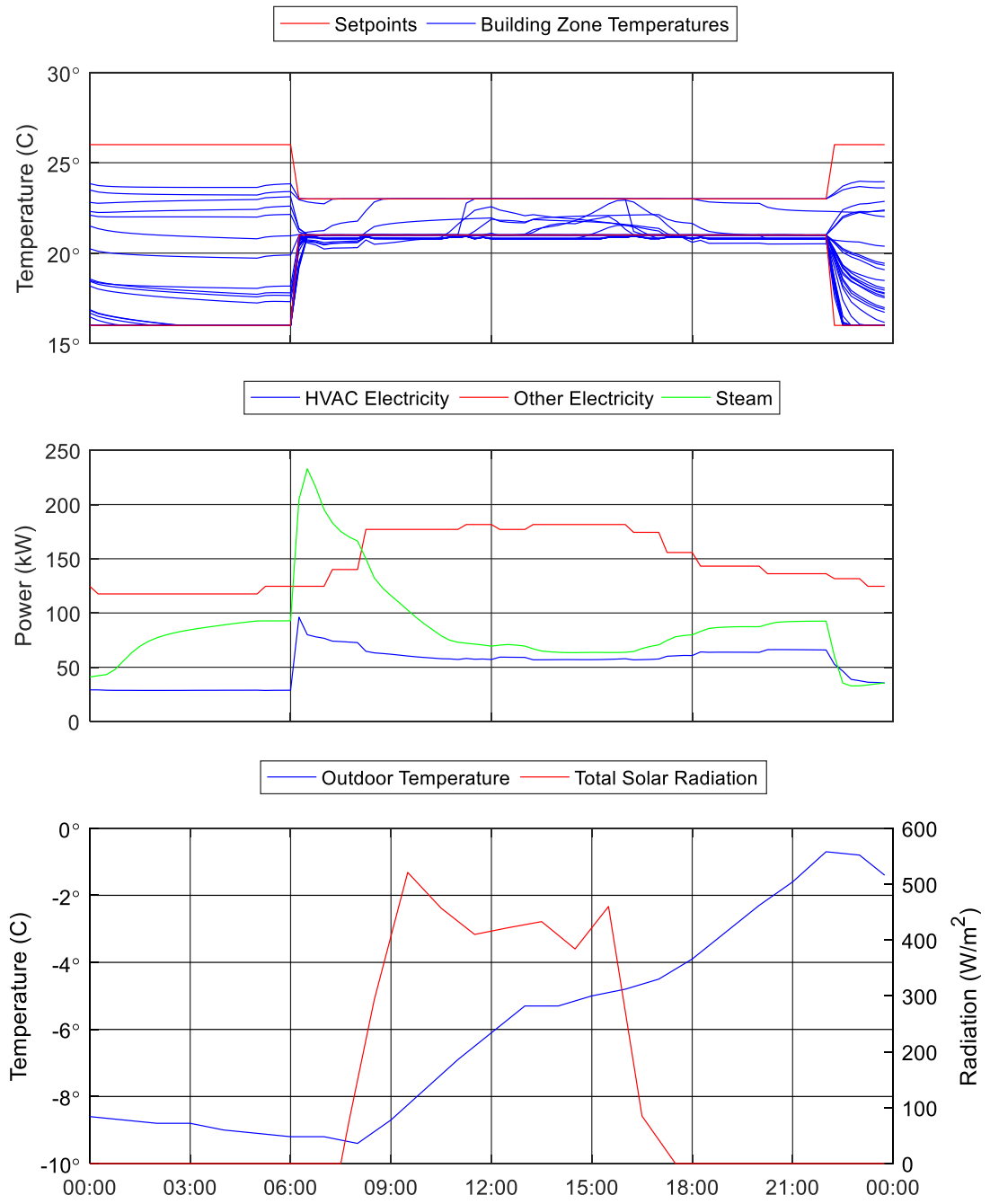


Figure 4.16 Winter zonal temperatures

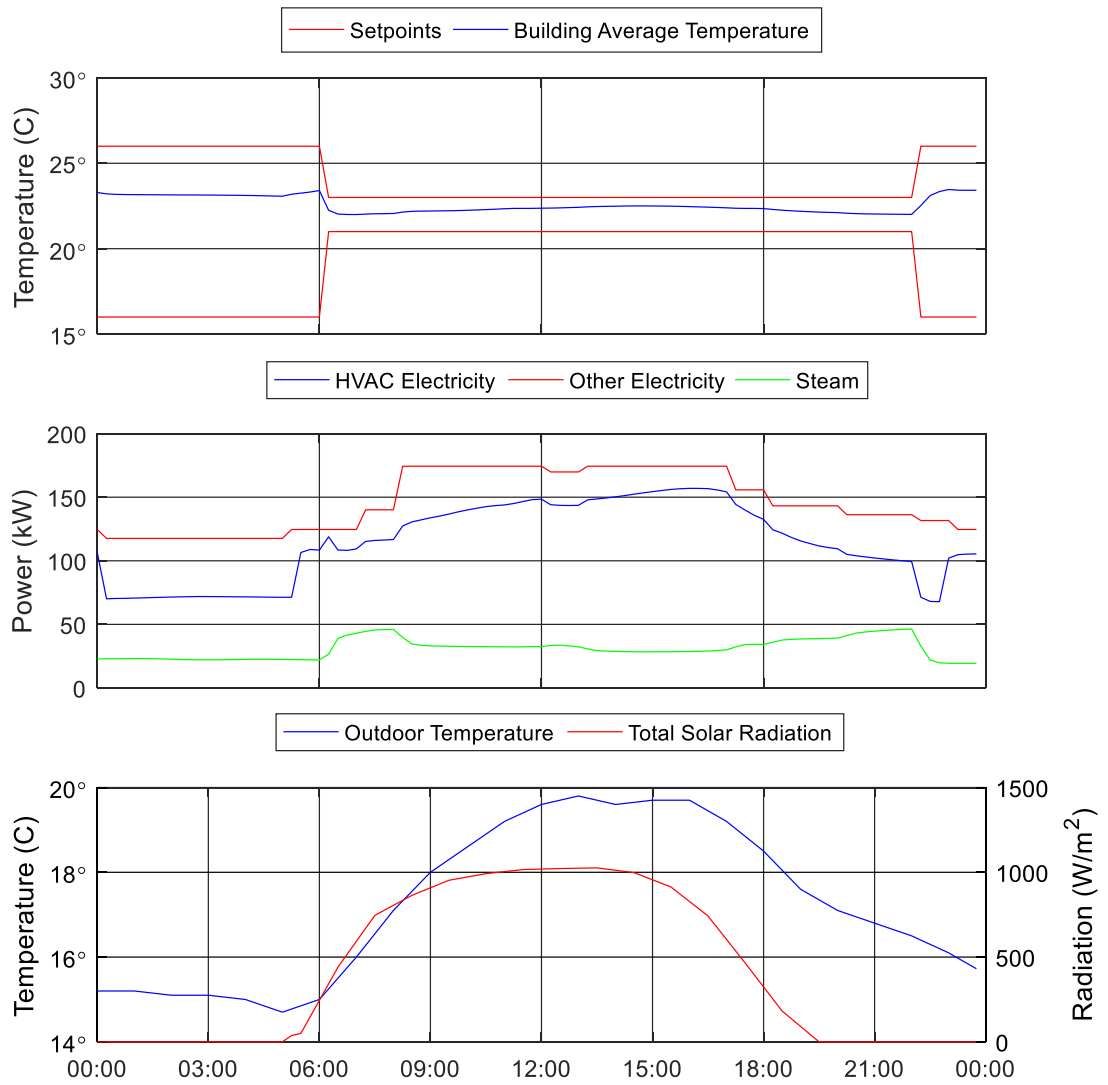


Figure 4.17 Energy consumption sources for August, hourly profile

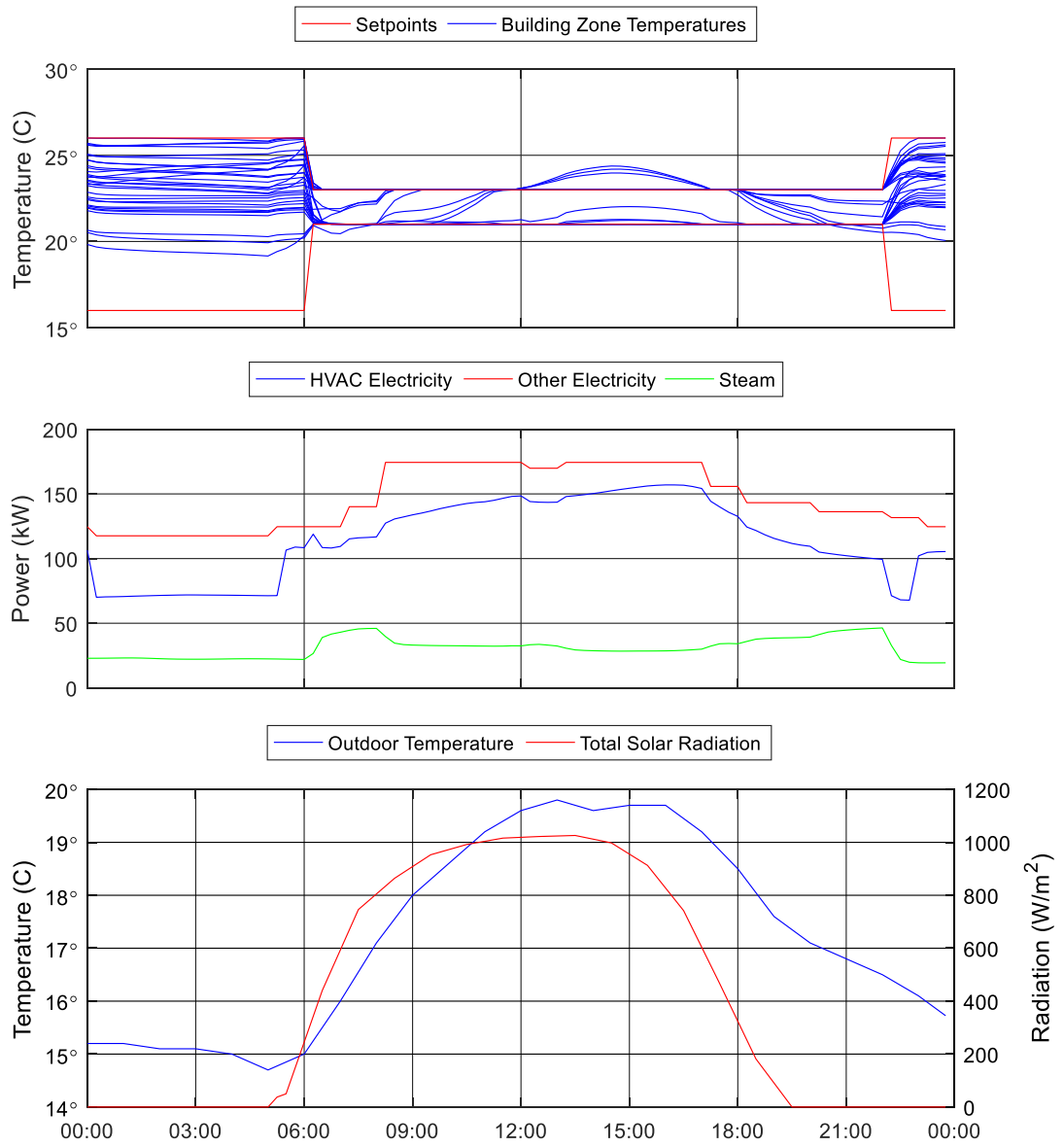


Figure 4.18 Summer zonal temperatures

4.7.2 Electricity by End Use

While the total monthly energy values meet ASHRAE Guideline 14 for energy calibration, it is important to verify that the energy is going to the correct sources. Figure 4.19 highlights the end energy use of electricity as simulated and as measured by submetered circuit groups. The total figures are in relative agreement, where the discrepancies can be attributed to building activities that occur outside of normal conditions that are not feasible to be modelled. A monthly breakdown by end use can be found in Figure 4.20.

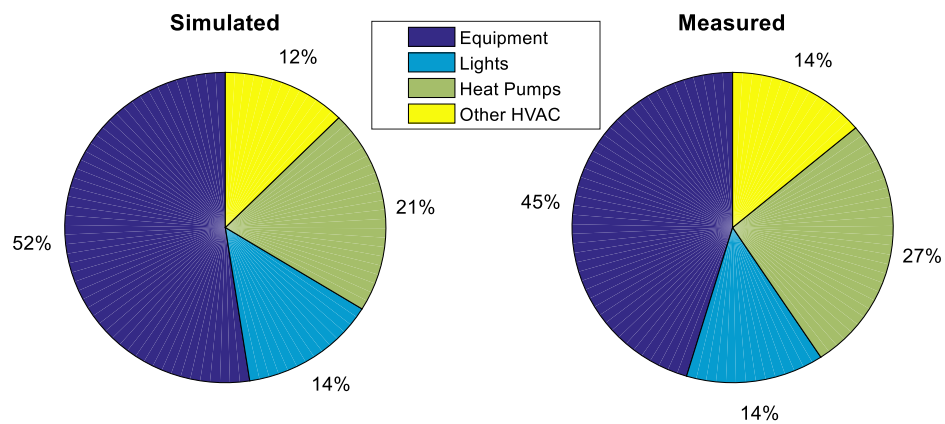


Figure 4.19 Annual electricity by end use

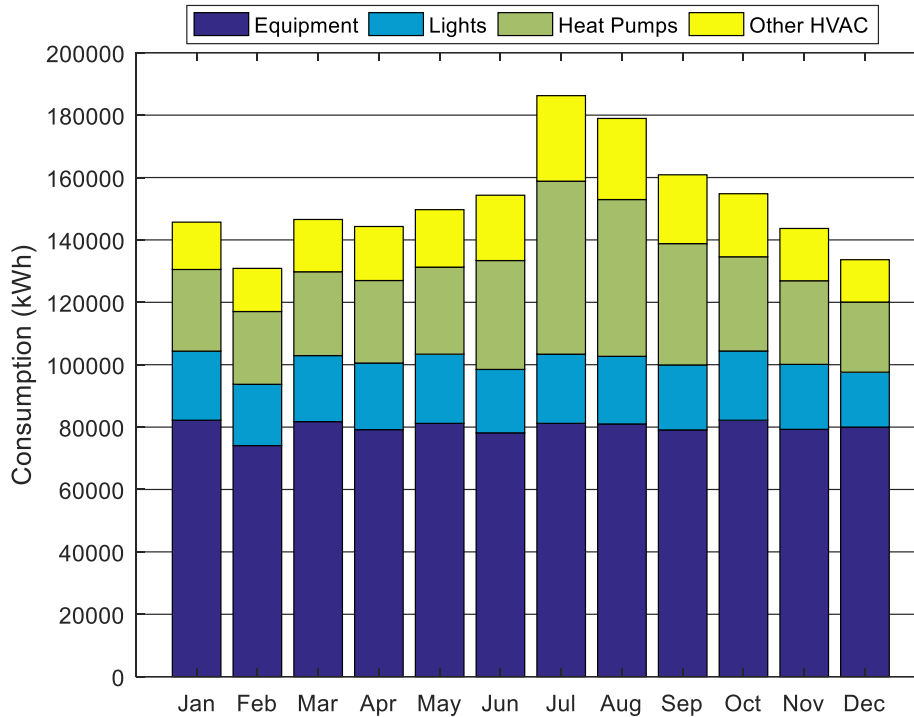


Figure 4.20 Monthly electricity by end use - simulated

The building currently only measures total steam provided, so detailed comparison to measured components is not possible. Engineering assumptions were made for hot water heating and system losses to account for the modelled control zones being at a higher level than the actual control implemented on the building. An example of this is that within one zone of E+, there are multiple HVAC control points that can be operating at different temperatures.

4.8 Conclusions of Building Energy Modelling

This chapter demonstrates the work undertaken to build a detailed and calibrated E+ model of the Mona Campbell building based on the provided utility bills and operational schedule. The model is calibrated to ASHRAE Guideline 14 [104] with the best available data at the beginning phase of the dissertation. This level of information also reflects the typical amount available from a commercial client (utility bills and nominal operating schedule), thus provides a baseline on commercial feasibility of MPC technology with current building practice.

The model is a necessary component for this research and it is used to generate data for the simplified prediction model for use in MPC (Chapter 6.1), and is also used as a virtual building for MPC simulation in Chapter 7 (treated as if it were a real building). Due to the importance of the tasks that rely on the detailed model, an accurate model was required and was developed from typical data from commercial clients.

Chapter 5 ZONE OPERATIVE TEMPERATURE

New control strategies that look to exploit the thermal mass and dynamic storage behavior of a building run the risk of having significant radiant impacts. By using the thermal mass of the building, a larger influence of zone mean radiant temperature (ZRT) is experienced. Thus, a comfort based metric that includes ZRT, such as zone operative temperature (ZOT), is an important factor to consider for thermal comfort. Unfortunately, ZOT is often not a readily available measurement in a commercial building. Only zone air temperature (ZAT) is measured. ZOT is commonly calculated as the average between ZAT and ZRT assuming low air speeds (Equation 5.1) [48], thus a method to predict ZRT can lead to ZOT utilizing the ZAT feedback from the building.

$$ZOT = \frac{ZRT + ZAT}{2} \quad 5.1$$

It was shown in Chapter 2.3 that changes in ZRT impact comfort on a similar level as changes in ZAT for Fanger's comfort models [49], which is widely used in simulation based studies for comfort [17] [73]. Due to the relationship between ZRT and comfort, a detailed investigation was conducted to understand the factors that influence ZRT in various zones within a building, and how they can be used to estimate it so that it can be used to enhance occupant comfort. EnergyPlus building performance modeling/simulation software was used for this work as a detailed model was already created, and the software has been shown to capture the effects of ZRT [107]. It should be noted that *E+* assumes fully-mixed air inside a thermal zone, which is reasonable for distributed furniture and air duct systems.

5.1 Zone Mean Radiant Temperature Analysis of Characteristic Zones

It was first necessary to characterize the differences between ZRT and ZAT for typical zones in the Mona Campbell building for trends. For this study, three characteristic zones were chosen:

- Interior zone (2C)
- Exterior zone with large windows facing north (2N)
- Exterior zone with small windows facing south (2SW)

The zones are controlled with an unoccupied night setback of 16 and 26 °C for ZAT from 23:00 to 05:45, which matches the baseline control of the Mona Campbell building (Chapter 4.4).

5.1.1 Interior Zone 2C

The first characteristic zone considered was an interior zone in the building. It was expected that the difference between the ZOT and ZAT would be minimal as the zone is not exposed to ambient conditions or solar radiation. A scatter plot of ZOT versus ZAT in Figure 5.1 shows a linear trend along the line of equal values. This relationship verifies that ZOT can be approximated using ZAT for interior spaces.

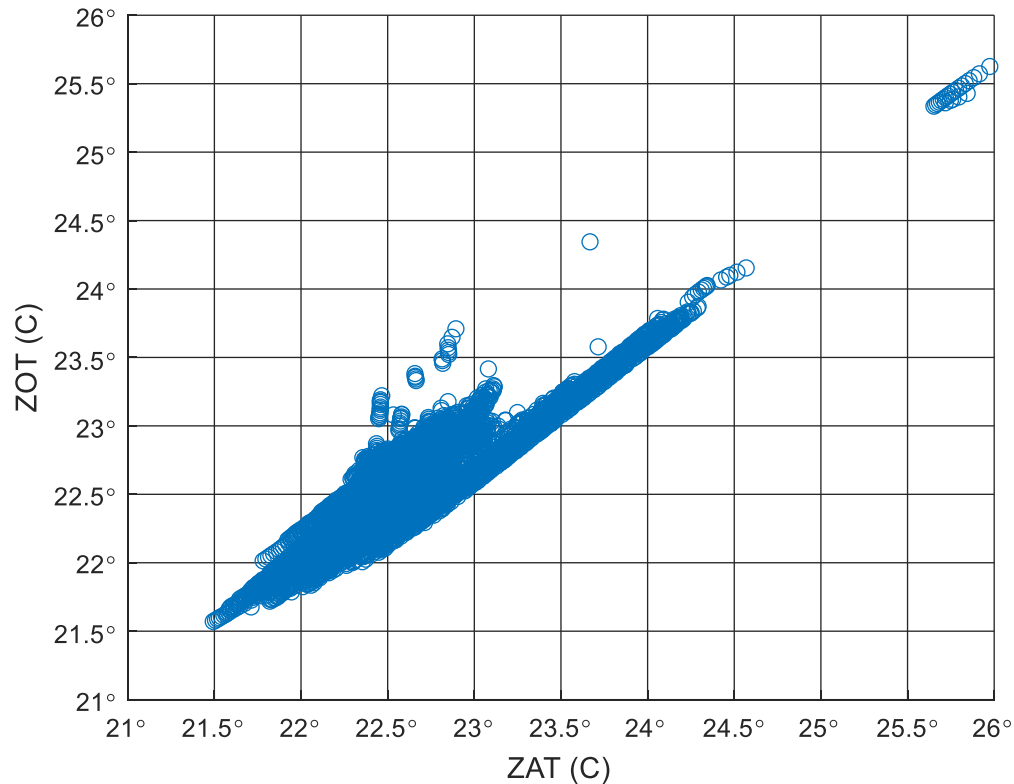


Figure 5.1 Scatter plot of ZOT versus ZAT for an interior zone

5.1.2 Exterior Zone with Large Windows 2N

The second characteristic zone examined is an exterior zone with large north facing windows. It is expected that the ZRT be a function of the outdoor ambient air temperature (conduction through the glass) and solar radiation (transmitted through the transparent glass). For a winter day as shown in Figure 5.2, the ZRT and ZAT are closely matched overnight, with a disparity occurring during the day hours when the HVAC system is operating. During the day the ZRT is lower than the ZAT, which is expected due to the low temperature of the glass. The difference between the ZRT and ZAT reduces when the solar radiation is strongest, highlighting the impact of solar radiation. Also of note is that the building is a primary air source heating system, thus when in heating mode is expected that the ZAT be greater than the surrounding surfaces through which energy is being lost.

Figure 5.3 illustrates a summer day where the ZRT exceeds the ZAT throughout the day. The ZRT peaks at the same time as the solar radiation, and begins to slowly decay when the solar radiation dissipates. The positive difference when the solar radiation is zero highlights the impact of the outdoor ambient temperature, and that the zone is in cooling mode where the air provided to the space is cool, thus driving the ZAT lower than the surroundings.

Figure 5.4 illustrates the results from a spring day, where the outdoor ambient air temperature appears to be at an equilibrium point for ZRT and the ZAT (i.e. minimal difference). The difference is driven primarily by the solar radiation, as there is little difference between ZRT and ZAT when there is no solar radiation.

Figure 5.5 illustrates the distribution of the differences between ZRT and ZAT. The range extends from -6 to 8 °C, with the majority of the data lying between -3 and 3 °C.

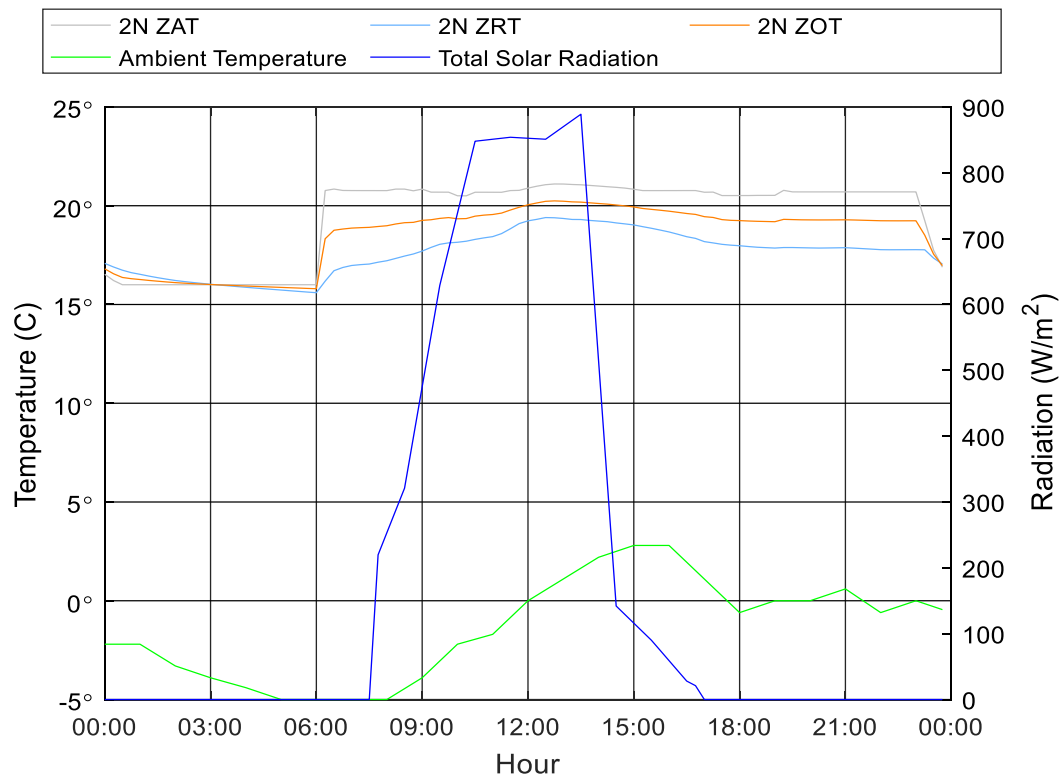


Figure 5.2 Exterior zone large windows winter day (January 8 2013)

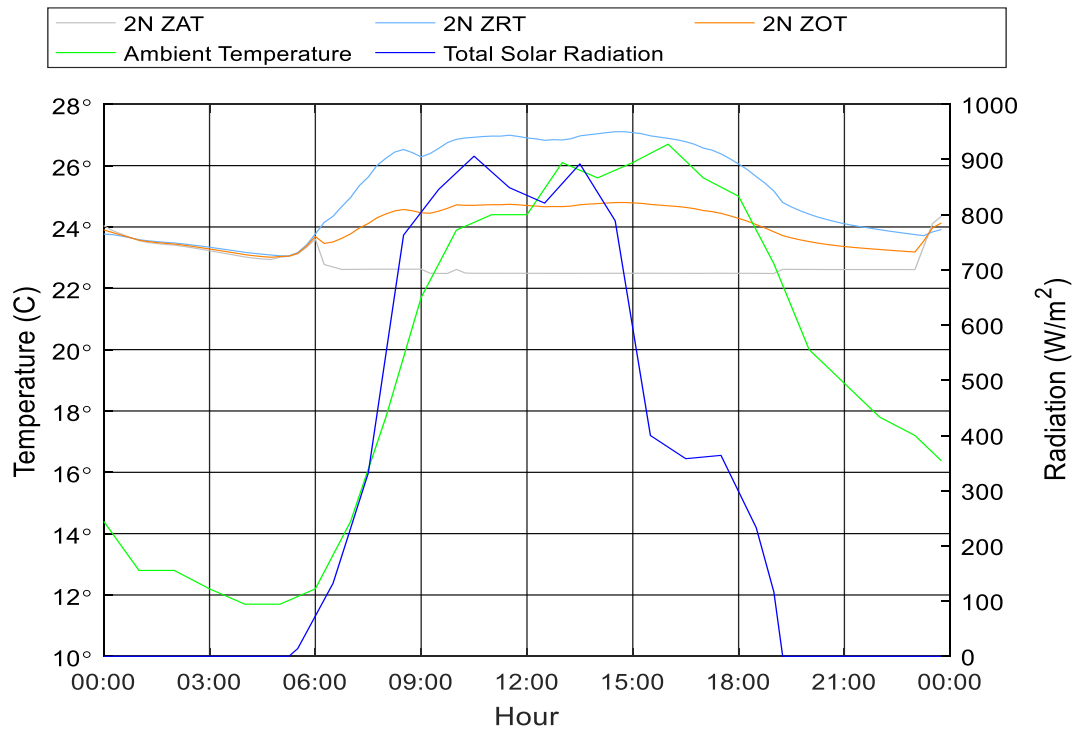


Figure 5.3 Exterior zone large windows summer day (August 8 2013)

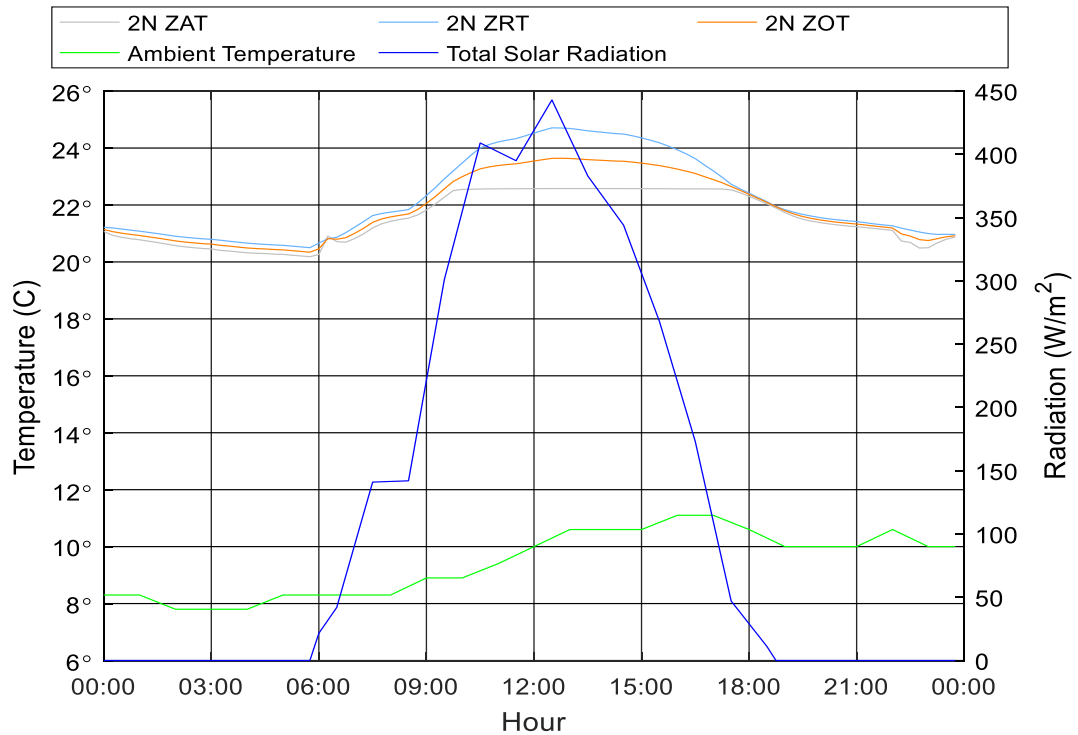


Figure 5.4 Exterior zone large windows spring day (April 6 2013)

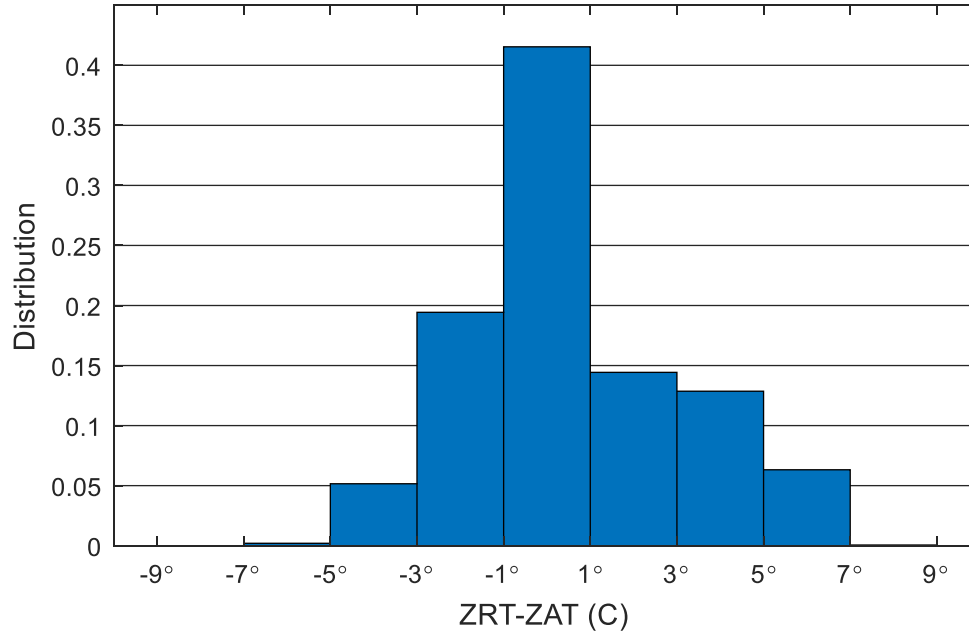


Figure 5.5 Distribution of variations between ZRT and ZAT for an exterior north-facing zone with large windows

5.1.3 Exterior Zone Small Windows 2SW

The final characteristic zone considered is that with small windows facing a southwest direction. It was expected that the zone would follow similar trends to zone 2N, but be more linked to solar radiation due to the increased outer wall thermal resistance, as well being south facing as opposed to north facing.

As shown in Figure 5.6 to Figure 5.8, the zone does indeed behave in a similar manner to the exterior zone with large windows. The key differences are that in winter the ZRT exceeds the ZAT, and that the zone appears to be more influenced by solar radiation due to the steeper slope changes in ZRT when solar radiation exists.

Figure 5.9 illustrates the distribution of differences between ZRT and ZAT, with a range from -3 to 9 °C. It is clear that a positive shift in differential exists, with a majority lying below 5 °C.

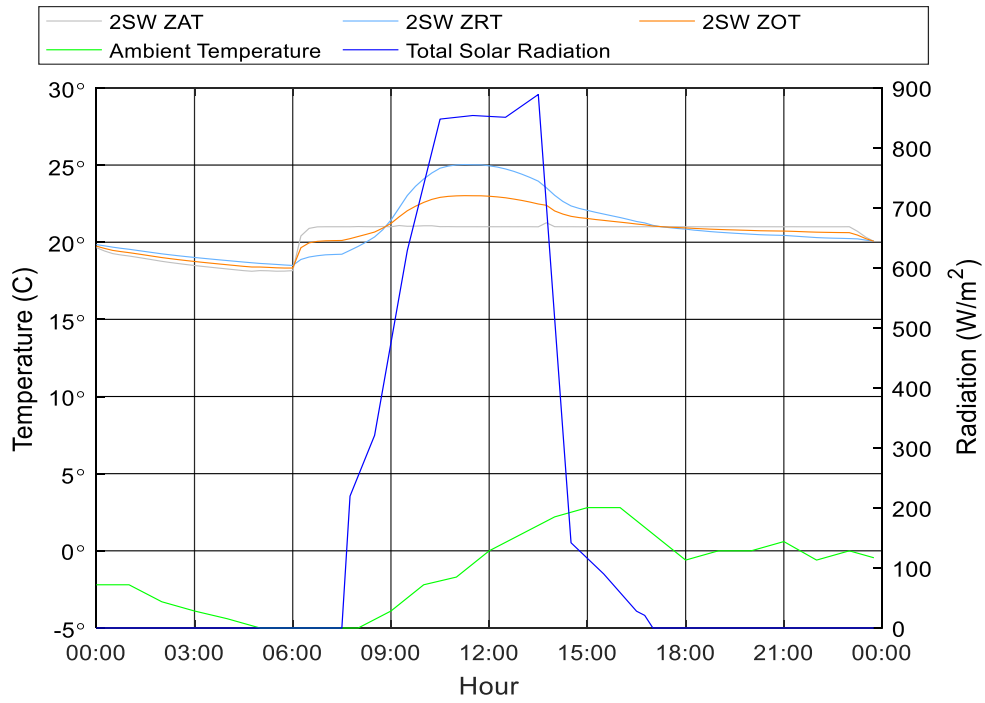


Figure 5.6 Exterior zone small windows winter day (January 8 2013)

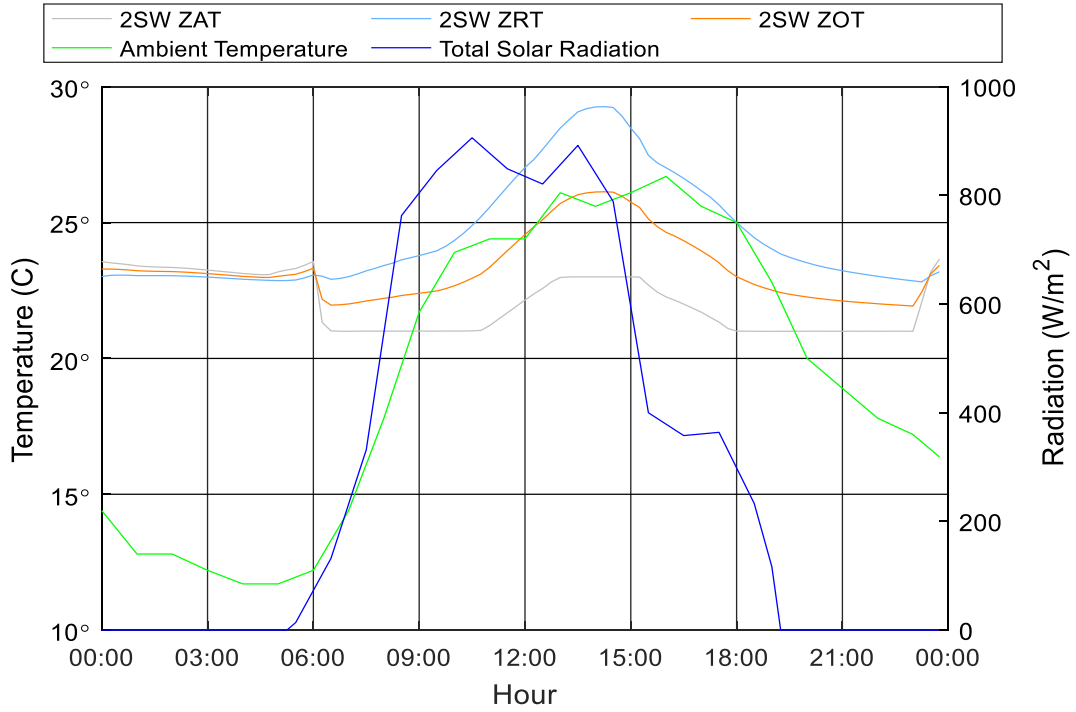


Figure 5.7 Exterior zone small windows summer day (August 8 2013)

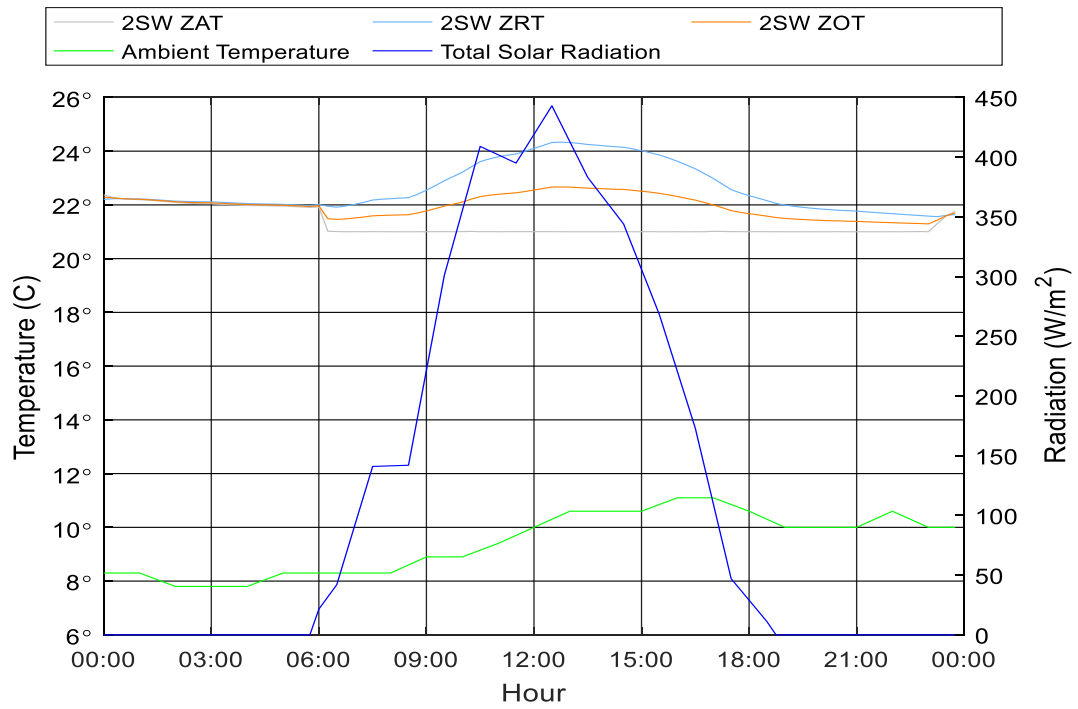


Figure 5.8 Exterior zone small windows spring day (April 6 2013)

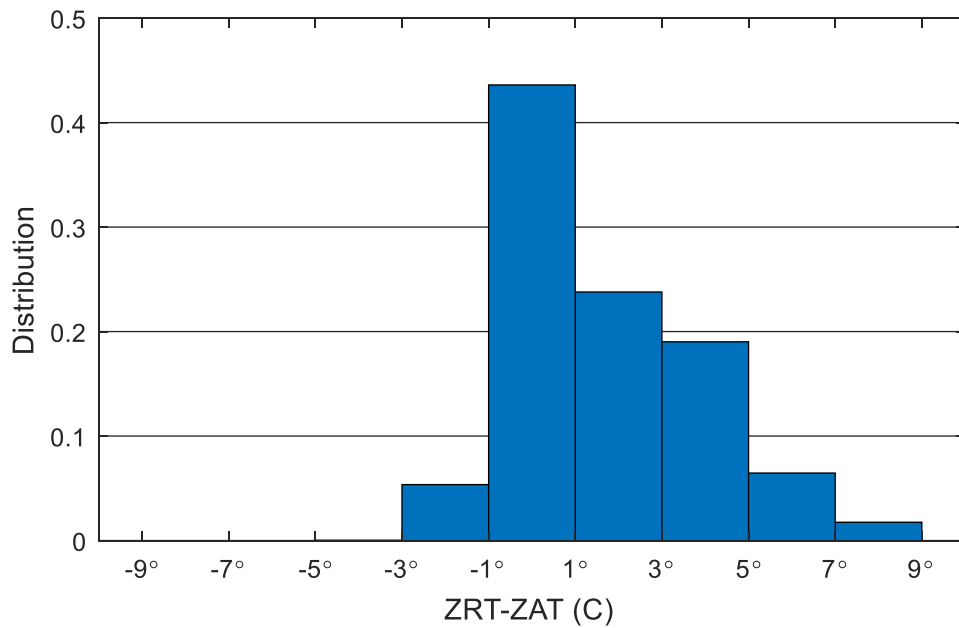


Figure 5.9 Distribution of variations between ZRT and ZAT for an exterior south-facing zone with small windows

5.1.4 Zone Radiant Temperature Difference from Zone Air Temperature Compared to Outdoor Ambient Air Temperature and Solar Radiation

While the initial analysis of ZRT shows different trends for each zone, the exterior zones tend to show a positive trend between the difference between ZRT and ZAT with solar radiation and outdoor ambient air temperature. The relationship with outdoor ambient air temperature for exterior zones is demonstrated in Figure 5.10, where a higher difference occurs with higher outdoor ambient air temperatures, and negative differences occur with lower temperatures. The interior zone (2C) shows a relatively flat trend which is expected as it has no exterior facing walls. Zone 2N shows a higher linear trend with the outdoor air temperature than 2SW, which is expected due to the higher window percentage and north facing directionality.

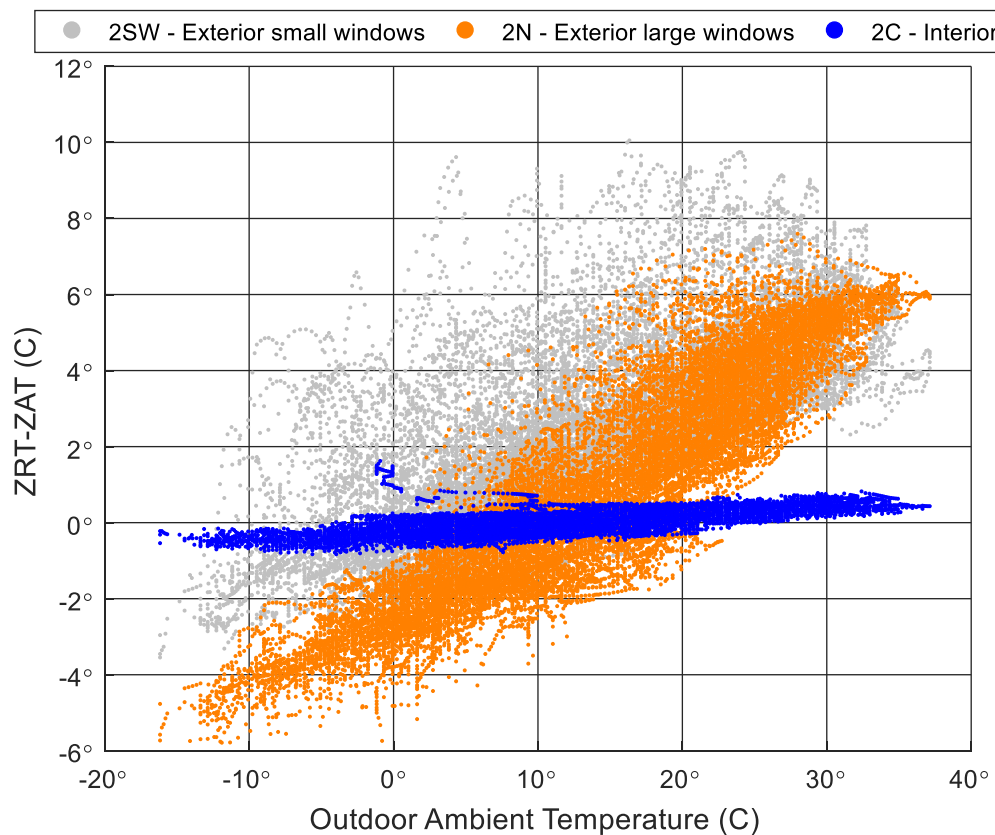


Figure 5.10 Difference of ZRT and ZAT vs outdoor ambient air temperature

A similar study was conducted to determine the relationship between the difference between ZRT and ZAT compared to solar radiation, which is shown in Figure 5.11. The interior zone (2C) shows a flat relationship between the difference in ZRT and ZAT and solar radiation. The outlying points above 1 °C occur during the first day of the year. In contrast to the outdoor ambient air temperature analysis, zone 2SW shows a stronger linear relationship than zone 2N, confirming that it is indeed influenced more heavily by solar radiation than zone 2N. A second key factor from the analysis is that the temperature difference for both zones appear to be positively correlated with both solar radiation and outdoor ambient air temperature for development of an approximation method.

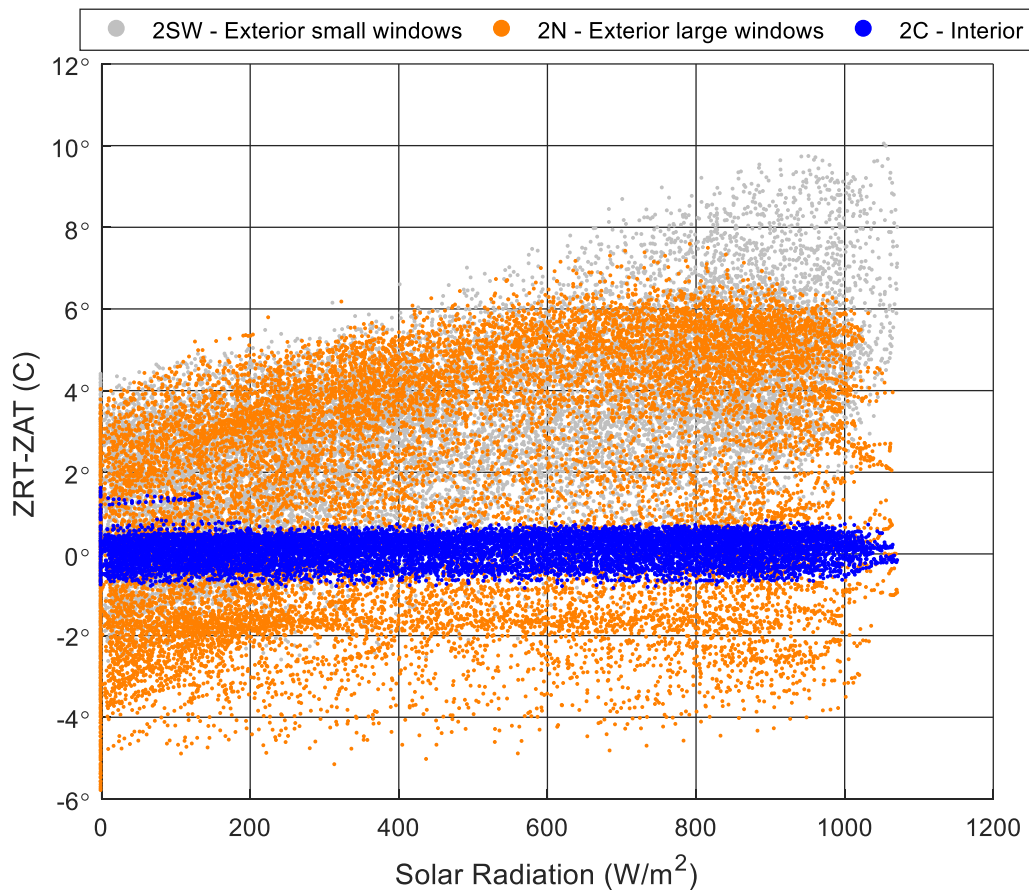


Figure 5.11 Difference between ZRT and ZAT vs solar radiation

5.1.5 Zone Radiant Temperature Difference from Zone Temperature Compared to Outdoor Ambient Air Temperature and Solar Radiation With 180 Degree Building Rotation

In an effort to isolate construction effects (such as window to wall ratio) from orientation effects (north facing vs south facing) on ZRT, a second simulation of the Mona Campbell building was run with a 180-degree rotation, such that the north zone now faced south, and the southwest zone northeast.

Figure 5.12 demonstrates the difference between ZRT and ZAT compared with outdoor ambient air temperature, while Figure 5.13 demonstrates the difference between ZRT and ZAT compared with solar radiation. When compared with Figure 5.10 and Figure 5.11, it is shown that orientation appears to have an influence on the temperature difference. As shown, zone 2N (now facing south) sees a larger swing in temperature difference than zone 2SW, as well as now having the stronger linear relationship with solar radiation. The effects of construction can also be gathered from the plots, where zone 2N has higher extremes when facing south, than what was experienced by zone 2SW, caused by its enlarged window to wall area.

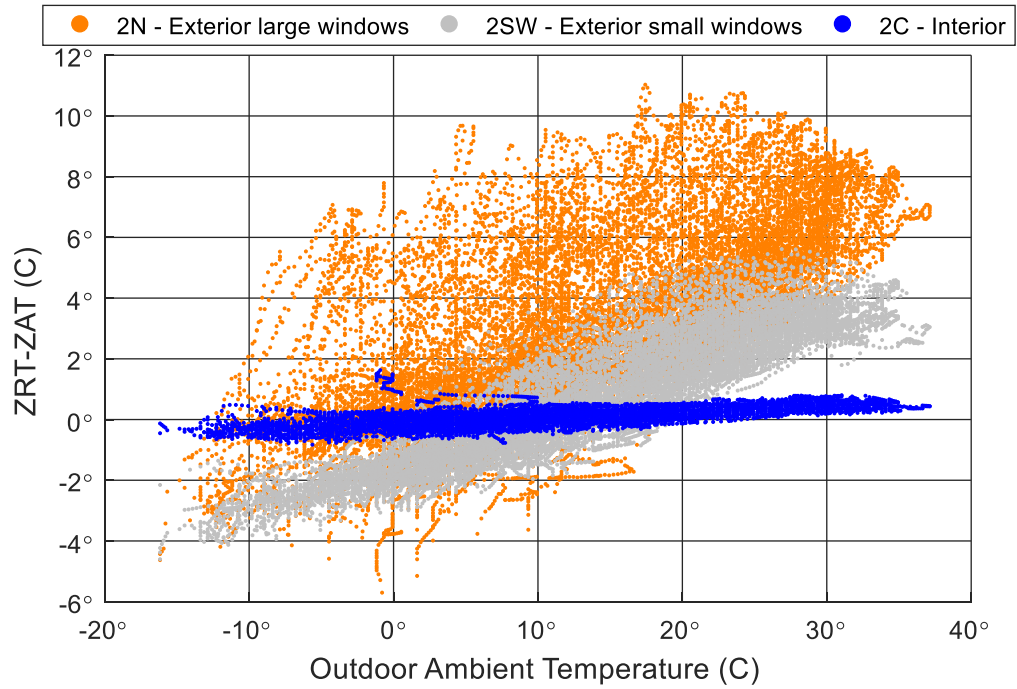


Figure 5.12 Difference between ZRT and ZAT vs outdoor temperature with the 180-degree rotation

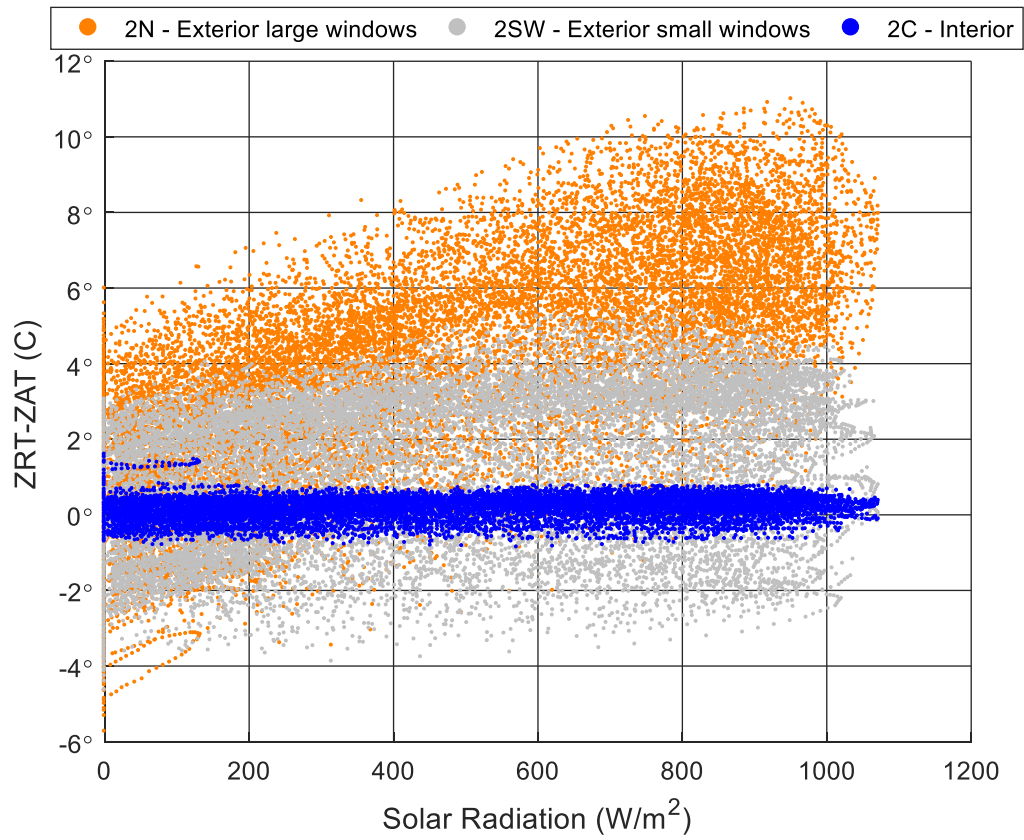


Figure 5.13 Difference between ZRT and ZAT vs solar radiation with the 180-degree rotation

5.2 Mean Radiant Temperature Differential from Zone Temperature Approximation Method

With an understanding that the difference between ZRT and ZAT has positive linear correlations with both solar radiation and outdoor ambient air temperature for external zones, an approximation method was developed using these values to predict the difference. Predicting the difference between ZRT and ZAT is fundamentally the same as predicting the ZRT, as the absolute error is the same in both scenarios, and by predicting the difference removes the ZAT as an input. This leads to the following approximation method (Equation 5.2):

$$ZRT - ZAT = a(\text{Solar radiation}) + b(\text{Outdoor temperature}) + c \quad 5.2$$

Where the coefficients a , b , and c can be found from linear regression analysis (such as LINEST least squares in Microsoft Excel), and are dependent on zone orientation, wall construction, and HVAC delivery method (air point vs. radiant based systems). Solar radiation is provided as W/m^2 and outdoor temperature as dry bulb $^{\circ}\text{C}$. The offset constant c carries any offset that occurs. Data filtering based on measurable information was used to improve the overall accuracy of the approximation. This separates the solution into:

- Filter 1: is the building in occupied or unoccupied mode, as indicated by the AHU system status (i.e. occupied daytime is when airflow is > 0). Thermal comfort is only of importance during occupancy, the unoccupied data is not analyzed.
- Filter 2: is detecting during the occupied period if the zone is in heating mode or is in cooling mode. This is determined based on present ZAT and applied temperature setpoints.

These filters lead to three distinct regression solutions: (i) occupied (heating or cooling); (ii) occupied heating; and (iii) occupied cooling.

The approximation method is applied to the exterior zones only, as the difference between ZRT and ZAT of the interior zones is insignificant and not directly impacted by outdoor conditions.

5.2.1 Exterior Zone Large Windows 2N Occupied Only Mode Filter

The first zone considered for analysis was zone 2N, in occupied mode with no concern for heating/cooling status. The resulting linear regression coefficients are found in Table 5.1, with an r^2 of 0.8667 indicating that the linear relationship assumption was justified. The approximation error has been plotted as a function of time of day (Figure 5.14) and of the temperature difference (Figure 5.15) to determine trends within the data. As shown, the largest prediction error occurs at 06:00, which is expected as this is when transient effects are occurring, which are neglected in the approximation method. The second visible trend is a negative correlation between error and temperature difference. This is due to the high concentration of temperature differences between -2 and 2 °C for which the fit occurs better than at the extremes. A distribution of errors is provided in Figure 5.16, for which 87% of errors are within -1.5 to 1.5 °C.

Table 5.1 Exterior zone large windows occupied only mode linear regression coefficients

Coefficient	a	b	c	r^2
Value	0.001367	0.2338	-2.885	0.867

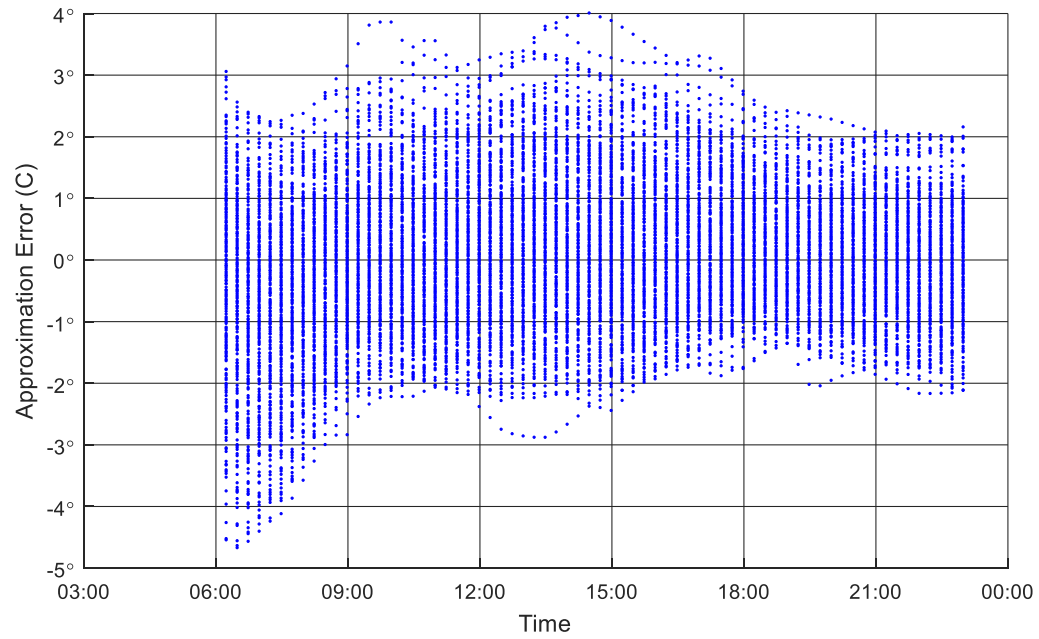


Figure 5.14 Exterior zone large windows occupied only mode approximation error vs time of day

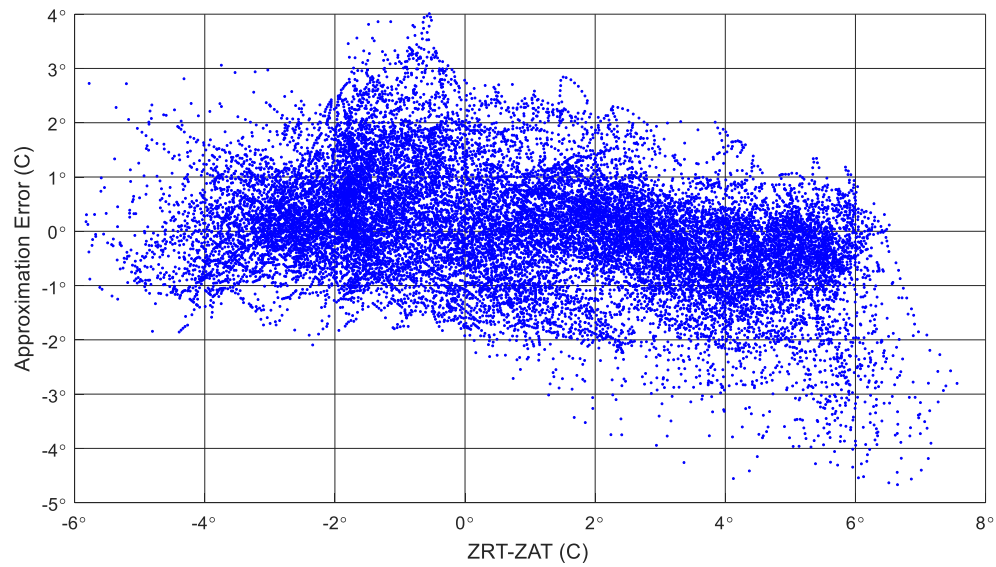


Figure 5.15 Exterior zone large windows occupied only mode approximation error vs temperature difference

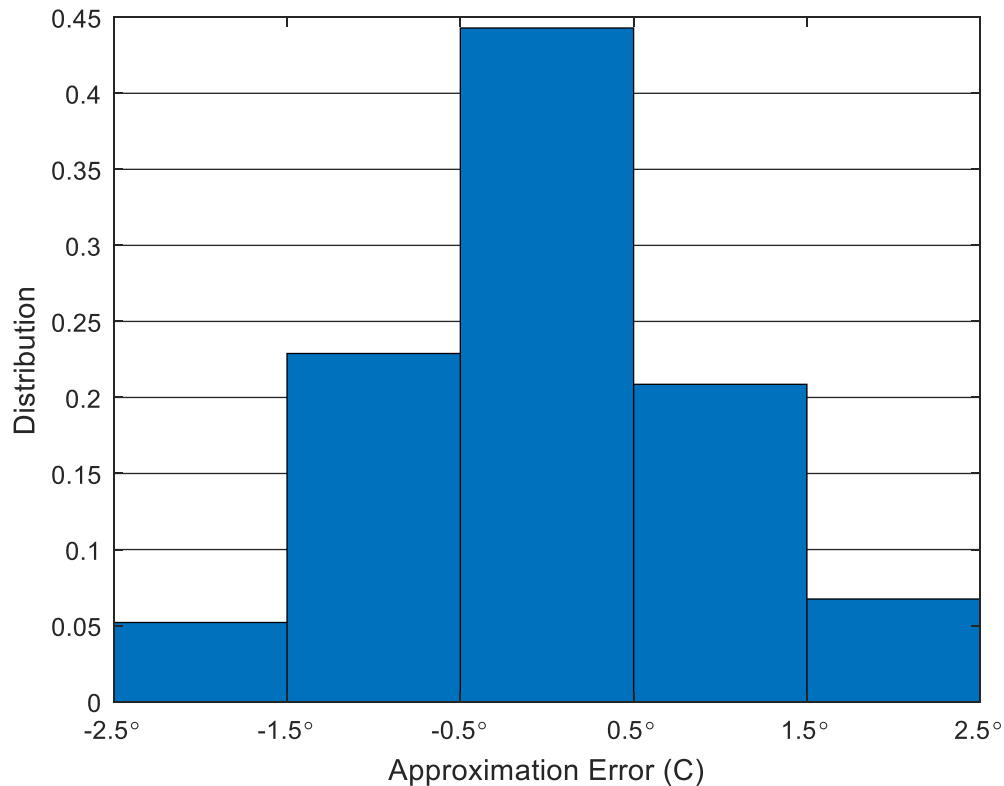


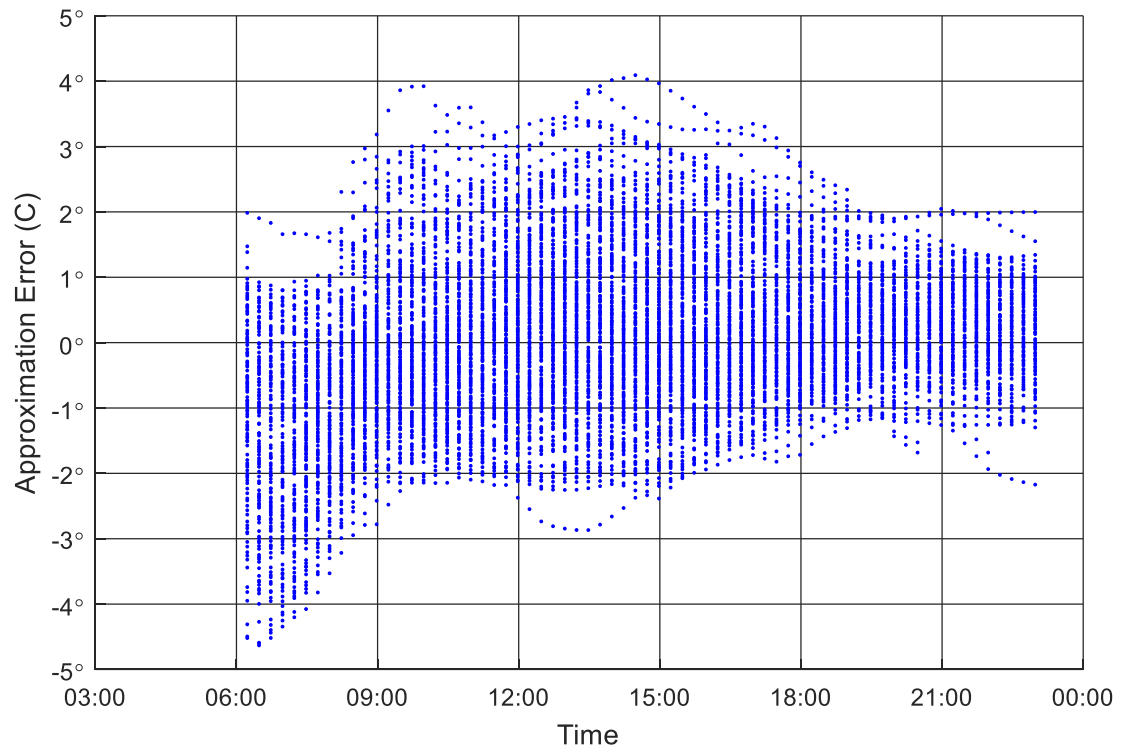
Figure 5.16 Exterior zone large windows occupied only mode approximation error distribution

5.2.2 Exterior Zone Large Windows 2N Occupied Cooling Mode Filter

In an attempt to improve the approximation errors, a data filter was applied using the ZAT. A high temperature filter was applied so that all data when the ZAT was above 21.5 °C (assumed to be cooling mode) would be analyzed for curve fitting. This threshold was chosen as it would be when the building was above the heating setpoint of 21 °C and likely in cooling or about to enter cooling mode. As shown in Table 5.2, the regression coefficients are similar to when occupied only filter is applied, and the r^2 value has decreased to 0.727. When considering the time of day analysis (Figure 5.17), approximation error is biased low in the morning, and reaches an equilibrium about zero around 09:00. Similar to the no filter case, the temperature differential comparison case (Figure 5.18) shows a distinct negative correlation. The distribution of approximation errors (Figure 5.19) also follows the same trend as the no filter case.

Table 5.2 Exterior zone large windows occupied cooling mode linear regression coefficients

Coefficient	a	b	c	r^2
Value	0.001413	0.2408	-2.998	0.727

**Figure 5.17 Exterior zone large windows occupied cooling mode approximation error vs time of day**

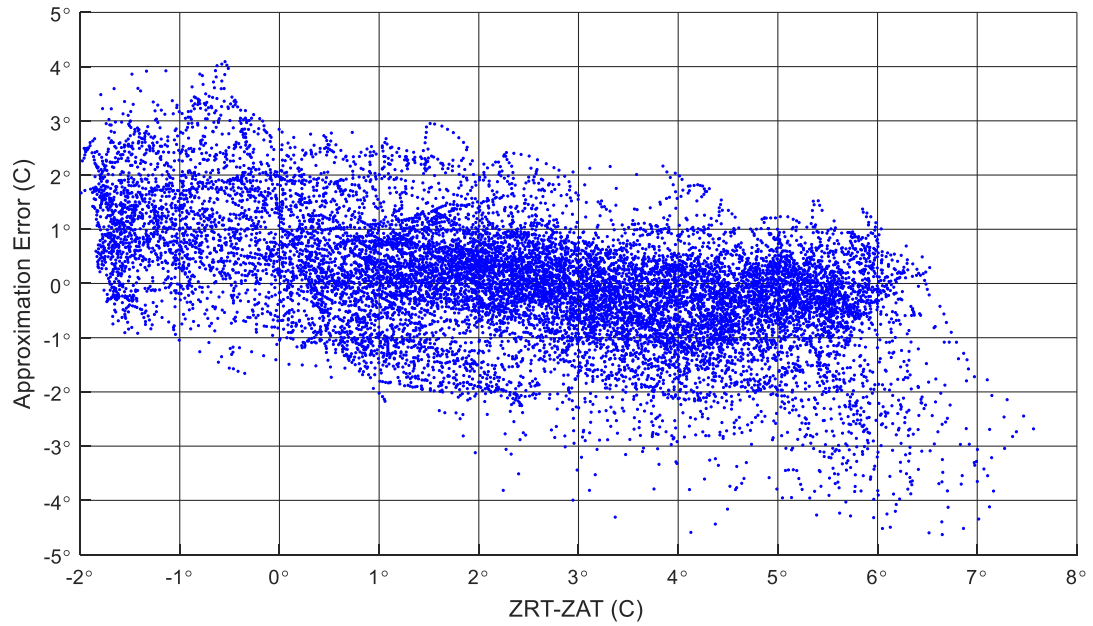


Figure 5.18 Exterior zone large windows occupied cooling mode approximation error vs temperature difference

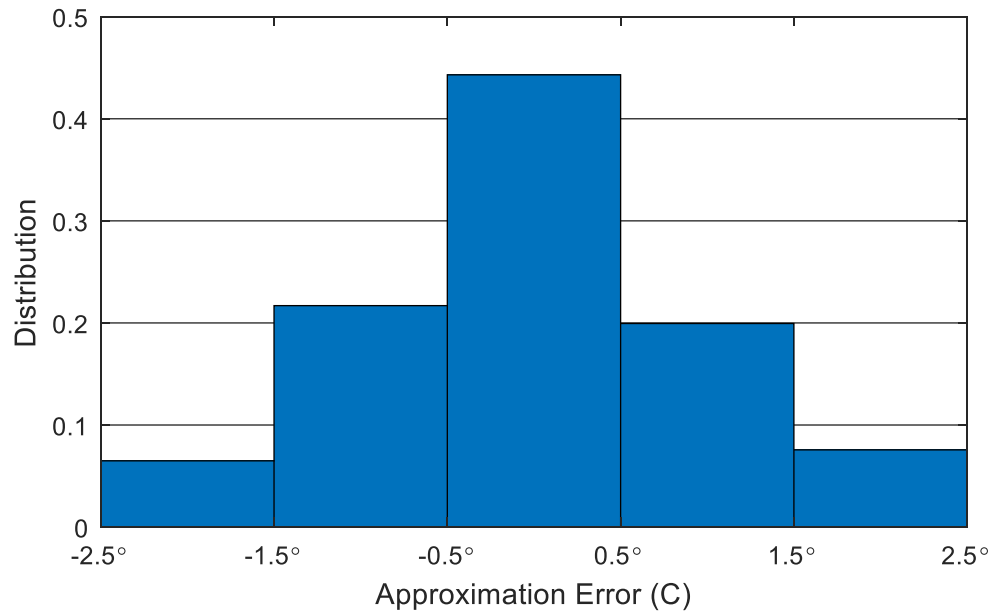


Figure 5.19 Exterior zone large windows occupied cooling mode approximation error distribution

5.2.3 Exterior Zone Large Windows 2N Occupied Heating Mode Filter

Similar to the cooling mode filter, a heating mode filter for when ZAT was less than 22 °C was applied to look for improved approximation performance. The value of 22 °C was chosen as values below this are likely to be in heating mode, or just after heating mode when characteristics should be similar. Once again, a lower r^2 correlation exists (Table 5.3) in comparison with the no data filter case. The time of day analysis (Figure 5.20) shows similar trends to the no filter case, as does the temperature difference analysis (Figure 5.21). The error distribution (Figure 5.22) is improved from the no filter case, with a higher percentage of errors between -1 and 1 °C.

Table 5.3 Exterior zone large windows occupied heating mode linear regression coefficients

Coefficient	a	b	c	r^2
Value	0.0007819	0.1744	-2.649	0.649

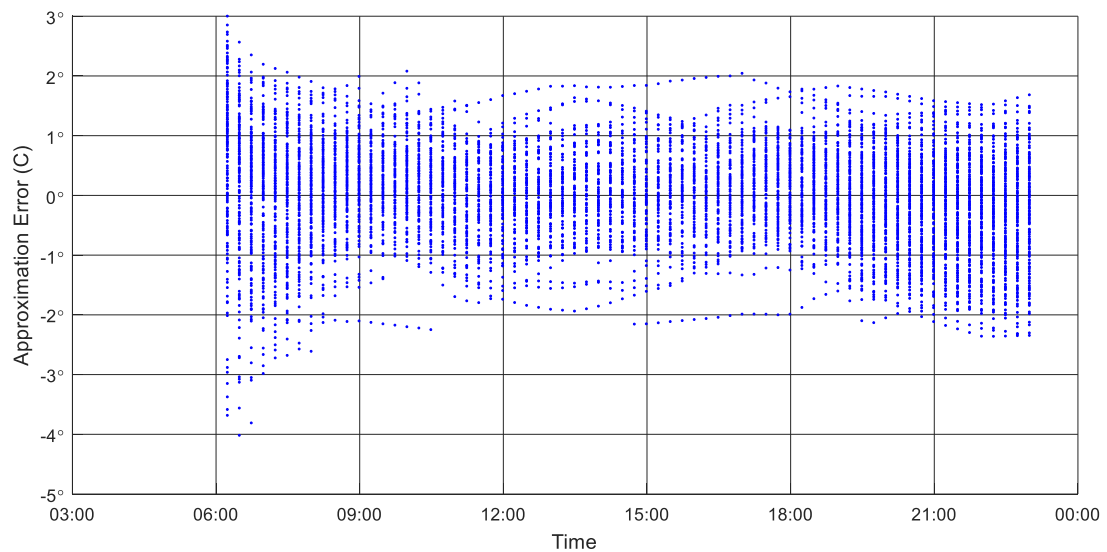


Figure 5.20 Exterior zone large windows occupied heating mode approximation error vs time of day

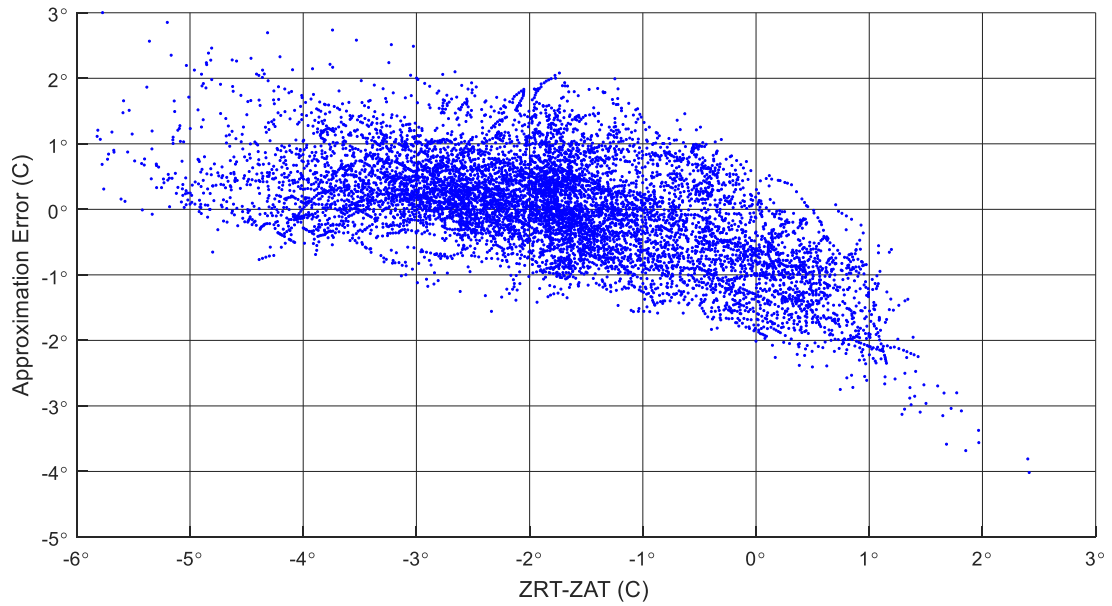


Figure 5.21 Exterior zone large windows occupied heating mode approximation error vs temperature difference

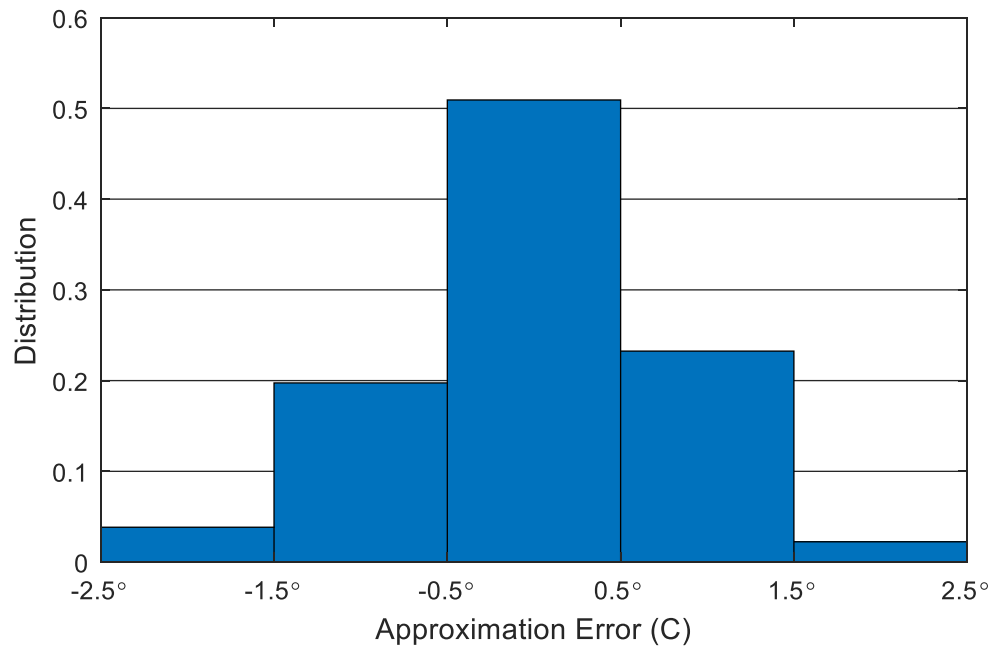


Figure 5.22 Exterior zone large windows occupied heating mode approximation error distribution

5.2.4 Exterior Zone Large Windows 2N Comparison of Filters

In order to better contrast the filtering methods, the distribution of approximation error of all methods is plotted in Figure 5.23, which shows similar behavior between the three filters. A comparison of coefficients is given in Table 5.4, which shows that heating mode filter has the largest deviation in coefficients, and that the mode specific filtered methods have a worse correlation. Due to the similar level of behavior and added challenge of implementation, filtering based on HVAC mode is not required.

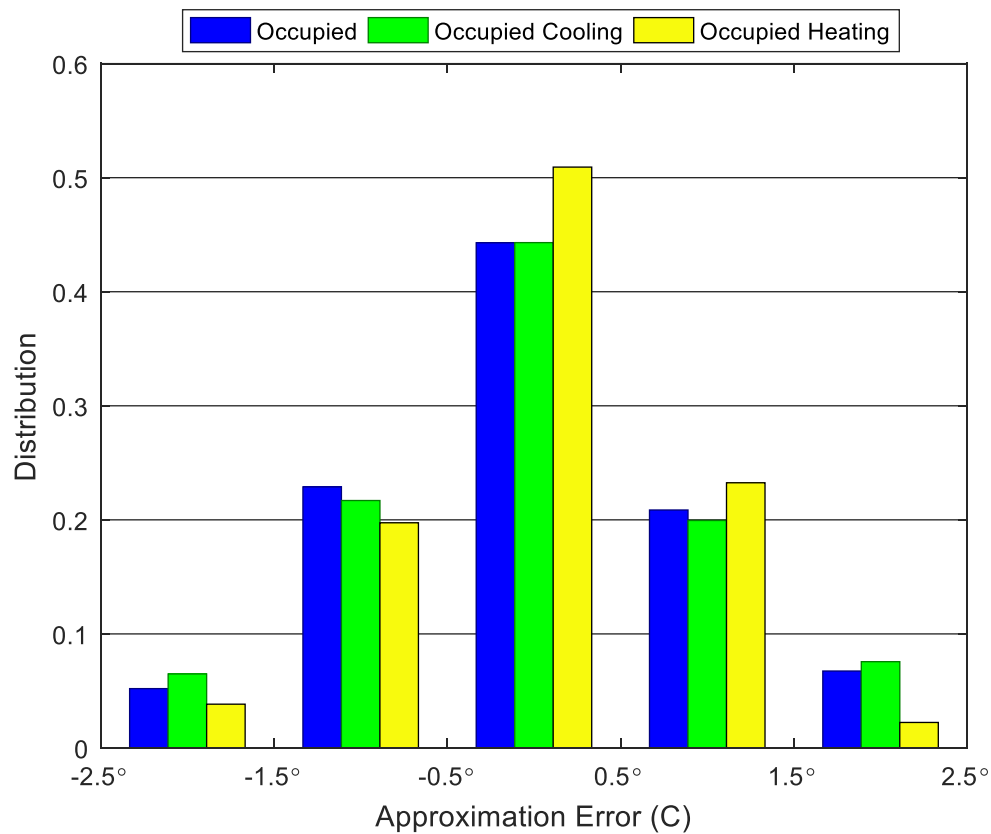


Figure 5.23 Comparison of filter error distribution

Table 5.4 Comparison of zone 2N large exterior windows

Mode	a	b	c	r ²
Occupied only	0.001367	0.2338	-2.885	0.867
Occupied cooling	0.001413	0.2408	-2.998	0.727
Occupied heating	0.0007819	0.1744	-2.649	0.649

5.2.5 Exterior Zone Small Windows 2SW

The same analysis as conducted for zone 2N was conducted for zone 2SW, and due to similar trends, only the tabular correlation results are presented in Table 5.5. As shown, the occupied only mode has similar correlation coefficients and high regression coefficients, similar to the occupied heating mode. This indicates that these two models accurately represent the difference between ZRT and ZAT. Cooling mode r² of 0.342 is quite low and indicates that filtering for heating and cooling mode has little value, and can lead to worse results.

Table 5.5 Exterior zone small windows linear regression coefficients

Mode	a	b	c	r ²
Occupied only	0.003338	0.1200	-0.4234	0.741
Occupied cooling	0.003105	-0.01934	3.672	0.342
Occupied heating	0.002569	0.1229	-0.3893	0.715

5.2.6 Summary of Zone and Mode Filters

While approximations have been developed for individual zones, it is important to draw conclusions from the analysis and compare the differences between the north and south facing zones.

- The filtering between cooling and heating mode during the occupied period appears to provide negligible changes to prediction accuracy (often reducing performance) and are not worth the extra computational effort to implement.
- Interior zones require no ZRT modifications because they have no solar impacts and no exterior facing walls. If the space was conditioned with a radiant heat source, additional factors would be required.
- Shown in Table 5.6 are differences in correlation coefficients for the occupied mode of the building zones. As shown, the south facing zone is more correlated with solar radiation (a coefficient; slope is almost three times higher) while the north zone is more correlated with outdoor ambient air temperature (b coefficient; almost double). Also of note is that the offset coefficients are negative for both cases, with the north zone experiencing a larger initial offset.

Table 5.6 Comparison of north and south facing correlation coefficients for occupied mode

Mode	a	b	c	r ²
2SW	0.003338	0.1200	-0.4234	0.741
2N	0.001367	0.2338	-2.885	0.867

5.2.7 Surface Level Forecasting – Total Solar Radiation

An expansion of the ZRT approximation method from using the global/site level forecasts to those of the GPL high resolution surface level forecasts (HRF) of total solar radiation was developed. The HRF forecasts consist of square meter surface level resolution of both direct and diffuse radiation, and can be aggregated to each surface. The goals were to improve prediction accuracy of ZRT-ZAT and improve the potential transferability from building to building (i.e. develop a universal model). The reference case in this evaluation using *E+* is that which uses the site level global horizontal solar radiation. The surface level total solar radiation is then used in Equation 5.2 as opposed to the site level values

for comparison. The results are shown in Table 5.7, where the use of HRF forecasts improves the overall prediction accuracy (higher r^2 and F statistic values), and shows more consistency in the solar radiation values (ranging from 0.0074 to 0.0139 compared to 0.0006 to 0.0033).

Table 5.7 HRF coefficients and r^2 compared to global level forecasts

Zone	Global Solar radiation					Total HRF solar radiation				
	Solar	Ambient Air	Offset	r^2	F	Solar	Ambient Air	Offset	r^2	F
2SW	0.0033	0.1200	-0.4233	0.741	21231	0.0098	0.1108	-0.396	0.838	37864
2N	0.0014	0.2338	-2.8851	0.867	50938	0.0118	0.2124	-2.997	0.912	80192

The improvement in performance is shown visually in Figure 5.24 through Figure 5.27, with narrower bands of error compared to what was found using site level forecasts. There appears to be minor changes in the ambient air and offset values. As for directionality, north facing zones have a larger offset and larger ambient air affect, due to the lower contributions of solar gains on these surfaces.

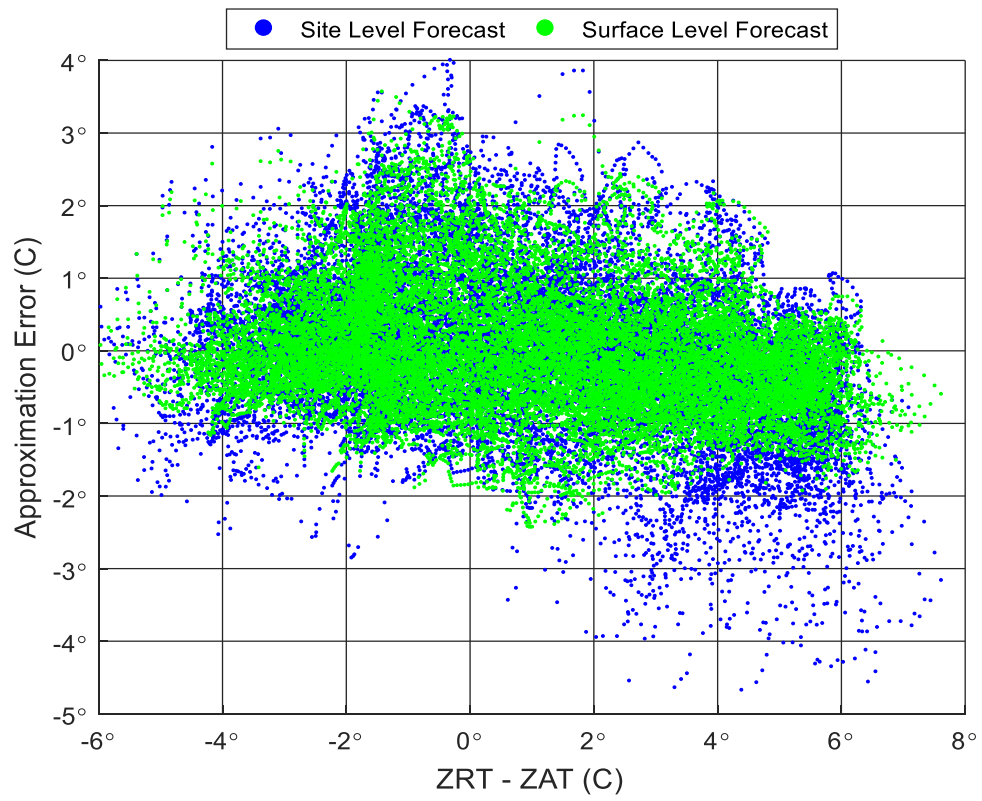


Figure 5.24 2N HRF approximation error vs ZRT-ZAT

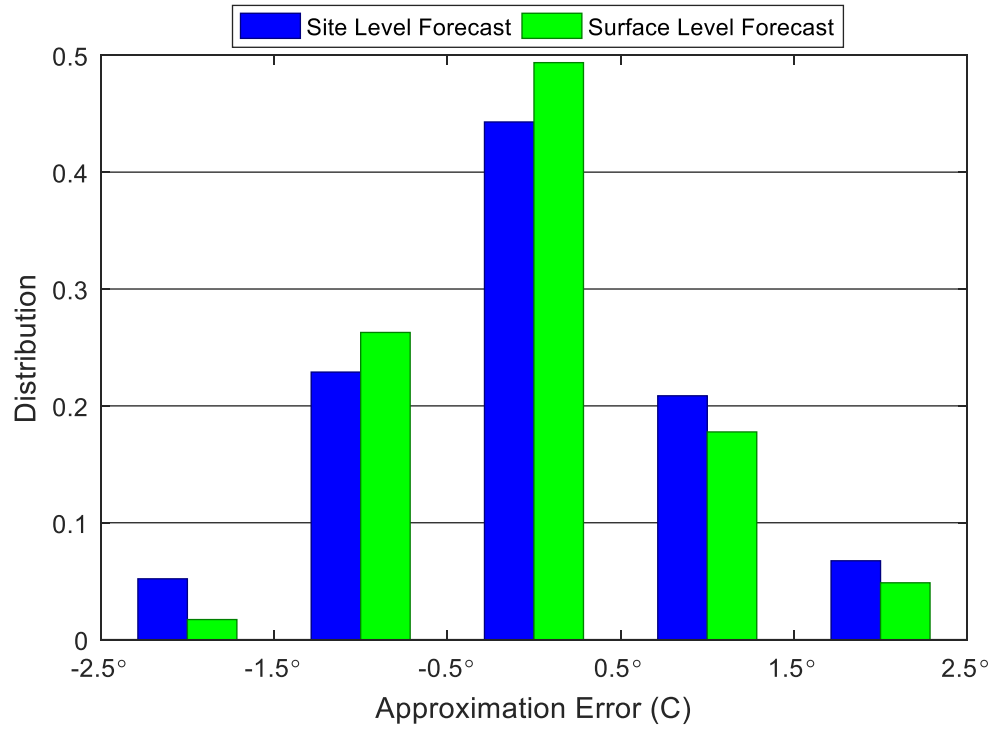


Figure 5.25 2N HRF ZRT-ZAT approximation error distribution

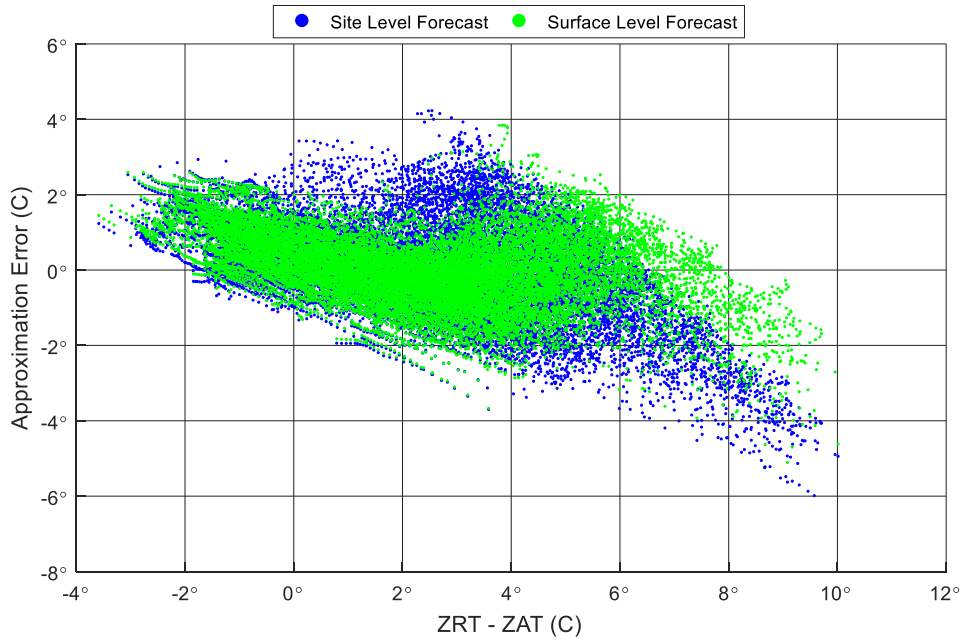


Figure 5.26 2SW HRF approximation error of ZRT-ZAT vs ZRT-ZAT

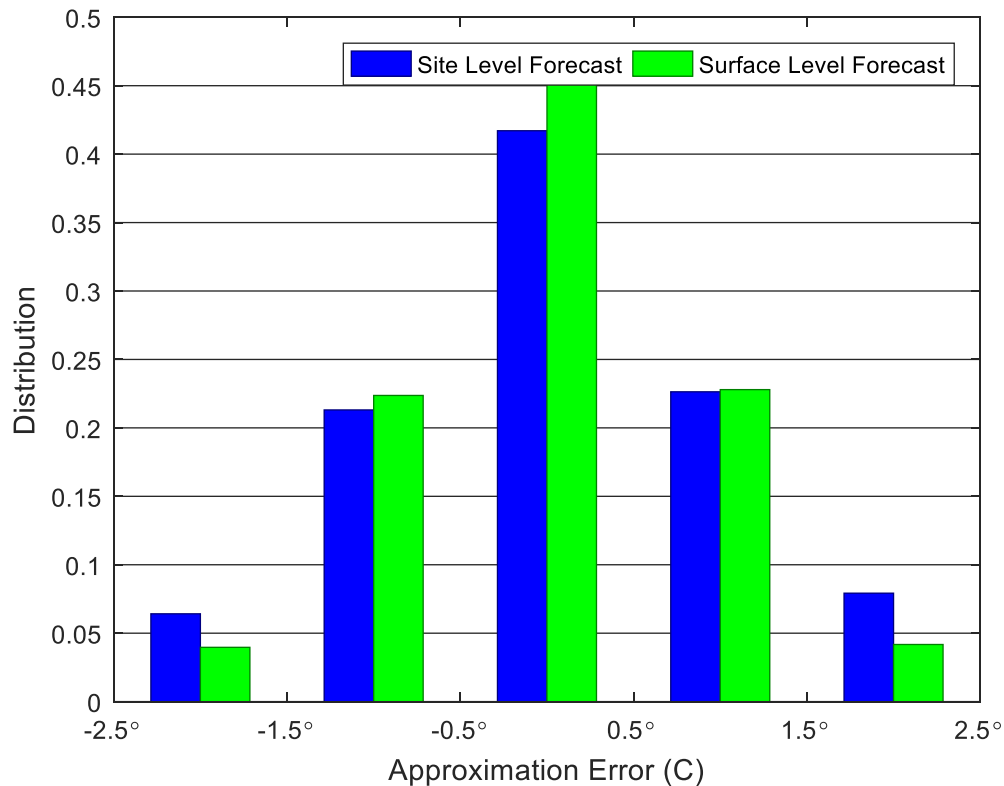


Figure 5.27 2SW HRF ZRT-ZAT approximation error distribution

5.2.8 Direct and Diffuse Solar Forecasting

In an attempt to further improve upon the total HRF solar forecasting results, the direct and diffuse solar radiation components were separated. It was expected that a further improvement should be gained as direct radiation should cause a larger increase in ZRT compared to the diffuse components. The new approximation equation to represent the components of solar radiation is listed below (Equation 5.3).

$$ZRT - ZAT = a(\text{Diffuse}) + b(\text{Direct}) + c(\text{Outdoor temperature}) + d \quad 5.3$$

Table 5.8 outlines the differences between Direct and Diffuse HRF and total HRF solar radiation, with the Direct and Diffuse form showing slight improvements in prediction accuracy. The performance is verified by Figure 5.28 through Figure 5.31, which visually show the minimal improvements from the total HRF solar radiation method discussed in

Chapter 5.2.7. Overall the components coefficients trend similarly to the general coefficient value, while the ambient air and offset coefficients remain unchanged.

Table 5.8 Comparison of total HRF to component (direct, diffuse) HRF forecasts

Zone	Total HRF solar radiation					Direct and Diffuse HRF solar radiation					
	Solar	Ambient Air	Offset	r^2	F	Diffuse	Direct	Ambient Air	Offset	r^2	F
2SW	0.0098	0.1108	-0.396	0.838	37864	0.0071	0.0114	0.116	-0.363	0.842	64576
2N	0.0118	0.2124	-2.997	0.912	80192	0.0102	0.0154	0.214	-2.966	0.914	55011

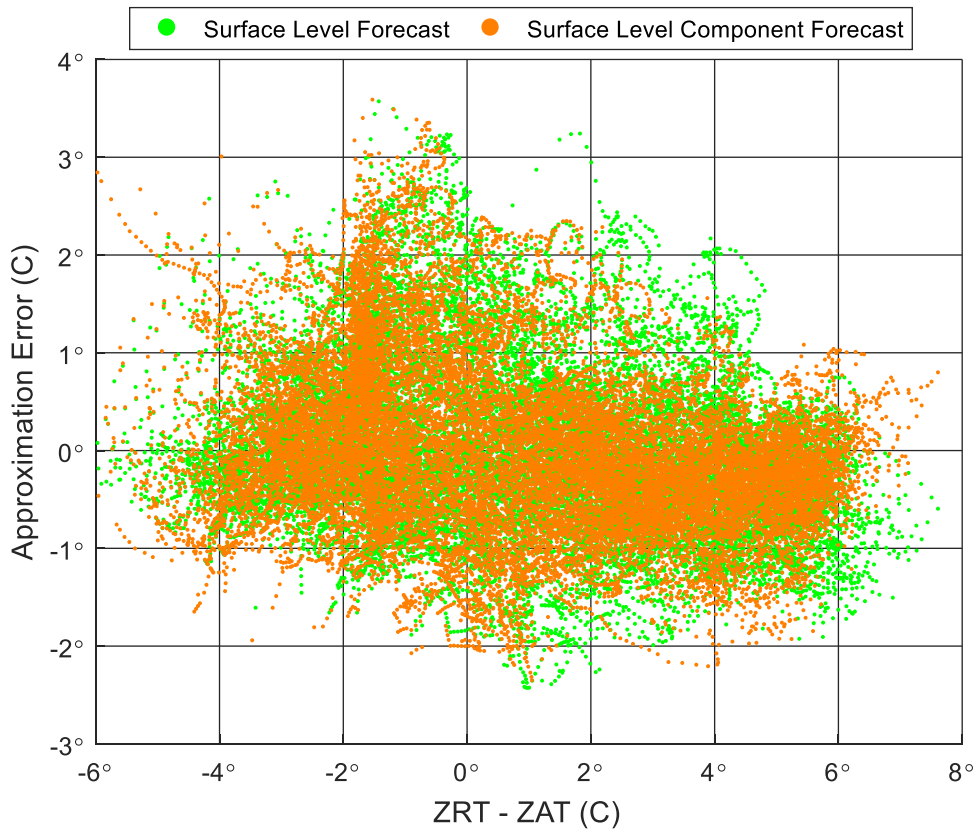


Figure 5.28 2N Direct and Diffuse ZRT-ZAT approximation error vs ZRT-ZAT

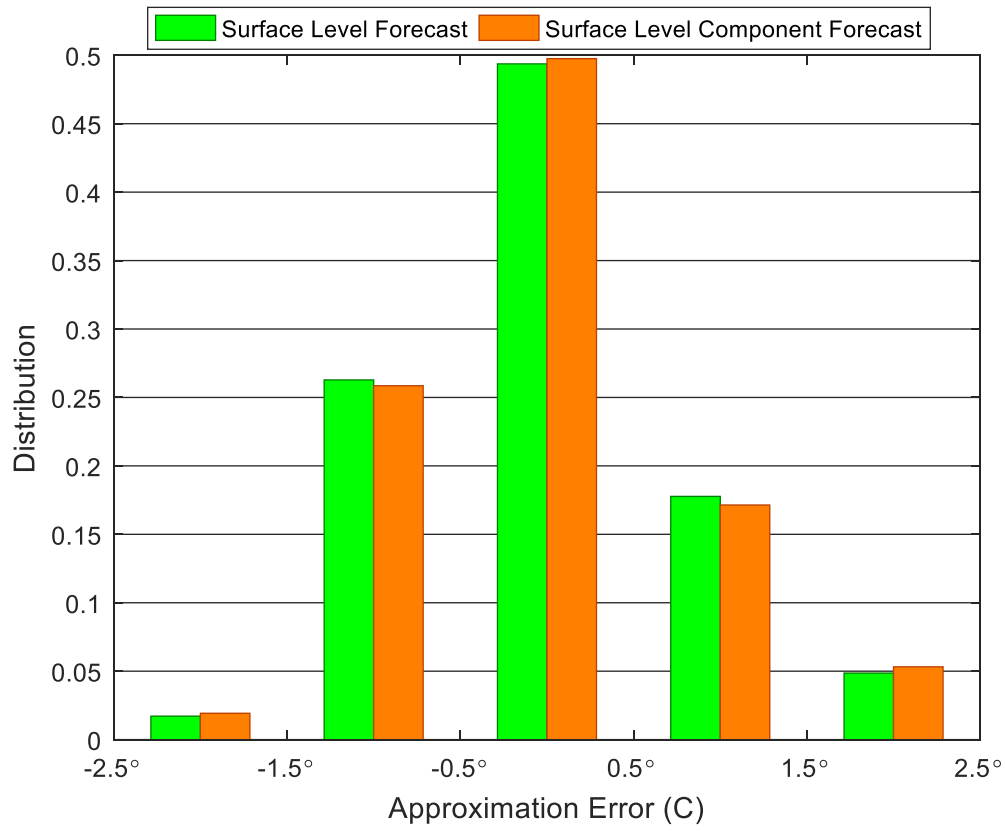


Figure 5.29 2N Direct and Diffuse ZRT-ZAT approximation error distribution

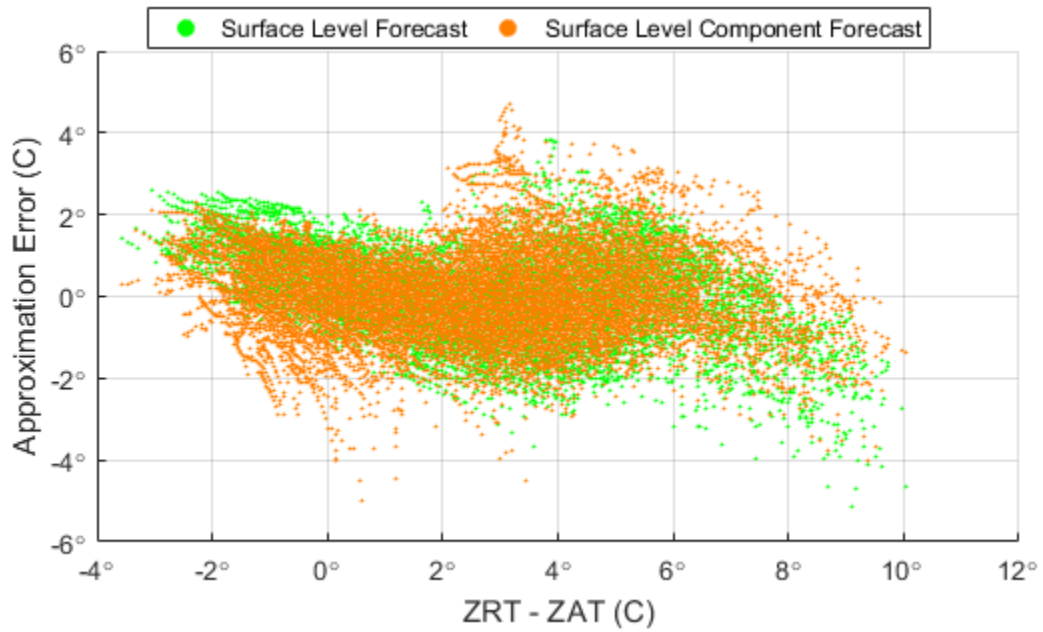


Figure 5.30 2SW Direct and Diffuse ZRT-ZAT approximation error vs ZRT-ZAT

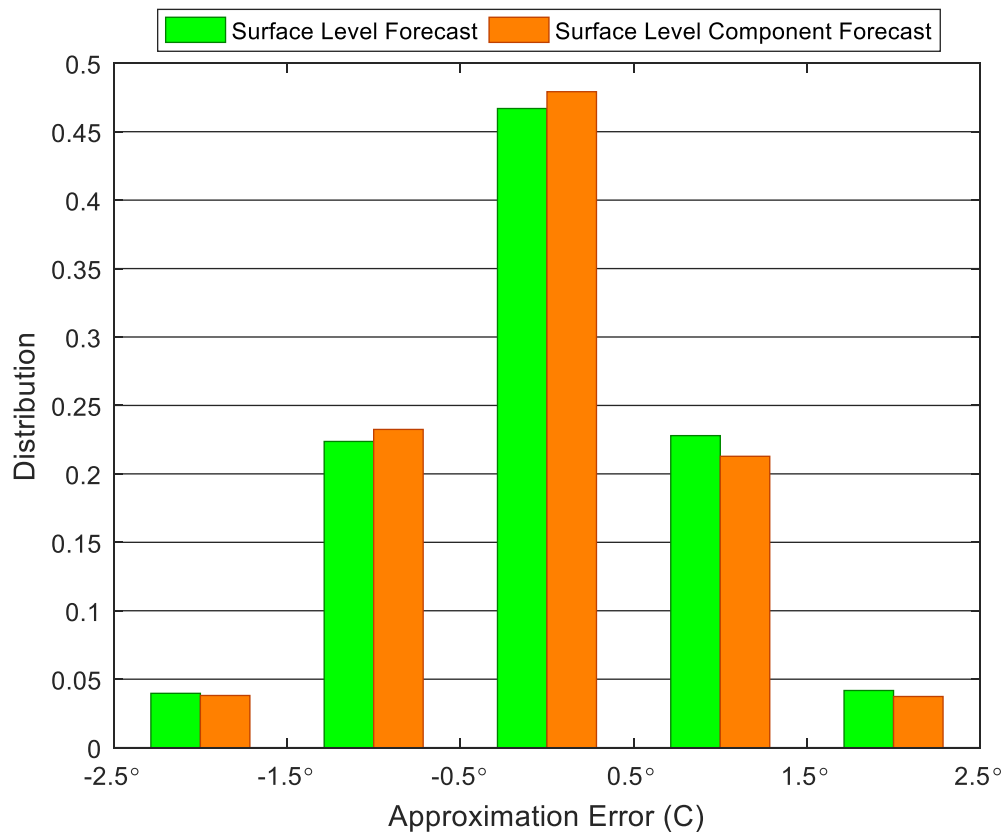


Figure 5.31 2SW Direct and Diffuse ZRT-ZAT approximation error distribution

Due to the improved performance and ability to capture the resolution of GPL's forecasting technology (both spatially and componentially), a full set of zone coefficients for the Mona Campbell building were generated and in Table 5.9. Several conclusions can be drawn from the numerical data outlined in the table:

- The south zones can be approximated as interior zones. This is due to their low percentage of exposed surface area with no windows. An analysis for the ZRT-ZAT difference shows a peak of 2 °C which is also in line with interior zones.
- The middle floor zones located on top of each other (2N and 3N, 2E and 3E, 2W and 3W) behave very similarly and likely can be satisfied with a single set of coefficients. This is due to having consistent boundary conditions and construction.

- Ground floor and roof zones have different characteristics due to their differing boundary layer conditions. The exposed boundary layers lower the offset values, while altering the other coefficients compared to middle floors with more constant boundary conditions.

Table 5.9 Mona Campbell coefficients

Floor	Direction	Diffuse	Direct	Ambient Air	Offset	r ²
1	N	0.0149	0.0094	0.119	-3.569	0.932
1	S	-0.0013	-0.0003	0.014	-0.333	0.297
1	SE	-0.0013	-0.0002	0.043	-0.406	0.675
1	SW	-0.0041	0.0006	0.059	-0.287	0.568
1	W	0.0047	0.0090	0.061	-2.499	0.821
2	E	0.0065	0.0066	0.137	-1.226	0.889
2	N	0.0102	0.0154	0.214	-2.966	0.914
2	S	-0.0015	-0.0003	0.019	-0.345	0.351
2	SE	-0.0010	-0.0004	0.053	-0.443	0.706
2	SW	0.0071	0.0114	0.116	-0.363	0.842
2	W	0.0027	0.0063	0.142	-1.386	0.865
3	E	0.0096	0.0075	0.131	-0.961	0.906
3	N	0.0112	0.0152	0.195	-2.394	0.917
3	S	-0.0012	-0.0004	0.026	-0.220	0.496
3	SE	-0.0010	-0.0010	0.095	-1.170	0.760
3	SW	0.0012	0.0063	0.153	-0.184	0.732
3	W	0.0048	0.0085	0.141	-0.776	0.893
4	A	0.0109	0.0136	0.097	-0.435	0.931
4	E	0.0109	0.0035	0.167	-0.649	0.803
4	N	0.0062	0.0075	0.223	-2.885	0.870
4	S	-0.0017	-0.0008	0.047	-0.443	0.671
4	W	0.0063	0.0066	0.175	-0.893	0.851
Penthouse	All	0.0014	0.0024	0.147	-0.999	0.807

The coefficients of Table 5.9 are visually represented in Figure 5.32 and Figure 5.33. Initially these were sorted by floor level, but it was found to only weakly influence the coefficients. Instead they are organized by zone orientation in color series, which does

show correlation. It can be seen in Figure 5.32 that the majority of the zones have similar diffuse and direct coefficients; indicating minimal performance gains from this change, and that using surface level forecasts accounts for orientation. Figure 5.33 shows that north facing zones have a much stronger ambient air coefficient than south facing zones.

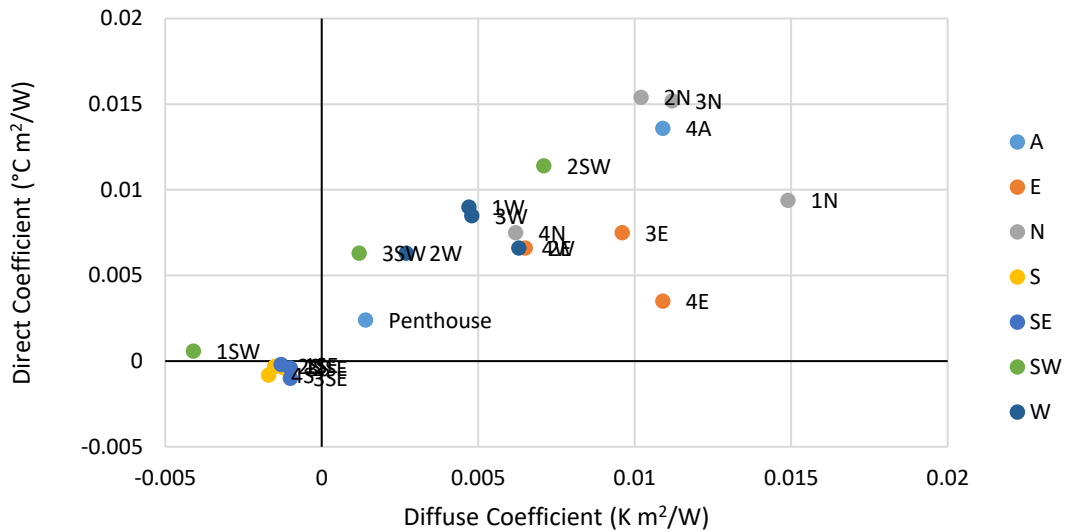


Figure 5.32 Comparison of direct and diffuse coefficients on the basis of zone orientation

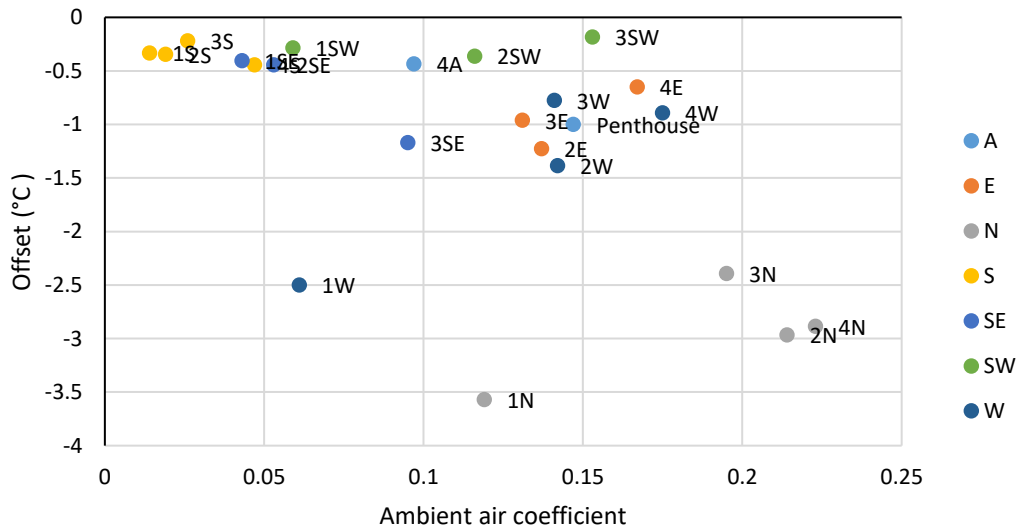


Figure 5.33 Comparison of the ambient air and offset coefficients on the basis of zone orientation

5.3 Conclusions of Zone Operative Temperature Analysis

The results of this chapter indicate that an approximation of ZRT utilizing ZAT, ambient air temperature, and surface level radiation is possible to be utilized for ZOT thermal comfort. The move to surface level forecasts helps reduce the impacts of orientation, however it does not account for construction characteristics (e.g. window to wall ratio, window type, insulation levels). Therefore, it is necessary to create unique coefficients for each zone to be controlled, as opposed to having a universal set of equations that govern prediction differences.

The use of ZOT as opposed to ZAT for thermal comfort is necessary due to MPC's ability to utilize the thermal mass and dynamics of a building to provide comfort, which are not adequately captured using strictly ZAT. The result of this change is improved thermal comfort, but at the potential expense of energy savings (e.g. if only ZAT is used, a later system initialization may occur that does not heat surrounding surfaces). However, due to the importance of occupant comfort the usage of ZOT is necessary for MPC.

While not explored in this dissertation, ZRT effects tend to be time lagged dependent upon thermal mass of the surfaces and how much energy it takes to increase their temperature. The ZRT of opaque surfaces is affected in real time by solar penetration of transparent surfaces, and the time delay due to conduction and thermal capacitance characteristics. Further exploration of these effects would be beneficial to help predict their effect, but would require additional models than what has been explored.

Chapter 6 MODEL PREDICTIVE CONTROL

METHODOLOGY

This chapter details the methodology used to develop the MPC scheme used for both simulation and experimental testing. As outlined in section 2.1, MPC has several key components: a prediction model, objective function, optimization, forecasts of future conditions (such as weather), and a system to control via a control variable (and to provide state feedback) as shown in Figure 6.1. For the work in this dissertation, the control variables are zone level heating and cooling air temperature setpoints. These points can be used to control the ZAT portion of ZOT and minimize the impact of ZRT on comfort. These were chosen as they are the values that determine if space conditioning is needed, and how much conditioning is required. This scheme is a supervisory control implementation similar to [64], and can be applied to all buildings, regardless of HVAC system type which is in contrast to many whole building studies to date that optimize the HVAC components as opposed to the space temperature.

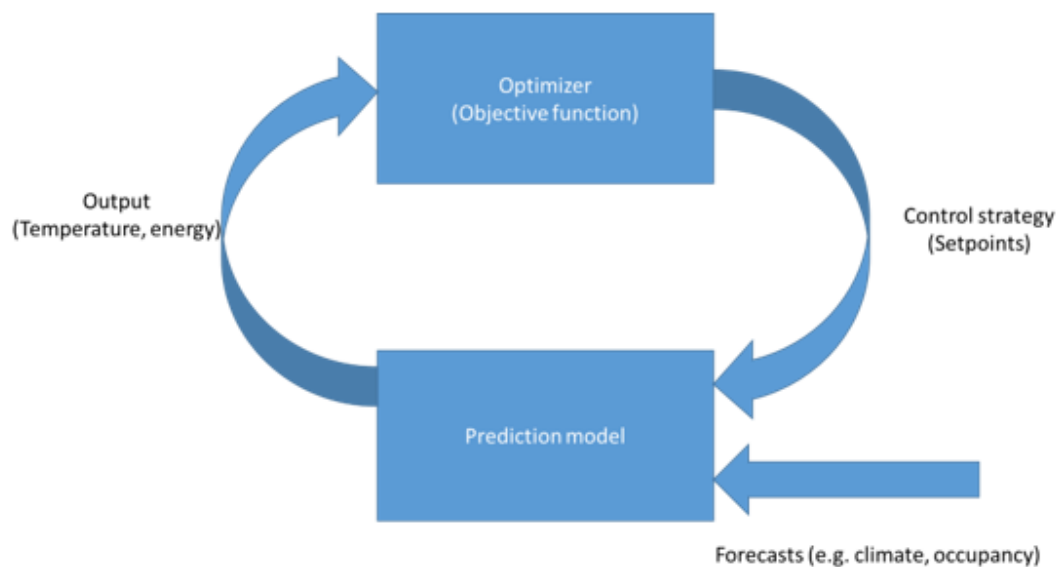


Figure 6.1 MPC optimization loop

In addition to the traditional MPC components outlined above, several additional unique new research components were added/modified for the simulation and experimental implementations. The first of the modified components was to split the optimization into three different time periods: morning start (06:00 to 08:00 Monday to Friday), occupied (08:00 to 22:00 Monday to Friday), and unoccupied (all other periods). This was done as to allow for the use of optimization and objective functions specific to each period. While adjusting terms in the objective function based on time of day is not entirely new (such as only penalizing temperature during the day in [62]), the use of different solution spaces and models was not found in literature. The second modification was to first run the MPC for the whole building to find a globally optimal solution, and then provide zone level adjustments to ensure comfort for zones in which the global solution would cause discomfort. While the work in [17] discusses using whole building energy measurements and zone level temperatures for control, many details are omitted. The layered approach was done due to the computational burden and overall complexity of optimizing all zones of a building at once. The final addition was the incorporation of occupant feedback (experiment only), in which occupants could adjust the range of thermal comfort from the whole building comfort band that was based on ASHRAE Standard 55. Shown in Figure 6.2 is the flow diagram used for the MPC (with no occupant feedback during simulation), where the whole building optimization incorporates the components of Figure 6.1.

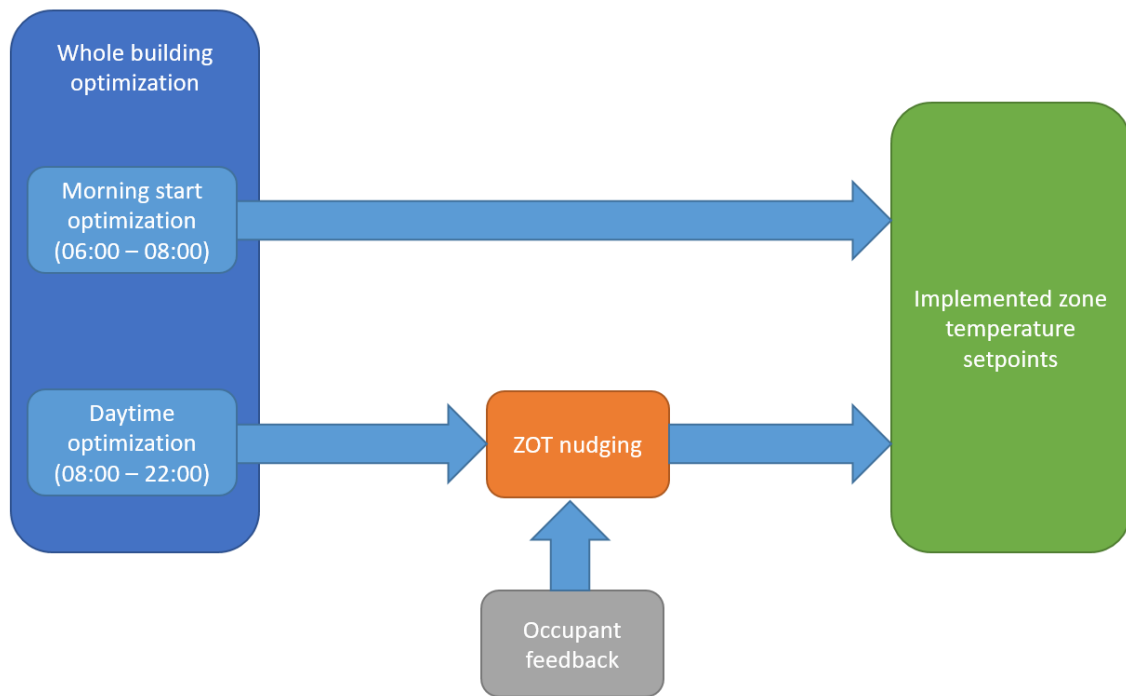


Figure 6.2 Flow diagram of MPC implementation

6.1 Research Tool Use

A method to implement MPC for both simulation and experimentally was needed. While *E+* has the *ExternalInterface* feature, it was originally designed to simply access separately provided files, such as a comma-delimited data file. It was thus necessary to find a software package designed to communicate with it and link to a separate program to perform the predictive controls. The program chosen for this task was the Building Controls Virtual Test Bed (BCVTB)²² which is intended for conducting co-simulation. BCVTB has been developed at the Lawrence Berkeley National Laboratory, and the developers are also involved with the development and maintenance of *E+*. BCVTB is a Java based program that utilizes the Ptolemy II programming language for actor-oriented design. BCVTB has native support for many software packages including Matlab, Modelica, *E+*, and TRNSYS.

For the development of the MPC prediction model and optimization, the statistical computing software *R* was chosen as it has many statistical models for developing a statistical building response model (BRM), and is also a free software package. While BCVTB does not natively support *R*, it does allow users to call custom programs and pass information to them as input arguments (similar to command line arguments), and reading the program outputs. By using this feature, *R* can be connected to BCVTB using *Rscript* to call the developed *R* MPC code. Figure 6.3 shows the flow of information between *E+* and *R* in BCVTB, with the *StringSubstring*, *ExpressionToToken*, *ElementsToArray*, and *ArrayToMatrix* blocks used to convert the output from *R* to a readable form for *E+*, while similar functionality is performed in the *R* code for the *E+* output.

²² <https://simulationresearch.lbl.gov/bcvtb>

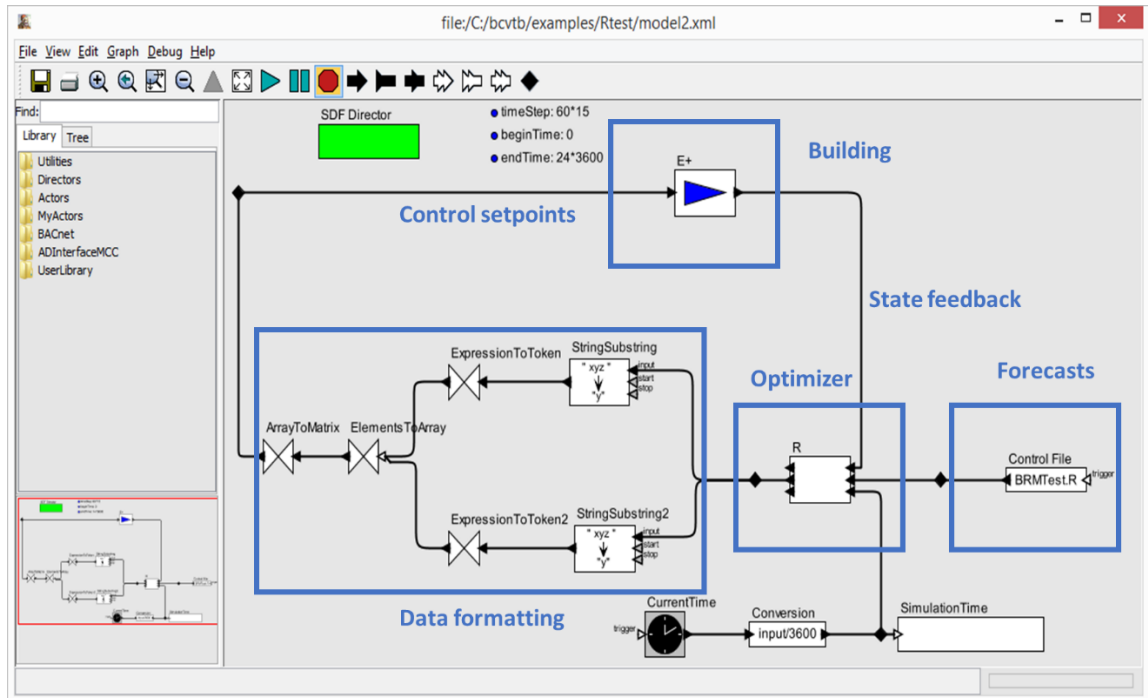


Figure 6.3 BCVTB Interface between *E+* and *R*

To simulate the Mona Campbell Building in *E+* for a full year simulation period takes approximately 30 minutes on a conventional computer core, based on the building complexity. When MPC is employed, several control strategies must be compared for each timestep. As a consequence, a weeklong simulation period of MPC requires about 36 hours to complete. In order to generate a full year of data for analysis it is necessary to divide the simulation into segments and run them in parallel and then assemble them into a single data file. This method is valid as all of the simulations begin and end during the overnight hours for which the setpoints are at the setback values, and all of the simulation methods experience the same conditions (i.e. simulate existing control strategies in the same piecewise manner). If differing setback values are used, or if MPC is not choosing the setback setpoints then error may be introduced by discontinuities at the transition period.

For parallel computing, the Atlantic Computational Excellence Network (ACEnet) has been used, for which *E+* and BCVTB had to be installed and tested. ACEnet is a Linux based high performance computing cluster that utilizes Red Hat Enterprise Linux 4, and contains over 7000 computing cores on 4 independent clusters. The simulations were

partitioned into 52 single week increments to allow for access to the most ACEnet resources and limit the runtime of approximately two days per simulation. This is due a single week of MPC simulation taking approximately 1.5 days of computing time. ACEnet has an increased runtime due to the age of its infrastructure.

For the experimental phase of the work, a Java based adaptor was developed by GPL to connect with Metasys (the building BAS software). The Java program reads in the weather forecasts produced by GPL, as well as the building state from Metasys. The information is then processed by the final operational MPC model (section 6.10) to send setpoints to all zones through a mapping of control points within Metasys.

6.2 Whole Building Model Predictive Control Modeling Method

While *E+* cannot serve as the prediction model, it has a built-in feature called *ExternalInterface* which has been designed for linking *E+* with other computing software for advanced control applications. When using the *ExternalInterface* feature, a co-simulation is performed, with the information flow as outlined in Figure 6.4. As shown, information is passed for every timestep execution of *E+*, where the MPC logic is implemented in the co-simulator that performs predictive analysis. These results are then returned to *E+* and it is allowed to step forward in time. This allows *E+* to serve as the virtual building for simulation.

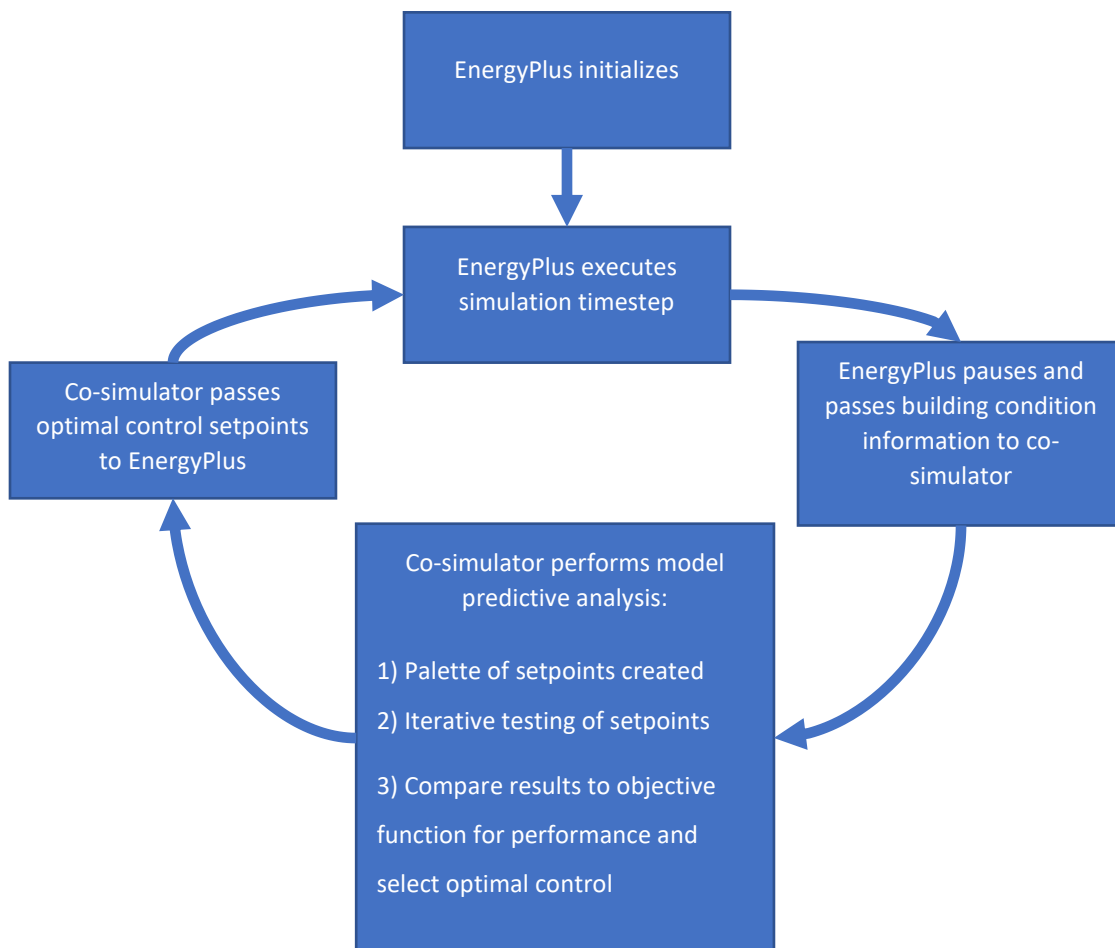


Figure 6.4 Co-simulation process

6.3 Building Response Model

As described in Chapter 2.1, a simplified building response model (BRM) that can be fed a palette of current and desired future conditions is required for the implementation of MPC. Recall that a simplified model is a statistical representation of a building with very fast model execution. Ideally, a building would have years of measurement information to use for the design of both a detailed $E+$ model as well as a BRM. However, most buildings have limited measured data available, and are often limited to monthly energy billing data. These allow an engineer/researcher to develop a detailed and calibrated energy model in software such as $E+$ to ASHRAE Guideline 14 [104]. Ideally the detailed model can be used as the BRM within MPC. However, MPC requires a BRM that can be executed in a short manner, iteratively, and for a variety of initial conditions. To create such a simplified model, a detailed energy model can be simulated for multiple years of climate data with various control strategies to generate training data for the BRM. This data can then be augmented with any measured timestep data from the site for improved accuracy when such data exists, either with a similar weighting to the existing data, or at a higher level of importance (which could be achieved by duplicating the data so it is a higher percentage of the data pool). Site data alone cannot often be used as it lacks the variation of control that MPC looks to exploit, such as various morning start times or daytime setpoints. The statistical model can then be retrained periodically with measured data from the site for improved accuracy and to account for any operational changes (i.e. new equipment, change in occupancy schedule)

To generate the data needed to create a BRM, a calibrated detailed energy model can be run with various control strategies for the same or varying climatic year. The various control strategies would alter the morning startup time between the current rule based start time and the nominal building occupancy, and consist of randomization on either the heating (nine sets) or cooling setpoint (nine sets) during unoccupied and morning start periods. For the Mona Campbell, there are nine start times between the initial rule based control (06:00) and expected occupancy (07:00), leading to a total of 18 training sets (nine with heating randomization, nine with cooling randomization). The randomization is

required for the model to understand the energy and thermal condition performance between heating and cooling as a simplified BRM has no physics incorporated. During the occupied period a deadband of 2 °C was applied, which varied up and down based on a probability weighted scheme (30% chance to increase by 0.5 °C, 30% chance to decrease by 0.5 °C, 40% constant) to create variations for the BRM, within a temperature band of 20 °C and 24 °C. These variations are needed to allow the BRM to provide the optimization function accurate predictions for deviating from the existing rule-based-control of 21 and 23 °C. An example of one of the training data profiles is given in Figure 6.5, where the cooling setpoint is randomized to allow the model to distinguish the differences between heating and cooling during the morning transition period.

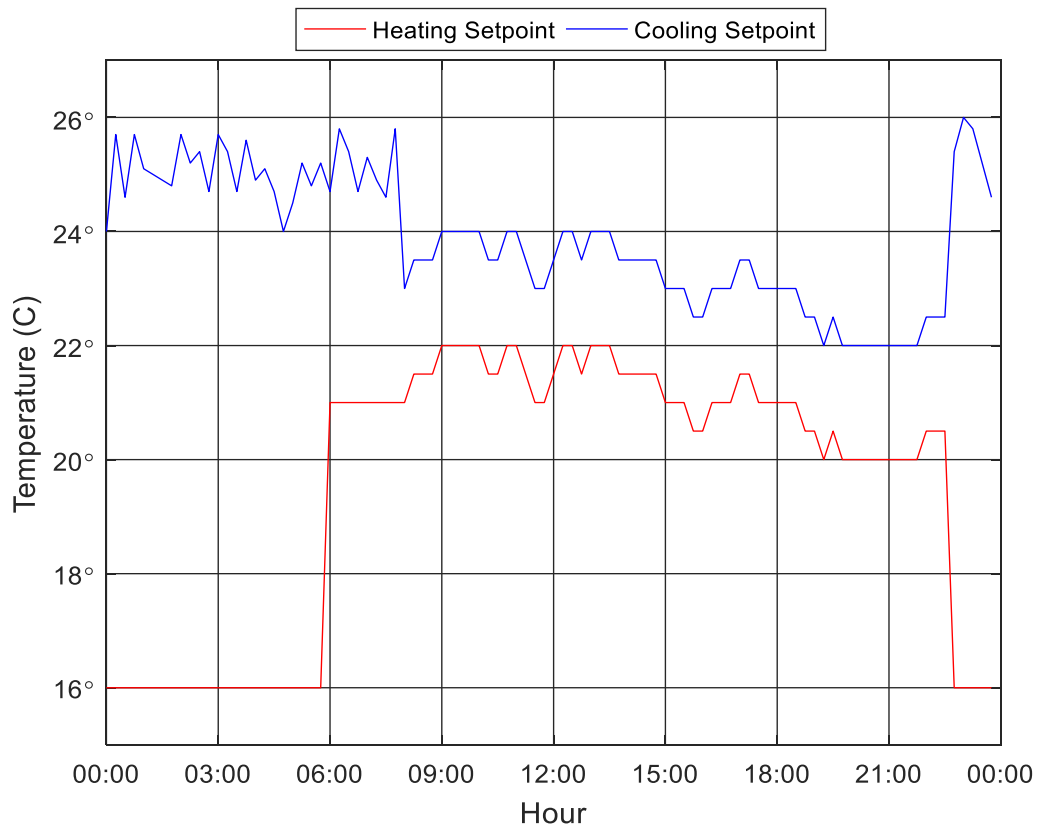


Figure 6.5 Sample training setpoint profile

It is critical an accurate prediction model is used to ensure proper control decisions are made. To achieve an accurate prediction model, a statistical BRM was created using the

randomForest classification model package for the statistical computing software *R* developed by Breiman and Cutler [108] in collaboration with industry research partner GPL. The *randomForest* model works by creating a series of classification trees based on the training data. After a series of trees are created, the *randomForest* model works by sending input data through each tree in the forest to find the most likely output. An example of a classification tree for electricity prediction is given in Figure 6.6, with the order of the branches determined by the model sensitivity to each input. The algorithm also determines the number of branches at each level based on the variability in the training data. Part of the randomization is in how the data is split between the trees, as to ensure no overfitting occurs.

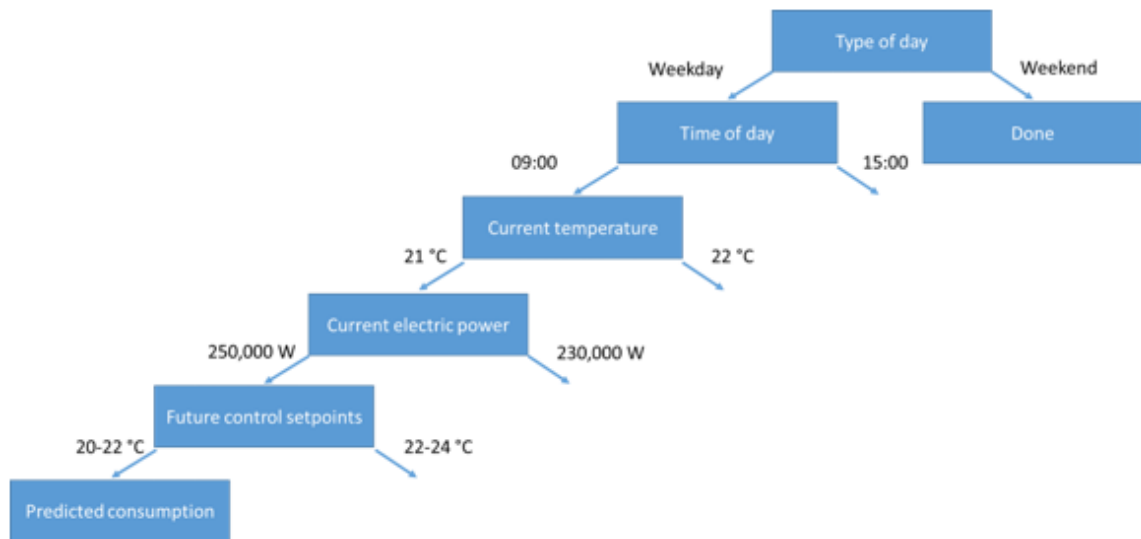


Figure 6.6 Example classification tree for electricity prediction

The *randomForest* model was chosen as it provided the best accuracy (lowest RMSE and percentile errors) when compared with linear regression and neural network models for the same input training data. The model takes as inputs the time of day, the type of day (workday vs non-workday) the current environment conditions (temperature, humidity, direct solar radiation, diffuse solar radiation), current average building ZAT, steam usage rate for the past timestep (15 minutes), electricity usage since the previous timestep, future environment conditions (one timestep ahead), and future zone setpoints (one timestep ahead). These values are chosen based on the ability to measure these values in the BAS.

From this set of information, the model produces estimates for steam usage rate for the next timestep, electricity usage during the next timestep, average building ZAT (as it is the feedback from the building) and average building ZOT (as it is the comfort constraint, see section 6.4) at the next timestep, with the specific details outlined in Table 6.1. The variables time of day and type of day are used to estimate the internal heat generation loads in the building as opposed to using a specific variable for this task. This was done as it can be difficult to measure sources of internal heat generation (such as number of occupants), but they tend to follow time of day patterns [109].

Table 6.1 Model inputs and outputs

Model	Inputs	Output
Electricity	<p>Current building average ZAT, ambient dry bulb temperature, direct solar radiation, diffuse solar radiation, ambient relative humidity, electricity consumption, time of day, type of day</p> <p>Future (1 timestep ahead) ambient temperature, direct solar radiation, diffuse solar radiation, ambient humidity control setpoints</p>	Future (1 timestep ahead) electricity consumption
Steam	<p>Current building average ZAT, ambient dry bulb temperature, direct solar radiation, diffuse solar radiation, ambient relative humidity, steam consumption, time of day, type of day</p> <p>Future (1 timestep ahead) ambient temperature, direct solar radiation, diffuse solar radiation, ambient humidity, building average control setpoints</p>	Future (1 timestep ahead) steam consumption
Building average ZAT	<p>Current building average ZAT, ambient temperature, direct solar radiation, diffuse solar radiation, ambient relative humidity, electricity consumption, steam consumption, time of day, type of day</p> <p>Future (1 timestep ahead) ambient temperature, direct solar radiation, diffuse solar radiation, ambient humidity, building average control setpoints</p>	Future (1 timestep ahead) building average ZAT
Building average ZOT	<p>Current building average ZAT, ambient temperature, direct solar radiation, diffuse solar radiation, ambient relative humidity, electricity consumption, steam consumption, time of day, type of day</p> <p>Future (1 timestep ahead) ambient temperature, direct solar radiation, diffuse solar radiation, ambient humidity, building average control setpoints</p>	Future (1 timestep ahead) building average ZOT

After training a BRM from 18 data sets similar to Figure 6.5, the results for a winter week (4-8 February 2013) and a summer week (5-9 August 2013) of the existing control strategy at the Mona Campbell are shown in Figure 6.7 and Figure 6.8. The results indicate that the BRM does indeed give good representation of “real building” energy demand (given as $E+$ values). Minimal error exists between the predicted value and measured value, with electricity having a peak error of 12 kW (or 3%) and RMSE of 1.8 kW, a steam a peak error of 35 kW (10%) and RMSE of 1.9 KW, and a peak temperature error of 0.3 °C and RMSE of 0.06 °C. The fit of the model is also confirmed by the r^2 values of 0.999 for electricity and temperature, and 0.997 for steam. The model statistics are tabulated in Table 6.2.

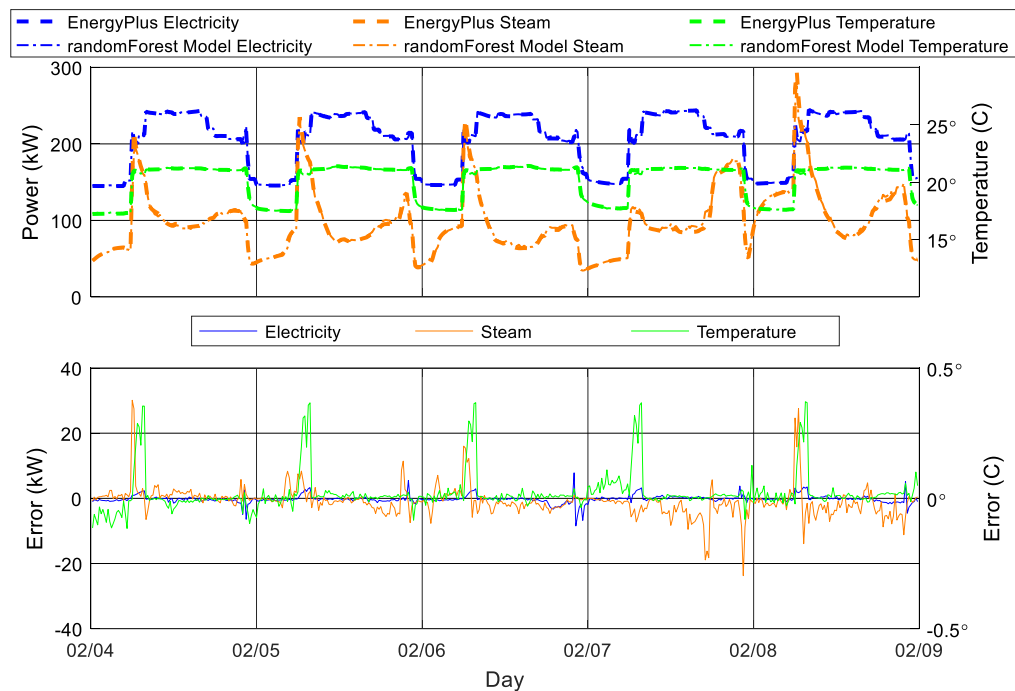


Figure 6.7 Winter BRM performance

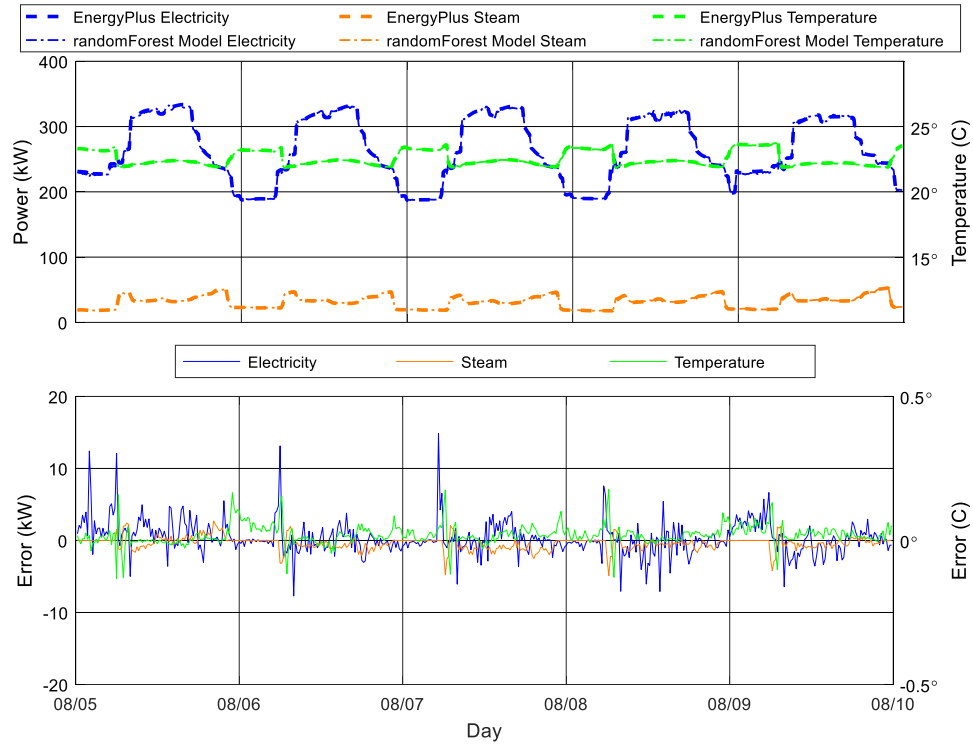


Figure 6.8 Summer BRM Performance

Table 6.2 Annualized BRM fit statistics to *E+* input data

Model	NMBE (%)	RMSE (kW/°C)	CV(RMSE) (%)	r ²
Electricity	0	1.8	2	0.999
Steam	1	1.9	4	0.997
Temperature	0	0.06	0	0.999

6.4 Objective Function

The design of the objective function (J) and corresponding variable weightings for the function to achieve the desired outcome must be defined. A minimization based objective function was constructed, where variable O represents a weighting for an energy source, and r represents the varying energy sources, and is shown in Equation 6.1. The summation represents the total objective “cost” at the end of n timesteps (the total horizon of interest). The weights of energy sources can be used to modify the objective function for varying purposes. For example, a dollar value can be applied to each energy source to make a cost optimization, or a greenhouse gas intensity factor can be used to minimize emissions. For the morning start, a constraint on thermal comfort is applied at the initial time of occupancy 08:00 (Equation 6.2), where if the constraint is not met, a penalty of 10^{50} was applied to artificially inflate the cost to indicate the constraint was not met. The comfort constraint is based on ASHRAE Standard 55 shown in Figure 6.9 using assumptions on clothing level (1 clo), metabolic rate (1-1.3 met), air speed (< 0.2 m/s), and relative humidity (20-60%) to build an operative temperature range from 20-26 °C.

$$J = \min \sum_{i=1}^n O \times r \quad 6.1$$

$$20^{\circ}\text{C} \leq T(08:00) \leq 26^{\circ}\text{C} \quad 6.2$$

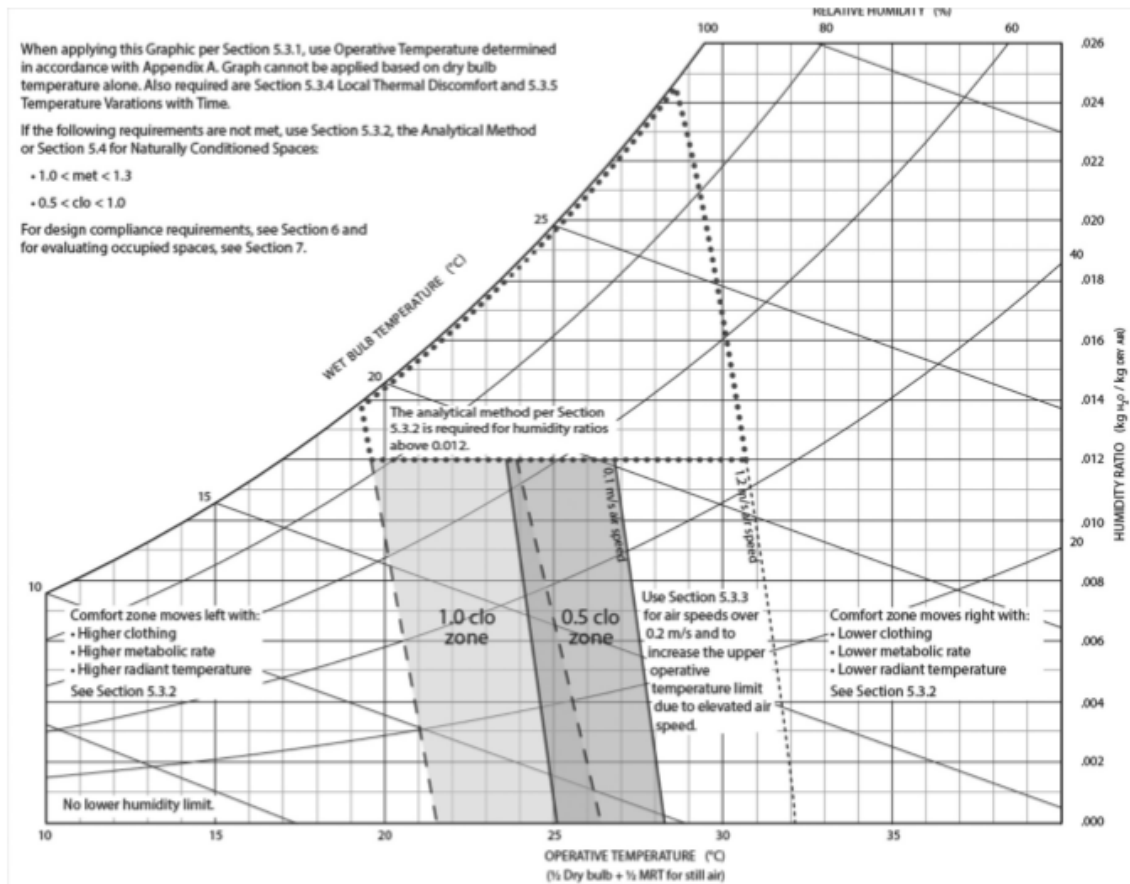


Figure 6.9 ASHRAE Standard 55 graphical comfort chart²³

Additional terms can be added to the cost function on an as needed basis, such as the inclusion of a demand charge term when doing cost optimization. The case of demand charge mitigation can be found in 6.3, where O_{Demand} represents the cost of increasing electric demand, $\max(r_{electricity})$ is the maximum value of electricity power predictions over the n timesteps, and $Peak_{electricity}$ is the current recorded peak electricity demand for the billing period. Note that the summation does not include the demand penalty term, as the

²³ ASHRAE standard by AMERICAN SOCIETY OF HEATING, REFRIGERATING AND AIR
Reproduced with permission of THE SOCIETY, in the format Republish in a thesis/dissertation via
Copyright Clearance Center.

peak demand of the entire forecast horizon of n steps is considered. If the value of $\max(r_{electricity})$ is lower than $Peak_{electricity}$, Equation 6.1 is used.

$$J = \sum_{i=1}^n (O_i \times r_i) + O_{Demand}(\max(r_{electricity}) - Peak_{electricity}) \quad 6.3$$

Additionally, a desire to reduce equipment cycling exist and can be implemented by incorporating a cycling penalty term into the objective function. This is done by penalizing a change in setpoints from their current value, with the penalty to switch decaying over time. An example of this is given in Equation 6.4 for when no electricity demand is considered, where Q represents the penalty to change from existing setpoints, and n_{change} is the number of timesteps since a change has occurred. Similar to the electricity demand mitigation term, the switching penalty is not part of the summation as it is only concerned with the current timestep. Equation 6.5 includes both the electricity demand mitigation and setpoint switching penalty terms, which are not part of the summation.

$$J = \sum_{i=1}^n (O_i \times r_i) + Q/n_{change} \quad 6.4$$

$$J = \sum_{i=1}^n (O_i \times r_i) + O_{demand}(\max(r_{electricity}) - Peak_{electricity}) + Q/n_{change} \quad 6.5$$

6.5 Optimization

With the BRM used to predict the building total electricity consumption, steam consumption, and an average zone temperature (either ZOT or ZAT depending on time of day), it was then necessary to develop an optimization strategy. The optimization is divided into three subsections: morning start, occupied, and unoccupied.

6.5.1 Morning Start

The first period for optimization was the morning start transition period. During the morning start, some limitations are applied to the optimization. The first is when the HVAC system is turned on, it must remain on to avoid unnecessary cycling of equipment. This limits the search space to nine options beginning at 06:00 (turn on any time between 06:00 and 08:00 in 15 minute intervals) down to two options at 07:45 (turn on now or at 08:00). A sample of the morning start transition setpoints can be found in Table 6.3. A brute force optimization method is then applied using the BRM model starting at 06:00 (to decide if turning on at 06:00 is necessary). If the optimal solution is any time other than 06:00 (option 9 in Table 6.3), then the setback is maintained. The optimization is then rerun at each timestep if the system is not enabled, to allow for the use of updated building feedback and forecasts, where the number of options to evaluate is reduced by one per timestep. During the morning transition period, a penalty of 10^{50} is applied if the predicted ZOT temperature of the building is outside of the comfort band at 08:00. If all the potential options have a cost greater than 10^{50} (i.e. none meet the comfort criterion) then the system is enabled in attempt to meet the comfort constraint.

Table 6.3 Morning start optimization heating setpoints (°C) at 06:00

Option	6:00	6:15	6:30	6:45	7:00	7:15	7:30	7:45	8:00
1	16	16	16	16	16	16	16	16	21
2	16	16	16	16	16	16	16	21	21
3	16	16	16	16	16	16	21	21	21
4	16	16	16	16	16	21	21	21	21
5	16	16	16	16	21	21	21	21	21
6	16	16	16	21	21	21	21	21	21
7	16	16	21	21	21	21	21	21	21
8	16	21	21	21	21	21	21	21	21
9	21	21	21	21	21	21	21	21	21

6.5.2 Occupied

A brute force optimization strategy was chosen for occupied optimization, as it allows for the storage of all possible solutions and to ensure the correct control option is chosen. The limitations of such an approach are computational time and the number of possible solutions evaluated. By storing all of the prediction information for each solution, it allowed for detailed system analysis, as any potential issues could be traced back to either the optimization algorithm or the BRM.

For brute force optimization, a set of control options needs to be specified along with the number of timesteps to look ahead. These two parameters determine the number of calculations required according to Equation 6.6. The optimizer has been limited to three options (low, medium, and high temperatures, Table 6.4 based on existing control strategy) and eight step look ahead (two hours at 15 minute timesteps), which lead to 6561 (3^8) solution paths per timestep. The two hour look ahead was chosen to align with the expected time for the building to achieve temperature and minimize computational demand based on the existing control strategy (the building was designed for HVAC to start at 06:00 for

occupancy at 08:00). Due to the exponent relationship, an expansion on the number of options from three to four increases the solution paths to 65536, where an increase in look ahead from eight to nine expands the solution paths to 19683. For the optimization of every zone (32 total) with three unique options and eight step look ahead, the MPC would compute 7.2×10^{15} solution paths (at 1 millisecond per path, a time of two billion hours per timestep), thus justifying the simplifying assumption of utilizing building temperature for optimization.

$$\text{Calculations} = \# \text{Options}^{\# \text{Look Ahead}} \quad 6.6$$

Table 6.4 Occupied period setpoint options (°C)

Option	Heating Setpoint	Cooling Setpoint
Low	20	22
Medium	21	23
High	22	24

The optimizer was coded as a feed forward loop, where the results from one timestep fed the next, constructed as a series of nested for loops. Figure 6.10 highlights this methodology, where the results from Step 1 feed into Step 2, all the way down to Step 8. The search begins by trying option one (low) for the first seven steps. Once at Step 8 all three setpoint options are carried out, and then the code goes back and executes control option two (medium) for Step 7, followed by all three options for Step 8. This continues until all 6561 options have been calculated. On the way down the steps, the cost is calculated at each level, and then summed to provide a total cost for the eight options selected. To determine the optimal solution, a search algorithm was used to find the minimum cost of all 6561 combinations, and then the optimized whole building performance setpoints are determined (the setpoints of step one for the minimum cost of the 6561 options). These setpoints are then compared to the range of allowable temperatures (section 6.7), where comfort based adjustments are made at the zone level prior to implementation. The search function is limited in that if multiple minima exist, it will select the first one that it encounters and use those values.

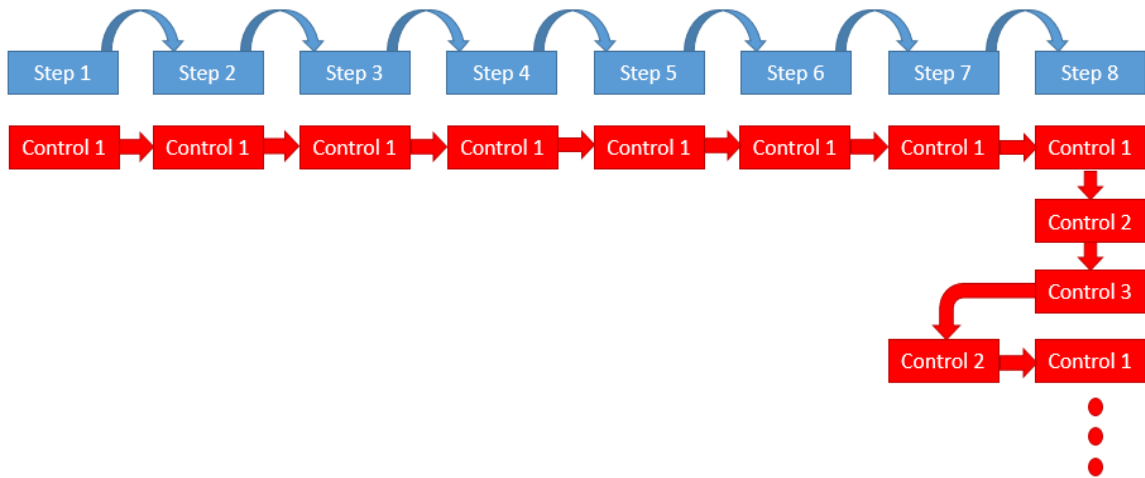


Figure 6.10 Brute force iterative methodology

6.5.3 Unoccupied


During the unoccupied period, the setpoints were set to be the night setback option of 16 and 26 °C. This was chosen as it provides the largest differential between setpoints that was designed for the building, and the morning start window is long enough to bring the building to temperature using the existing HVAC equipment for the setpoint pair.

6.6 Occupant Feedback

While the comfort range developed is based on ASHRAE standards for comfort [48], during the experiment individual offices had the ability to adapt to user preferences through occupant feedback. This mapping is done at each discrete zone. The occupant feedback is used to adjust the occupants band of ZOT comfort.

To gather feedback from occupants, a web based comfort portal was created by Green Power Labs for each occupant in an individual office, with the interface shown in Figure 6.11. The users input their room, and then select from three options: comfortable, too cold, or too warm. The comfortable option maintains the current ZOT comfort band, while the too cold or too warm options increase or decrease the ZOT band by 0.5 °C. This user adjustment was reset after 2 hours as the MPC points which caused the discomfort likely changed (e.g. due to forecasting errors, communication issues), and a return to MPC settings enables further energy savings. Feedback could be given at any time, but would only be implemented during the next 15-minute timestep interval. If no feedback was given, it was assumed the occupant was comfortable with the current space conditions. This feedback collection mechanism is similar to methods used in [110] and [17]. If an occupant provides consistent feedback, adjustments to their comfort range are made (i.e. if a user is always too cold, then an increase in the ZOT comfort range is made for them permanently).

Predictive Building Control

Hello pbcdiem 

Client Request:

Room:

My feeling:
Comfortable
Too cold
Too Warm




Figure 6.11 Client feedback portal

6.7 Zone Operative Temperature Comfort

Due to computational load, a whole building optimization is conducted to find a building average optimal solution. However, zones on various sides of the building experience different ambient conditions (i.e. more sun on the south side than north in North America), which can impact the ZOT through the ZRT. These differences can cause zones to not meet the comfort criteria and require modification to their setpoints. This is done by estimating the difference between ZRT and ZAT (Δ) utilizing ambient temperature, direct radiation, and diffuse radiation. A linear estimation was developed to calculate this parameter according to Equation 6.7. The parameters a , b , and c are scaling factors for the ambient conditions, while d is the offset which can account for construction, thermal mass, and other zone parameters that would influence the ZRT and ZAT relationship.

$$ZRT = a(Diffuse) + b(Direct) + c(Outdoor\ temperature) + d + ZAT \quad 6.7$$

After the optimization is run for the whole building, a ZOT comfort based nudging technique can be applied in the following manner:

1. Only calculate nudges for the occupied period, as thermal comfort is only required during occupancy.
2. Use whole building optimization to create a global, or zone averaged, zone air temperature setpoints prediction, ZAT_{MPC} (results of section 6.5).
3. On a per zone basis, calculate ZRT using Equation 6.7.
4. Apply ZRT to create a ZAT band of comfort using the following equation, where ZOT_{band} is the ZOT comfort range for the zone (20-26 °C based on ASHRAE as outlined in section 6.4, plus occupant feedback adjustments as shown in Figure 6.2):

$$ZAT_{band} = ZOT_{band} - (ZRT - ZOT_{band})$$

5. Check to see if ZAT_{MPC} lies within the ZAT_{band} . The focus should be placed on the setpoint closest to the current zone air temperature as this will be the driving force in changing thermal comfort.
 - a. If True: then $ZAT_{zone} = ZAT_{MPC}$, where ZAT_{zone} is the zone level setpoints to be applied.
 - b. If False: $ZAT_{zone} =$ nearest value within the ZAT_{band} for the setpoint of interest (i.e. heating if below comfort band) plus a differential for the other setpoint.
6. Apply ZAT_{zone} at the per zone level.

An example of how the ZOT nudging shifts setpoints is given in Figure 6.12 for a cloudy, cold day. Due to the cold ZRT (due to windows close to ambient conditions), the space ZOT after applying the whole building MPC setpoints falls outside the comfort band by 0.5 °C. In order to maintain comfort, the setpoint for the zone is boosted by 1 °C such that the ZOT falls within the comfort range of 20 to 26 °C.

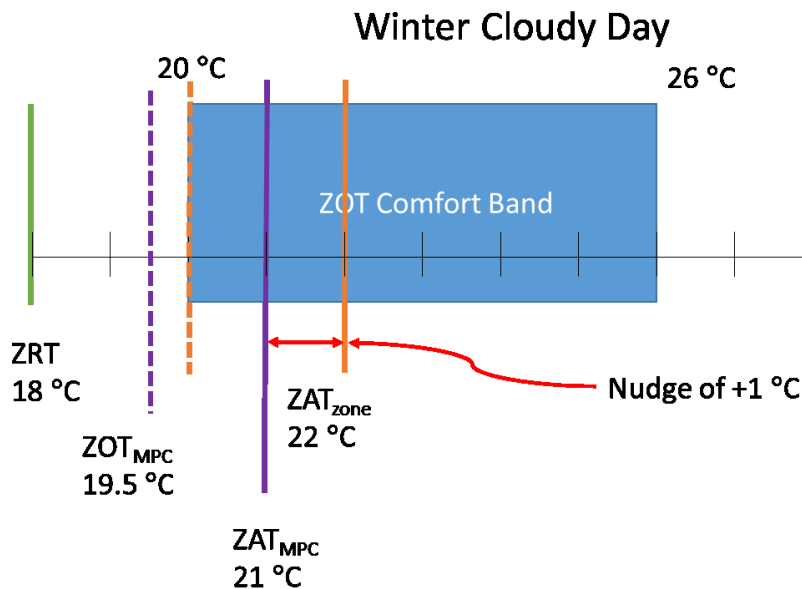


Figure 6.12 Example of ZOT based nudging for thermal comfort

By applying the ZOT thermal comfort as a layer after the energy/cost optimization problem in sections 6.4 and 6.5, thermal comfort is prioritized. This is important as occupant comfort outweighs the value of energy savings, and having comfort as the last layer of the MPC problem ensures it is given the highest priority. This is a key differentiating feature of the research in comparison to other published literature.

6.8 Forecasts

For the simulation based work, perfect weather forecasts were utilized by previously simulating the same weather year for the building, and storing the outputs in a file for later retrieval. The perfect weather forecasts include the site level conditions of dry bulb temperature, humidity, wind speed, wind direction, direct solar radiation, diffuse solar radiation. It also includes surface level forecasts of direct and diffuse radiation for each external face per zone, as calculated by *E+* from the site level data and building geometry. This allows for a theoretical limit estimate of the MPC performance, as real forecasts do contain errors. No occupancy forecasts were used as they are built into the BRM through the use of time of day and type of day as variables.

In the experimental work, weather forecasts were produced by GPL using their SolarSatData²⁴ platform, which produces forecasts of both direct and diffuse on a square meter basis, as well as overall site forecasts for temperature, humidity, wind speed, and wind direction. These values can then be aggregated to match the building surface level discretization produced by *E+*. The forecasts are used as an input to both the BRM and the ZOT comfort nudging as outlined in section 6.7. Predictions are generated through numerical weather predictions, using multiple sources of input data such as ECCC²⁵ and the National Oceanic and Atmospheric Administration²⁶.

²⁴ <https://greenpowerlabs.com/smart-solar-plan-deploy-operate/>

²⁵ https://weather.gc.ca/model_forecast/global_e.html

²⁶ <https://www.ncdc.noaa.gov/data-access/model-data/model-datasets/global-forecast-system-gfs>

6.9 Emulated Model Predictive Control Method

Portions of this section have been submitted to Science and Technology for the Built Environment for publication with Ms. Ref. No.: STBE-00075-2017, coauthored by Dr. Lukas Swan, 23 pgs.

Trent Hilliard is the principal researcher and author of the article. He conducted the research as part of his PhD. Thus, while he received supervision and guidance from his supervisor Dr. Lukas Swan, he carried out the work, wrote the article, and communicated with the editor of the journal. Minor grammatical and content changes have been made to integrate the article within this dissertation.

In addition to the traditional MPC, an optimal morning start-up “emulated MPC” was conducted using an *E+* model as opposed to the BRM, as a benchmark for what the “perfect” traditional MPC using BRM would achieve. By using the detailed energy model, inaccuracies of BRM are eliminated, providing a perfect scenario for comparison. A limitation of the method is that a convergence period is required after the optimization, thus it is limited to once a day task such as morning start (when followed by constant daytime conditions).

Emulated MPC was completed by conducting *E+* simulations of each distinct morning start-up (setpoints and AHU flow) times for every day over the 06:00 to 08:00 period, while maintaining constant conditions otherwise. The time of morning start was shifted by 15 minutes from the RBC values of 06:00 to the occupancy time of 08:00. This results in nine unique options and thus nine simulation runs to analyze, as shown in Figure 6.13. For the morning start-up, both the setpoint temperatures and AHU state were controlled simultaneously to optimize energy usage.

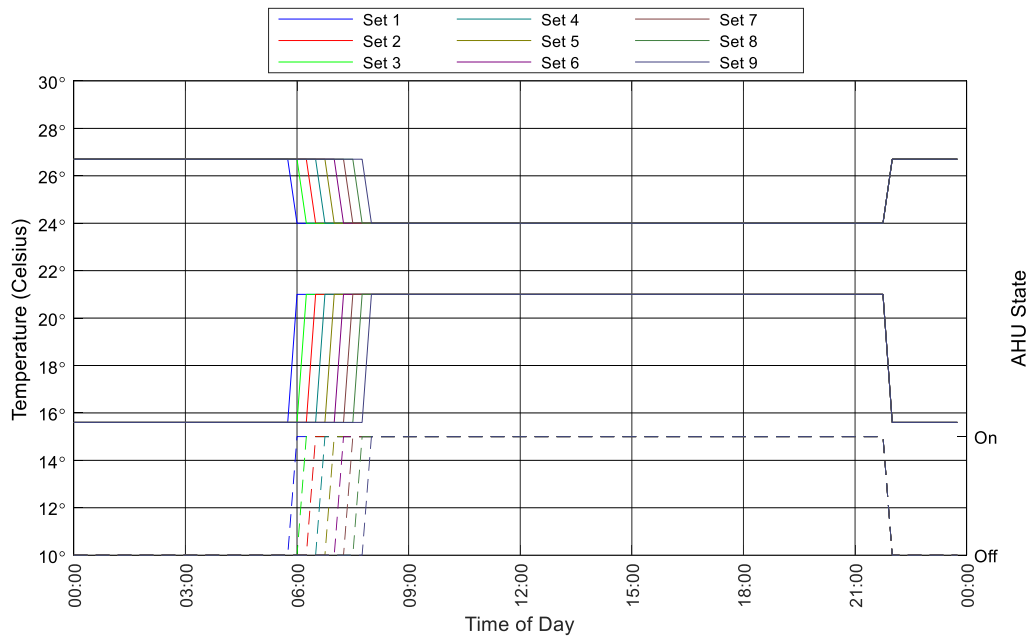


Figure 6.13 Nine unique sets for delayed morning start-up, with zone heating/cooling temperature setpoints (solid) and AHU state control (dashed)

Each of the simulation runs were then analyzed for each weekday (Monday-Friday) to determine if the comfort criterion was met (ZOT of 20 °C to 26 °C at 08:00), how much energy was consumed that day, and peak power demand for the day. An example of this is shown in Figure 6.14, where a setpoint change at 07:15 causes the building to reach the comfort operative temperature (20 °C) by 08:00. Setpoint changes prior to 07:15 heat the building up too early, using additional energy, and setpoint changes after 07:15 do not achieve the necessary comfort temperature until after 08:00.

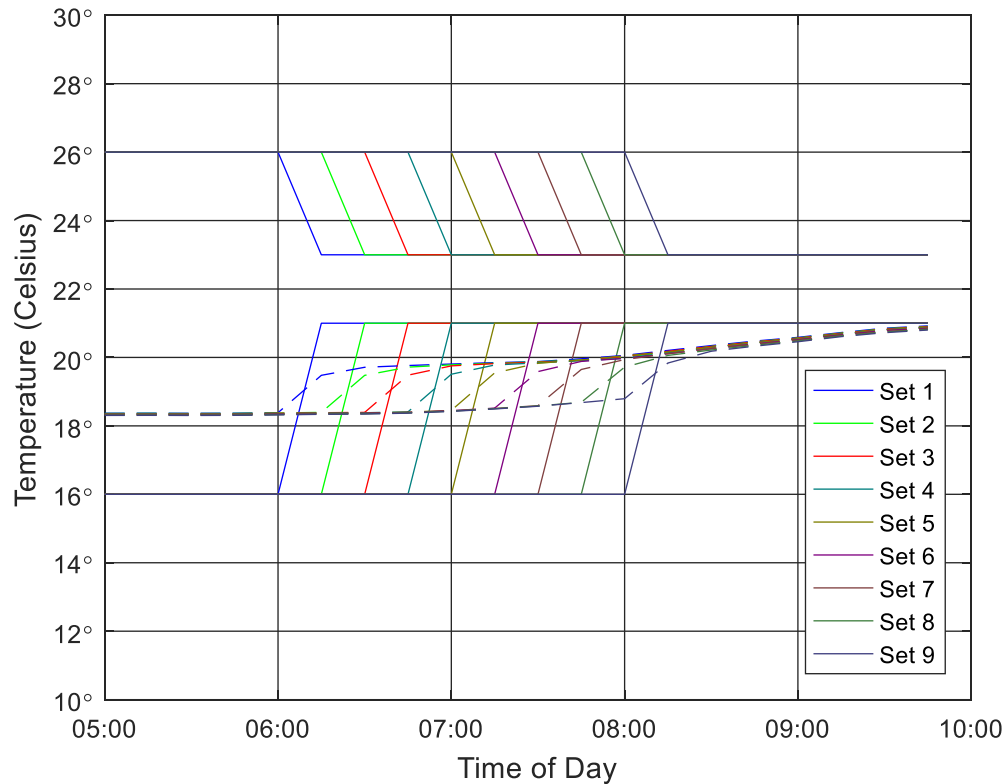


Figure 6.14 Example of nine start-up heating/cooling temperature setpoint scenarios (solid) and the resultant average zone operative temperature (dashed)

After creating matrices of comfort criteria satisfaction, energy consumption for the day, and peak electrical power, analysis could be conducted based on the desired objective function (examples provided in section 6.4). This analysis was conducted for each day of the year to construct a so-called “emulated MPC” file for the year period by placing the selected setpoint transition time for each day into a single file. An example would be if the best start time simulation for January 4th was 06:00 (simulation run 1), and then 07:45 (simulation run 8) for January 5th, the building simulation performance data (i.e. energy, runtime, operation) from the 06:00 simulation for January 4th and 07:45 simulation for January 5th would be pieced together to construct a yearlong period. An example of the start time variation for these days is given in Figure 6.15. This stitching together of control solution days is appropriate given that the simulation results converge during the constant setpoint daytime period, and identical overnight conditions. Finally, the energy

performance results (hourly, daily, monthly, annual) of the emulated MPC can be compared to that of the traditional MPC selections to identify the degradation in MPC performance due to the BRM, or due to other MPC parameters such as the forecast horizon or timestep.

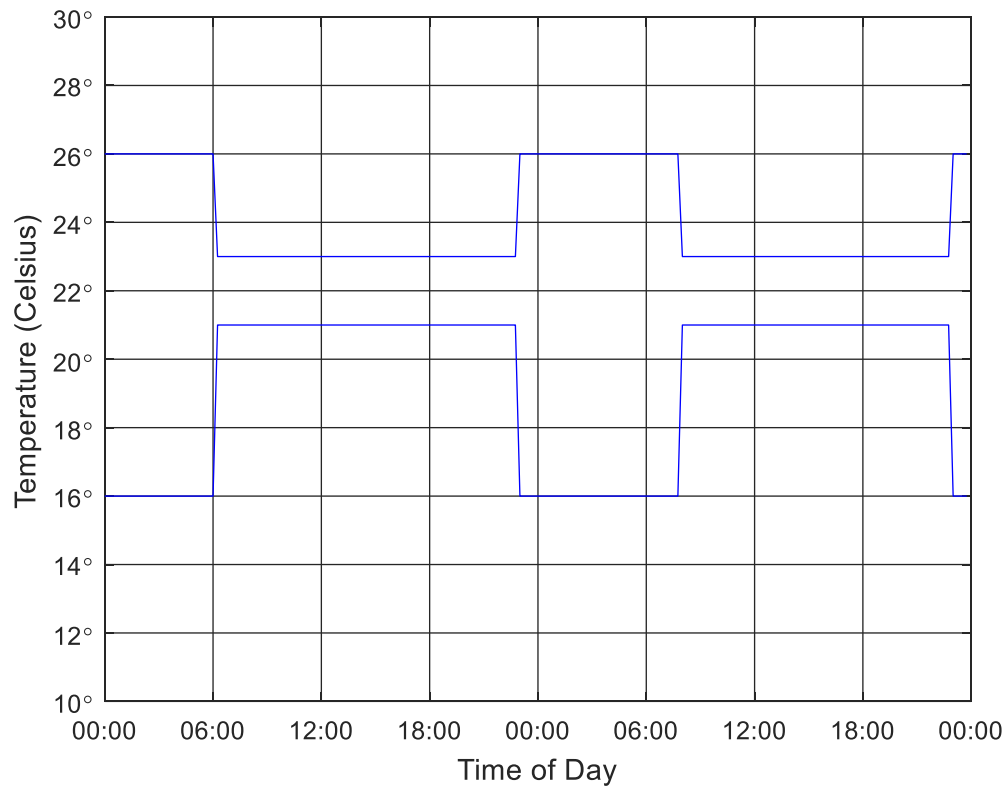


Figure 6.15 Sample of varying emulated MPC start times

6.10 Model Predictive Control Modifications for Experimental Implementation

In order to efficiently implement the MPC on a building in a real-time setting, several modifications to the simulation based approach described were needed. The changes were focused on reducing the runtime of the system, such that a final operational MPC model using weather and current state as in input could be implemented. Figure 6.16 outlines the overall workflow for the experimental implementation. These runtime reductions were necessary due to hardware scan limitations on the BACnet system.

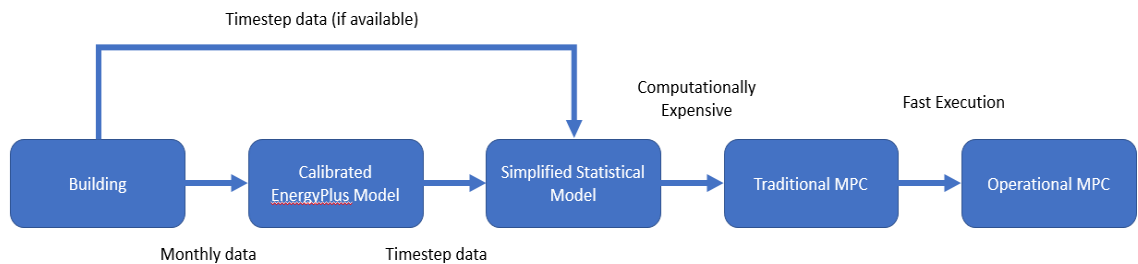


Figure 6.16 Operational MPC workflow

For the morning start, instead of using the BRM and brute force search algorithm, instead the results for emulated MPC were used, with weather forecasts over the time period to determine when to initialize the system. To achieve this, a clustering of results was done using ‘k-means’ clustering [111] to identify the relevant patterns between weather forecasts, current building state, and system initialization time. A total of nine clusters were used to match the potential start times. Clustering of the data works by separating the results into a number of groups, where a selected setpoint pattern can represent the behavior of the entire group. The desired input conditions for each group are then analyzed to find the relationships that then effectively create a look-up table between the inputs and outputs. Clustering was done as it more computationally efficient and utilizes information from the detailed $E+$ model as opposed to relying on the simplified BRM.

During the occupied period, the optimization method was changed from a brute force optimizer to a genetic algorithm. The genetic algorithm utilized 100 options per generation for 10 generations, with the 10 best options carried forward to the next generation. The change in optimizer was done in conjunction with GPL, and was chosen as the entire search space between 20 and 24 °C can be used in contrast to the discrete points utilized by brute force. The genetic algorithm works by first trying 100 random setpoint patterns and compares the results using the objective function. The best 10 results are then carried over to the next generation, with the remaining 90 patterns generated at random, but with a weighting towards the 10 previous results. The process repeats over the 10 generations, where the optimal solution for the last generation is chosen. The use of a genetic algorithm should improve the energy savings performance, as a larger search space is provided. For increased computational speed, a full year simulation using the genetic algorithm was run, and the results were once again clustered using 'k-means' methods based on weather forecasts, this time with five clusters for each two-hour forecast window. By utilizing the same clustering methodology, the results can be appended into a single operational MPC model that uses weather forecasts to determine the control setpoints via the clustered results of both morning start and occupied periods. The use of the clustered solutions reduces the simulation time from two days for one week of results, to 24 hours for one year of results.

Similar to the simulation based setpoint switching penalty in Equations 6.4 and 6.5, a method to limit equipment cycling was needed. To reduce or eliminate HVAC cycling, a threshold change in setpoints of at least 0.5 °C was required before actual setpoints were updated. This is due to the minimal impact on thermal comfort of these small changes, while creating a deadband which minimizes equipment cycling. An additional benefit of the limit was a reduction in network traffic, as only new setpoints needed to be sent to the BAS system.

Chapter 7 MODEL PREDICTIVE CONTROL SIMULATION RESULTS

This chapter details the simulation based results of the developed MPC. First the traditional MPC approach is analyzed, followed by further investigations of total cost reduction inclusive of demand charge utilizing the emulated MPC approach.

7.1 Fixed Energy Prices

The first pricing structure examined was that of fixed energy prices. The pricing information used for electricity was the NSP General Tariff for commercial consumers with a cost of 11.671 ¢/kWh, and a demand charge of 10.497 \$/kW (15-minute average). The pricing for steam was set to 7.4 ¢/kWh²⁷, based on the annual average rate for a class 1 commercial customer with Heritage Gas.

7.1.1 Rule Based Control

To provide a baseline for cost savings, the existing rule-based control strategy for the Mona Campbell building was simulated. For reference, the building runs in occupied mode Monday to Friday from 06:00 to 22:00 with setpoints of 21 and 23 °C. during the unoccupied period, the setpoints are set back to 16 and 26 °C. The sample monthly costs are shown in Figure 7.1 (also in Table 7.1), with electricity energy costs being dominant, followed by the electricity demand charge, and finally the cost for steam. A sample winter week is provided in Figure 7.2, which shows RBC keeps the building in a comfortable range above the lower limit of 20 °C. The electricity demand peaks in the morning when the HVAC system is turned on. The bottom of Figure 7.2 shows the costs associated with the timestep energy consumption (blue, left hand axis), as well the electricity demand charge associated with the week (grey, right hand axis). This visualization demonstrates

²⁷ Actual price varies from 8.5 ¢/kWh in winter to 5.8 ¢/kWh in the summer. The selected 7.4 ¢/kWh is biased towards winter pricing when usage increases.

that the electricity demand charge is set on the first day of the week, as no other day reaches as high of a peak. A similar plot is given for summer in Figure 7.3, where the key differences are that the electricity peak occurs in the afternoon due to space cooling, and steam usage is minimized (only for domestic hot water).

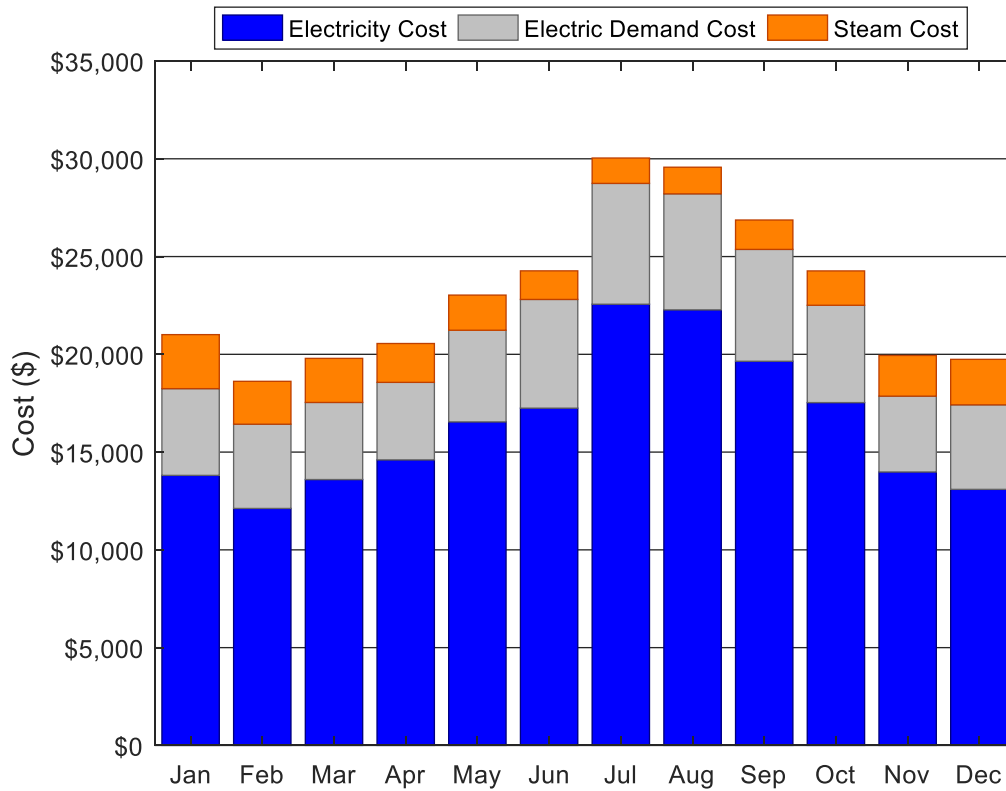


Figure 7.1 RBC monthly costs by source with constant energy prices

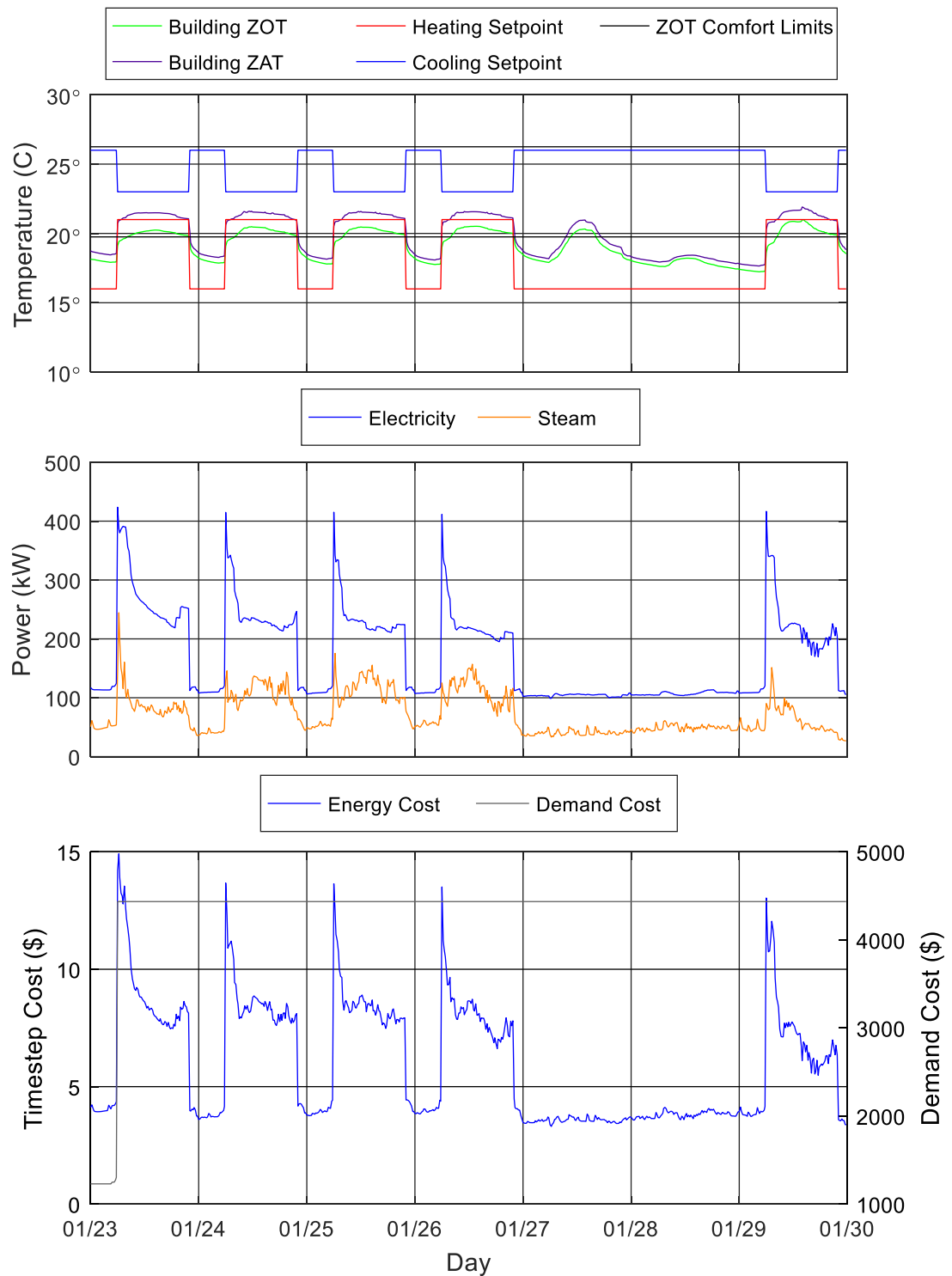


Figure 7.2 RBC winter temperature (top), energy consumption (middle), and costs (bottom) with constant energy prices

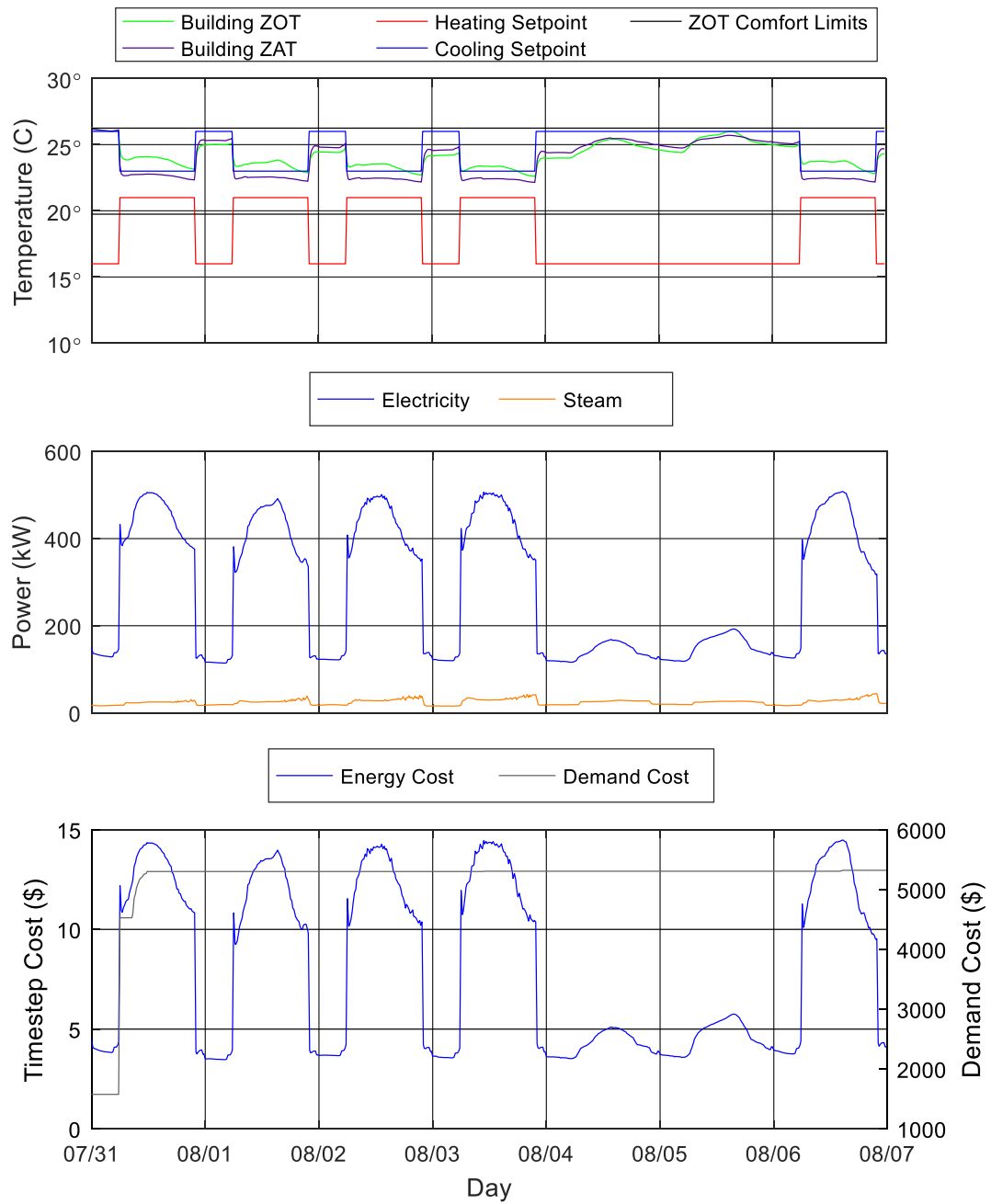


Figure 7.3 RBC summer temperatures (top), energy consumption (middle), and costs (bottom) with constant energy prices

Table 7.1 Monthly RBC energy consumption and costs with fixed energy prices

Month	Total Electricity (kWh)	Total Steam (kWh)	Peak Electricity Demand (kW)	Electricity Energy Cost (\$)	Steam Energy Cost (\$)	Total Energy Cost (\$)	Electricity Demand Cost (\$)	Total Cost (\$)
Jan	125,544	39,472	424	13,810	2,763	16,573	4,435	21,008
Feb	110,176	31,320	412	12,119	2,192	14,312	4,308	18,620
Mar	123,602	32,202	377	13,596	2,254	15,850	3,943	19,794
Apr	132,770	28,394	378	14,605	1,988	16,592	3,962	20,555
May	150,433	25,669	448	16,548	1,797	18,344	4,685	23,030
Jun	156,796	20,901	531	17,248	1,463	18,711	5,560	24,271
Jul	205,126	18,545	590	22,564	1,298	23,862	6,178	30,040
Aug	202,513	19,452	567	22,276	1,362	23,638	5,933	29,571
Sep	178,602	21,477	546	19,646	1,503	21,150	5,720	26,869
Oct	159,384	25,109	475	17,532	1,758	19,290	4,977	24,266
Nov	127,136	29,721	356	13,985	2,080	16,065	3,877	19,942
Dec	119,041	33,224	413	13,095	2,326	15,420	4,324	19,744
Annual	1,791,122	325,486	590	197,023	22,784	219,808	57,902	277,710

7.1.2 Model Predictive Control with Energy Optimization

The first MPC scenario tested was that of pure energy minimization, with no concerns on various energy costs or electric demand charges. The cost value of both electricity and steam was set to 1 to allow for energy minimization, with the cost function outlined in Equation 7.1.

$$J = \sum_{i=1}^8 (O_{\text{electricity}_i} \times \text{electricity}_i + O_{\text{steam}_i} \times \text{steam}_i) \quad 7.1$$

The results for the MPC are tabulated in Table 7.2. A comparison between MPC for energy minimization and RBC was conducted. Figure 7.4 illustrates the monthly costs, which show that for most months, the MPC has a lower cost. The data is tabulated in Table 7.3 which demonstrates that for all months the energy minimization has a lower energy cost, but at the expense of a higher demand cost. In April, May June, and November the increase in demand cost is larger than the reduction in energy costs, leading to an increase in overall operating costs. Overall a cost savings of \$1,273 is achieved, or 0.5%, however a total building energy reduction of 2% is achieved. When analyzing the HVAC components a 5% reduction in consumption exists. Example winter performance is demonstrated in Figure 7.5, which clearly shows the delay in HVAC system initialization, as well as the lower daytime temperatures used to achieve savings. Figure 7.6 shows a sample summer week, where the delay in start drives savings. An evening dip in setpoints occurs in an effort to save steam energy while maintaining electricity levels, however increases in electricity negate the effects.

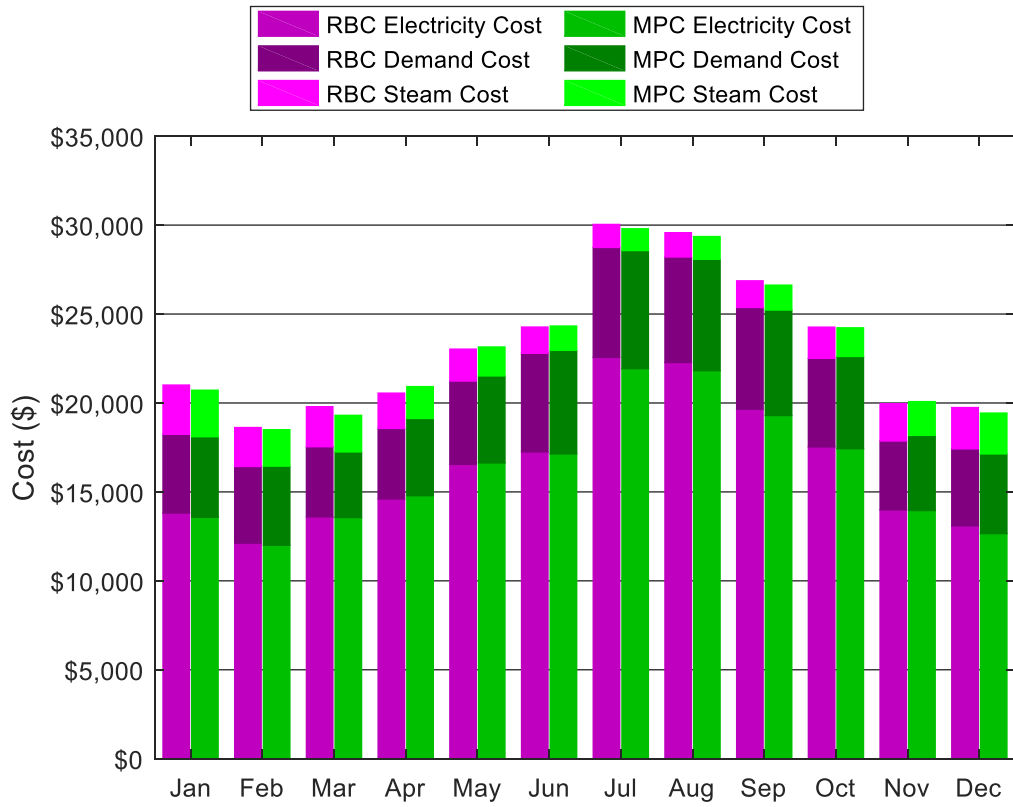


Figure 7.4 Cost comparison of MPC energy minimization vs RBC by source

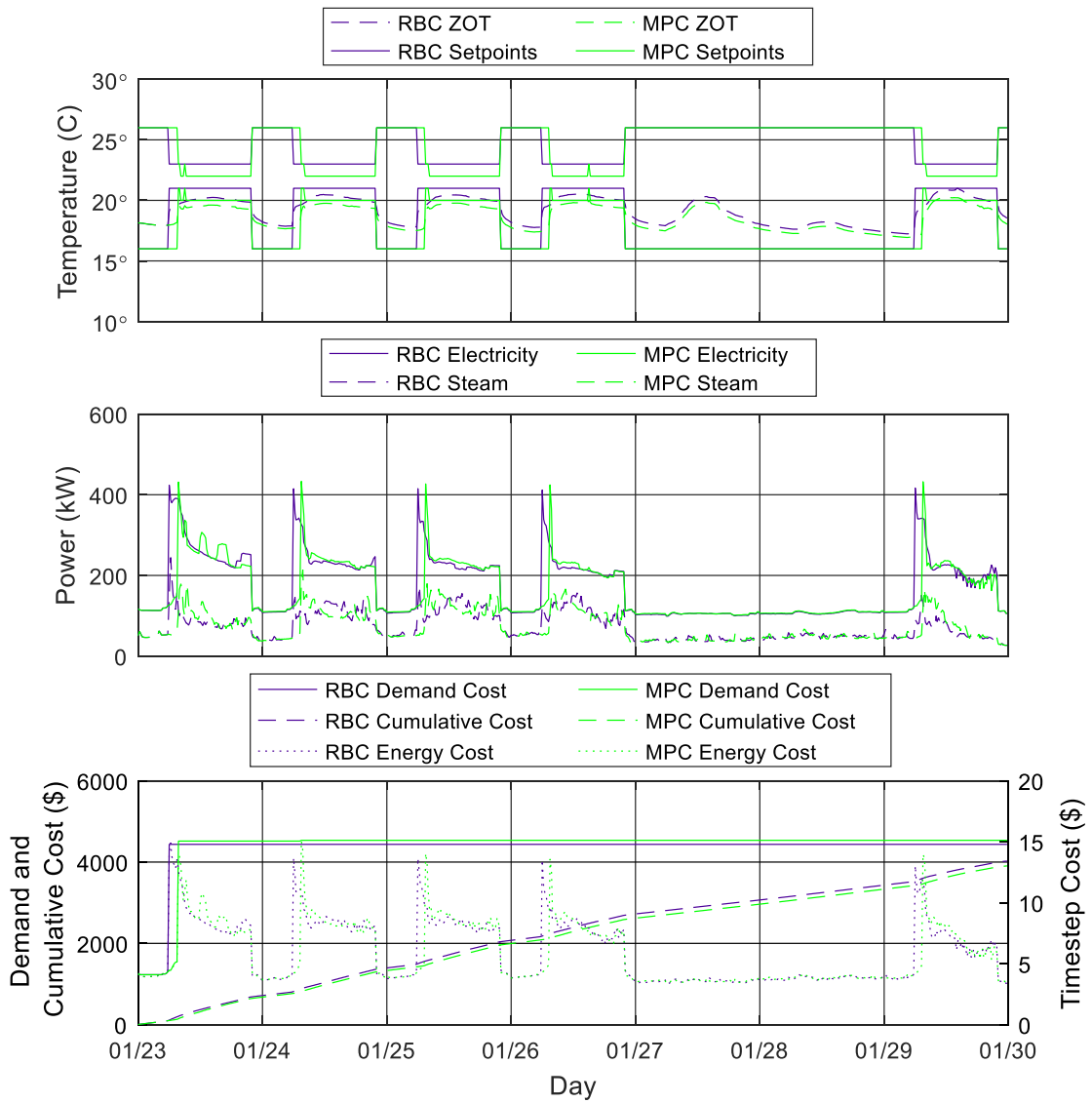


Figure 7.5 Comparison of MPC energy minimization vs RBC winter temperature (top), energy consumption (middle), and costs (bottom)

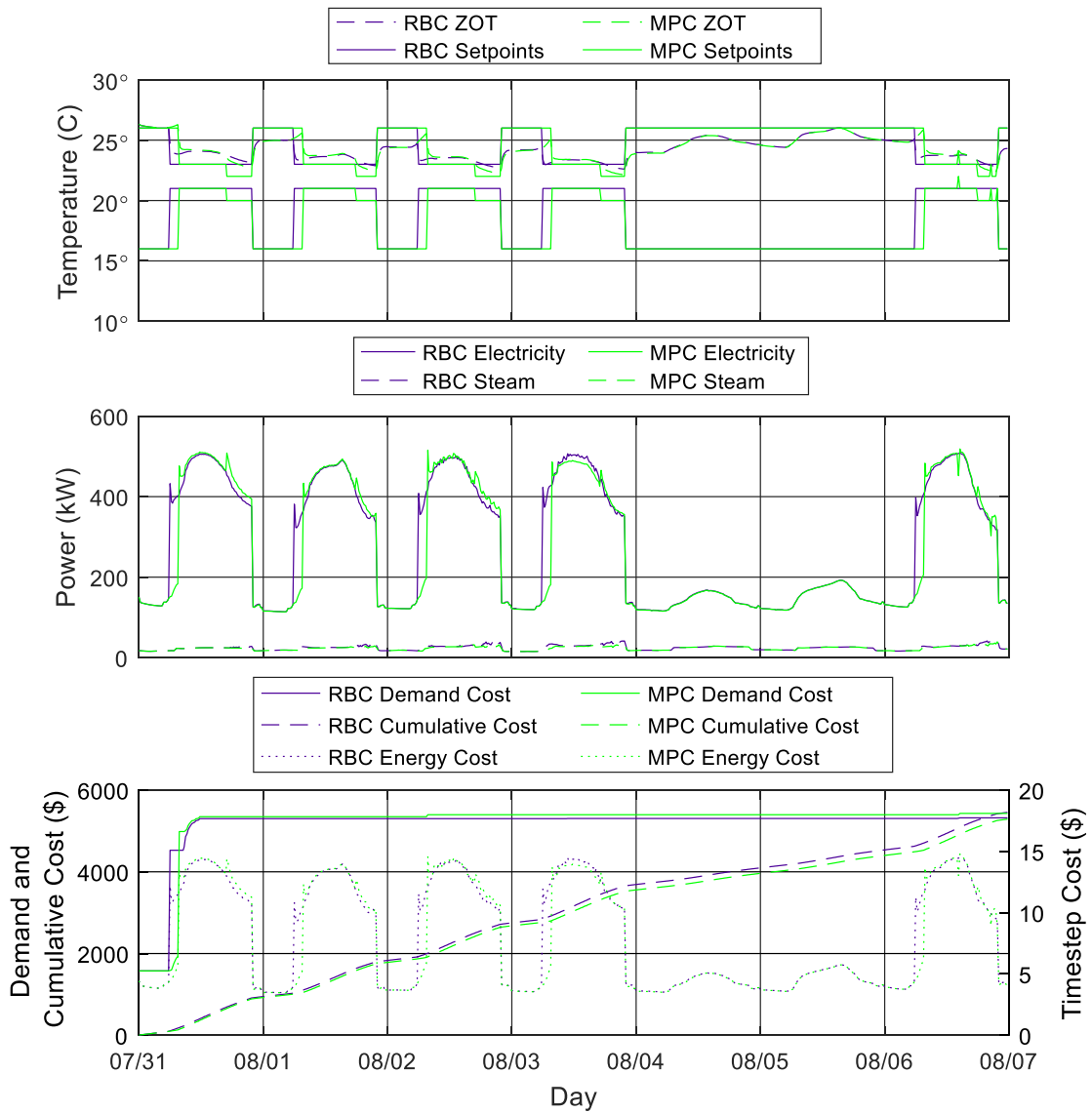


Figure 7.6 Comparison of MPC energy minimization vs RBC summer temperature (top), energy consumption (middle), and costs (bottom)

Table 7.2 Energy minimization MPC energy consumption and costs with fixed energy prices

Month	Total Electricity (kWh)	Total Steam (kWh)	Peak Electricity Demand (kW)	Electricity Energy Cost (\$)	Steam Energy Cost (\$)	Total Energy Cost (\$)	Electricity Demand Cost (\$)	Total Cost (\$)
Jan	123,342	37,390	433	13,568	2,617	16,185	4,535	20,720
Feb	109,094	29,197	425	12,000	2,044	14,044	4,448	18,492
Mar	123,256	29,417	352	13,558	2,059	15,617	3,690	19,307
Apr	134,432	25,641	414	14,788	1,795	16,582	4,339	20,921
May	151,191	23,276	467	16,631	1,629	18,260	4,890	23,150
Jun	155,750	19,576	556	17,132	1,370	18,503	5,824	24,327
Jul	199,364	17,542	634	21,930	1,228	23,158	6,637	29,795
Aug	198,302	18,325	598	21,813	1,283	23,096	6,264	29,360
Sep	175,401	20,048	566	19,294	1,403	20,697	5,929	26,626
Oct	158,445	23,056	495	17,429	1,614	19,043	5,185	24,228
Nov	126,810	27,148	361	13,949	1,900	15,849	4,228	20,077
Dec	115,038	32,841	428	12,654	2,299	14,953	4,482	19,435
Annual	1,770,426	303,457	634	194,747	21,242	215,989	60,448	276,437

Table 7.3 Energy minimization MPC vs RBC monthly cost comparison with fixed energy prices

Month	MPC Electricity Energy Cost	MPC Steam Energy Cost	MPC Electricity Demand Cost	RBC Electricity Energy Cost	RBC Steam Energy Cost	RBC Electricity Demand Cost	Total MPC Cost	Total RBC Cost	Total Savings
Jan	13,568	2,617	4,535	13,810	2,763	4,435	20,720	21,008	289
Feb	12,000	2,044	4,448	12,119	2,192	4,308	18,492	18,620	128
Mar	13,558	2,059	3,690	13,596	2,254	3,943	19,307	19,794	486
Apr	14,788	1,795	4,339	14,605	1,988	3,962	20,921	20,555	-367
May	16,631	1,629	4,890	16,548	1,797	4,685	23,150	23,030	-120
Jun	17,132	1,370	5,824	17,248	1,463	5,560	24,327	24,271	-56
Jul	21,930	1,228	6,637	22,564	1,298	6,178	29,795	30,040	245
Aug	21,813	1,283	6,264	22,276	1,362	5,933	29,360	29,571	211
Sep	19,294	1,403	5,929	19,646	1,503	5,720	26,626	26,869	243
Oct	17,429	1,614	5,185	17,532	1,758	4,977	24,228	24,266	39
Nov	13,949	1,900	4,228	13,985	2,080	3,877	20,077	19,942	-135
Dec	12,654	2,299	4,482	13,095	2,326	4,324	19,435	19,744	309
Annual	194,747	21,242	60,448	197,023	22,784	57,902	276,437	277,710	1,273

7.1.3 Model Predictive Control with Total Cost Minimization

The development of the MPC for cost optimization with electricity demand mitigation involved two key changes from the previously developed energy minimization. The first is converting the energy consumed into a cost based on the energy pricing provided in section 7.1. The second key change was to store and monitor the peak measured electricity demand, which is then compared with the predicted electricity demand values. If the difference in values is greater than 0 (i.e. predicting an increase in electricity demand), this value is multiplied by the electricity demand cost factor and added to the total cost accumulated over the look ahead period (8 timesteps). This method is outlined in Equation 7.2 when the predicted electricity peak exceeds the measured peak electricity:

$$J = \sum_{i=1}^8 (O_{electricity_i} \times r_{electricity_i} + O_{steam_i} \times r_{steam_i}) + O_{Demand}(\max(r_{electricity}) - Peak_{electricity}) \quad 7.2$$

Or when the measured electricity peak is smaller than the recorded peak in Equation 7.3:

$$J = \sum_{i=1}^8 (O_{electricity_i} \times r_{electricity_i} + O_{steam_i} \times r_{steam_i}) \quad 7.3$$

An analysis of the MPC performance is in Table 7.5. A direct comparison is conducted between RBC and MPC for total cost to identify where the MPC worked well, and potential areas for improvement. The first comparison was done on monthly costs, shown in Figure 7.7 and Table 7.5. The MPC performs best in the summer months, where savings of approximately \$1000 per month are realized. This is due to the building being in cooling mode, where the only energy source to optimize is the electrical energy used for cooling the space.

During the winter months, smaller cost savings are realized due to the competing nature of the cost optimization (i.e. electricity wants higher setpoints, steam lower setpoints) causing the optimization to oscillate between options in an effort to save money. This competing nature can be seen in Figure 7.8, where the MPC cycles between heating and cooling mode, with an actual savings in steam compared to RBC when going from higher to lower setpoints. Overall the MPC has a slightly higher electricity peak demand due to shifting

the HVAC loads closer to the building non-HVAC electricity loads, but offsets the increased electricity demand cost through energy cost savings. The majority of the savings during these months is generated through the optimal start time, and not through daytime efforts.

The summer comparison is provided in Figure 7.9, which clearly shows energy savings related to both morning start optimization, and daytime setpoint optimization. A disappointing finding is that the peak electricity demand is higher for MPC case, which is likely due to an under prediction by the BRM of the peak power. This prediction issue has not been a problem when only optimizing energy consumption, as relative gains manifest themselves as savings. However, because maximum demand only ratchets upwards, actual magnitude accuracy is required. Even with the noted shortcomings, an annual cost savings of \$6,527 is achieved, representing 2.4% of total costs, or 5.9% of the HVAC costs.

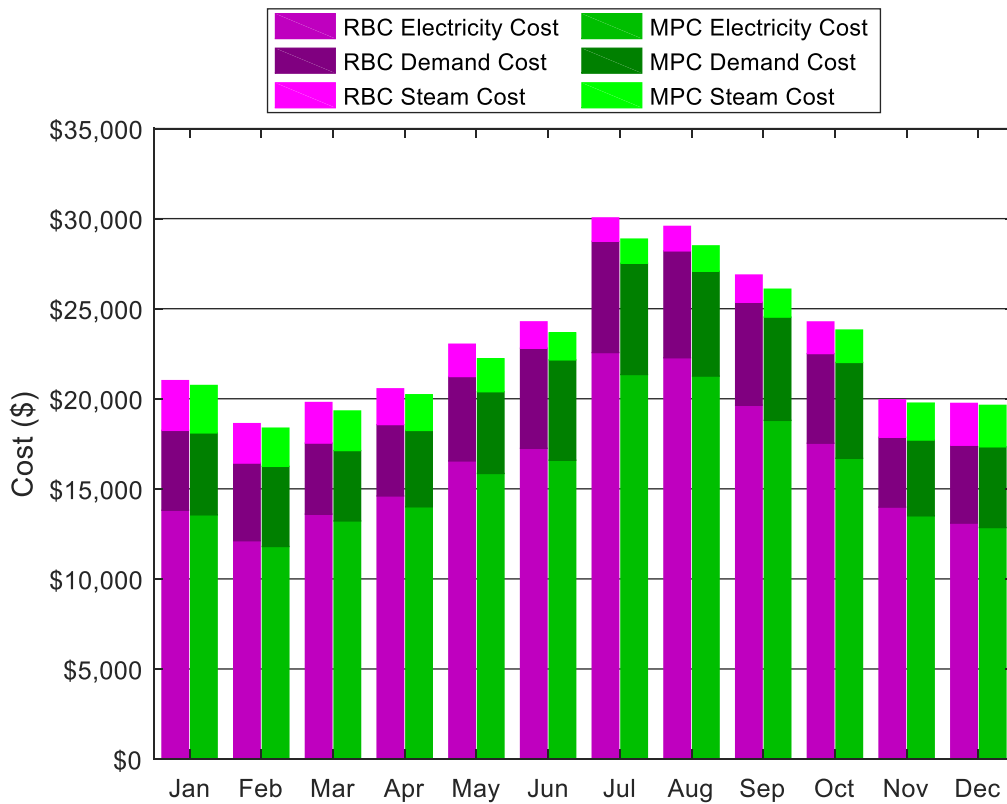


Figure 7.7 Cost comparison of MPC total cost minimization vs RBC by source

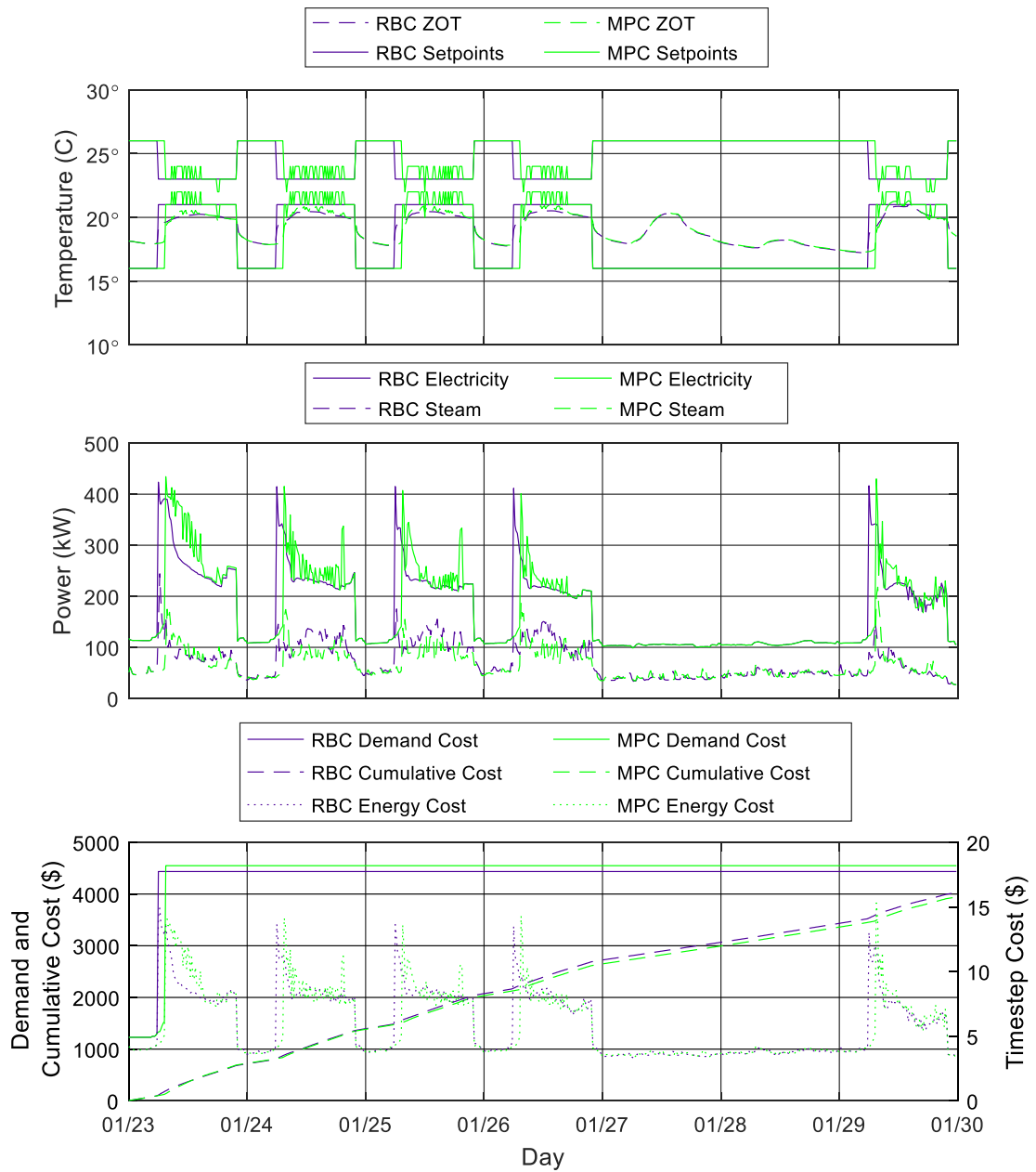


Figure 7.8 Comparison of MPC total cost minimization vs RBC winter temperature (top), energy consumption (middle), and costs (bottom)

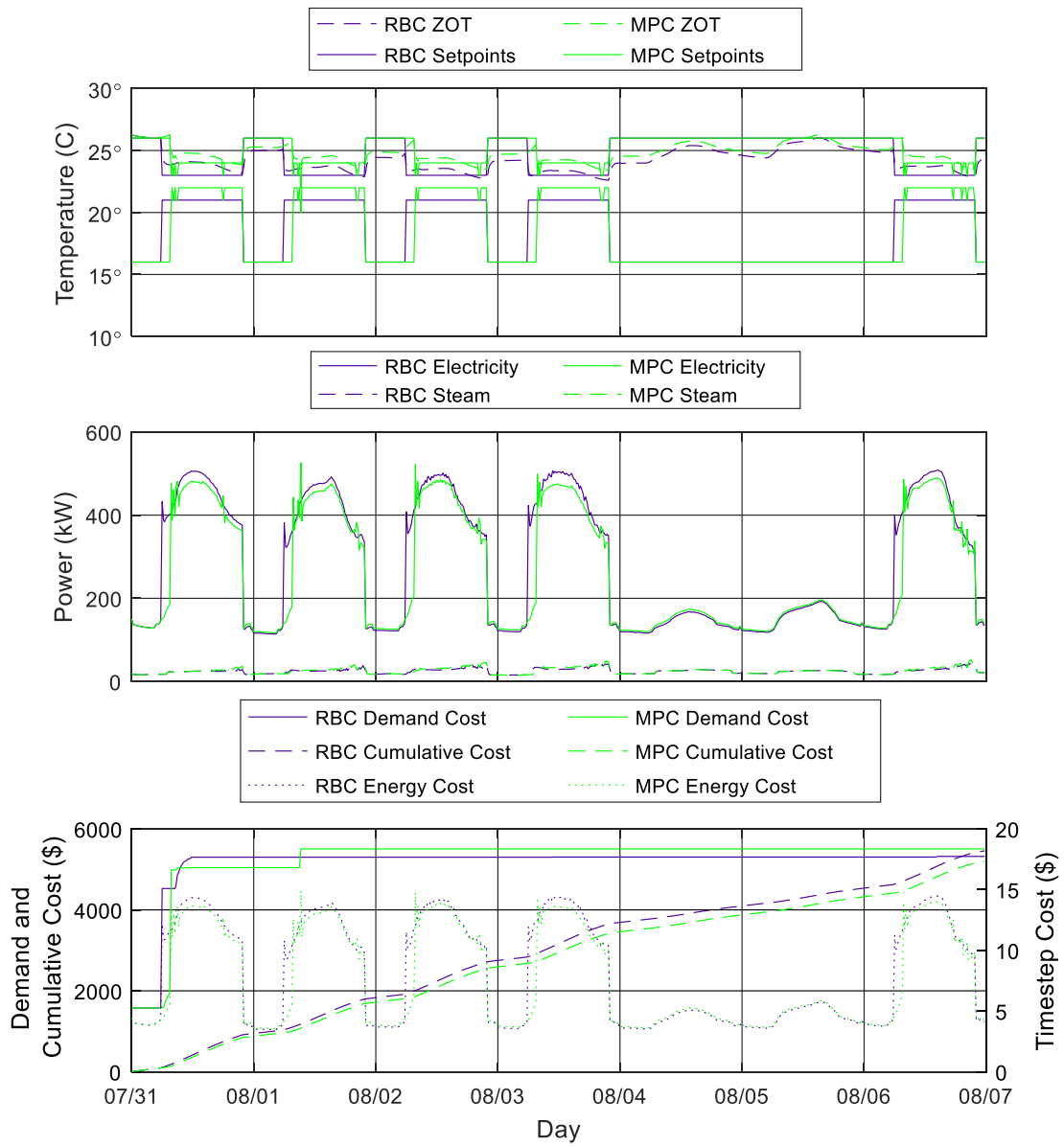


Figure 7.9 Comparison of MPC total cost minimization vs RBC summer temperatures (top), energy consumption (middle), and costs (bottom)

Table 7.4 Total cost minimization MPC energy consumption and costs with fixed energy prices

Month	Total Electricity (kWh)	Total Steam (kWh)	Peak Electricity Demand (kW)	Electricity Energy Cost (\$)	Steam Energy Cost (\$)	Total Energy Cost (\$)	Electricity Demand Cost (\$)	Total Cost (\$)
Jan	123,240	37,627	434	13,556	2,634	16,190	4,548	20,739
Feb	107,264	30,318	425	11,799	2,122	13,921	4,448	18,369
Mar	120,167	31,405	373	13,218	2,198	15,417	3,905	19,322
Apr	127,288	28,362	405	14,002	1,985	15,987	4,239	20,226
May	144,116	26,181	433	15,853	1,833	17,685	4,538	22,223
Jun	150,817	21,429	532	16,590	1,500	18,090	5,568	23,658
Jul	194,060	19,176	590	21,347	1,342	22,689	6,176	28,865
Aug	193,256	20,106	556	21,258	1,407	22,666	5,824	28,490
Sep	170,906	22,150	547	18,800	1,551	20,350	5,732	26,082
Oct	151,765	25,714	508	16,694	1,800	18,494	5,321	23,815
Nov	122,742	29,303	393	13,502	2,051	15,553	4,205	19,758
Dec	116,824	32,893	428	12,851	2,303	15,153	4,482	19,635
Annual	1,722,447	324,665	590	189,469	22,727	212,196	58,987	271,182

Table 7.5 Total cost minimization MPC vs RBC monthly cost comparison with fixed energy prices

Month	MPC Electricity Energy Cost	MPC Steam Energy Cost	MPC Electricity Demand Cost	RBC Electricity Energy Cost	RBC Steam Energy Cost	RBC Electricity Demand Cost	Total MPC Cost	Total RBC Cost	Total Savings
Jan	13,556	2,634	4,548	13,810	2,763	4,435	20,739	21,008	270
Feb	11,799	2,122	4,448	12,119	2,192	4,308	18,369	18,620	251
Mar	13,218	2,198	3,905	13,596	2,254	3,943	19,322	19,794	472
Apr	14,002	1,985	4,239	14,605	1,988	3,962	20,226	20,555	328
May	15,853	1,833	4,538	16,548	1,797	4,685	22,223	23,030	806
Jun	16,590	1,500	5,568	17,248	1,463	5,560	23,658	24,271	612
Jul	21,347	1,342	6,176	22,564	1,298	6,178	28,865	30,040	1,175
Aug	21,258	1,407	5,824	22,276	1,362	5,933	28,490	29,571	1,081
Sep	18,800	1,551	5,732	19,646	1,503	5,720	26,082	26,869	787
Oct	16,694	1,800	5,321	17,532	1,758	4,977	23,815	24,266	451
Nov	13,502	2,051	4,205	13,985	2,080	3,877	19,758	19,942	184
Dec	12,851	2,303	4,482	13,095	2,326	4,324	19,635	19,744	109
Annual	189,469	22,727	58,987	197,023	22,784	57,902	271,182	277,710	6,527

7.1.4 Addition of a Switching Penalty to Total Cost Minimization

Due to the excessive equipment cycling found in section 7.1.2, a method to minimize equipment cycling was introduced. This was done by adding a penalty term (Q in dollars) associated with a change in setpoints, that decreases the longer the setpoints remain constant (n_{change} represents the number of timesteps since the last setpoint change). This penalty term is only invoked when the first setpoints of a MPC sequence differs from the currently implemented setpoints. This makes a new objective function in Equation 7.4 (same as Equation 6.5 as discussed in Section 6.5).

$$J = \sum_{i=1}^8 (O_{electricity_i} \times r_{electricity_i} + O_{steam_i} \times r_{steam_i}) + O_{Demand}(\max(r_{electricity}) - Peak_{electricity}) + Q/n_{change} \quad 7.4$$

When there is no change in setpoints from the currently implemented values, the cost function of Equation 7.2 or Equation 7.3 was used. The various combinations of the cost functions were invoked via *if-else* statements that filter based on a comparison to see if the initial sequence setpoint differs from the last recorded value, and if the peak electricity demand for a sequence exceeds the recorded peak.

To help determine an optimal value for the fluctuation penalty term, a quick analysis of the difference between the highest and lowest cost options for a single timestep was undertaken. This found a typical spread of \$20 when no demand charge changes were present between the highest cost option (approximately \$80 for the two hours ahead) and lowest cost option for a timestep (\$60 for the two hours ahead). This led to the choice of 3 trial penalty values of 1, 2, and 5 as the goal was to prevent unnecessary cycling of equipment, while still allowing for the MPC to choose an optimal cost path. Thus, it was expected that there exists an optimal penalty value that eliminates the minimal differences between options that causes equipment cycling (under a dollar over the two-hour forecast horizon) while still allowing the MPC to switch options to save costs.

The first penalty magnitude considered was 1 (Table 7.6) which showed a reduced oscillation frequency in winter (Figure 7.10) as a direct result of the penalty term. This led

to increased cost savings compared to the total cost minimization MPC (section 7.2.3) due to the reduced equipment cycling. The impact during summer appears minimal (Figure 7.11). The second penalty term explored was a magnitude of 2 (Table 7.7) where the winter performance showed an even further reduction in oscillations, indicating that the penalty term was working as intended. A final penalty term of 5 (Table 7.8) was implemented to help determine the optimal penalty term magnitude, as it was expected that too large of a term would negatively impact cost savings. The winter performance showed further reductions in oscillations, and appeared to possibly be reaching the point of negative impact (i.e. taking too long to correct an incorrect choice). The summer performance also experienced a delay in switching to the upper setpoint level, leading to a loss in potential savings as shown in Figure 7.11.

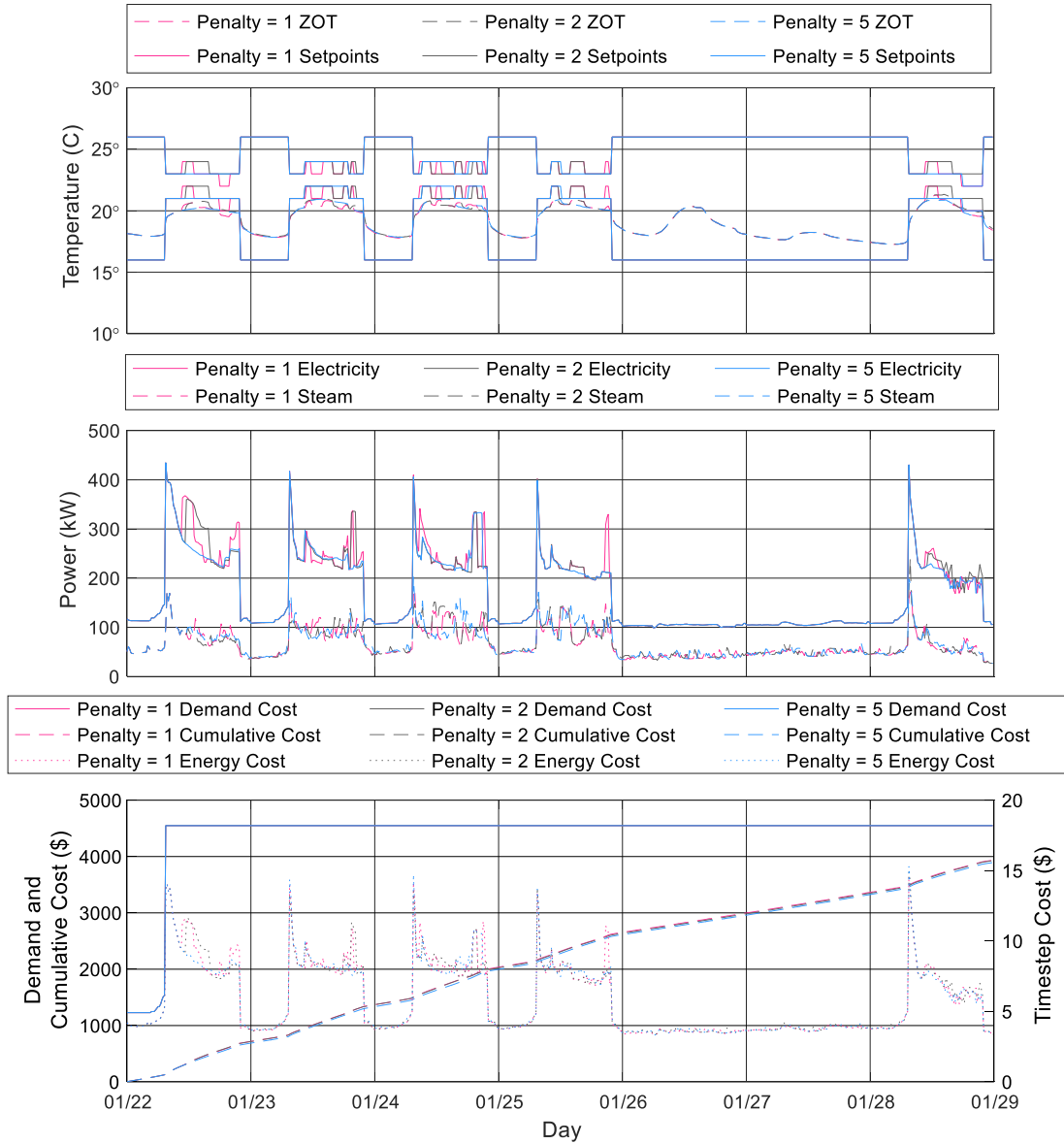


Figure 7.10 Comparison of decay penalty values in winter temperature (top), energy consumption (middle), and cost (bottom)

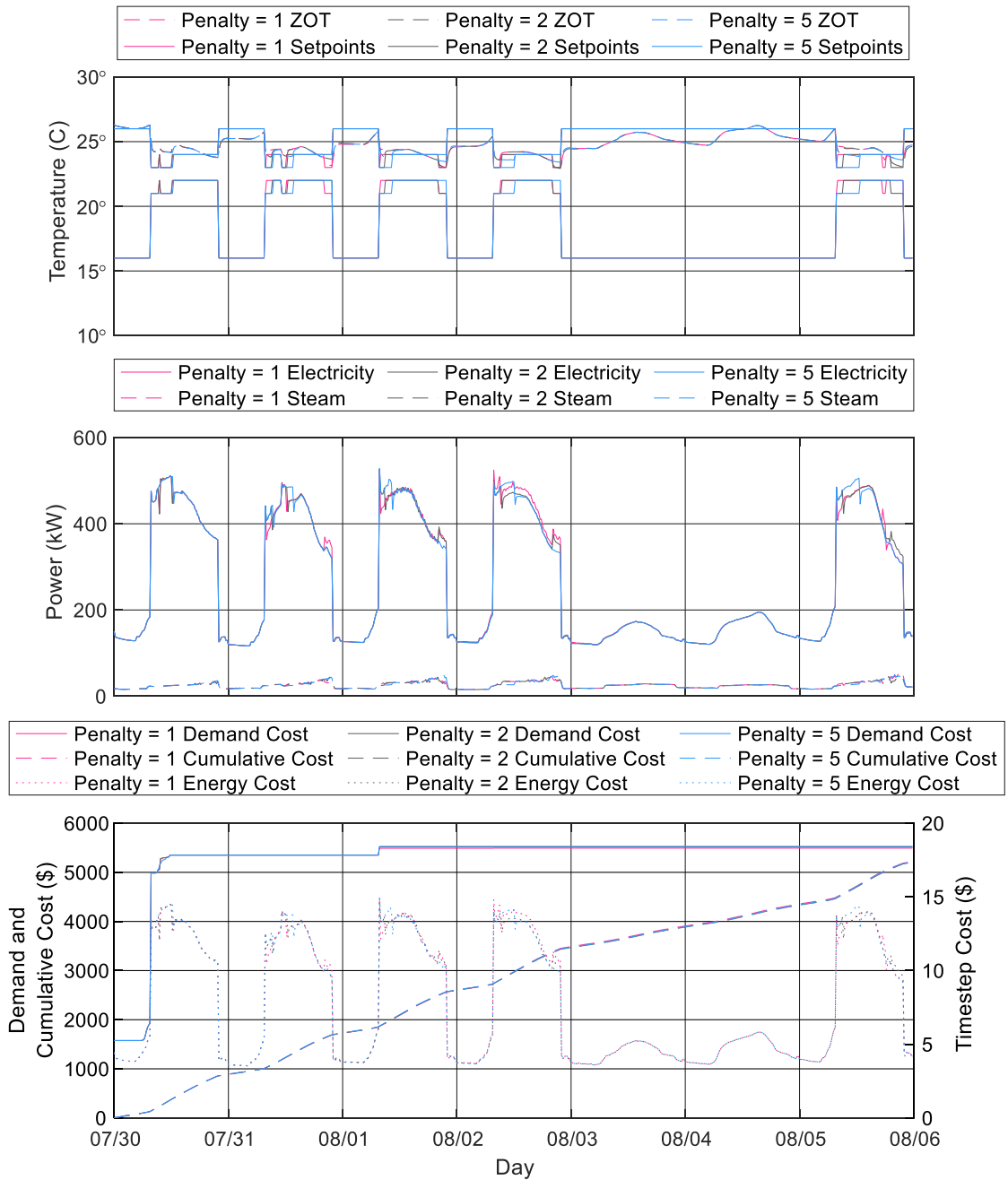


Figure 7.11 Comparison of decay penalty values in summer temperature (top), energy consumption (middle), and cost (bottom)

Table 7.6 Decay penalty = 1 monthly costs and energy consumption with fixed energy prices

Month	Total Electricity (kWh)	Total Steam (kWh)	Peak Electricity Demand (kW)	Electricity Energy Cost (\$)	Steam Energy Cost (\$)	Total Energy Cost (\$)	Electricity Demand Cost (\$)	Total Cost (\$)
Jan	122,764	37,663	434	13,504	2,636	16,140	4,548	20,689
Feb	106,829	30,609	425	11,751	2,143	13,894	4,448	18,341
Mar	119,897	31,419	373	13,189	2,199	15,388	3,905	19,293
Apr	127,157	28,330	363	13,987	1,983	15,970	3,804	19,775
May	144,359	25,994	476	15,879	1,820	17,699	4,980	22,679
Jun	150,687	21,384	532	16,576	1,497	18,073	5,568	23,641
Jul	194,174	19,052	590	21,359	1,334	22,693	6,176	28,869
Aug	193,421	19,995	551	21,276	1,400	22,676	5,773	28,449
Sep	170,821	22,031	568	18,790	1,542	20,333	5,948	26,281
Oct	152,302	25,523	483	16,753	1,787	18,540	5,060	23,600
Nov	122,471	29,383	353	13,472	2,057	15,529	3,712	19,241
Dec	116,653	32,294	428	12,832	2,261	15,092	4,482	19,574
Annual	1,721,537	323,677	590	189,369	22,657	212,026	58,403	270,429

Table 7.7 Decay penalty = 2 monthly costs and energy consumption with fixed energy prices

Month	Total Electricity (kWh)	Total Steam (kWh)	Peak Electricity Demand (kW)	Electricity Energy Cost (\$)	Steam Energy Cost (\$)	Total Energy Cost (\$)	Electricity Demand Cost (\$)	Total Cost (\$)
Jan	122,566	37,874	434	13,482	2,651	16,133	4,548	20,682
Feb	106,771	30,668	425	11,745	2,147	13,892	4,448	18,339
Mar	119,885	31,440	373	13,187	2,201	15,388	3,905	19,293
Apr	127,137	28,313	399	13,985	1,982	15,967	4,177	20,144
May	144,382	26,005	475	15,882	1,820	17,702	4,975	22,677
Jun	151,415	21,317	532	16,656	1,492	18,148	5,568	23,716
Jul	194,664	19,020	590	21,413	1,331	22,744	6,176	28,920
Aug	193,771	19,813	557	21,315	1,387	22,702	5,833	28,535
Sep	171,053	21,936	568	18,816	1,536	20,351	5,948	26,300
Oct	152,220	25,455	470	16,744	1,782	18,526	4,916	23,442
Nov	122,446	29,363	355	13,469	2,055	15,525	3,721	19,246
Dec	116,192	32,350	428	12,781	2,265	15,046	4,482	19,527
Annual	1,722,502	323,555	590	189,475	22,649	212,124	58,697	270,821

Table 7.8 Decay penalty = 5 monthly costs and energy consumption with fixed energy prices

Month	Total Electricity (kWh)	Total Steam (kWh)	Peak Electricity Demand (kW)	Electricity Energy Cost (\$)	Steam Energy Cost (\$)	Total Energy Cost (\$)	Electricity Demand Cost (\$)	Total Cost (\$)
Jan	122,392	37,844	434	13,463	2,649	16,112	4,548	20,661
Feb	107,166	30,455	425	11,788	2,132	13,920	4,448	18,368
Mar	120,212	31,306	373	13,223	2,191	15,415	3,905	19,320
Apr	127,448	28,314	363	14,019	1,982	16,001	3,804	19,805
May	144,909	25,855	460	15,940	1,810	17,750	4,812	22,562
Jun	151,616	21,373	532	16,678	1,496	18,174	5,568	23,742
Jul	194,555	19,097	594	21,401	1,337	22,738	6,222	28,960
Aug	193,853	19,986	528	21,324	1,399	22,723	5,531	28,254
Sep	171,615	21,885	563	18,878	1,532	20,410	5,895	26,304
Oct	152,460	25,459	470	16,771	1,782	18,553	4,916	23,468
Nov	122,940	29,339	381	13,523	2,054	15,577	3,985	19,562
Dec	115,902	32,505	428	12,749	2,275	15,025	4,482	19,506
Annual	1,725,070	323,418	594	189,758	22,639	212,397	58,115	270,512

7.1.5 Results Comparison for Fixed Energy Pricing

After analyzing the decay penalty results, a comparison between the decay penalty results, RBC, and total cost minimization MPC was done to determine what an optimal penalty for the Mona Campbell would be. A monthly cost comparison is provided in Figure 7.12, which shows that all MPC methods save money, and that the penalty terms save more in winter months. For the summer months, as the penalty increases there tends to be a decrease in the savings. These findings are confirmed in Table 7.9, which also highlights that the ideal penalty term annually is a value of 1 due to it having the most savings. Overall the penalty terms generate more savings on an annual basis than the no penalty scenario. The savings peak at \$7,280, or 2.6% of the total annual energy cost of the building, or 6.1% of the HVAC costs of the building.

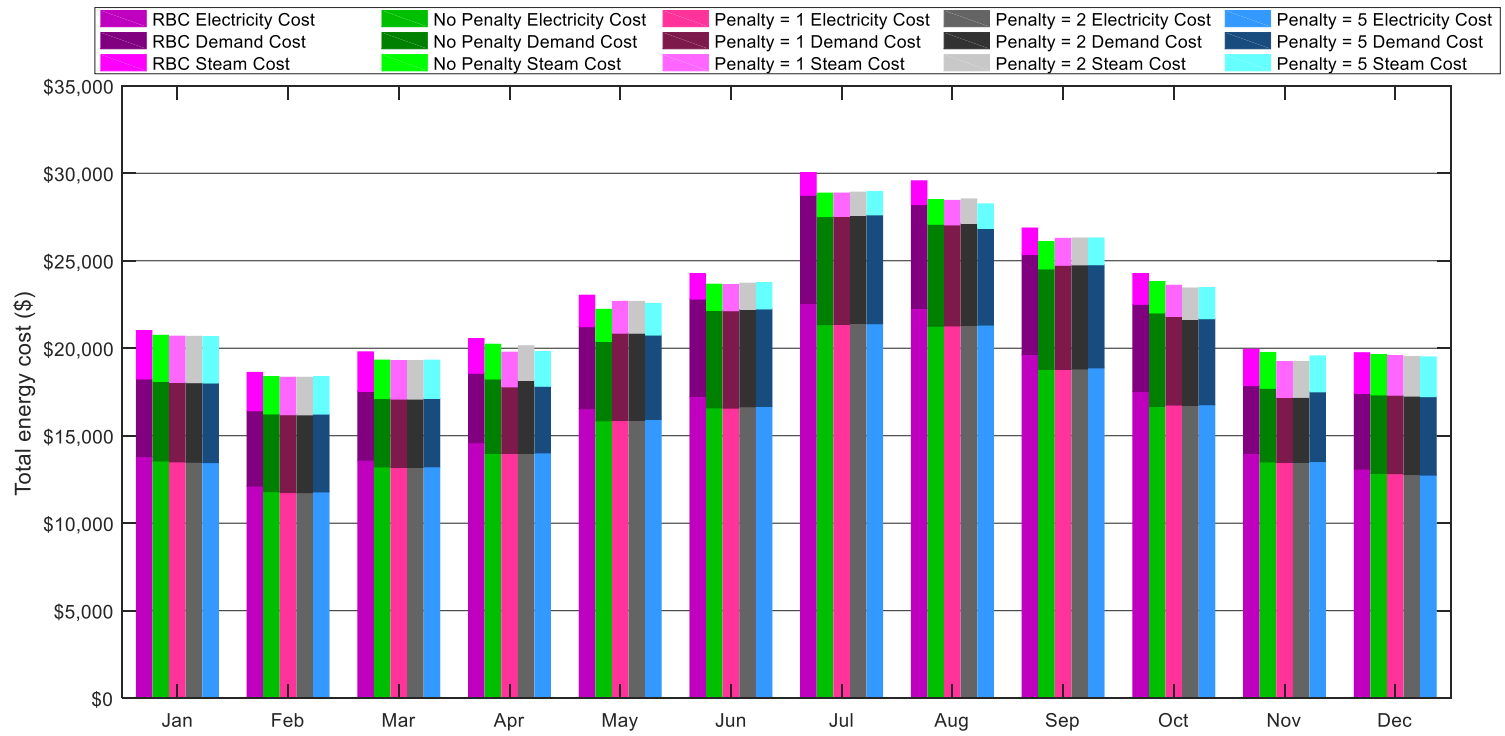


Figure 7.12 Decay penalty monthly cost comparison by source

Table 7.9 Decay penalty cost comparison with fixed energy prices

Month	RBC Total Cost	No Penalty Total Cost	Penalty = 1 Total Cost	Penalty = 2 Total Cost	Penalty = 5 Total Cost	No Penalty Savings	Penalty = 1 Savings	Penalty = 2 Savings	Penalty = 5 Savings
Jan	21,008	20,739	20,689	20,682	20,661	270	319	326	348
Feb	18,620	18,369	18,341	18,339	18,368	251	279	281	253
Mar	19,794	19,322	19,293	19,293	19,320	472	501	501	474
Apr	20,555	20,226	19,775	20,144	19,805	328	780	410	749
May	23,030	22,223	22,679	22,677	22,562	806	351	353	468
Jun	24,271	23,658	23,641	23,716	23,742	612	630	554	528
Jul	30,040	28,865	28,869	28,920	28,960	1,175	1,171	1,120	1,080
Aug	29,571	28,490	28,449	28,535	28,254	1,081	1,122	1,036	1,317
Sep	26,869	26,082	26,281	26,300	26,304	787	589	570	565
Oct	24,266	23,815	23,600	23,442	23,468	451	667	825	798
Nov	19,942	19,758	19,241	19,246	19,562	184	702	697	381
Dec	19,744	19,635	19,574	19,527	19,506	109	170	217	238
Annual	277,710	271,182	270,429	270,821	270,512	6,527	7,280	6,889	7,198

7.2 Electricity Demand Mitigation Only

Due to the lack of apparent electricity demand charge savings in the total cost minimization MPCs of section 7.1, a separate MPC with only the demand mitigation term was run to see if the issue was related to BRM predictions or with the variable energy source pricing (steam vs electricity) and MPC causing an increase in electricity demand. The cost function was as outlined below in Equation 7.5, and if the maximum predicted electricity value was below the recorded peak, then no limitations were implemented.

$$J = O_{\text{demand}}(\text{Max}(\text{PredictedElectricity}) - \text{PeakElectricity}) \quad 7.5$$

As shown in Table 7.13, the demand mitigation only strategy does not work for most months, with March and May the only month to see electricity demand cost savings (which are minimal). The poor performance is linked to an under-prediction of peak electricity demands compared to the actual peak demands from $E+$. This is demonstrated in Table 7.10 (BRM predictions) and Figure 7.13 (actual values) where the BRM predicts an electricity value of 518 kW compared to the building actual consumption of 540 kW at 14:00. This under-prediction leads to missing the correct decision to increase the temperature to avoid an increase in demand charges. Table 7.11 and Table 7.12 demonstrate BRM predictions for the 8 start options available at 06:00, and show clearly that the BRM recognizes that a change in setpoints causes a jump in electricity. However, if this jump peak is inaccurate than incorrect paths may be chosen. This is due to demand mitigation relying on high accuracy of magnitude prediction as opposed to relative accuracy.

Table 7.10 August 5th at 14:00 predictions (kW for power, °C for temperature)

Heating Setpoint	Cooling Setpoint	Electricity Prediction	Steam Prediction	Temp Prediction	Electricity Actual	Steam Actual	Temp Actual	Electricity Delta	Steam Delta	Temp Delta
16	26	422	35	24.1	N/A	N/A	N/A	N/A	N/A	N/A
20	22	518	34	23.5	540	27	23.2	-22	7	0.3
21	23	482	36	23.8	N/A	N/A	N/A	N/A	N/A	N/A
22	24	452	40	24.1	N/A	N/A	N/A	N/A	N/A	N/A

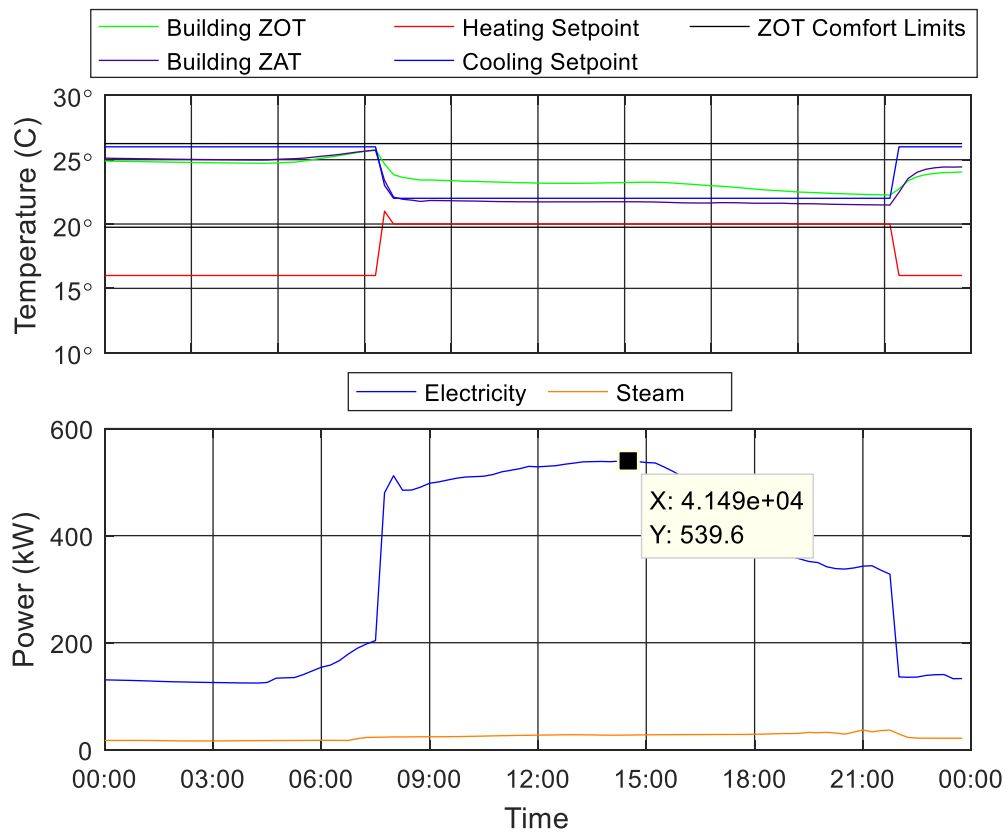


Figure 7.13 August 5th temperature profile (top) and energy consumption (bottom)

Table 7.11 Summer start electricity demand predictions (kW)

Option	06:15	06:30	06:45	07:00	07:15	07:30	07:45	08:00
1	138	159	171	184	177	179	184	403
2	138	159	171	184	177	179	401	409
3	138	159	171	184	177	399	408	410
4	138	159	171	184	387	401	407	409
5	138	159	171	383	393	403	407	409
6	138	159	383	380	393	402	407	409
7	138	370	365	380	392	402	407	409
8	138	362	362	379	391	401	406	403

Table 7.12 Winter start electricity demand predictions (kW)

Option	06:15	06:30	06:45	07:00	07:15	07:30	07:45	08:00
1	115	134	133	138	145	145	146	269
2	115	134	133	138	145	145	284	261
3	115	134	133	138	145	289	275	260
4	115	134	133	138	277	271	275	260
5	115	134	133	291	263	271	275	259
6	115	134	292	271	263	271	275	259
7	115	290	264	270	262	270	275	259
8	333	260	261	271	262	270	275	259

Table 7.13 Comparison of electricity demand mitigation only costs (all units in \$)

Month	MPC Electricity Energy Cost	MPC Steam Energy Cost	MPC Electricity Demand Cost	RBC Electricity Energy Cost	RBC Steam Energy Cost	RBC Electricity Demand Cost	Total MPC Cost	Total RBC Cost	Total Savings
Jan	13,554	2,624	4,548	13,810	2,763	4,435	20,726	21,008	282
Feb	11,976	2,047	4,448	12,119	2,192	4,308	18,470	18,620	150
Mar	13,560	2,066	3,905	13,596	2,254	3,943	19,531	19,794	263
Apr	14,787	1,799	4,262	14,605	1,988	3,962	20,849	20,555	- 294
May	16,743	1,625	4,664	16,548	1,797	4,685	23,032	23,030	- 2
Jun	17,459	1,352	6,226	17,248	1,463	5,560	25,037	24,271	- 767
Jul	22,249	1,226	6,541	22,564	1,298	6,178	30,015	30,040	25
Aug	22,162	1,258	6,583	22,276	1,362	5,933	30,003	29,571	- 432
Sep	19,646	1,360	6,055	19,646	1,503	5,720	27,061	26,869	- 192
Oct	17,664	1,582	5,190	17,532	1,758	4,977	24,436	24,266	- 170
Nov	13,928	1,896	4,253	13,985	2,080	3,877	20,077	19,942	- 134
Dec	12,617	2,299	4,482	13,095	2,326	4,324	19,397	19,744	347
Ann	196,344	21,134	6,583	197,023	22,784	6,178	278,634	277,710	- 924

7.3 Time of Use Electricity Pricing

For the variable energy pricing structure, a time of use electricity tariff based on Ontario Energy Board²⁸ residential prices, shown in Figure 7.14 was implemented. Residential Data was used because it is easily accessed/implemented, and it acts as a proxy of the wholesale Independent Electricity System Operator²⁹ rates. The summer period runs from May 1 (week 17) to October 1 (week 39), with winter representing the remaining months.

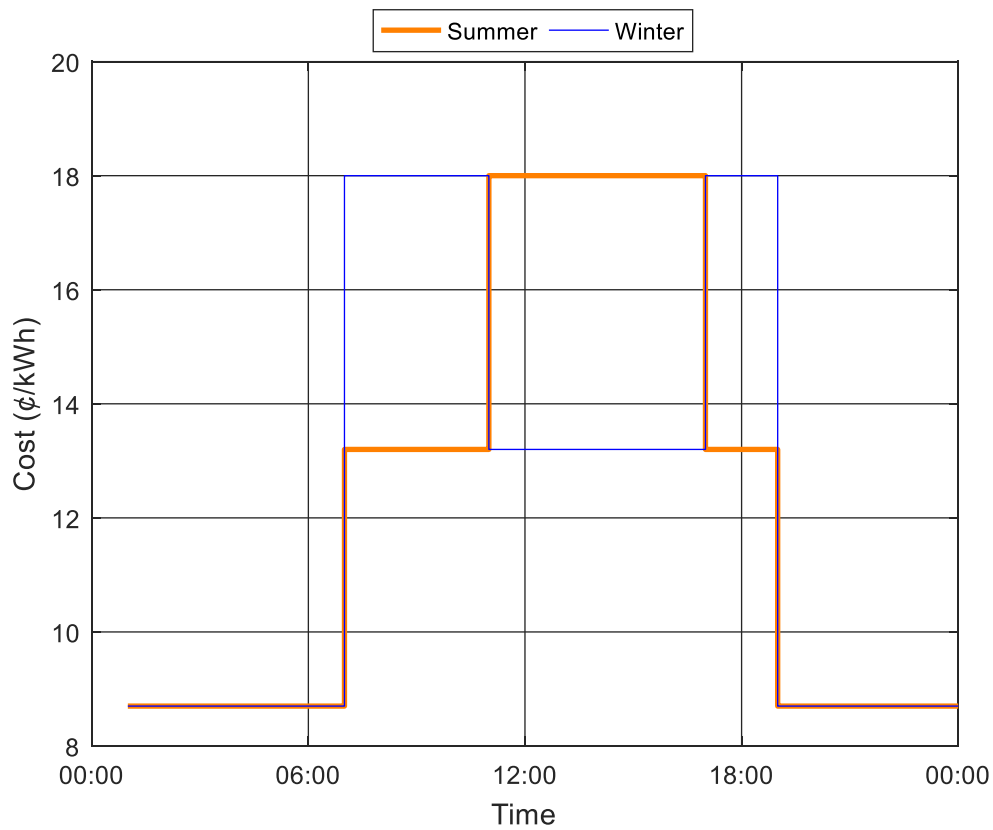


Figure 7.14 Time of use electricity profiles

While time of use pricing is not currently in use for commercial customers in many jurisdictions, it represents a trend towards the future of energy supply and demand through

²⁸ <http://www.ontarioenergyboard.ca/OEB/Consumers/Electricity/Electricity+Prices#tou>

²⁹ <http://www.ieso.ca/>

features such as smart grid. The first step in this evolution is the demand charge, which is meant to minimize peak draws to provide electricity suppliers stability and improve the life of current infrastructure. Time of use energy pricing is the next step in the process with fixed tariffs such as used in the residential sector. This is then followed by real-time pricing and smart grid operational strategy, where only a fixed supply of electricity is available. This approximation is the first step towards these expected changes in the electricity market place, and while time of use for commercial customers may be skipped for more advanced technologies, it is a good test bed for their applicability.

7.3.1 Rule Based Control

The rule based control strategy as in Chapter 7.1.1 was applied, but updated with the new time of use electricity pricing structure as described in Chapter 7.3. The monthly costs are shown in Figure 7.15 contrasted against constant price RBC (and detailed in Table 7.14). As shown, the fluctuations in price cause an increase in costs throughout the year, with a larger increase in the summer. This is due to an increased usage of electricity in the summer months, and the peak periods of use coinciding with the higher price structure. Overall the change to time of use electricity rates appears to skew the cost ratio higher towards electricity energy in comparison to steam and electricity demand.

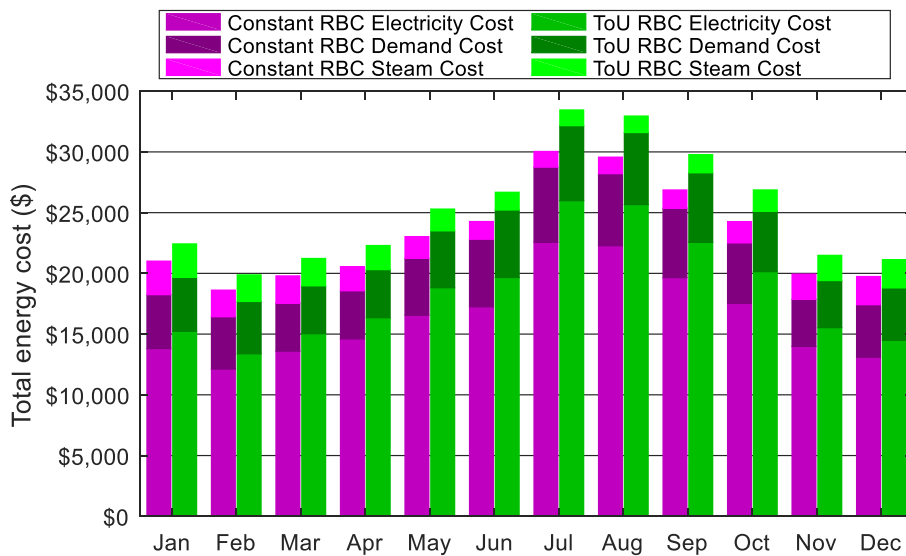


Figure 7.15 RBC monthly costs comparison by source

Table 7.14 RBC monthly energy consumption and costs

Month	Total Electricity (kWh)	Total Steam (kWh)	Peak Electricity Demand (kW)	Electricity Energy Cost (\$)	Steam Energy Cost (\$)	Total Energy Cost (\$)	Electricity Demand Cost (\$)	Total Cost (\$)
Jan	125,544	39,472	424	15,229	2,763	17,992	4,435	22,428
Feb	110,176	31,320	412	13,377	2,192	15,570	4,308	19,878
Mar	123,602	32,202	377	15,030	2,254	17,284	3,943	21,227
Apr	132,770	28,394	378	16,345	1,988	18,333	3,962	22,295
May	150,433	25,669	448	18,814	1,797	20,610	4,685	25,296
Jun	156,796	20,901	531	19,655	1,463	21,118	5,560	26,678
Jul	205,126	18,545	590	25,981	1,298	27,279	6,178	33,457
Aug	202,513	19,452	567	25,661	1,362	27,022	5,933	32,955
Sep	178,602	21,477	546	22,559	1,503	24,062	5,720	29,782
Oct	159,384	25,109	475	20,138	1,758	21,896	4,977	26,873
Nov	127,136	29,721	356	15,528	2,080	17,609	3,877	21,486
Dec	119,041	33,224	413	14,479	2,326	16,805	4,324	21,128
Annual	1,791,122	325,486	590	222,796	22,784	245,580	57,902	303,482

7.3.2 Total Cost Minimization with a Switching Penalty of 1

Based on the results of fixed energy prices, only a comparison to the best performing scenario (fluctuation penalty = 1) is given in detail. The results for penalty = 1 are tabulated in Table 7.15, and direct comparison to RBC with monthly data in Figure 7.16. Similar to the constant price scenario, more cost savings are achieved during the summer than the winter. Figure 7.17 clearly illustrates the impact of time of use pricing on cost, where the middle portion of the day has a reduced cost compared to the morning and evening. During the summer (Figure 7.18), the impact of the MPC is more noticeable, with the building being chilled prior to or at the very start of the high price period. Due to the lack of thermal mass on the Mona Campbell, the time of minimal energy consumption (i.e. no active cooling during transition) is minimal, and the savings are generated by setpoints that require less cooling.

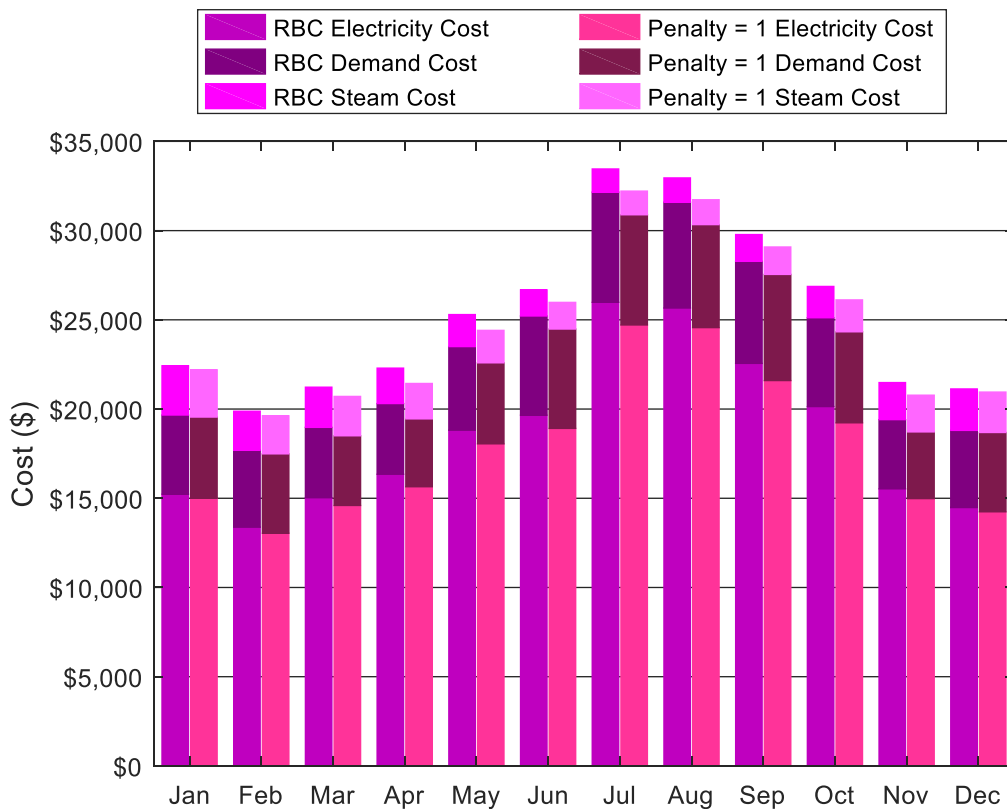


Figure 7.16 Decay penalty = 1 monthly costs by source

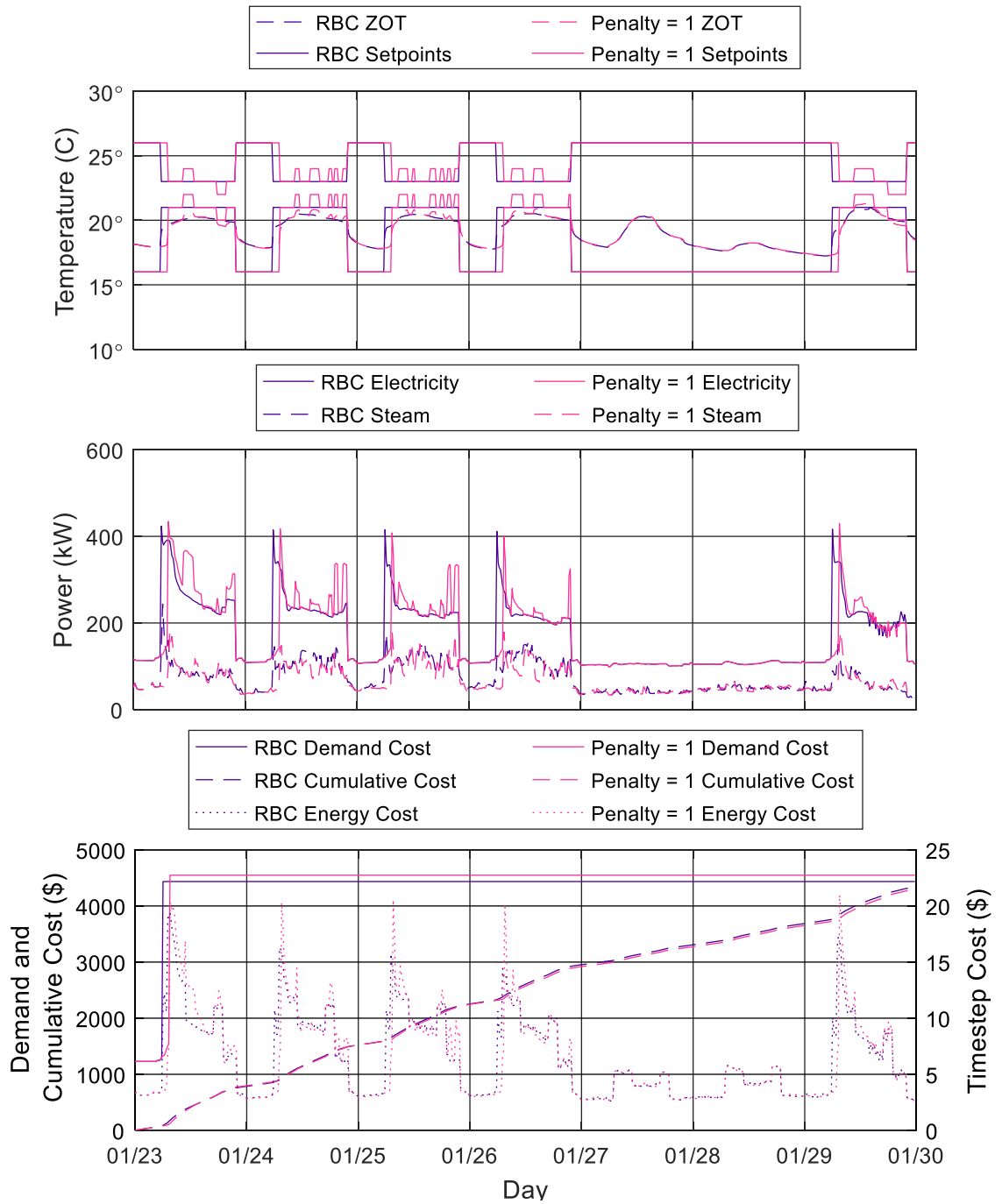


Figure 7.17 Decay penalty = 1 vs RBC sample winter temperatures (top), energy consumption (middle), and costs (bottom)

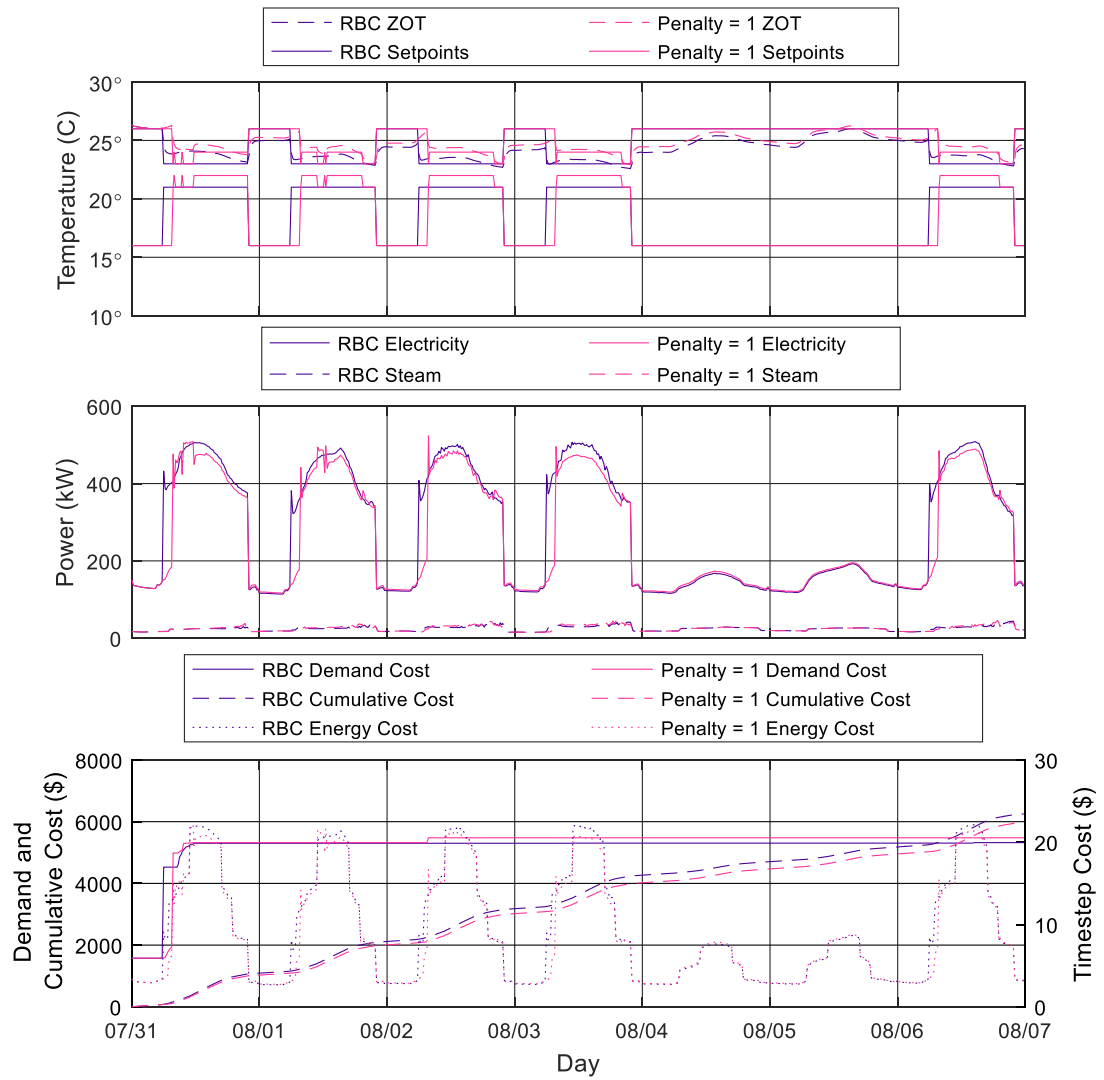


Figure 7.18 Decay penalty = 1 vs RBC sample summer temperatures (top), energy consumption (middle), and costs (bottom)

Table 7.15 Decay penalty = 1 energy consumption and costs

Month	Total Electricity (kWh)	Total Steam (kWh)	Peak Electricity Demand (kW)	Electricity Energy Cost (\$)	Steam Energy Cost (\$)	Total Energy Cost (\$)	Electricity Demand Cost (\$)	Total Cost (\$)
Jan	122,830	37,871	434	15,002	2,651	17,653	4,548	22,201
Feb	106,859	30,491	425	13,040	2,134	15,175	4,448	19,622
Mar	119,764	31,562	373	14,595	2,209	16,804	3,905	20,709
Apr	127,067	28,379	363	15,645	1,987	17,631	3,804	21,436
May	144,162	26,018	434	18,049	1,821	19,871	4,540	24,411
Jun	150,658	21,373	532	18,915	1,496	20,411	5,568	25,980
Jul	194,319	18,983	590	24,712	1,329	26,041	6,176	32,216
Aug	193,296	19,958	551	24,562	1,397	25,960	5,773	31,732
Sep	170,794	21,999	568	21,595	1,540	23,135	5,948	29,084
Oct	152,007	25,581	487	19,228	1,791	21,019	5,099	26,119
Nov	122,517	29,442	357	14,980	2,061	17,041	3,737	20,778
Dec	116,291	32,392	424	14,241	2,267	16,509	4,444	20,953
Annual	1,720,563	324,050	590	214,566	22,684	237,249	57,992	295,241

7.3.3 Results Comparison for Time of Use Electricity Pricing

The MPC with greatest savings for time of use electricity pricing is that of the MPC with a penalty term of 1. This is verified in Figure 7.19 and Table 7.16, where all the MPC scenarios provide energy savings. The results highlight the addition of a penalty term on switching setpoints is valid for both constant electricity pricing and time of use electricity pricing. In terms of magnitude, a maximum savings of \$8,248 is achieved, representing 2.7% of the operating costs of the building, or 6.1% of the HVAC costs.

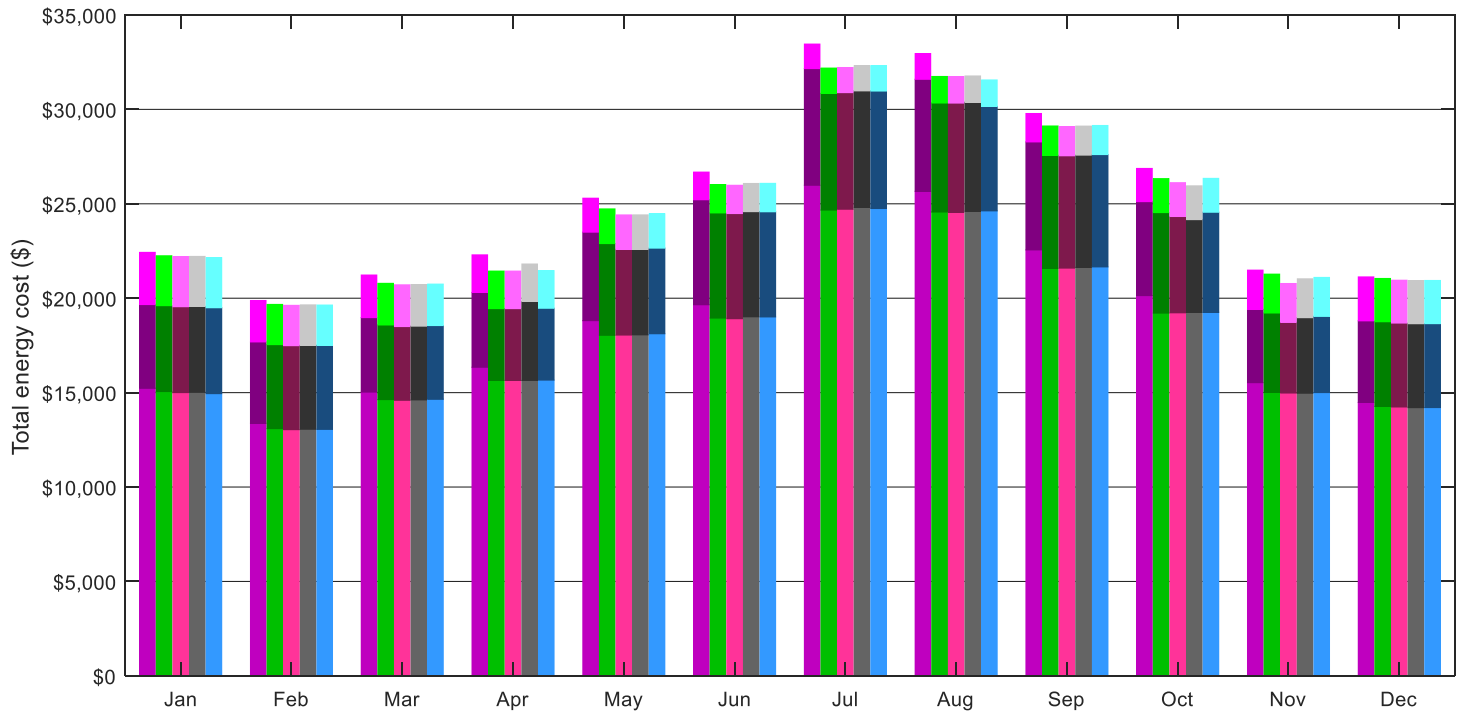
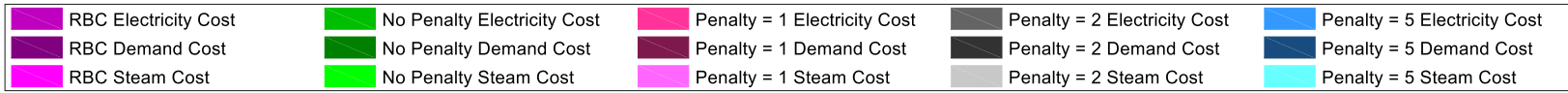


Figure 7.19 Time of use electricity pricing monthly cost comparisons

Table 7.16 Time of use electricity price cost comparison

Month	RBC Total Cost	No Penalty Total Cost	Penalty = 1 Total Cost	Penalty = 2 Total Cost	Penalty = 5 Total Cost	No Penalty Savings	Penalty = 1 Savings	Penalty = 2 Savings	Penalty = 5 Savings
Jan	22,428	22,247	22,201	22,213	22,148	181	226	215	279
Feb	19,878	19,671	19,622	19,647	19,637	207	256	232	241
Mar	21,227	20,787	20,709	20,723	20,746	440	518	504	481
Apr	22,295	21,436	21,436	21,810	21,460	859	859	485	834
May	25,296	24,729	24,411	24,412	24,470	567	885	884	826
Jun	26,678	26,017	25,980	26,076	26,081	661	698	602	597
Jul	33,457	32,186	32,216	32,310	32,313	1,271	1,241	1,147	1,144
Aug	32,955	31,743	31,732	31,769	31,559	1,212	1,223	1,186	1,396
Sep	29,782	29,120	29,084	29,114	29,147	662	698	668	635
Oct	26,873	26,333	26,119	25,950	26,346	540	754	922	526
Nov	21,486	21,274	20,778	21,026	21,101	211	708	459	385
Dec	21,128	21,045	20,953	20,936	20,940	83	175	193	189
Ann	303,482	296,589	295,241	295,986	295,949	6,893	8,242	7,496	7,533

7.4 Comparison of Time of Use Electricity Pricing to Constant Pricing

In order to better understand the impact of time of use electricity pricing on MPC decision making, a comparison between the MPC with constant pricing and time of use pricing was conducted. The comparison is done between the MPCs with a decay penalty of 1 as they were the best performing MPC for both pricing structures. Shown in Figure 7.20 are the monthly pricing comparisons, where similar to the RBC case a larger cost differential is located in the summer months. Figure 7.21 shows the annual costs by fuel source, where the primary difference in cost is that of electricity energy. A sample winter week of comparison is shown in Figure 7.22, where minimal differences in setpoints exist and appear to be unaffected by the time of use electricity rates. A similar conclusion can be drawn for the summer week in Figure 7.23, where there are minimal differences in setpoints between the MPCs. This is not surprising due to the low thermal mass of the Mona Campbell building allowing for a minimal amount of energy storage for latter periods with higher prices.

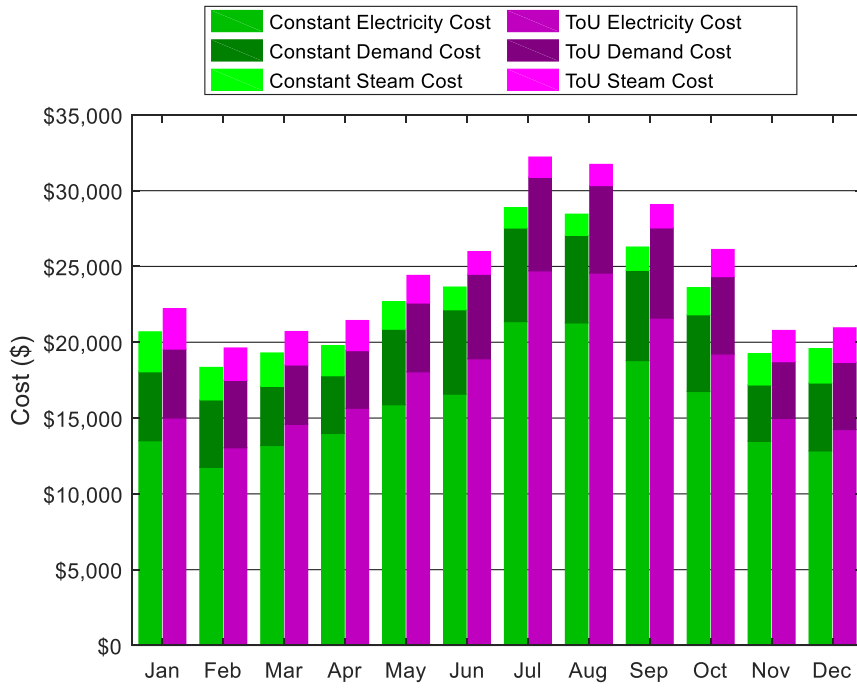


Figure 7.20 Monthly cost comparison of time of use and constant price electricity for MPC with penalty = 1

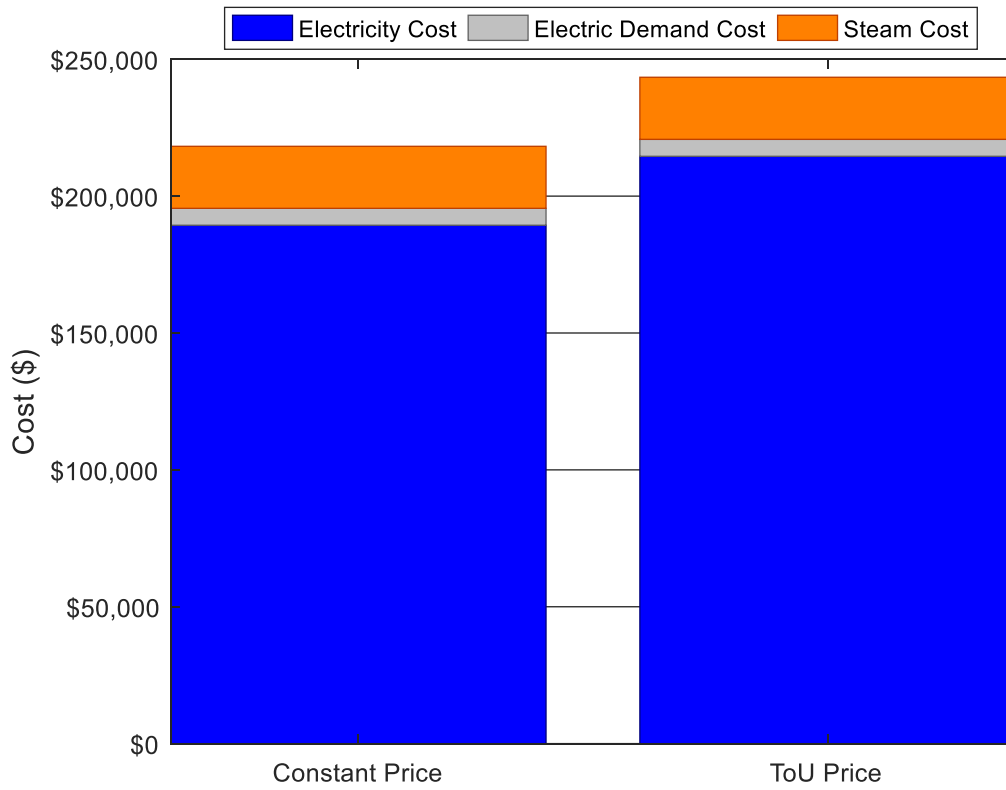


Figure 7.21 Annual cost comparison between constant and time of use electricity pricing MPC with penalty = 1

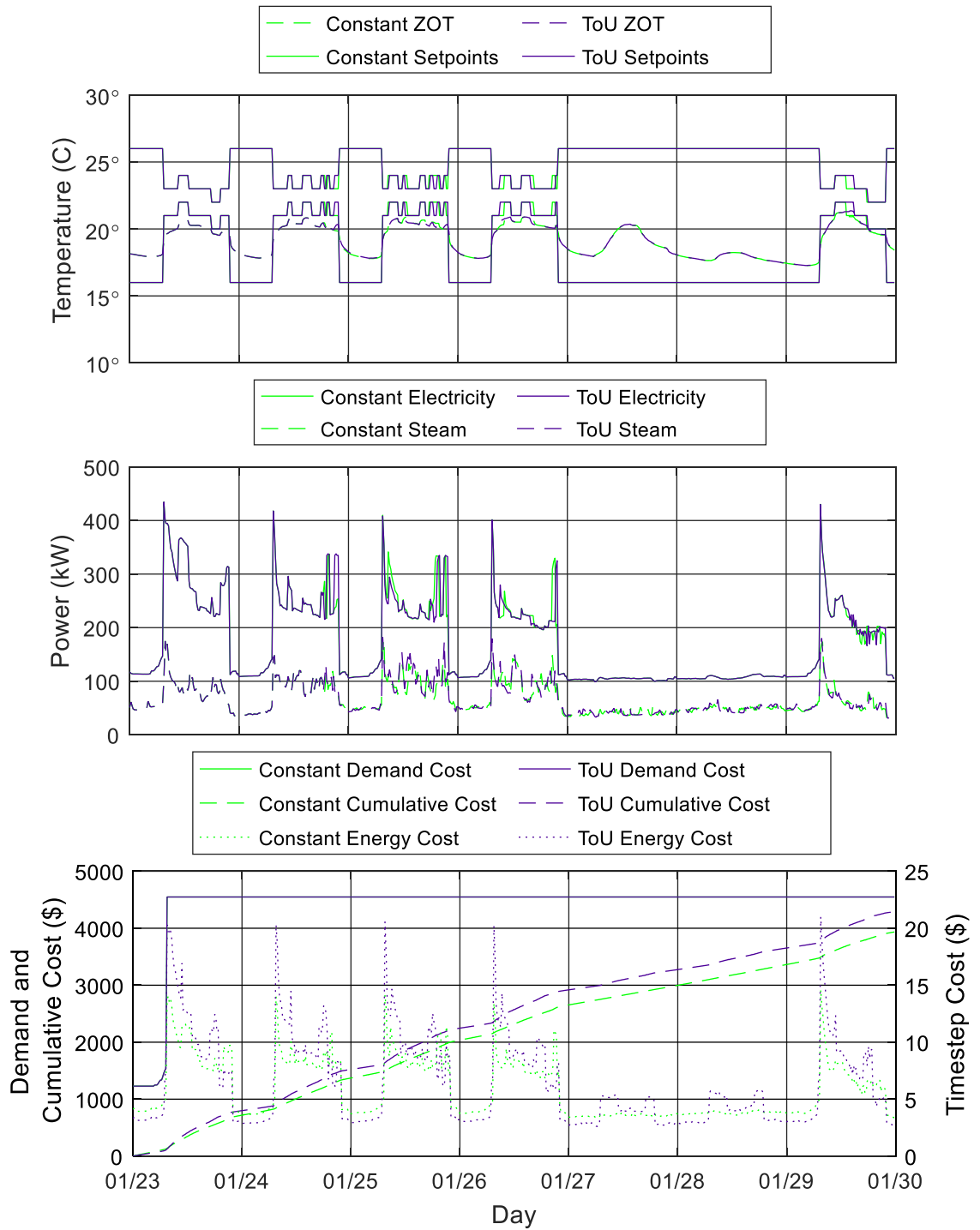


Figure 7.22 Penalty = 1 MPC comparison between time of use and constant electricity pricing winter temperature (top), energy consumption (middle) and cost (bottom)

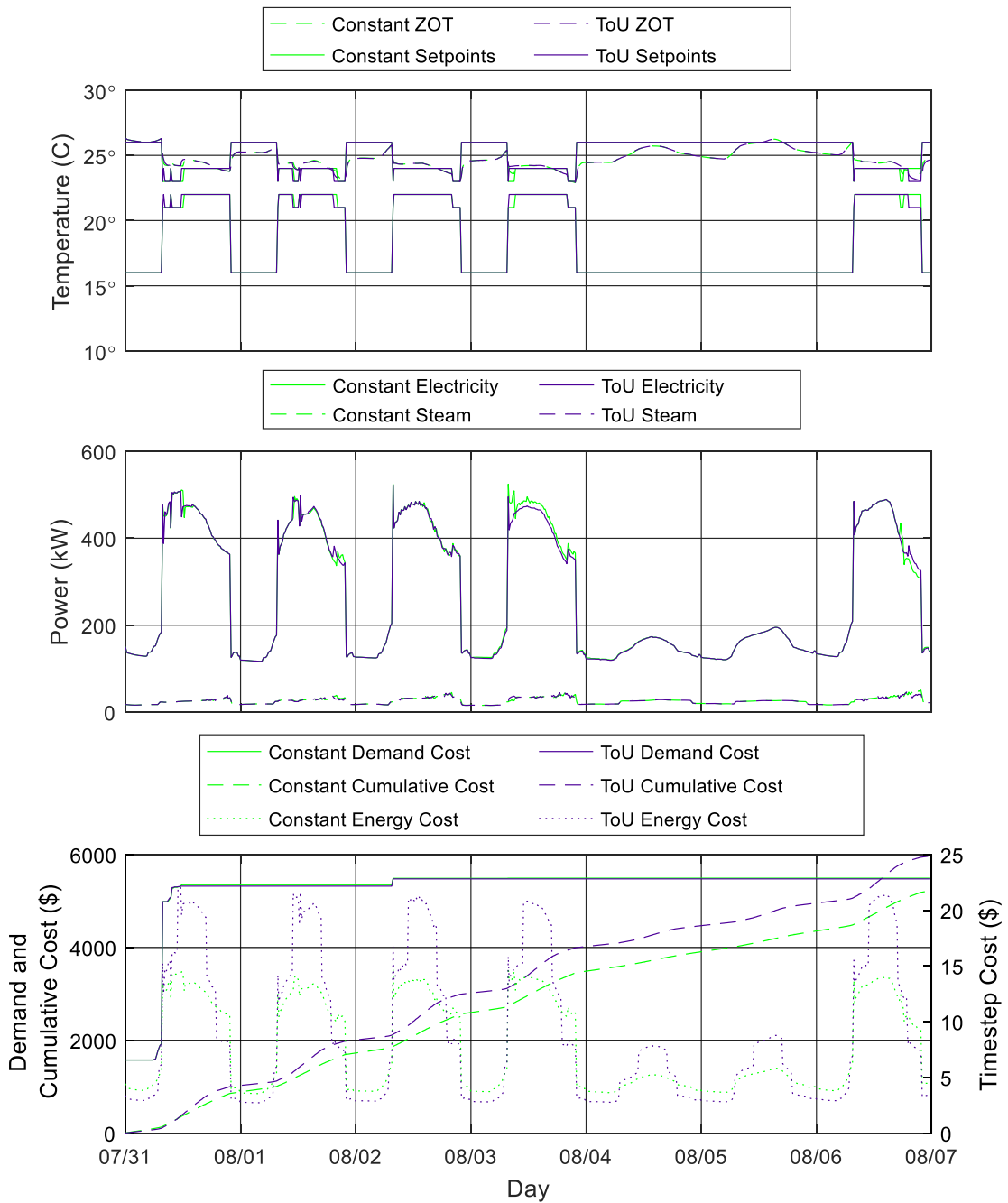


Figure 7.23 Penalty = 1 MPC comparison between time of use and constant electricity pricing summer temperature (top), energy consumption (middle) and cost (bottom)

While there appears to be minimal change in setpoint choices due to the pricing structure in electricity, an analysis of the cost savings shows differences. Table 7.17 outlines the costs and savings for the penalty of 1 MPC in both price structures. As shown, the time of use price structure saves an additional \$968, but only increases the percentage savings from 2.6% to 2.7% of operating costs of the building. This is due to the increased cost of operating the building under a time of use electricity pricing structure.

Table 7.17 Cost and savings comparison between constant and time of use electricity pricing (\$)

Month	Constant Price	Constant Price	Constant Price	ToU RBC	ToU MPC	ToU Savings
	RBC Total Cost	MPC Total Cost	Savings	Total Cost	Total Cost	
Jan	21,008	20,689	319	22,428	22,201	226
Feb	18,620	18,341	279	19,878	19,622	256
Mar	19,794	19,293	501	21,227	20,709	518
Apr	20,555	19,775	780	22,295	21,436	859
May	23,030	22,679	351	25,296	24,411	885
Jun	24,271	23,641	630	26,678	25,980	698
Jul	30,040	28,869	1,171	33,457	32,216	1,241
Aug	29,571	28,449	1,122	32,955	31,732	1,223
Sep	26,869	26,281	589	29,782	29,084	698
Oct	24,266	23,600	667	26,873	26,119	754
Nov	19,942	19,241	702	21,486	20,778	708
Dec	19,744	19,574	170	21,128	20,953	175
Annual	277,710	270,429	7,280	303,482	295,241	8,242

7.5 Conclusions of Model Predictive Control Simulations

The results of this chapter can be summarized as follows:

- A pure total cost minimization strategy produces energy savings, but has an unrealistic amount of setpoint changes during the winter months. This is due to a competing balance between the steam cost (increases as setpoints increase) and electricity cost (predicted to increase as setpoints decrease due to core space cooling). Any prediction inaccuracies that cause a change in setpoints where the expected savings are not realized will cause a corresponding switch in setpoints again leading to an unstable feedback loop.
- A switching penalty was introduced to prevent the oscillations as found in Chapter 7.1.3. Values of 1, 2, and 5 were tested, with a penalty of 1 providing the best balance between oscillation minimization and allowing for corrections when necessary.
- Demand mitigation requires high magnitude accuracy of electricity demand as opposed to relative accuracy, which the BRM (and most simplified models) appears incapable of producing. The BRM has a tendency to under predict the peak demand. Due to these BRM inaccuracies a pure electricity demand mitigation strategy does not work.
- A minimal difference between time of use and constant electricity prices was found in terms of setpoint choices and percentage savings (2.6% vs 2.7%). A higher dollar savings was achieved with the time of use rates, due to the higher base cost of operating the building. This is due to the Mona Campbell building being rather light from its bubble deck construction which provides good thermal resistance but has less mass with a limited ability to store energy for shifting.
- A challenge for the Mona Campbell is that HVAC electricity is only 41% of the measured total loads and 33% of the simulated loads. The building also has minimal thermal mass due to the use of a bubble deck construction (bubbles of air are placed

within the concrete to reduce mass). These properties make it a less than ideal test facility as there is little thermal mass to manipulate, and an efficient HVAC system has smaller room for improvements. In contrast, typical building construction contains more mass (no air bubbles within the concrete), and has less efficient HVAC systems (upwards of 50% energy consumption for the site as opposed to 41%). When HVAC is a larger component of the building costs, a larger net savings can be achieved as MPC only has a direct influence on the HVAC loads.

- It is expected for heavier buildings (i.e. more thermal mass) that a larger impact from the implementation of time of use electricity rates would be realized, but should be further investigated.

Chapter 8 EMULATED MODEL PREDICTIVE CONTROL SIMULATIONS

In an effort to isolate the effects of BRM prediction error on MPC decision making, a version of emulated MPC was conducted. The driving factor was the struggle that BRM had to predict peak electricity consumption as outlined in section 7.2. By using emulated MPC, these errors in prediction can be overcome as an exact system model is used. The downside is that only morning start optimization can be implemented, which does not directly influence the peak demand period (afternoon). A second area that is explored using emulated MPC is the impact of the forecast horizon on MPC results. It is expected that longer forecast horizons with perfect information perform better than shorter horizons. These effects are expected to be most noticeable on electricity demand mitigation, which is billed on a monthly basis.

To achieve the one month shrinking window look ahead horizon, the initial one day horizon MPC was run for an entire month, with the peak electrical demand stored. The one day horizon MPC was then rerun with monthly electric demand peak value (as opposed to the peak to date value) to allow for the MPC to make decisions based on the largest electric demand limit. Using the new limit prevents the wasted energy usage when attempting to maintain the current peak electricity demand prior to an unavoidable electricity demand peak.

The emulated MPC was run using the optimization algorithms from Chapter 7.1.2 for energy minimization and Chapter 7.1.3 for cost minimization, utilizing time-of-use electricity pricing. It is expected that the results for the cost optimization should mirror those of the energy minimization, with slight changes due to the time latency of changes in start time (i.e. it takes several hours to reach a similar level of energy consumption, with delayed starts using more energy until convergence happens). Any demand savings that occur compared to the energy minimization scenario are due to shifting the peak in winter, or the transient convergence process in summer.

A further exploration into an emulated MPC method is required in order to truly capture demand savings due to demand peaks occurring during the daytime as opposed to during the morning start. While the results from emulated MPC will not be optimal for pure demand mitigation, a better understanding of how demand mitigation influences MPC choices can be gained by comparing to pure energy minimization.

8.1 Results of Emulated Model Predictive Control

A comparison between 4 different operating scenarios is given for emulated MPC: RBC, energy minimization, total cost minimization with a one day forecast, and total cost minimization with a one month forecast. Monthly costs are plotted in Figure 8.1 with totals tabulated in Table 8.1, electricity demand costs in Table 8.2, electricity energy costs in Table 8.3, and steam energy costs in Table 8.4. The results indicate that the one month forecast has the best performance by saving \$6,685 (2.1% total costs, 5.7% HVAC costs). This is due to the forecast horizon matching the billing period for demand, such that those savings can be accurately captured along with energy savings.

The next best scenario was the energy minimization scenario, with savings of \$6,208 (2.1% total cost, 5.6% HVAC cost). The result is driven by pure energy reduction, where total energy savings outweigh the increase in demand costs. Due to the use of steam for heating and low percentage of electricity used for HVAC, pure energy minimization appears to be a feasible strategy to employ. Buildings with higher HVAC electricity percentages (such as electrically heated buildings) may not have similar findings. The pricing structure of energy may also play a factor, where jurisdictions with higher demand charges a lower energy costs (such as Quebec) may require attention paid to the demand portion of costs.

The one day horizon cost MPC performs worse than a pure energy minimization MPC due to having an insufficient forecast horizon, with savings of \$6,171 (2.1% total cost, 5.6% HVAC). By only considering one day ahead, the MPC strives to maintain peak demand over a smaller window (from when the billing cycle began to the day ahead compared to the whole month). Due to this smaller window, the actual peak demand of a billing period is not seen until a day before it occurs. This leads to extra energy usage to maintain the

incorrect lower electricity demand peak value. Examples of this can be seen in Figure 8.2 and Figure 8.3 where the one day forecast MPC initializes the HVAC system sooner than the energy minimization and one month forecast MPC to maintain the incorrect lower electric demand peak.

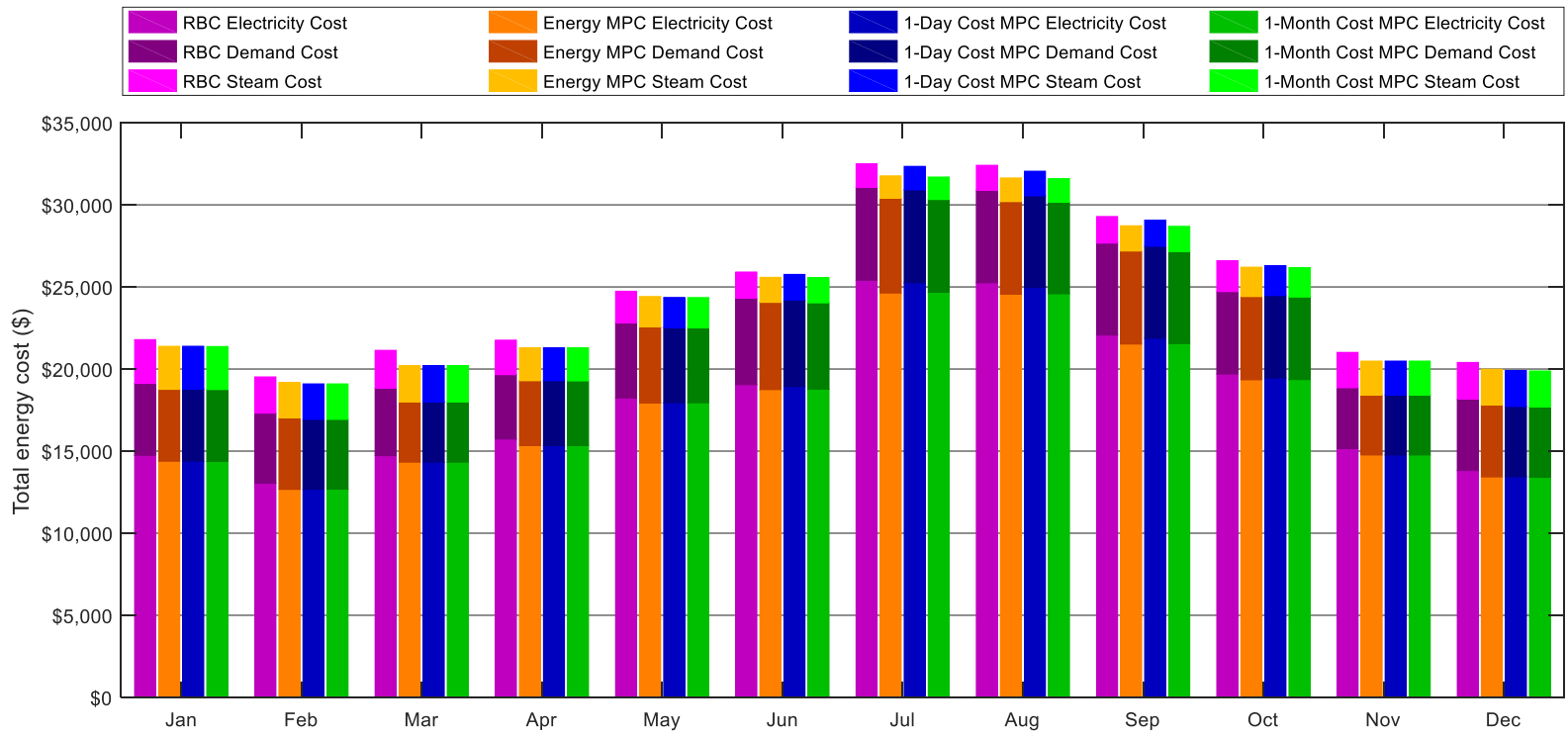


Figure 8.1 Emulated MPC monthly cost comparison

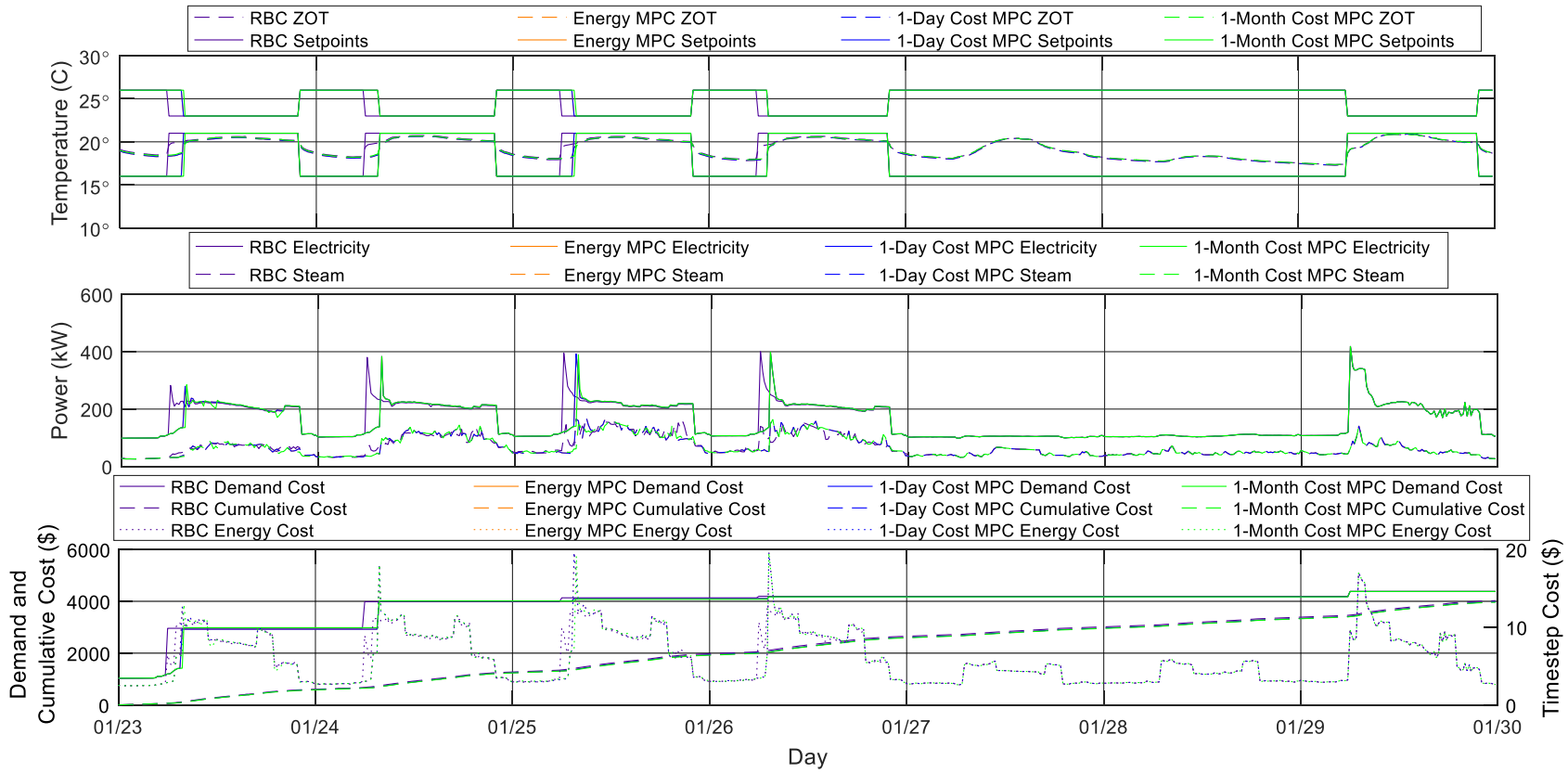


Figure 8.2 Emulated MPC winter comparison

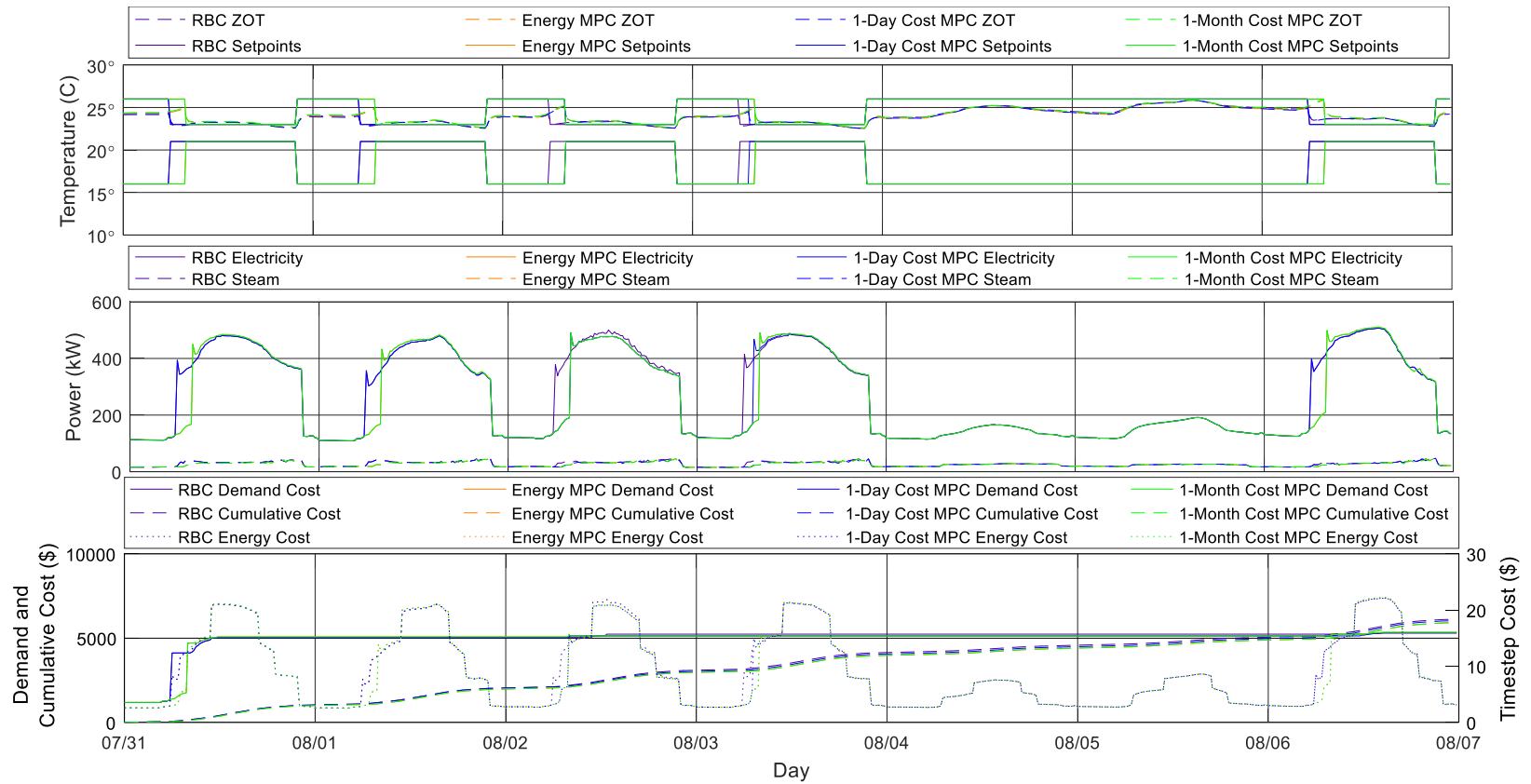


Figure 8.3 Emulated MPC summer comparison

Table 8.1 Monthly comparison of total costs for emulated MPC scenarios (\$)

Month	RBC Total Cost	Energy MPC Total Cost	1-Day MPC Total Cost	1-Month MPC Total Cost	Energy MPC Savings	1-Day MPC Savings	1-Month MPC Savings
Jan	21,791	21,382	21,368	21,368	409	423	423
Feb	19,519	19,184	19,100	19,094	335	419	425
Mar	21,138	20,209	20,209	20,209	929	929	929
Apr	21,761	21,287	21,309	21,280	474	452	481
May	24,737	24,418	24,386	24,355	319	351	382
Jun	25,908	25,584	25,660	25,557	324	248	351
Jul	32,504	31,766	31,828	31,693	738	676	811
Aug	32,409	31,637	31,683	31,597	772	726	812
Sep	29,289	28,725	28,787	28,692	564	502	597
Oct	26,600	26,203	26,199	26,173	397	401	427
Nov	21,013	20,483	20,483	20,483	530	530	530
Dec	20,400	19,983	19,887	19,881	417	513	519
Ann	297,070	290,862	290,899	290,382	6,208	6,171	6,688

Table 8.2 Monthly comparison of electricity demand costs for emulated MPC scenarios (\$)

Month	RBC Electricity Demand Cost	Energy MPC Electricity Demand Cost	1-Day MPC Electricity Demand Cost	1-Month MPC Electricity Demand Cost	Energy MPC Savings	1-Day MPC Savings	1-Month MPC Savings
Jan	4,380	4,380	4,380	4,380	0	0	0
Feb	4,261	4,353	4,254	4,254	-92	7	7
Mar	4,112	3,664	3,664	3,664	448	448	448
Apr	3,923	3,942	3,918	3,918	-19	5	5
May	4,566	4,650	4,566	4,566	-84	0	0
Jun	5,259	5,315	5,259	5,259	-56	0	0
Jul	5,657	5,773	5,657	5,657	-116	0	0
Aug	5,639	5,633	5,557	5,571	6	82	68
Sep	5,601	5,667	5,601	5,601	-66	0	0
Oct	5,023	5,070	5,023	5,023	-47	0	0
Nov	3,677	3,661	3,661	3,661	16	16	16
Dec	4,351	4,379	4,282	4,282	-28	69	69
Ann	56,449	56,486	55,820	55,834	-37	629	615

Table 8.3 Monthly comparison of electricity energy costs for emulated MPC scenarios (\$)

Month	RBC Electricity Energy Cost	Energy MPC Electricity Energy Cost	1-Day MPC Electricity Energy Cost	1-Month MPC Electricity Energy Cost	Energy MPC Savings	1-Day MPC Savings	1-Month MPC Savings
Jan	14,743	14,381	14,366	14,370	362	377	373
Feb	13,050	12,667	12,682	12,677	383	368	373
Mar	14,724	14,324	14,324	14,324	400	400	400
Apr	15,736	15,343	15,380	15,358	393	356	378
May	18,236	17,925	17,965	17,941	311	271	295
Jun	19,049	18,743	18,857	18,769	306	192	280
Jul	25,403	24,626	24,789	24,668	777	614	735
Aug	25,253	24,562	24,672	24,583	691	581	670
Sep	22,068	21,520	21,636	21,549	548	432	519
Oct	19,693	19,344	19,378	19,356	349	315	337
Nov	15,180	14,764	14,764	14,764	416	416	416
Dec	13,818	13,425	13,425	13,421	393	393	397
Ann	216,954	211,592	212,238	211,779	5,362	4,716	5,175

Table 8.4 Monthly comparison of steam energy costs for emulated MPC scenarios (\$)

Month	RBC Steam Energy Cost	Energy MPC Steam Energy Cost	1-Day MPC Steam Energy Cost	1-Month MPC Steam Energy Cost	Energy MPC Savings	1-Day MPC Savings	1-Month MPC Savings
Jan	2,669	2,621	2,623	2,619	48	46	50
Feb	2,207	2,163	2,165	2,163	44	42	44
Mar	2,301	2,221	2,222	2,222	80	79	79
Apr	2,101	2,003	2,011	2,005	98	90	96
May	1,936	1,844	1,855	1,848	92	81	88
Jun	1,600	1,527	1,544	1,529	73	56	71
Jul	1,444	1,367	1,383	1,369	77	61	75
Aug	1,517	1,442	1,454	1,444	75	63	73
Sep	1,619	1,538	1,550	1,542	81	69	77
Oct	1,884	1,790	1,797	1,793	94	87	91
Nov	2,156	2,058	2,058	2,058	98	98	98
Dec	2,232	2,179	2,180	2,180	53	52	52
Ann	23,667	22,747	22,841	22,771	920	826	896

8.2 Conclusions from Emulated Model Predictive Control Simulations

Several conclusions can be drawn from the results of running emulated MPC and isolating the effects of the BRM on system performance. The first is that high magnitude accuracy of the $E+$ model used within emulated MPC does lead to improved electricity demand mitigation. All months either maintain the RBC electricity demand or lower the value through optimal morning start choice. This is in contrast with the results of Chapter 7, where only 6 months either reduced or maintained the peak electricity demand. The error introduced by simplified models in predicting magnitude values makes optimizing for electricity demand a challenge, as most simplified models have excellent trend following and low overall error, but can still miss the peak demand.

A second finding is that the forecast horizon has an impact on system performance. Using a forecast of one month had an improved performance over the forecast horizon of one day. The improvement is due to estimating the proper electricity demand value for the entire billing period, which allows for more energy savings. This is difficult to implement in practice due to uncertainties in weather forecasts over such a time period. Using a shorter window still achieves the demand reduction, but at the expense of using more energy prior to the monthly peak entering the horizon window. This is due to the efforts to minimize demand early in a billing period uses more energy at that time. When a later peak occurs, all this extra energy used to mitigate the previous demand peaks is wasted as demand is billed on the highest peak.

A final finding is that when morning start alone is being optimized for the Mona Campbell Building, a pure energy minimization provides similar performance to cost reduction strategies utilizing electricity demand charges. The energy minimization performs similarly due to the morning start having a larger impact on morning heating in the Halifax climate, which is serviced primarily by steam. A second factor is that the electricity peak typically occurs in the afternoon for cooling, meaning the choices made for morning start have minimal impact on the electricity peak demand. The efficient HVAC system of the Mona Campbell also minimizes the amount of potential savings due an already low amount

of energy consumption. A final contributing factor is the energy pricing structure, where the energy cost represents the largest portion of costs. In jurisdictions/buildings where demand charges are a larger component of total cost, a larger emphasis is likely to be placed on electricity demand mitigation.

Chapter 9 EXPERIMENTAL RESULTS

Portions of this chapter have been submitted to Building and Environment for publication with Ms. Ref. No.: BAE-D-17-00886, coauthored by Dr. Lukas Swan and Dr. Zheng Qin, 27 pgs.

Trent Hilliard is the principal researcher and author of the article. He conducted the research as part of his PhD. Thus, while he received supervision and guidance from his coauthors Dr. Lukas Swan and Dr. Zheng Qin, he carried out the work, wrote the article, and communicated with the editor of the journal. Minor grammatical and content changes have been made to integrate the article within this dissertation.

9.1 Introduction

An experimental test was conducted on the Mona Campbell building to verify MPC performance in a real-world setting. Based on the results of Chapter 8 which indicate simplified models struggle with demand charges, an energy minimization scheme was employed. Data was collected from the existing building BAS on 15 minute timesteps, with ZAT setpoints applied to the BAS for implementation. Data was collected starting May 2, 2016. The MPC was implemented on the building from August 8, 2016 to November 28, 2016, providing 4 months of data for comparison. MPC was implemented as described in section 6.10, where the emulated MPC results were used for morning start, and the BRM based MPC results for the occupied period. The objective function was the same as in section 7.1.3. The system was run first offline, with the results then clustered using ‘k means’ clustering to create a real-time operational system. The clustered results act as a look-up table where weather and building state are the inputs, with the optimal building setpoints as the output. The ZOT comfort layer is then applied across the building utilizing the forecasts produced by GPL. Building system performance was monitored for energy savings performance, while the client feedback portal was used to monitor thermal comfort of the occupants. Limits were provided to the output setpoints from the MPC to be in the range of 19 to 26 °C during the daytime period. A heartbeat function was included that if no information was gathered or written for three consecutive timesteps in a row the building would revert back to the existing rule based control.

9.2 Building Response Model

For the whole building optimization, a simplified BRM was required for the occupied period of the MPC due to computational time constraints of *E+*. The *randomForest* modeling technique as employed in Chapter 6.1 was used with the following data sources:

- Simulated data from a calibrated *E+* model.
- Measured data from the building.

The data consisted of 90% *E+* simulation data, and 10% measure data from the building. No additional weighting was placed on the measured data, and the *randomForest* model was allowed to split the data between trees as it saw fit.

A validation was conducted on the BRM predictions (temperature and power) to the measured site data. Figure 9.1 is a comparison of BRM predictions to measured data for a summer day (August 22) for the occupied period of 08:00 to 22:00 when the BRM was used for MPC. As shown, the electricity model predicts well with minimal deviations. The steam appears to have a consistent offset, with the model predicting constant usage while the site measurements are sporadic. A comparison of zone temperature shows a consistent daytime offset of approximately 1 °C, with the BRM underpredicting. Figure 9.2 is a comparison for fall (October 5) and represents some of the colder ambient conditions during data collection. As shown, the electricity model shows a similar level of performance as in the summer months, with steam showing an improvement in performance, but still trends on the overprediction side. The temperature performance has a similar 1 °C offset. The data gap at 11:30 is due to a communication error and shows that there is minor impact on the simplified model prediction performance (drop of 1 °C in temperature prediction, increase in steam prediction), indicating that the model can withstand a sensor issue and still provide usable predictions. A statistical fit between the BRM and measured data is provided in Table 9.1, which shows worse performance than the *E+* comparison. This is due to the fact that the majority of training data was from *E+*, and due to operational changes that occurred at the building between the period of used for

model calibration and when the MPC system was tested. These changes include the moving of several servers to a different building (November 2015), isolating steam heating to domestic hot water during the summer (June 2106), and changes to the cooling equipment within the server room (November 2014). The overprediction errors (as outlined in the NMBE) are in line with the changes, as electrical load was removed from the building, and the steam was disabled.

Based on the model fit with the *E+* data (90% of the training data for the model), a future iteration of the model trained with a majority of data from the actual building should result in improved model predictions when compared to the measured building data.

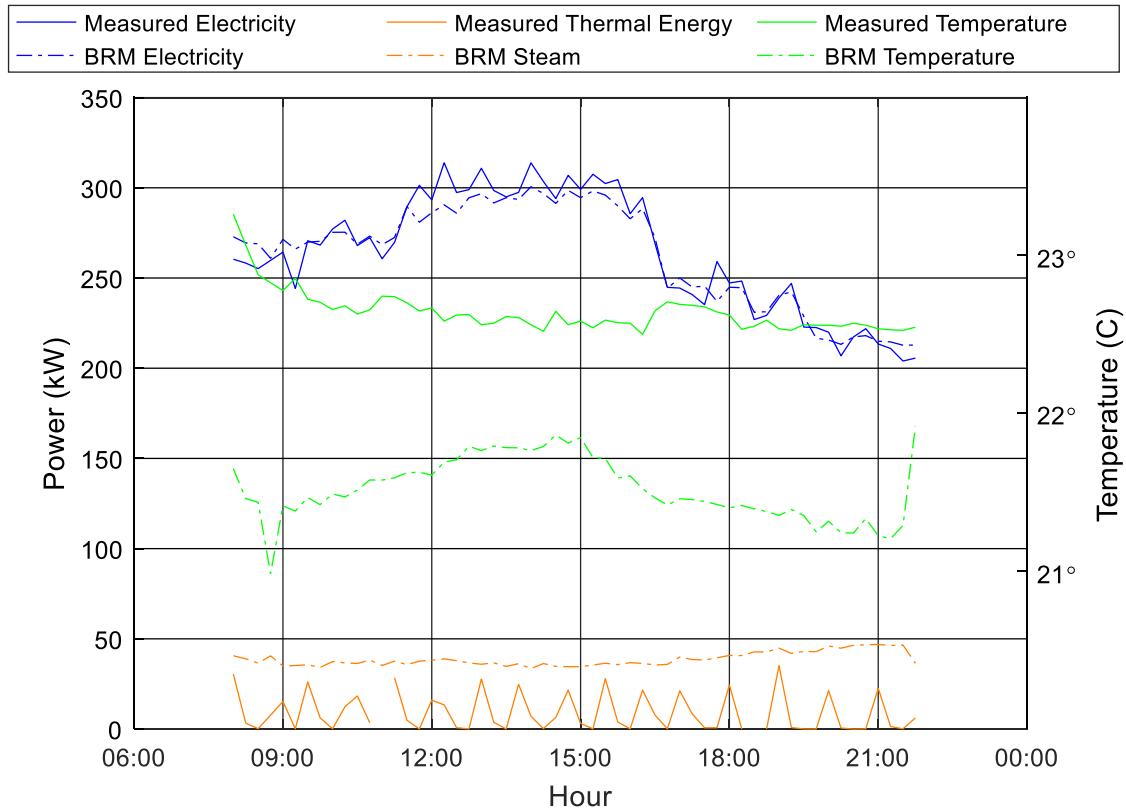


Figure 9.1 Comparison of measured data to BRM predictions in summer

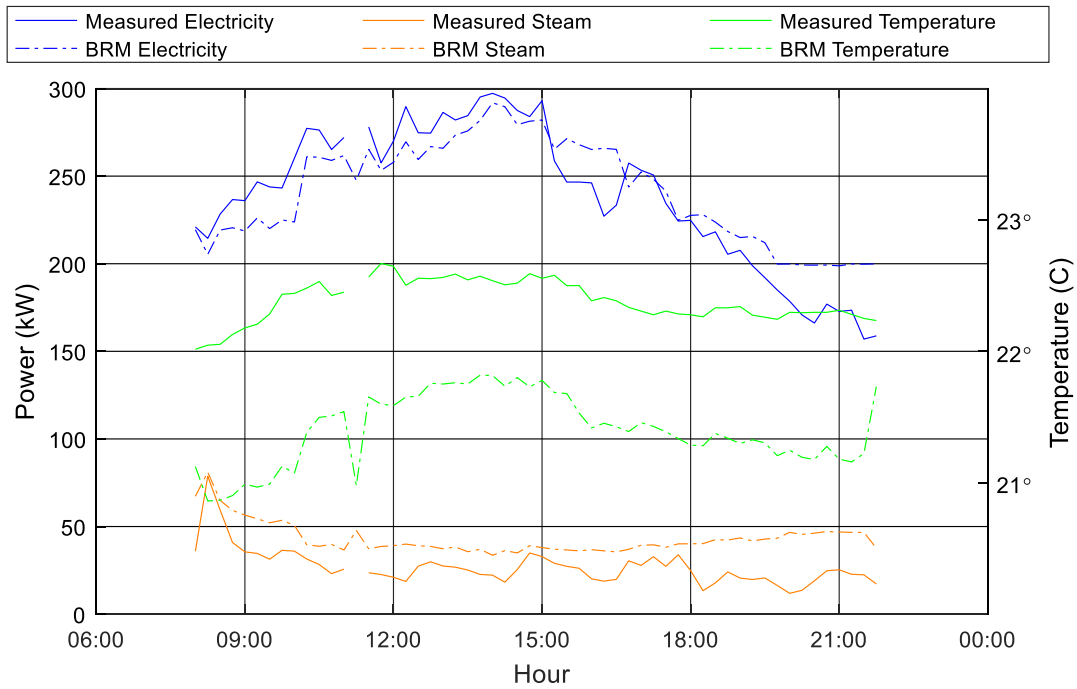


Figure 9.2 Comparison of measured data to BRM predictions in winter

Table 9.1 BRM model fit to measured site data

Model	NMBE (%)	RMSE (kW/°C)	CV(RMSE) (%)
Electricity	28	69.4	37
Steam	191	27.0	188
Temperature	-3	0.755	3

9.3 Energy Savings

The first quantifiable measure in the success of the MPC scheme is that energy savings exist and are generated by both the optimized start and daytime optimization of the MPC. There were several non-HVAC operational changes made in previous years that make comparison to historical data difficult. These changes include the moving of several servers to a different building (November 2015), isolating steam heating to domestic hot water during the summer (June 2106), and changes to the cooling equipment within the server room (November 2014). Due to these changes a comparison to historical whole building data would not provide an accurate representation of MPC savings. Instead, dedicated sub-meters on the HVAC system were used to determine the impact of the MPC. This is an appropriate comparison meter as it only considers the portion of electrical load affected by MPC (the server room cooling equipment was measured separately from the remainder of the HVAC load).

A comparison to historical HVAC electricity is given in Figure 9.3, while steam is given in Figure 9.4, with a weather comparison of heating degree days and cooling degree days given in Figure 9.5. Note that the plotted data is the supplied monthly data. The test period of August to November 2016 is shaded a darker green. As shown in Figure 9.3, the historical HVAC energy appears to have an upward trend in usage from 2014 through 2015 and into the beginning of 2016. The first decline begins in August 2016 after the MPC technology was employed with the decrease being maintained until December when the MPC trial period ended. In comparison to 2015, a total HVAC electricity reduction of 29% was achieved for the trial period of MPC (August through November 2016). Figure 9.4 clearly shows that the steam was isolated in June of 2016, and was re-enabled in late September for the beginning of the heating season. The marked decreases in October and November can be attributed to the implementation of the MPC to the site, where the usage in December re-approaches historical levels when the MPC technology was not used. A decrease in steam for October and November of 63% compared to 2015 was achieved and can be directly related to the MPC implementation. The weather trends in Figure 9.5 show

that the climate is a heating dominated climate, and that there was minor variability year to year.

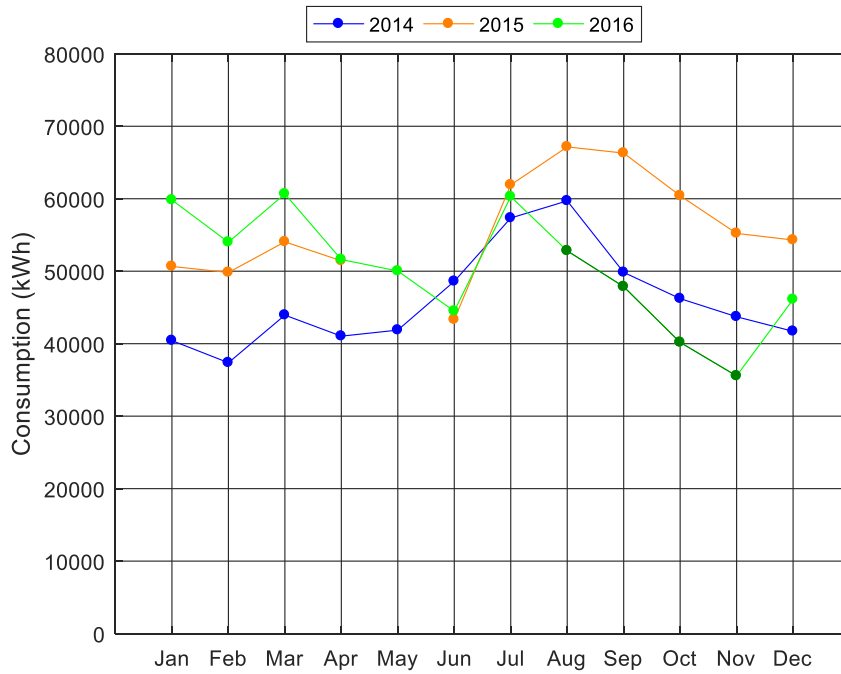


Figure 9.3 Historical HVAC electricity usage

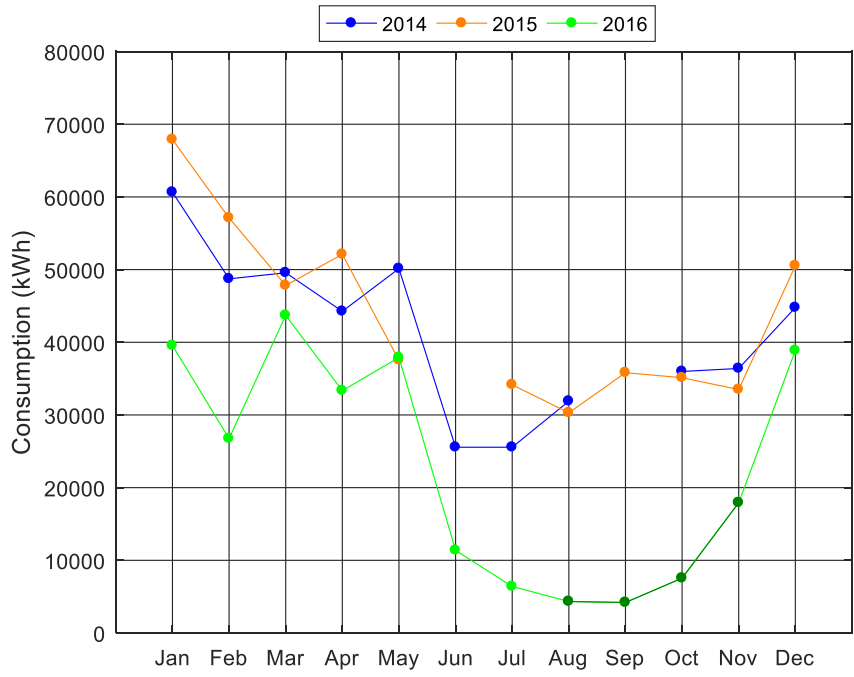


Figure 9.4 Historical steam consumption

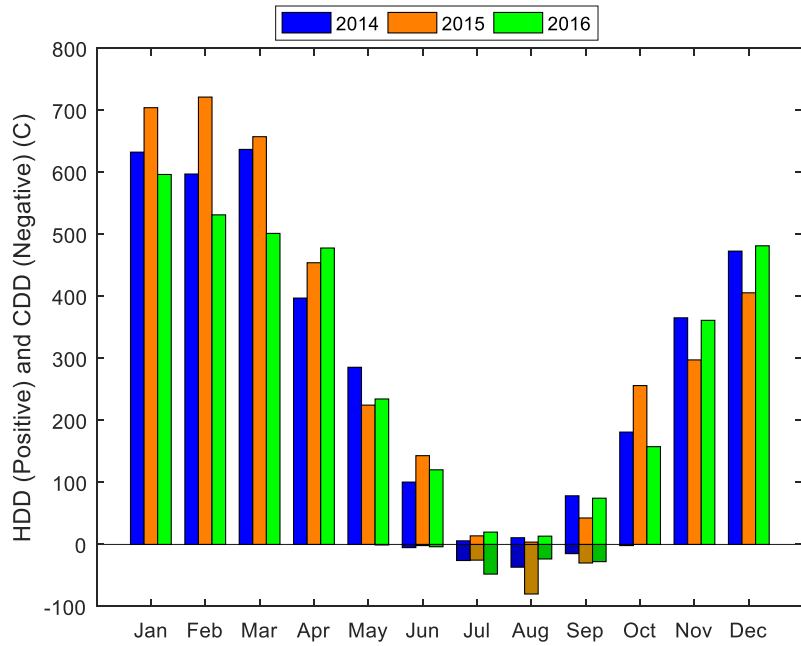


Figure 9.5 Historical ambient condition trends as defined by HDD and CDD

To better understand how the MPC saved energy, a comparison between the last full week prior to the MPC and first full week after MPC implementation was undertaken, with the results in Figure 9.6 and weather in Figure 9.7, which demonstrated similar ambient conditions. The temperature profile shows the change from the constant setpoints being used by the building (week 31) to when the MPC scheme is activated (week 33) where night setbacks become employed, and several daytime changes can be seen.

Larger savings were generated during constant external conditions (such as Tuesday and Wednesday), while fluctuating ambient conditions cause more changes in control setpoints, thus more equipment cycling occurred and led to energy usage. The fluctuations are driven by the competing nature of ZOT comfort requirements and energy minimization. Morning start optimization savings can be seen by the delay in reaching the daytime nominal operating value, where week 31 has a peak that drops down, while week 33 exhibits smoother behavior. An example of this occurs on Wednesday, when the week 31 has a first peak of 237 kW at 07:30, while week 33 has a first peak at 09:30 of 227 kW. The daytime savings are noticeable by the offset between the peak values for week 31 and week 33, with a reduction of 30 kW on Wednesday (279 kW for week 31 and 249 kW for week 33).

Savings were achieved overnight and on weekends due to the implementation of setback temperature setpoints. The AHU schedules had previously had night shutdown implemented. The reduction in weekend electricity usage was due to the fresh air system being engaged over the weekend, but with using the setback temperatures less energy was required as a tight temperature band was no longer being maintained. Overnight savings were also achieved due to smaller loads required to maintain the setback conditions.

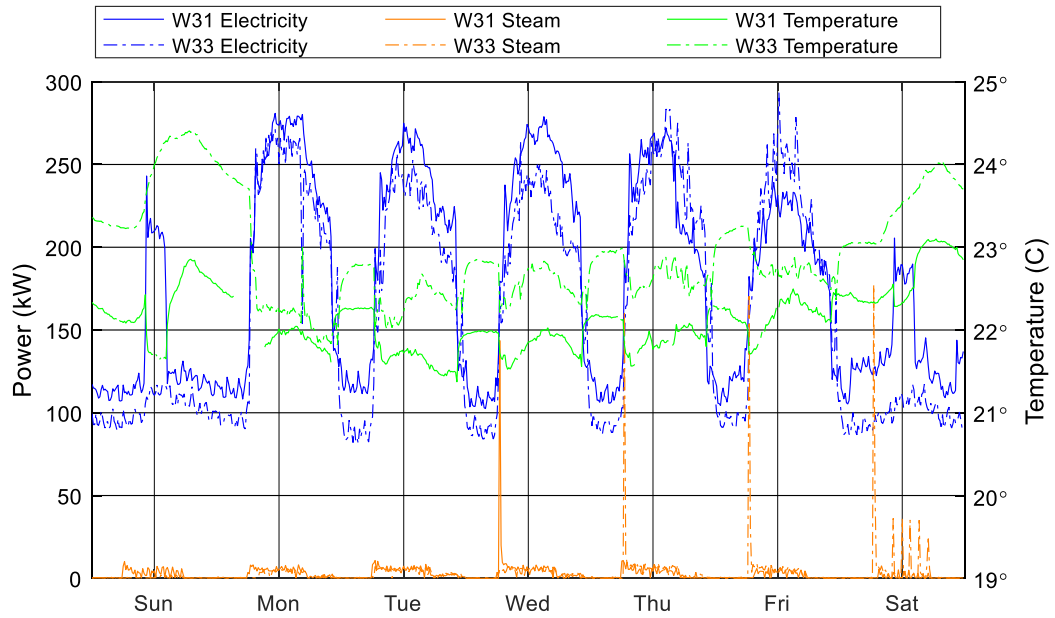


Figure 9.6 Comparison prior to (week 31 – solid) and after (week 33 – dashed) MPC integration electricity, steam, and temperature

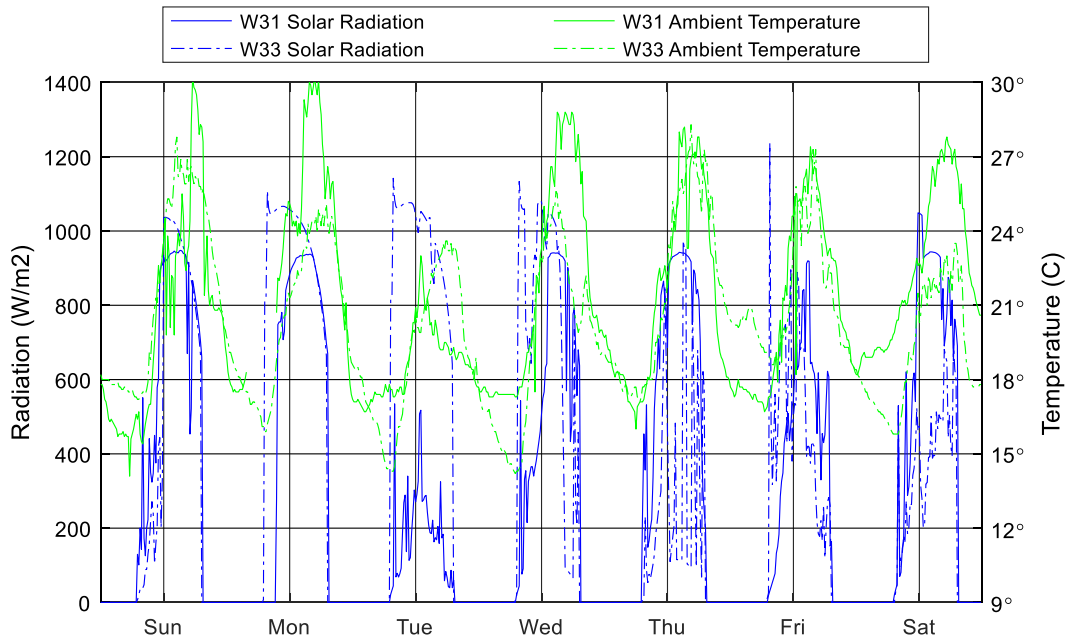


Figure 9.7 Weather comparison prior to (week 31 – solid) and after (week 33 - dashed) MPC integration

In addition to the comparison to measured data, a regression based models for steam and HVAC electricity were developed. The 2014 and 2015 data was used to create the regression models. For steam, the sole regressor used was HDD (steam is only used for heating), while for electricity both HDD and CDD were used (the heat pumps provide both heating and cooling). The model statistics are outlined in Table 9.2, which show that the steam model appears to have a better fit than electricity due to the higher r^2 and higher F statistic.

Table 9.2 Regression model statistics

Model	HDD Coefficient	CDD Coefficient	Intercept	r^2	F
Electricity	-6.1	262	50164	0.51	10.3
Steam	39.9	N/A	28973	0.76	62.6

A comparison between the regression model and measured electricity data for 2016 is given in Figure 9.8, which shows that savings during the MPC period exist throughout the 95% confidence range. The percent savings range from 10% to 29%, with the nominal model predictions showing 19% savings. A p-value of 0.049 statistically validates the savings. The results for steam are shown in Figure 9.9, where the range of savings within the 95% confidence interval are 69% to 86%, with the nominal model prediction showing a 78% reduction for the months of October and November (August and September were omitted due to operational changes that were reverted in late September). A p-value of 0.024 demonstrates the statistical significance of the results. The test period from August to November is shaded to highlight when MPC was run on the building. The results for electricity are tabulated in Table 9.3, and steam in Table 9.4.

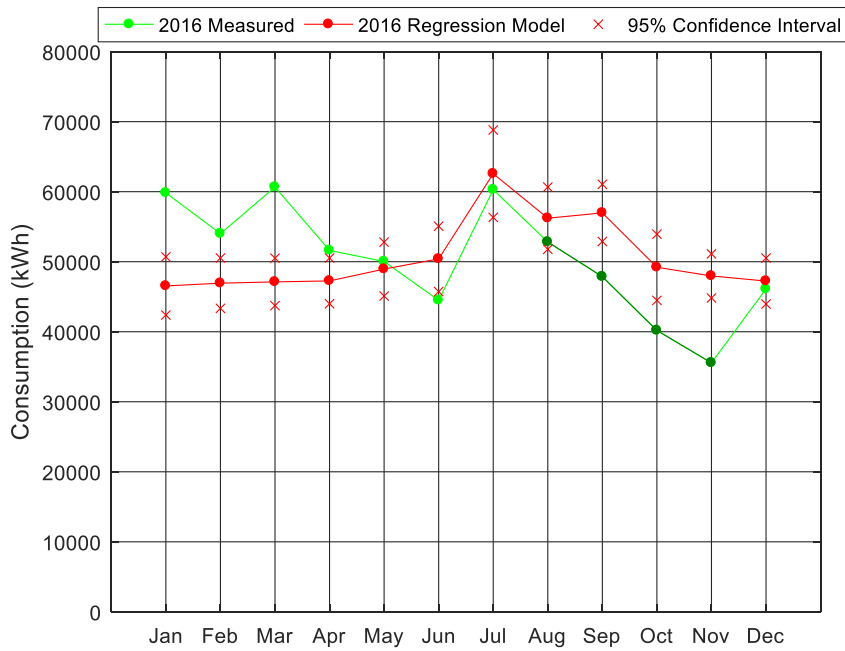


Figure 9.8 Comparison between measured data and regression model for electricity

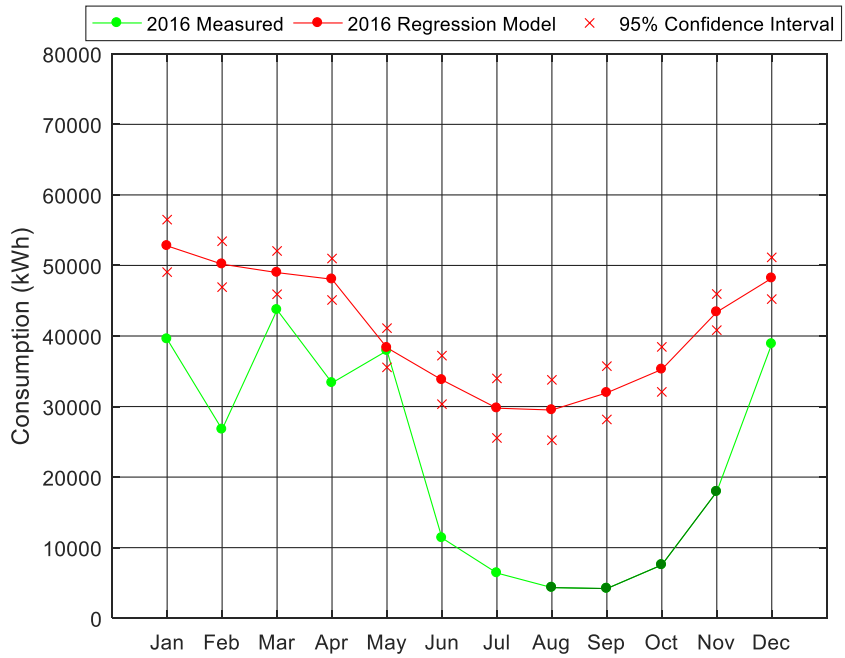


Figure 9.9 Comparison between measured and regression model for steam

Table 9.3 Monthly electricity consumption (kWh), MPC savings in bold

Month	2014	2015	2016	2016 Regression	Savings vs 2015	Savings vs Regression
January	40429	50657	59825	46538	9168	13287
February	37372	49828	54007	46934	4179	7073
March	43941	54049	60661	47116	6612	13545
April	41038	51434	51614	47259	180	4355
May	41874	N/A	50028	48948	N/A	1080
June	48601	43318	44490	50402	1172	-5912
July	57339	61911	60289	62568	-1622	-2279
August	59705	67150	52813	56214	-14337	-3401
September	49836	66297	47864	56969	-18433	-9105
October	46219	60416	40181	49205	-20235	-9024
November	43715	55217	35554	47967	-19663	-12413
December	41708	54301	46104	47237	-8197	-1133

Table 9.4 Monthly steam consumption (kWh), MPC savings in bold

Month	2014	2015	2016	2016 Regression	Savings vs 2015	Savings vs Regression
January	60643	67895	39559	52776	-28336	-13217
February	48729	57111	26757	50178	-30354	-23421
March	49566	47816	43706	48985	-4110	-5279
April	44260	52105	33352	48044	-18753	-14692
May	50138	37540	37911	38332	371	-421
June	25561	N/A	11372	33776	N/A	-22404
July	25561	34157	6399	29766	-27758	-23367
August	31898	30297	4333	29507	-25964	-25174
September	N/A	35818	4197	31949	-31621	-27752
October	35981	35123	7545	35264	-27578	-27719
November	36400	33501	17926	43392	-15575	-25466
December	44774	50526	38865	48187	-11661	-9322

9.4 Zone Operative Temperature Adjustment

In addition to the whole building setpoint changes, a verification of the ZOT comfort adjustments was also undertaken. An example of the ZOT based adjustments for a western facing zone can be shown in Figure 9.10 for Thursday of week 33. The setpoints are reduced during the afternoon period when direct sunlight would be entering the zone, and the intermittent nature of adjustments occurs due to the fluctuating solar load. While these adjustments typically expend more energy, the improvement in thermal comfort is considered more important than the additional energy cost. As shown, the changes in setpoint are used to lower the ZAT, which in turns lowers the ZOT of the zone to maintain comfort.

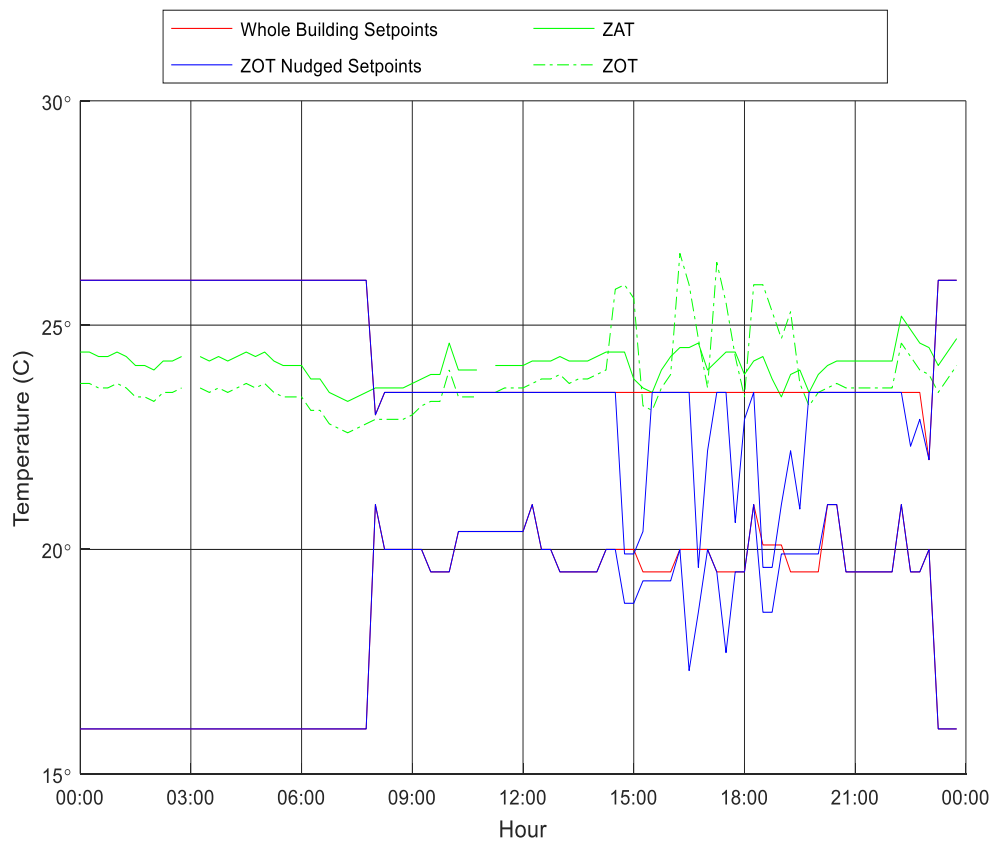


Figure 9.10 ZOT based thermal comfort adjustments – first floor west

9.5 User Feedback

The client feedback portal became operation on September 16, 2016 for the remainder of the trial period. The portal recorded 636 instances of feedback from occupants. The feedback consisted of 23 comfortable (3.6%), 197 too cold (31.0%), and 416 too warm (65.4%). The high percentage of uncomfortable complaints (as a percent of total feedback) is not unexpected as the use of the portal was voluntary. It was assumed that a comfortable occupant would not log in to provide feedback. Feedback was registered by 22 of the 63 full-time occupants of the building, with 79% of the feedback coming from just 5 rooms (all single offices) in the building. The highest feedback room accounted for 44% of all feedback from a user whose desired comfort lied outside the ASHRAE comfort range (preferred a much cooler temperature). One of the high complaint rooms was found to have a thermostat mapping issue within the original BAS. This information was passed to the building operator, with the point being corrected and an immediate reduction in the rate of comfort complaints occurred. When compared to a total number of MPC control timesteps during the occupancy period (08:00-22:00 Monday-Friday) the 636 feedback points represent 0.4% of the 173,600 (63 people for 2800 timesteps) which lies far below the Fanger stated discomfort level of 10% of people dissatisfied [48].

9.6 Conclusions of Experimental Implementation

A hybrid, multilayered MPC approach for optimal building control while maintaining occupant comfort through the use of zone level ZOT adjustments and a client feedback portal was experimentally implemented on an academic building. During the period of operation, a HVAC energy reduction of 29% for electricity and 63% for steam was achieved on-site compared to 2105 usage utilizing the existing rule based control with individual occupant control. A linear regression based model built on HDD and CDD was built to confirm the savings, which the savings are 19% for HVAC electricity and 78% for steam, with p-values of 0.049 for HVAC electricity and 0.024 for steam statistically validating the savings. The client feedback portal registered only 0.4% complaints of discomfort over the nominal occupied period. These results justify that treating the whole building average for optimization (to minimize computational complexity) and then applying local thermal comfort adjustments is indeed a viable approach to the optimization problem. The low level of complaints also verifies the decision to use ZOT as the comfort metric as opposed to ZAT, due to the incorporation of radiation based effects. The MPC (including the energy modeling portion) only uses information readily available in the BAS and/or provided by the building manager (such as occupancy hours and design drawings) to provide a low-cost solution that requires no on-site installation beyond a data connection to the BAS.

While the BRM energy predictions did differ from the actual energy use of the building, the fit with the simulated training data (which compromised 90% of training data) indicate that a retraining of the model should provide better performance. Even with the prediction errors, the relative gains seen by the model are enough for optimal decisions to be made when using an energy minimization scheme. The savings exceed those found in the simulation study, and can be attributed to several of the assumptions built into the model. The first area is the implementation of setbacks, which had been in use but manually overridden between the model calibration period (2013 data) and the MPC testing in 2016. A second factor is the uniformity of the zone setpoints in $E+$ compared to on site, where variability in thermostats existed. To overcome these issues, a finer resolution model in $E+$

would be required. This extra work for such a model is not trivial. Secondly, the current zoning groups rooms based on their expected ZOT comfort range, as they should experience similar ambient conditions, thus it should be sufficient for development of the MPC.

Chapter 10 CONCLUSIONS AND FUTURE WORK

The results of this dissertation demonstrate a model predictive control (MPC) approach for whole building control utilizing surface level forecasts can be implemented, and can provide energy reduction through the experimental study conducted, with simulations showing smaller savings potential.

10.1 Conclusions

The results are made possible through the steps outlined in this thesis, starting with an accurate source of data to train the building response model (BRM) for MPC. The data was generated using a calibrated EnergyPlus (*E+*) model of the building to ASHRAE Guideline 14, and supplemented with measured data from the building automation system (BAS). The importance of the advanced energy model cannot be understated, as it was used to generate the BRM, and the primary source of data for development zone operative temperature (ZOT) prediction methodology.

Building energy model

While a calibrated model was developed for use within the MPC, the quality of the calibration can be questioned. The model was calibrated using the best data available for the time period of historical energy data, which included setbacks in the control strategy. Data monitoring prior to the implementation of MPC indicated that setpoint setbacks were not being used, but the main air handling equipment was being turned off overnight. While this leads to differences in the energy model absolute results, the daytime trends remain similar as was shown in Section 9.2, which allows MPC to make the right decision. These differences highlight the challenges of energy modelling, as there are many uncertainties in the model (e.g. construction quality, control strategy) that can be tuned to achieve a calibrated model.

Building response model

The use of the *randomForest* model as the BRM was a success, as it was capable of providing energy savings for all MPC scenarios tested. Best performance occurred with energy minimization tasks. The energy minimization scheme is a relative based decision – find the path that uses the least energy, regardless of the quantity. In contrast, demand mitigation requires high prediction accuracy, as the predictions are compared to a measured peak for savings. Instead of determining which option has the smallest peak, the magnitude of the peaks is what drives cost savings. The BRM based MPC struggled with demand savings due to the need for high precision in peak prediction values. Many simplified models struggle to predict the correct peak magnitude (even detailed models can struggle, hence it is not included in ASHRAE Guideline 14). The struggle with electricity demand events indicate that design of the objective function should account for the capabilities of the simplified model.

Thermal comfort metric

In this dissertation, a more advanced thermal comfort metric than zone air temperature (ZAT) was explored. ZOT was chosen due to its prescribed use in industry standards, and potential ease of measurement. While other researchers have attempted to use PMV/PPD, the number of variables to be measured to produce such calculations is large, and many variables are not readily measured in buildings currently. By contrast, ZOT only requires ZAT (already measured) and zone radiant temperature (ZRT) (which can be measured, or approximated), where standard approximations can be made for variables such as clothing, metabolic rate, air speed, and humidity to account for their impact on comfort.

Due to a typical building not having ZRT measurements, a linear estimation was developed based on simulation data to approximate the ZRT based on the surface level weather forecasts (ambient temperature, direct radiation, and diffuse radiation) for each building zone. The method allows for the use of detailed weather forecasting to improve the comfort across the building, as individual zone radiant effects are incorporated.

The ZOT based comfort was implemented as a modifying layer after a whole building energy optimization. This is a key advancement, as optimizing for all zones simultaneously is a large problem that is computationally challenging, and not feasible for real time application due to computing time. The implementation is done by first solving a whole building energy minimization, followed by a zone level adjustment to maintain comfort. By solving a much simpler whole building energy optimization, the computational burden is vastly reduced compared to optimizing all the zones simultaneously. With the comfort metric as the last layer, it ensures thermal comfort is not compromised for energy savings. The importance of comfort cannot be understated, as it is the primary function of buildings.

Optimization objectives

Several advanced simulation scenarios were explored to determine their effectiveness and suitability with the MPC system as designed. A pure energy minimization (no preference between energy source) was first explored, which showed cost savings of 0.5% over rule-based control with fixed energy pricing. While the energy consumption was minimized (2% total reduction and 5% HVAC reduction), a lack of total cost savings was due to the resulting increase in demand costs. The total savings are in line with the lower end of the surveyed literature, and is due to the low thermal mass and highly efficient HVAC system installed on the building. The next scenario explored was implementing a total cost minimization problem that included energy prices (constant but different for each source) and an electric demand mitigation term. The initial simulation showed an oscillatory behavior between control options as the system tried to balance the savings of the various energy sources, leading to undesirable performance. A second trend noticed was the lack of demand savings. The addition of a switching penalty was introduced to minimize equipment cycling and act as a rate of change limit. This improved performance (2.6% total cost savings, 6.1% HVAC cost savings) while limiting the oscillations in the system. The use of time-of-day electricity pricing was then conducted to assess their impact on performance and the same trends occurred where a fluctuation penalty was needed, and a total cost savings of 2.7% was achieved, or 6.1% of HVAC costs. The majority of the

savings were generated through the morning start optimization (80%), while the daytime period accounted for the remaining savings.

Forecasting and horizon

To explore the impact of forecast horizon and remove and BRM related errors, an emulated MPC scenario was conducted to include a larger horizon window (one day and one month as opposed to two hours) with both energy minimization and total cost minimization. Simulations were conducted with time of use electricity pricing (one day and one month forecasts). The one day forecast emulated MPC performed worse than energy minimization, in that it saved less money than the energy minimization strategy (\$104 difference). However, the one month forecast with time of use forecasting did save more money than the energy minimization method (\$480), indicating that the issue was with the forecast horizon, and not the objective function or optimization technique. The reason for energy minimization outperforming cost minimization with a short horizon window is that the cost minimization was trying to maintain the electricity demand peak currently experienced, not the expected peak for the billing period. By using a lower peak early in a month, extra energy is consumed to maintain the current electricity demand level. However, when an unavoidable peak occurs later in the billing cycle, all the energy consumed to maintain the lower peak is now waste, and led to the lower savings when compared with energy minimization. The results of the forecast horizon study indicate the need to carefully design the objective function around the forecast horizon, as attempting to optimize for effects that last longer than the forecast horizon can result in worse performance.

Experimental testing

An experimental test was conducted on-site to quantify the performance of the MPC scheme on a real building. Slight changes were made from the simulation testing in that a multi-model approach was used to optimization. This was done by using the calibrate *E+* model to do morning start optimization utilizing emulated MPC, while the BRM was used for daytime optimization. This was done due to the higher confidence in the *E+* model. A

second change was the usage of a genetic algorithm to solve the optimization problem as opposed to the brute force methodology used in simulation. The change was made to improve operational runtime and to increase the range of possible solutions after simulations with a limited number of options showed savings. These results were translated into a look-up table based on forecasted weather and current building temperature using ‘k-means’ clustering for even less computational burden during real-time operation. The clustered results act as a look-up table where the weather forecast and current building state are used to determine the optimal control setpoints. Overall, the implemented MPC was run from August 2, 2016 to November 28, 2016 and showed a 29% reduction in HVAC electricity and 63% in steam usage, equating to a 30% total HVAC energy reduction. This is in contrast to the energy minimization simulation which showed a 5% HVAC energy reduction. These numbers exceed the simulation results due to the simulation having a more optimal baseline (the simulations assumed uniform setpoints and setbacks as provided by the building operator, while this was not true on site). The savings in both the experimental and simulation systems validate the MPC was successful for energy reduction in buildings.

10.2 Recommendations

While the results of this dissertation have proven successful, there are still some further areas that could be explored. The first area is a study on the impact of the simulation timestep on MPC performance. It was shown that forecast horizon should dictate the type of optimization conducted (or vice versa), and it is expected that the simulation timestep has a similar property. An example of this is that if demand is billed on a 15-minute peak, a simulation timestep of 1-hour likely will miss the peak demand period due to the larger averaging period. A second key area for future work is the application of the MPC developed to various buildings, particularly those with more thermal mass and slower HVAC systems. By evaluating performance on different buildings, a better understanding of what factors are best for applying MPC can be realized, and help aid in commercialization of the technology. An expansion of the MPC objectives from morning

start and daytime optimization to include optimal shutdown and free cooling should also be added for higher energy savings potential.

A second area for further exploration is the method used to predict ZRT for ZOT control. The current method requires sensors typically not installed in buildings, or the development of a detailed energy model to generate the relationships. It is expected that the linear regression coefficients are related to the construction parameters of the space (window to wall ratio, construction materials, zone aspect ratio), where the use of surface level forecasting eliminates the effects of orientation. More work is needed to try and develop a method of producing suitable coefficients without developing a detailed energy model for cases where buildings have a large amount of stored data accessible within the BAS. Additionally, exploration of the time lag effect of ZRT would provide better information to the MPC, however additional models would be needed for this scope of work, in addition to adding to the computational burden of the MPC.

In order to become a commercially viable solution, MPC must be transferable from building to building, and require minimal preparation. Currently a detailed energy model is required, which requires weeks of work from an expert in energy modeling. Methods to create models more efficiently, or translate the results to not require a detailed energy model are needed. One key aspect of the work that does allow it to be transferable is that it attempts to optimize the amount of energy needed by a space, as opposed to the efficiency of the delivery system. For improved savings, a layer of system optimization can be employed, but would be a custom solution on a per building basis, as opposed to a general methodology that can be applied regardless of the HVAC system.

The scope of MPC for buildings and its applications could be further explored. An example would be using MPC to better utilize on-site renewable resources that must be used on-site or else curtailed. A prediction of renewable generation can be included with the forecast information, and an additional objective function term added to ensure the building load matches the renewable generation. The result may lead to increased energy usage during peak renewable generation to match load, while reducing the amount of imported energy

to the site. A second potential expansion of MPC with buildings is to help balance the electrical grid. A forecast of grid power production can be used as a MPC input, where the building may shift its usage profile to smooth out the grid demand profile. Changes to the MPC timestep and forecast horizon may be needed for grid applications as the response time of the electrical grid is much faster than a building (order of seconds compared to minutes), depending on the service provided. If doing peak load shedding, the frequency of response aligns well with buildings, while services such as frequency regulation require a faster response. A key component for allowing the expansion of MPC to other applications is the inclusion of energy storage, either thermally or electrically. The more storage capability a building has, the more impactful it can be in providing the ancillary services discussed.

REFERENCES

- [1] Y. Huang, "Drivers of rising global energy demand: The importance of spatial lag and error dependence," *Energy*, vol. 76, pp. 254-263, 2014.
- [2] X. Liu, A. Vedlitz, J. W. Stoutenborough and S. Robinson, "Scientists' views and positions on global warming and climate change: A content analysis of congressional testimonies," *Climatic Change*, vol. 131, no. 4, pp. 487-503, 2015.
- [3] United Nations, "Paris Agreement," United Nations, Paris, 2015.
- [4] Natural Resources Canada, "Energy Use Data Handbook: 1990 - 2010," Natural Resources Canada, 2013.
- [5] Natural Resources Canada, "Survey of commercial and institutional energy use – buildings 2009," Natural Resources Canada, Ottawa, Ontario, 2012.
- [6] L. Perez-Lombard, J. Ortiz and C. Pout, "A review on buildings energy consumption information," *Energy and Buildings*, pp. 394-398, 2008.
- [7] M. Gwerder, D. Gyalistras, C. Sagerschnig, R. S. Smith and D. Sturzenegger, "Final Report: Use of Weather And Occupancy Forecasts For Optimal Building Climate Control – Part II: Demonstration (OptiControl-II)," Automatic Control Laboratory, Zurich, 2013.
- [8] S. Wang, "Energy modeling of ground source heat pump vs. variable refrigerant flow systems in representative US climate zones," *Energy and Buildings*, vol. 72, pp. 222-228, 2014.
- [9] Y. Ma, F. Borrelli, B. Hency, B. Coffey, S. Benghea and P. Haves, "Model predictive control for the operation of building cooling systems," *IEEE Transactions on Control Systems Technology*, vol. 20, no. 3, pp. 796-803, 2012.
- [10] D. F. Dicaire and H. Tezel, "Regeneration and efficiency characterization of hybrid adsorbent for thermal energy storage of excess and solar heat," *Renewable Energy*, vol. 36, no. 3, pp. 986-992, 2011.
- [11] S. Kahwaji, M. B. Johnson, A. C. Kheirabadi, D. Groulx and M. A. White, "Stable, low-cost phase change material for building applications: The eutectic mixture of decanoic and tetradecanoic acid," *Applied Energy*, vol. 168, pp. 457-464, 2016.

- [12] S. D. Zwanzig, Y. Lian and E. G. Brehob, "Numerical simulation of phase change material composite wallboard in a multi-layered building envelope," *Energy Conversion and Management*, vol. 69, pp. 27-40, 2013.
- [13] A. Zidan, H. A. Gabbar and A. Eldessouky, "Optimal planning of combined heat and power systems within microgrids," *Energy*, vol. 93, no. 1, pp. 235-244, 2015.
- [14] A. H. Abdel-Salam and C. J. Simonson, "State-of-the-art in liquid desiccant air conditioning equipment and systems," *Renewable and Sustainable Energy Reviews*, vol. 58, pp. 1152-1183, 2016.
- [15] M. R. Abdel-Salam, R. W. Besant and C. J. Simonson, "Design and testing of a novel 3-fluid liquid-to-air membrane energy exchanger (3-fluid LAMEE)," *International Journal of Heat and Mass Transfer*, vol. 92, pp. 312-329, 2016.
- [16] T. Hilliard, L. Swan, M. Kavacic, Z. Qin and P. Lingras, "Development of a whole building model predictive control strategy for a LEED silver community college," *Energy and Buildings*, pp. 224-232, 2016.
- [17] S. R. West, J. K. Ward and J. Wall, "Trial results from a model predictive control and optimisation system for commercial building HVAC," *Energy and Buildings*, vol. 72, pp. 271-279, 2014.
- [18] J. Siroky, F. Oldewurtel, J. Cigler and S. Privara, "Experimental analysis of model predictive control for an energy efficient building heating system," *Applied Energy*, vol. 88, no. 9, pp. 3079-3087, 2011.
- [19] S. C. Benghea, A. D. Kelman, F. Borrelli, R. Taylor and S. Narayanan, "Implementation of model predictive control for an HVAC system in a mid-size commercial building," *HVAC and R Research*, vol. 20, no. 1, pp. 121-135, 2014.
- [20] W. O'Brien and G. H. Burak, "The contextual factors contributing to occupants' adaptive comfort behaviors in offices – A review and proposed modeling framework," *Building and Environment*, vol. 77, pp. 77-87, 2014.
- [21] G. R. Newsham, H. Xue, C. Arsenault, J. J. Valdes, E. Scarlett, S. G. Kruithof and W. Shen, "Testing the accuracy of low-cost data streams for determining single-person office occupancy and their use for energy reduction of building services," *Energy and Buildings*, vol. 135, pp. 137-147, 2017.

- [22] T. Labeodan, W. Zeiler, G. Boxem and Y. Zhao, "Occupancy measurement in commercial office buildings for demand-driven control applications - A survey and detection system evaluation," *Energy and Buildings*, vol. 93, pp. 303-314, 2015.
- [23] M. De Felice, A. Alessandri and P. M. Ruti, "Electricity demand forecasting over Italy: Potential benefits using numerical weather prediction models," *Electric Power Systems Research*, vol. 104, no. 11, pp. 71-79, 2013.
- [24] J. Grosso, C. Ocampo-Martinez and V. Puig, "Learning-based tuning of supervisory model predictive control for drinking water network," *Engineering Applications of Artificial Intelligence*, vol. 26, no. 7, pp. 1741-1750, 2013.
- [25] J. F. Kreider, X. A. Wang, D. Anderson and J. Dow, "Expert systems, neural networks and artificial intelligence applications in commercial building HVAC operations," *Automation in Construction*, vol. 1, no. 3, pp. 225-238, 1992.
- [26] H. B. Gunay, J. Bursill, B. Huchuk, W. O'Brien and I. Beausoleil-Morrison, "Shortest-prediction-horizon model-based predictive control for individual offices," *Building and Environment*, vol. 82, pp. 408-419, 2014.
- [27] M. Sourbron, C. Verhelst and L. Helsen, "Building models for model predictive control of office buildings with concrete core activation," *Journal of Building Performance Simulation*, pp. 175-198, 2013.
- [28] J. (. Feng, F. Chuang, F. Borrelli and F. Bauman, "Model predictive control of radiant slab systems with evaporative cooling sources," *Energy and Buildings*, vol. 87, pp. 199-210, 2015.
- [29] L. He, B. Lei, H. Bi and T. Yu, "Simplified Building Thermal Model Used for Optimal Control of Radiant Cooling System," *Mathematical Problems in Engineering*, pp. 1-15, 2016.
- [30] D. Zhang, X. Xia and N. Cai, "A dynamic simplified model of radiant ceiling cooling integrated with underfloor ventilation system," *Applied Thermal Energy*, vol. 106, pp. 415-422, 2016.
- [31] M. Soleimani-Mohseni, B. Thomas and P. Fahlen, "Estimation of operative temperature in buildings using artificial neural networks," *Energy and Buildings*, vol. 38, no. 6, pp. 635-640, 2006.
- [32] F. Frontini and T. E. Kuhn, "The influence of various internal blinds on thermal comfort: A new method for calculating the mean radiant temperature in office spaces," *Energy and Buildings*, vol. 54, pp. 527-533, 2012.

- [33] K. Ka-Lun Lau, C. Ren, J. Ho and E. Ng, "Numerical modelling of mean radiant temperature in high-density sub-tropical urban environment," *Energy and Buildings*, vol. 114, pp. 80-86, 2016.
- [34] S. Thorsson, F. Lindberg, I. Eliasson and B. Holmer, "Different methods for estimating the mean radiant temperature in an outdoor urban setting," *INTERNATIONAL JOURNAL OF CLIMATOLOGY*, vol. 27, pp. 1983-1993, 2007.
- [35] A. H. Neto, "Comparison between detailed model simulation and artificial neural network for forecasting building energy consumption," *Energy and Buildings*, vol. 40, no. 12, pp. 2169-2176, 2008.
- [36] T. Lu, "A hybrid numerical-neural-network model for building simulation: A case study for the simulation of unheated and uncooled indoor temperature," *Energy and Buildings*, vol. 86, pp. 723-734, 2015.
- [37] P. Ferreira, A. Ruano, S. Silva and E. Conceicao, "Neural network based predictive control for thermal comfort and energy savings in public buildings," *Energy and Buildings*, pp. 238-251, 2012.
- [38] K. A. Antonopolous and T. C., "Finite-difference prediction of transient indoor temperature and related correlation based on the building time constant," *International journal of energy research*, vol. 20, no. 6, pp. 507-520, 1996.
- [39] A. Afram and F. Janabi-Sharifi, "Theory and applications of HVAC control systems - A review of model predictive control (MPC)," *Building and Environment*, pp. 343-355, 2014.
- [40] R. Z. Homod, K. S. M. Sahari, H. A. Almurib and F. H. Nagi, "Double cooling coil model for non-linear HVAC system using RLF method," *Energy and Buildings*, vol. 43, no. 9, pp. 2043-2054, 2011.
- [41] S. Wang and Z. Ma, "Supervisory and Optimal Control of Building HVAC Systems: A Review," *HVAC&R Research*, pp. 3-32, 2008.
- [42] R. Findeisen and F. Allgoewer, "An introduction to nonlinear model predictive control," in *21st Benelux Meeting on Systems and Control*, 2002.
- [43] J. A. Clarke, *Energy simulation in building design*, Routledge, 2001.
- [44] L. Swan, "Residential Sector Energy and GHG Emissions Model for the Assessment of New Technologies," Dalhousie University, Halifax, 2010.

- [45] X. Jin, X. Zhang, Y. Cao and G. Wang, "Thermal performance evaluation of the wall using heat flux time lag and decrement factor," *Energy and Buildings*, vol. 47, pp. 369-374, 2012.
- [46] T. T. Steve, "Cost effective HVAC managing energy and performance," in *World Energy Engineering Congress 2007*, 2007.
- [47] A. Saari, T. Tissari, E. Valkama and O. Seppanen, "The effect of a redesigned floor plan, occupant density and the quality of indoor climate on the cost of space, productivity and sick leave in an office building—A case study," *Building and Environment*, pp. 1961-1972, 2006.
- [48] ASHRAE, "ASHRAE Standard 55- 2013: Thermal Environmental Conditions for Human Occupancy," ASHRAE, 2013.
- [49] P. O. Fanger, *Thermal Comfort*, Danish Technical Press, 1970.
- [50] J. Sykes, "Sick Building Syndrome," *Building services engineering research and technology*, vol. 10, no. 1, pp. 1-11, 1989.
- [51] ASHRAE, "ASHRAE Standard 62.1-2016 Ventilation for Acceptable Indoor Air Quality," ASHRAE, 2016.
- [52] R. Dales, L. Liu, A. J. Wheeler and N. L. Gilbert, "Quality of indoor residential air and health," *Canadian Medical Association Journal*, vol. 179, no. 2, pp. 147-152, 2008.
- [53] ISO, "ISO 7730 - Ergonomics of the thermal environment - Analytical determination and interpretation of thermal comfort using calculation of the PMV and PPD indices and local thermal comfort criteria," ISO, Geneva, 2005.
- [54] British Standards/CEN, "BS EN 15251:2007 - Indoor environmental input parameters for design and assessment of energy performance of buildings addressing indoor air quality, thermal environment, lighting and acoustics," British Standards, Brussels, 2007.
- [55] T. Hilliard, M. Kavacic and L. Swan, "Model predictive control for buildings: trends and opportunities," *Advances in Building Energy Research*, 2015.
- [56] B. Lehmann, G. D. M. Gwerder, K. Wirth and S. Carl, "Intermediate complexity model for model predictive control of integrated room automation," *Energy and Buildings*, vol. 58, pp. 250-262, 2013.

- [57] H. A. Neto, "Comparison between detailed model simulation and artificial neural network for forecasting building energy consumption," *Energy and Buildings*, vol. 40, no. 12, pp. 2169-2176, 2008.
- [58] S. Privara, J. Siroky, L. Ferkl and J. Cigler, " Model predictive control of a building heating system: The first experience," *Energy and Buildings*, vol. 43, no. 2-3, pp. 564-572, 2011.
- [59] S. Privara, Z. Vana, E. Zacekova and J. Cigler, "Building modeling: Selection of the most appropriate model for predictive control," *Energy and Buildings*, pp. 341-350, 2012.
- [60] H. B. Gunay, W. O'Brien and I. Beausoleil-Morrison, "Control-oriented inverse modeling of the thermal characteristics in an office," *Science and Technology for the Built Environment*, pp. 586-605, 2016.
- [61] M. Killian and M. Kozek, "Ten questions concerning model predictive control for energy efficient buildings," *Building and Environment*, vol. 105, pp. 403-412, 2016.
- [62] P.-D. Morosan, R. Bourdais, D. Dumur and J. Buisson, "Building temperature regulation using a distributed model predictive control," *Energy and Buildings*, vol. 42, no. 9, pp. 1445-1452, 2010.
- [63] A. Aswani, N. Master, J. Taneja, D. Culler and C. Tomlin, "Reducing transient and steady state electricity consumption in HVAC using learning-based model predictive control," *Proceedings of the IEEE*, vol. 100, no. 1, pp. 240-253, 2012.
- [64] Z. Ma and S. Wang, "Fault-tolerant supervisory control of building condenser cooling water systems for energy efficiency," *HVAC&R Research*, vol. 18, pp. 126-146, 2012.
- [65] M. Avci, M. Erkok, A. Rahmani and S. Asfour, "Model predictive HVAC load control in buildings using real-time electricity pricing," *Energy and Buildings*, vol. 60, pp. 199-209, 2013.
- [66] B. Coffey, "Approximating model predictive control with existing building simulation tools and offline optimization," *Journal of Building Performance Simulation*, pp. 220-235, 2013.
- [67] V. Putta, G. Zhu, D. Kim, J. Hu and J. Braun, "Comparative evaluation of model predictive control strategies for a building HVAC system," in *2013 American Control Conference*, Washington, DC, 2013.
- [68] F. Oldewurtel, A. Parisio, C. N. Jones, M. Morari, D. Gyalistras, G. M. V. Stauch, B. Lehmann and K. Wirth, "Energy efficient building climate control using stochastic model predictive control and weather," in *2010 American Control Conference*, Baltimore, 2010.

- [69] W. J. Cole, E. T. Hale and T. F. Edgar, "Building energy model reduction for model predictive control using OpenStudio," in *2013 American Control Conference*, Washington DC, 2013.
- [70] G. Huang, S. Wang and X. Xu, "Robust Model Predictive Control of VAV Air-Handling Units Concerning Uncertainties and Constraints," *HVAC&R Research*, vol. 16, pp. 15-33, 2010.
- [71] J. Ma, J. Qin, T. Salsbury and P. Xu, "Demand reduction in building energy systems based on economic model predictive control," *Chemical Engineering Science*, vol. 67, no. 1, pp. 92-100, 2012.
- [72] P. May-Ostendorp, G. P. Henze, C. D. Corbin, B. Rajagopalan and C. Felsman, "Model-predictive control of mixed-mode building with rule extraction," *Building and Environment*, pp. 428-437, 2011.
- [73] I. Hazyuk, C. Ghiaus and D. Penhouet, "Optimal temperature control of intermittently heated buildings using Model Predictive Control: Part II – Control algorithm," *Building and Environment*, vol. 51, pp. 388-394, 2012.
- [74] C. D. Corbin and G. P. M.-O. P. Henze, "A model predictive control optimization environment for real-time commercial building application," *Journal of Building Performance Simulation*, vol. 6, no. 3, pp. 159-174, 2013.
- [75] J. Zhao, K. P. Lam and B. E. Ydstie, "EnergyPlus model based predictive control (EPMPC) by using matlab/simulink and MLE," in *13th Conference of the International Building Performance Simulation Association*, Le Bourget Du Lac, 2013.
- [76] H. Huang, L. Chen and E. Hu, "A new model predictive control scheme for energy and cost savings in commercial buildings: An airport terminal building case study," *Building and Environment*, vol. 89, pp. 203-216, 2015.
- [77] M. Schmelas, T. Feldmann and E. Bollin, "Adaptive predictive control of thermo-active building systems (TABS) based on a multiple regression algorithm," *Energy and Buildings*, vol. 103, pp. 14-28, 2015.
- [78] D. Sturzenegger, D. Gyalistras, M. Morari and R. S. Smith, "Model predictive climate control of a swiss office building: implementation, results, and cost-benefit analysis," *IEEE TRANSACTIONS ON CONTROL SYSTEMS TECHNOLOGY*, vol. 24, no. 1, pp. 1-12, 2016.

- [79] A. Schirrer, M. Brandstetter, I. Leobner, S. Hauer and M. Kozek, "Nonlinear model predictive control for a heating and cooling system of a low energy office building," *Energy and Buildings*, vol. 125, pp. 86-98, 2016.
- [80] D. Schwingschackl, J. Rehrl and M. Horn, "LoLiMoT based MPC for air handling units in HVAC systems," *Building and Environment*, vol. 96, pp. 250-259, 2016.
- [81] S. Salakij, N. Yu, S. Paolucci and P. Antsaklis, "Model-Based Predictive Control for building energy management. I:," *Energy and Buildings*, vol. 133, pp. 345-358, 2016.
- [82] N. Yu, S. Salakij, R. Chavez, S. Paolucci, M. Sen and P. Antsaklis, "Model-based predictive control for building energy management: Part II – Experimental validations," *Energy and Buildings*, vol. 146, pp. 19-26, 2017.
- [83] D. Kim and J. E. Braun, "Reduced-ordered building modeling for application to model-based predictive control," in *SimBuild 2012*, Madison, Wisconsin, 2012.
- [84] Z. O'Neill, S. Narayanan and R. Brahme, "Model-based thermal load estimation in buildings," in *SimBuild 2010*, New York City, New York, 2010.
- [85] H. Huang, L. Chen, M. Mohammadzaheri, E. Hu and M. Chen, "Multi-zone temperature prediction in a commercial building using artificial neural network model," in *10th IEEE International Conference on Control and Automation (ICCA)*, Hangzhou, China, 2013.
- [86] M. Kavgic, T. Hilliard, L. Swan and Z. Qin, "Method for validation of statistical energy models," in *eSim 2016 Building Performance Simulation Conference*, Hamilton, Ontario, 2016.
- [87] S. Privara, J. Cigler, Z. Vana, F. Oldewurtel, C. Sagerschnig and E. Zacekova, "Building modeling as a crucial part for building predictive control," *Energy and Buildings*, pp. 8-22, 2013.
- [88] S. Wang and X. Xu, "Simplified building model for transient thermal performance estimation using GA-based parameter identification," *International Journal of Thermal Science*, pp. 419-432, 2006.
- [89] A. P. Melo, D. Costola, R. Lamberts and J. L. M. Hensen, "Assessing the accuracy of a simplified building energy simulation model using BESTEST: The case study of Brazilian regulation," *Energy and Buildings*, pp. 219-228, 2012.
- [90] D. Hsu, "Identifying key variables and interactions in statistical models of building energy consumption using regularization," *Energy*, pp. 144-155, 2015.

- [91] A. Florita and G. Henze, "Comparison of Short-Term Weather Forecasting Models for Model Predictive Control," *HVAC&R Research*, vol. 15, no. 5, pp. 835-853, 2009.
- [92] G. Rutledge, J. Aplert and W. Ebuisaki, "NOMADS: A Climate and Weather Model Archive at the National Oceanic and Atmospheric Administration," *Bulletin of the American Meteorological Society*, vol. 87, no. 3, pp. 327-341, 2006.
- [93] Y. Sun, S. Wang, F. Xiao and D. Gao, "Peak load shifting control using different cold thermal energy storage facilities in commercial buildings: A review," *Energy Conversion and Management*, vol. 71, pp. 101-114, 2013.
- [94] M. Humphreys, J. Nicol and I. Raja, "Field studies of indoor thermal comfort and the progress of the adaptive approach," *Advances in Building Energy Research*, vol. 1, no. 1, pp. 55-88, 2007.
- [95] L. Mavromatidis, M. El Mankibi, P. Michel, A. Bykalyuk and M. Santamouris, "Guidelines to study numerically and experimentally reflective insulation systems as applied to buildings," *Advances in Building Energy Research*, vol. 6, no. 1, pp. 2-35, 2012.
- [96] S. Emmerich and A. K. Persily, "Analysis of U.S. commercial building envelope air leakage database to support sustainable building design," *International Journal of Ventilation*, vol. 12, no. 4, pp. 331-344, 2014.
- [97] H. Fennel and J. Haehnel, "Setting airtightness standards," *ASHRAE Journal*, vol. 47, no. 9, pp. 26-31, 2005.
- [98] A. K. Persily, "Myths about building envelopes," *ASHRAE Journal*, vol. 41, no. 2-3, pp. 39-47, 1999.
- [99] M. Sherman and R. Chan, "Building airtightness: Research and practice," Lawrence Berkeley National Laboratory, Berkeley, 2004.
- [100] M. Deru, K. Field, D. Studer, K. Benne, B. Griffith, P. Torcellini, B. Liu, M. Halverson, D. Winiarski, M. Rosenberg, M. Yazdanian, J. Huang and D. Crawley, "U.S. Department of Energy Commercial Reference Building Models of the National Building Stock," National Renewable Energy Laboratory, Golden, Colorado, 2011.
- [101] D. Wei and X. Liu, "Research on multi-zone VAV air conditioning system modeling," in *10th World Congress on Intelligent Control and Automation*, Beijing, 2012.
- [102] J. Li, Y. Chen and R. Qu, "PID control of VAV system based on elman neural network," *Journal of Convergence Information Technology*, vol. 8, no. 10, pp. 407-414, 2013.

- [103] U.S. Department of Energy, Input - Output Reference EnergyPlus 8.5.0, 2016.
- [104] ASHRAE, "Guideline 14-2014 -- Measurement of Energy, Demand, and Water Savings," ASHRAE, 2014.
- [105] ASHRAE, "ASHRAE Standard 189.1-2009 Standard for the Design of High-Performance, Green Buildings," ASHRAE, 2009.
- [106] CBCL Limited, "Mona Campbell Building Measurement and Verification of Energy and Water Systems," CBCL Limited, Halifax, 2013.
- [107] C. Chantrasrisalai, V. Ghatti, D. E. Fisher and D. G. Scheatzle, "Experimental Validation of the EnergyPlus Low-Temperature Radiant Simulation," *ASHRAE Transactions*, vol. 109, no. 2, pp. 614-623, 2003.
- [108] A. Liaw and M. Wiener, "Classification and Regression by randomForest," *R News*, vol. 2/3, pp. 18-22, 2002.
- [109] T. McKinley and A. G. Alleyne, "Identification of building model parameters and loads using on-site data logs," in *Third National Conference of IBPSA-USA*, Berkeley, California, 2008.
- [110] S. K. Gupta, S. Atkinson, I. O'Boyle, J. Drogo, K. Kar, S. Mishra and J. T. Wen, "BEES: Real-time occupant feedback and environmental learning framework for collaborative thermal management in multi-zone, multi-occupant buildings," *Energy and Buildings*, vol. 125, pp. 142-152, 2016.
- [111] J. MacQueen, "Some methods for classification and analysis of multivariate observations," in *5th Berkeley Symposium on Mathematics, Statistics and Probability*, Berkeley, 1967.

Appendix A – Taylor and Francis Publishing Agreement

What follows are the rights retained by an author of an article in the Advances in Building Energy Research. A complete list of rights and further copyright details can be found on the Publisher's website at: <http://www.tandf.co.uk/journals/authorrights.pdf>

“The rights that you retain as Author In assigning Taylor & Francis or the journal proprietor copyright, or granting an exclusive licence to publish, you retain:

1) the right to be identified as the Author of an article whenever and wherever the Article is published;

2) patent rights, trademark rights, or rights to any process, product or procedure described in an article;

3) the right to share with colleagues print or electronic ‘preprints’ (i.e., versions of the article created prior to peer review) of an unpublished Article, perhaps in the form and content as submitted for publication;

... 9) the right to facilitate the distribution of the Article if the Article has been produced within the scope of an Author's employment, so that the Author's employer may use all or part of the Article internally within the institution or company provided that acknowledgement to prior publication in the relevant Taylor & Francis journal is made explicit;

10) the right to include an article in a thesis or dissertation that is not to be published commercially, provided that acknowledgement to prior publication in the relevant Taylor & Francis journal is made explicit;

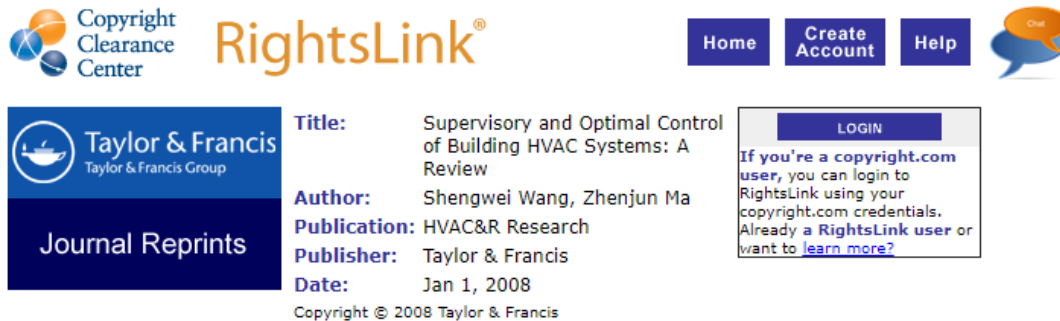
11) the right to present an article at a meeting or conference and to distribute printed copies of the Article to the delegates attending the meeting provided that this is not for commercial purposes and provided that acknowledgement to prior publication in the relevant Taylor & Francis journal is made explicit;

12) the right to use the Article in its published form in whole or in part without revision or modification in personal compilations [in print or electronic form] or other publications of an Author's own articles, provided that acknowledgement to prior publication in the relevant Taylor & Francis journal is made explicit;

13) The right to expand an article into book-length form for publication provided that acknowledgement to prior publication in the relevant Taylor & Francis journal is made explicit.”

Appendix B – Reprint of Figures/Tables Licences

Wang and Ma (2008)



The screenshot shows the RightsLink interface. At the top left is the Copyright Clearance Center logo. To its right is the RightsLink logo. Further right are navigation buttons for Home, Create Account, and Help, along with a chat icon. On the left side, there is a Taylor & Francis logo and a 'Journal Reprints' button. The main content area displays the following information:

Title: Supervisory and Optimal Control of Building HVAC Systems: A Review
Author: Shengwei Wang, Zhenjun Ma
Publication: HVAC&R Research
Publisher: Taylor & Francis
Date: Jan 1, 2008

Below this information is a 'Copyright © 2008 Taylor & Francis' notice. To the right of the article information is a 'LOGIN' button and a text box that reads: 'If you're a copyright.com user, you can login to RightsLink using your copyright.com credentials. Already a RightsLink user or want to learn more?' At the bottom of the interface are 'BACK' and 'CLOSE WINDOW' buttons.

Thesis/Dissertation Reuse Request

Taylor & Francis is pleased to offer reuses of its content for a thesis or dissertation free of charge contingent on resubmission of permission request if work is published.

BACK

CLOSE WINDOW

Copyright © 2017 Copyright Clearance Center, Inc. All Rights Reserved. [Privacy statement](#). [Terms and Conditions](#).
 Comments? We would like to hear from you. E-mail us at customer care@copyright.com

B. Lehmann, D. Gyalistras, M. Gwerder, K. Wirth, S. Carl (2013)

ELSEVIER LICENSE
TERMS AND CONDITIONS

Jun 15, 2017

This Agreement between Mr. Trent Hilliard ("You") and Elsevier ("Elsevier") consists of your license details and the terms and conditions provided by Elsevier and Copyright Clearance Center.

License Number

4130231268660

License date

Jun 15, 2017

Licensed Content Publisher

Elsevier

Licensed Content Publication

Energy and Buildings

Licensed Content Title

Intermediate complexity model for Model Predictive Control of Integrated Room Automation

Licensed Content Author

B. Lehmann,D. Gyalistras,M. Gwerder,K. Wirth,S. Carl

Licensed Content Date

Mar 1, 2013

Licensed Content Volume

58

Licensed Content Issue

n/a

Licensed Content Pages

13

Start Page

250

End Page

262

Type of Use

reuse in a thesis/dissertation

Portion

figures/tables/illustrations

Number of figures/tables/illustrations

2

Format

both print and electronic

Are you the author of this Elsevier article?

No

Will you be translating?

No

Order reference number

Thesis_1

Original figure numbers

Table 1, 2

Title of your thesis/dissertation

Whole building model predictive control with optimization for HVAC systems utilizing surface level weather forecasts

Expected completion date

Aug 2017

Estimated size (number of pages)

266

Elsevier VAT number

GB 494 6272 12

Requestor Location

Mr. Trent Hilliard

804-2393 Robie Street

Halifax, NS B3K 6S2

Canada

Attn: Mr. Trent Hilliard

Total

0.00 CAD

Terms and Conditions

INTRODUCTION

1. The publisher for this copyrighted material is Elsevier. By clicking "accept" in connection with completing this licensing transaction, you agree that the following terms

and conditions apply to this transaction (along with the Billing and Payment terms and conditions established by Copyright Clearance Center, Inc. ("CCC"), at the time that you opened your Rightslink account and that are available at any time at <http://myaccount.copyright.com>).

GENERAL TERMS

2. Elsevier hereby grants you permission to reproduce the aforementioned material subject to the terms and conditions indicated.

3. Acknowledgement: If any part of the material to be used (for example, figures) has appeared in our publication with credit or acknowledgement to another source, permission must also be sought from that source. If such permission is not obtained then that material may not be included in your publication/copies. Suitable acknowledgement to the source must be made, either as a footnote or in a reference list at the end of your publication, as follows:

"Reprinted from Publication title, Vol /edition number, Author(s), Title of article / title of chapter, Pages No., Copyright (Year), with permission from Elsevier [OR APPLICABLE SOCIETY COPYRIGHT OWNER]." Also Lancet special credit - "Reprinted from The Lancet, Vol. number, Author(s), Title of article, Pages No., Copyright (Year), with permission from Elsevier."

4. Reproduction of this material is confined to the purpose and/or media for which permission is hereby given.

5. Altering/Modifying Material: Not Permitted. However figures and illustrations may be altered/adapted minimally to serve your work. Any other abbreviations, additions, deletions and/or any other alterations shall be made only with prior written authorization of Elsevier Ltd. (Please contact Elsevier at permissions@elsevier.com). No modifications can be made to any Lancet figures/tables and they must be reproduced in full.

6. If the permission fee for the requested use of our material is waived in this instance, please be advised that your future requests for Elsevier materials may attract a fee.

7. Reservation of Rights: Publisher reserves all rights not specifically granted in the combination of (i) the license details provided by you and accepted in the course of this

licensing transaction, (ii) these terms and conditions and (iii) CCC's Billing and Payment terms and conditions.

8. License Contingent Upon Payment: While you may exercise the rights licensed immediately upon issuance of the license at the end of the licensing process for the transaction, provided that you have disclosed complete and accurate details of your proposed use, no license is finally effective unless and until full payment is received from you (either by publisher or by CCC) as provided in CCC's Billing and Payment terms and conditions. If full payment is not received on a timely basis, then any license preliminarily granted shall be deemed automatically revoked and shall be void as if never granted. Further, in the event that you breach any of these terms and conditions or any of CCC's Billing and Payment terms and conditions, the license is automatically revoked and shall be void as if never granted. Use of materials as described in a revoked license, as well as any use of the materials beyond the scope of an unrevoked license, may constitute copyright infringement and publisher reserves the right to take any and all action to protect its copyright in the materials.

9. Warranties: Publisher makes no representations or warranties with respect to the licensed material.

10. Indemnity: You hereby indemnify and agree to hold harmless publisher and CCC, and their respective officers, directors, employees and agents, from and against any and all claims arising out of your use of the licensed material other than as specifically authorized pursuant to this license.

11. No Transfer of License: This license is personal to you and may not be sublicensed, assigned, or transferred by you to any other person without publisher's written permission.

12. No Amendment Except in Writing: This license may not be amended except in a writing signed by both parties (or, in the case of publisher, by CCC on publisher's behalf).

13. Objection to Contrary Terms: Publisher hereby objects to any terms contained in any purchase order, acknowledgment, check endorsement or other writing prepared by you, which terms are inconsistent with these terms and conditions or CCC's Billing and

Payment terms and conditions. These terms and conditions, together with CCC's Billing and Payment terms and conditions (which are incorporated herein), comprise the entire agreement between you and publisher (and CCC) concerning this licensing transaction. In the event of any conflict between your obligations established by these terms and conditions and those established by CCC's Billing and Payment terms and conditions, these terms and conditions shall control.

14. **Revocation:** Elsevier or Copyright Clearance Center may deny the permissions described in this License at their sole discretion, for any reason or no reason, with a full refund payable to you. Notice of such denial will be made using the contact information provided by you. Failure to receive such notice will not alter or invalidate the denial. In no event will Elsevier or Copyright Clearance Center be responsible or liable for any costs, expenses or damage incurred by you as a result of a denial of your permission request, other than a refund of the amount(s) paid by you to Elsevier and/or Copyright Clearance Center for denied permissions.

LIMITED LICENSE

The following terms and conditions apply only to specific license types:

15. **Translation:** This permission is granted for non-exclusive world **English** rights only unless your license was granted for translation rights. If you licensed translation rights you may only translate this content into the languages you requested. A professional translator must perform all translations and reproduce the content word for word preserving the integrity of the article.

16. **Posting licensed content on any Website:** The following terms and conditions apply as follows: Licensing material from an Elsevier journal: All content posted to the web site must maintain the copyright information line on the bottom of each image; A hyper-text must be included to the Homepage of the journal from which you are licensing at <http://www.sciencedirect.com/science/journal/xxxxx> or the Elsevier homepage for books at <http://www.elsevier.com>; Central Storage: This license does not include permission for a scanned version of the material to be stored in a central repository such as that provided by Heron/XanEdu.

Licensing material from an Elsevier book: A hyper-text link must be included to the Elsevier homepage at <http://www.elsevier.com> . All content posted to the web site must maintain the copyright information line on the bottom of each image.

Posting licensed content on Electronic reserve: In addition to the above the following clauses are applicable: The web site must be password-protected and made available only to bona fide students registered on a relevant course. This permission is granted for 1 year only. You may obtain a new license for future website posting.

17. **For journal authors:** the following clauses are applicable in addition to the above:

Preprints:

A preprint is an author's own write-up of research results and analysis, it has not been peer-reviewed, nor has it had any other value added to it by a publisher (such as formatting, copyright, technical enhancement etc.).

Authors can share their preprints anywhere at any time. Preprints should not be added to or enhanced in any way in order to appear more like, or to substitute for, the final versions of articles however authors can update their preprints on arXiv or RePEc with their Accepted Author Manuscript (see below).

If accepted for publication, we encourage authors to link from the preprint to their formal publication via its DOI. Millions of researchers have access to the formal publications on ScienceDirect, and so links will help users to find, access, cite and use the best available version. Please note that Cell Press, The Lancet and some society-owned have different preprint policies. Information on these policies is available on the journal homepage.

Accepted Author Manuscripts: An accepted author manuscript is the manuscript of an article that has been accepted for publication and which typically includes author-incorporated changes suggested during submission, peer review and editor-author communications.

Authors can share their accepted author manuscript:

- immediately
 - via their non-commercial person homepage or blog

- by updating a preprint in arXiv or RePEc with the accepted manuscript
- via their research institute or institutional repository for internal institutional uses or as part of an invitation-only research collaboration work-group
- directly by providing copies to their students or to research collaborators for their personal use
- for private scholarly sharing as part of an invitation-only work group on commercial sites with which Elsevier has an agreement
- After the embargo period
 - via non-commercial hosting platforms such as their institutional repository
 - via commercial sites with which Elsevier has an agreement

In all cases accepted manuscripts should:

- link to the formal publication via its DOI
- bear a CC-BY-NC-ND license - this is easy to do
- if aggregated with other manuscripts, for example in a repository or other site, be shared in alignment with our hosting policy not be added to or enhanced in any way to appear more like, or to substitute for, the published journal article.

Published journal article (JPA): A published journal article (PJA) is the definitive final record of published research that appears or will appear in the journal and embodies all value-adding publishing activities including peer review co-ordination, copy-editing, formatting, (if relevant) pagination and online enrichment.

Policies for sharing publishing journal articles differ for subscription and gold open access articles:

Subscription Articles: If you are an author, please share a link to your article rather than the full-text. Millions of researchers have access to the formal publications on ScienceDirect, and so links will help your users to find, access, cite, and use the best available version.

Theses and dissertations which contain embedded PJAs as part of the formal submission can be posted publicly by the awarding institution with DOI links back to the formal publications on ScienceDirect.

If you are affiliated with a library that subscribes to ScienceDirect you have additional private sharing rights for others' research accessed under that agreement. This includes use for classroom teaching and internal training at the institution (including use in course packs and courseware programs), and inclusion of the article for grant funding purposes.

Gold Open Access Articles: May be shared according to the author-selected end-user license and should contain a [CrossMark logo](#), the end user license, and a DOI link to the formal publication on ScienceDirect.

Please refer to Elsevier's [posting policy](#) for further information.

18. **For book authors** the following clauses are applicable in addition to the above: Authors are permitted to place a brief summary of their work online only. You are not allowed to download and post the published electronic version of your chapter, nor may you scan the printed edition to create an electronic version. **Posting to a repository:** Authors are permitted to post a summary of their chapter only in their institution's repository.

19. **Thesis/Dissertation:** If your license is for use in a thesis/dissertation your thesis may be submitted to your institution in either print or electronic form. Should your thesis be published commercially, please reapply for permission. These requirements include permission for the Library and Archives of Canada to supply single copies, on demand, of the complete thesis and include permission for Proquest/UMI to supply single copies, on demand, of the complete thesis. Should your thesis be published commercially, please reapply for permission. Theses and dissertations which contain embedded PJAs as part of the formal submission can be posted publicly by the awarding institution with DOI links back to the formal publications on ScienceDirect.

Elsevier Open Access Terms and Conditions

You can publish open access with Elsevier in hundreds of open access journals or in nearly 2000 established subscription journals that support open access publishing.

Permitted third party re-use of these open access articles is defined by the author's choice of Creative Commons user license. See our [open access license policy](#) for more information.

Terms & Conditions applicable to all Open Access articles published with Elsevier:

Any reuse of the article must not represent the author as endorsing the adaptation of the article nor should the article be modified in such a way as to damage the author's honour or reputation. If any changes have been made, such changes must be clearly indicated. The author(s) must be appropriately credited and we ask that you include the end user license and a DOI link to the formal publication on ScienceDirect.

If any part of the material to be used (for example, figures) has appeared in our publication with credit or acknowledgement to another source it is the responsibility of the user to ensure their reuse complies with the terms and conditions determined by the rights holder.

Additional Terms & Conditions applicable to each Creative Commons user license:

CC BY: The CC-BY license allows users to copy, to create extracts, abstracts and new works from the Article, to alter and revise the Article and to make commercial use of the Article (including reuse and/or resale of the Article by commercial entities), provided the user gives appropriate credit (with a link to the formal publication through the relevant DOI), provides a link to the license, indicates if changes were made and the licensor is not represented as endorsing the use made of the work. The full details of the license are available at <http://creativecommons.org/licenses/by/4.0>.

CC BY NC SA: The CC BY-NC-SA license allows users to copy, to create extracts, abstracts and new works from the Article, to alter and revise the Article, provided this is not done for commercial purposes, and that the user gives appropriate credit (with a link to the formal publication through the relevant DOI), provides a link to the license, indicates if changes were made and the licensor is not represented as endorsing the use made of the work. Further, any new works must be made available on the same conditions. The full details of the license are available at <http://creativecommons.org/licenses/by-nc-sa/4.0>.

CC BY NC ND: The CC BY-NC-ND license allows users to copy and distribute the Article, provided this is not done for commercial purposes and further does not permit distribution of the Article if it is changed or edited in any way, and provided the user gives appropriate credit (with a link to the formal publication through the relevant DOI), provides a link to the license, and that the licensor is not represented as endorsing the use made of the work. The full details of the license are available at <http://creativecommons.org/licenses/by-nc-nd/4.0>. Any commercial reuse of Open Access articles published with a CC BY NC SA or CC BY NC ND license requires permission from Elsevier and will be subject to a fee.

Commercial reuse includes:

- Associating advertising with the full text of the Article
- Charging fees for document delivery or access
- Article aggregation
- Systematic distribution via e-mail lists or share buttons

Posting or linking by commercial companies for use by customers of those companies.

20. Other Conditions:

v1.9

Questions? customercare@copyright.com or +1-855-239-3415 (toll free in the US) or +1-978-646-2777.

Xing Jin, Xiaosong Zhang, Yiran Cao, Geng Wang (2012)

ELSEVIER LICENSE
TERMS AND CONDITIONS

Jun 15, 2017

This Agreement between Mr. Trent Hilliard ("You") and Elsevier ("Elsevier") consists of your license details and the terms and conditions provided by Elsevier and Copyright Clearance Center.

License Number

4130231268660

License date

Jun 15, 2017

Licensed Content Publisher

Elsevier

Licensed Content Publication

Energy and Buildings

Licensed Content Title

Thermal performance evaluation of the wall using heat flux time lag and decrement factor

Licensed Content Author

Xing Jin,Xiaosong Zhang,Yiran Cao,Geng Wang

Licensed Content Date

Apr 1, 2012

Licensed Content Volume

47

Licensed Content Issue

n/a

Licensed Content Pages

6

Start Page

369

End Page

374

Type of Use

reuse in a thesis/dissertation

Portion

figures/tables/illustrations

Number of figures/tables/illustrations

1

Format

both print and electronic

Are you the author of this Elsevier article?

No

Will you be translating?

No

Order reference number

Thesis_2

Original figure numbers

Figure 1

Title of your thesis/dissertation

Whole building model predictive control with optimization for HVAC systems utilizing surface level weather forecasts

Expected completion date

Aug 2017

Estimated size (number of pages)

266

Elsevier VAT number

GB 494 6272 12

Requestor Location

Mr. Trent Hilliard

804-2393 Robie Street

Halifax, NS B3K 6S2

Canada

Attn: Mr. Trent Hilliard

Total

0.00 CAD

Terms and Conditions

INTRODUCTION

1. The publisher for this copyrighted material is Elsevier. By clicking "accept" in connection with completing this licensing transaction, you agree that the following terms

and conditions apply to this transaction (along with the Billing and Payment terms and conditions established by Copyright Clearance Center, Inc. ("CCC"), at the time that you opened your Rightslink account and that are available at any time at <http://myaccount.copyright.com>).

GENERAL TERMS

2. Elsevier hereby grants you permission to reproduce the aforementioned material subject to the terms and conditions indicated.

3. Acknowledgement: If any part of the material to be used (for example, figures) has appeared in our publication with credit or acknowledgement to another source, permission must also be sought from that source. If such permission is not obtained then that material may not be included in your publication/copies. Suitable acknowledgement to the source must be made, either as a footnote or in a reference list at the end of your publication, as follows:

"Reprinted from Publication title, Vol /edition number, Author(s), Title of article / title of chapter, Pages No., Copyright (Year), with permission from Elsevier [OR APPLICABLE SOCIETY COPYRIGHT OWNER]." Also Lancet special credit - "Reprinted from The Lancet, Vol. number, Author(s), Title of article, Pages No., Copyright (Year), with permission from Elsevier."

4. Reproduction of this material is confined to the purpose and/or media for which permission is hereby given.

5. Altering/Modifying Material: Not Permitted. However figures and illustrations may be altered/adapted minimally to serve your work. Any other abbreviations, additions, deletions and/or any other alterations shall be made only with prior written authorization of Elsevier Ltd. (Please contact Elsevier at permissions@elsevier.com). No modifications can be made to any Lancet figures/tables and they must be reproduced in full.

6. If the permission fee for the requested use of our material is waived in this instance, please be advised that your future requests for Elsevier materials may attract a fee.

7. Reservation of Rights: Publisher reserves all rights not specifically granted in the combination of (i) the license details provided by you and accepted in the course of this

licensing transaction, (ii) these terms and conditions and (iii) CCC's Billing and Payment terms and conditions.

8. License Contingent Upon Payment: While you may exercise the rights licensed immediately upon issuance of the license at the end of the licensing process for the transaction, provided that you have disclosed complete and accurate details of your proposed use, no license is finally effective unless and until full payment is received from you (either by publisher or by CCC) as provided in CCC's Billing and Payment terms and conditions. If full payment is not received on a timely basis, then any license preliminarily granted shall be deemed automatically revoked and shall be void as if never granted. Further, in the event that you breach any of these terms and conditions or any of CCC's Billing and Payment terms and conditions, the license is automatically revoked and shall be void as if never granted. Use of materials as described in a revoked license, as well as any use of the materials beyond the scope of an unrevoked license, may constitute copyright infringement and publisher reserves the right to take any and all action to protect its copyright in the materials.

9. Warranties: Publisher makes no representations or warranties with respect to the licensed material.

10. Indemnity: You hereby indemnify and agree to hold harmless publisher and CCC, and their respective officers, directors, employees and agents, from and against any and all claims arising out of your use of the licensed material other than as specifically authorized pursuant to this license.

11. No Transfer of License: This license is personal to you and may not be sublicensed, assigned, or transferred by you to any other person without publisher's written permission.

12. No Amendment Except in Writing: This license may not be amended except in a writing signed by both parties (or, in the case of publisher, by CCC on publisher's behalf).

13. Objection to Contrary Terms: Publisher hereby objects to any terms contained in any purchase order, acknowledgment, check endorsement or other writing prepared by you, which terms are inconsistent with these terms and conditions or CCC's Billing and

Payment terms and conditions. These terms and conditions, together with CCC's Billing and Payment terms and conditions (which are incorporated herein), comprise the entire agreement between you and publisher (and CCC) concerning this licensing transaction. In the event of any conflict between your obligations established by these terms and conditions and those established by CCC's Billing and Payment terms and conditions, these terms and conditions shall control.

14. **Revocation:** Elsevier or Copyright Clearance Center may deny the permissions described in this License at their sole discretion, for any reason or no reason, with a full refund payable to you. Notice of such denial will be made using the contact information provided by you. Failure to receive such notice will not alter or invalidate the denial. In no event will Elsevier or Copyright Clearance Center be responsible or liable for any costs, expenses or damage incurred by you as a result of a denial of your permission request, other than a refund of the amount(s) paid by you to Elsevier and/or Copyright Clearance Center for denied permissions.

LIMITED LICENSE

The following terms and conditions apply only to specific license types:

15. **Translation:** This permission is granted for non-exclusive world **English** rights only unless your license was granted for translation rights. If you licensed translation rights you may only translate this content into the languages you requested. A professional translator must perform all translations and reproduce the content word for word preserving the integrity of the article.

16. **Posting licensed content on any Website:** The following terms and conditions apply as follows: Licensing material from an Elsevier journal: All content posted to the web site must maintain the copyright information line on the bottom of each image; A hyper-text must be included to the Homepage of the journal from which you are licensing at <http://www.sciencedirect.com/science/journal/xxxxx> or the Elsevier homepage for books at <http://www.elsevier.com>; Central Storage: This license does not include permission for a scanned version of the material to be stored in a central repository such as that provided by Heron/XanEdu.

Licensing material from an Elsevier book: A hyper-text link must be included to the Elsevier homepage at <http://www.elsevier.com> . All content posted to the web site must maintain the copyright information line on the bottom of each image.

Posting licensed content on Electronic reserve: In addition to the above the following clauses are applicable: The web site must be password-protected and made available only to bona fide students registered on a relevant course. This permission is granted for 1 year only. You may obtain a new license for future website posting.

17. **For journal authors:** the following clauses are applicable in addition to the above:

Preprints:

A preprint is an author's own write-up of research results and analysis, it has not been peer-reviewed, nor has it had any other value added to it by a publisher (such as formatting, copyright, technical enhancement etc.).

Authors can share their preprints anywhere at any time. Preprints should not be added to or enhanced in any way in order to appear more like, or to substitute for, the final versions of articles however authors can update their preprints on arXiv or RePEc with their Accepted Author Manuscript (see below).

If accepted for publication, we encourage authors to link from the preprint to their formal publication via its DOI. Millions of researchers have access to the formal publications on ScienceDirect, and so links will help users to find, access, cite and use the best available version. Please note that Cell Press, The Lancet and some society-owned have different preprint policies. Information on these policies is available on the journal homepage.

Accepted Author Manuscripts: An accepted author manuscript is the manuscript of an article that has been accepted for publication and which typically includes author-incorporated changes suggested during submission, peer review and editor-author communications.

Authors can share their accepted author manuscript:

- immediately
 - via their non-commercial person homepage or blog

- by updating a preprint in arXiv or RePEc with the accepted manuscript
 - via their research institute or institutional repository for internal institutional uses or as part of an invitation-only research collaboration work-group
 - directly by providing copies to their students or to research collaborators for their personal use
 - for private scholarly sharing as part of an invitation-only work group on commercial sites with which Elsevier has an agreement
- After the embargo period
 - via non-commercial hosting platforms such as their institutional repository
 - via commercial sites with which Elsevier has an agreement

In all cases accepted manuscripts should:

- link to the formal publication via its DOI
- bear a CC-BY-NC-ND license - this is easy to do
- if aggregated with other manuscripts, for example in a repository or other site, be shared in alignment with our hosting policy not be added to or enhanced in any way to appear more like, or to substitute for, the published journal article.

Published journal article (JPA): A published journal article (PJA) is the definitive final record of published research that appears or will appear in the journal and embodies all value-adding publishing activities including peer review co-ordination, copy-editing, formatting, (if relevant) pagination and online enrichment.

Policies for sharing publishing journal articles differ for subscription and gold open access articles:

Subscription Articles: If you are an author, please share a link to your article rather than the full-text. Millions of researchers have access to the formal publications on ScienceDirect, and so links will help your users to find, access, cite, and use the best available version.

Theses and dissertations which contain embedded PJAs as part of the formal submission can be posted publicly by the awarding institution with DOI links back to the formal publications on ScienceDirect.

If you are affiliated with a library that subscribes to ScienceDirect you have additional private sharing rights for others' research accessed under that agreement. This includes use for classroom teaching and internal training at the institution (including use in course packs and courseware programs), and inclusion of the article for grant funding purposes.

Gold Open Access Articles: May be shared according to the author-selected end-user license and should contain a [CrossMark logo](#), the end user license, and a DOI link to the formal publication on ScienceDirect.

Please refer to Elsevier's [posting policy](#) for further information.

18. For book authors the following clauses are applicable in addition to the above: Authors are permitted to place a brief summary of their work online only. You are not allowed to download and post the published electronic version of your chapter, nor may you scan the printed edition to create an electronic version. **Posting to a repository:** Authors are permitted to post a summary of their chapter only in their institution's repository.

19. Thesis/Dissertation: If your license is for use in a thesis/dissertation your thesis may be submitted to your institution in either print or electronic form. Should your thesis be published commercially, please reapply for permission. These requirements include permission for the Library and Archives of Canada to supply single copies, on demand, of the complete thesis and include permission for Proquest/UMI to supply single copies, on demand, of the complete thesis. Should your thesis be published commercially, please reapply for permission. Theses and dissertations which contain embedded PJAs as part of the formal submission can be posted publicly by the awarding institution with DOI links back to the formal publications on ScienceDirect.

Elsevier Open Access Terms and Conditions

You can publish open access with Elsevier in hundreds of open access journals or in nearly 2000 established subscription journals that support open access publishing.

Permitted third party re-use of these open access articles is defined by the author's choice of Creative Commons user license. See our [open access license policy](#) for more information.

Terms & Conditions applicable to all Open Access articles published with Elsevier:

Any reuse of the article must not represent the author as endorsing the adaptation of the article nor should the article be modified in such a way as to damage the author's honour or reputation. If any changes have been made, such changes must be clearly indicated.

The author(s) must be appropriately credited and we ask that you include the end user license and a DOI link to the formal publication on ScienceDirect.

If any part of the material to be used (for example, figures) has appeared in our publication with credit or acknowledgement to another source it is the responsibility of the user to ensure their reuse complies with the terms and conditions determined by the rights holder.

Additional Terms & Conditions applicable to each Creative Commons user license:

CC BY: The CC-BY license allows users to copy, to create extracts, abstracts and new works from the Article, to alter and revise the Article and to make commercial use of the Article (including reuse and/or resale of the Article by commercial entities), provided the user gives appropriate credit (with a link to the formal publication through the relevant DOI), provides a link to the license, indicates if changes were made and the licensor is not represented as endorsing the use made of the work. The full details of the license are available at <http://creativecommons.org/licenses/by/4.0>.

CC BY NC SA: The CC BY-NC-SA license allows users to copy, to create extracts, abstracts and new works from the Article, to alter and revise the Article, provided this is not done for commercial purposes, and that the user gives appropriate credit (with a link to the formal publication through the relevant DOI), provides a link to the license, indicates if changes were made and the licensor is not represented as endorsing the use made of the work. Further, any new works must be made available on the same conditions. The full details of the license are available at <http://creativecommons.org/licenses/by-nc-sa/4.0>.

CC BY NC ND: The CC BY-NC-ND license allows users to copy and distribute the Article, provided this is not done for commercial purposes and further does not permit distribution of the Article if it is changed or edited in any way, and provided the user gives appropriate credit (with a link to the formal publication through the relevant DOI), provides a link to the license, and that the licensor is not represented as endorsing the use made of the work. The full details of the license are available at <http://creativecommons.org/licenses/by-nc-nd/4.0>. Any commercial reuse of Open Access articles published with a CC BY NC SA or CC BY NC ND license requires permission from Elsevier and will be subject to a fee.

Commercial reuse includes:

- Associating advertising with the full text of the Article
- Charging fees for document delivery or access
- Article aggregation
- Systematic distribution via e-mail lists or share buttons

Posting or linking by commercial companies for use by customers of those companies.

20. Other Conditions:

v1.9

Questions? customercare@copyright.com or +1-855-239-3415 (toll free in the US) or +1-978-646-2777.

ASHRAE Figure Reprints

ASHRAE standard Permission type: Republish or display content Type of use: Republish in a thesis/dissertation TERMS AND CONDITIONS The following terms are individual to this publisher: None Other Terms and Conditions: STANDARD TERMS AND CONDITIONS 1. Description of Service; Defined Terms. This Republication License enables the User to obtain licenses for republication of one or more copyrighted works as described in detail on the relevant Order Confirmation (the “Work(s)”). Copyright Clearance Center, Inc. (“CCC”) grants licenses through the Service on behalf of the rightsholder identified on the Order Confirmation (the “Rightsholder”). “Republication”, as used herein, generally means the inclusion of a Work, in whole or in part, in a new work or works, also as described on the Order Confirmation. “User”, as used herein, means the person or entity making such republication. 2. The terms set forth in the relevant Order Confirmation, and any terms set by the Rightsholder with respect to a particular Work, govern the terms of use of Works in connection with the Service. By using the Service, the person transacting for a republication license on behalf of the User represents and warrants that he/she/it (a) has been duly authorized by the User to accept, and hereby does accept, all such terms and conditions on behalf of User, and (b) shall inform User of all such terms and conditions. In the event such person is a “freelancer” or other third party independent of User and CCC, such party shall be deemed jointly a “User” for purposes of these terms and conditions. In any event, User shall be deemed to have accepted and agreed to all such terms and conditions if User republishes the Work in any fashion. 3. Scope of License; Limitations and Obligations. 3.1 All Works and all rights therein, including copyright rights, remain the sole and exclusive property of the Rightsholder. The license created by the exchange of an Order Confirmation (and/or any invoice) and payment by User of the full amount set forth on that document includes only those rights expressly set forth in the Order Confirmation and in these terms and conditions, and conveys no other rights in the Work(s) to User. All rights not expressly granted are hereby reserved. 3.2 General Payment Terms: You may pay by credit card or through an account with us payable at the end of the month. If you and we agree that you may establish a standing account with CCC, then the following terms apply: Remit Payment to: Copyright Clearance Center, 29118 Network Place, Chicago, IL 60673-1291. Payments Due: Invoices are payable upon their delivery to you (or upon our notice to you that they are available to you for downloading). After 30 days, outstanding amounts will be subject to a service charge of 1-1/2% per month or, if less, the maximum rate allowed by applicable law. Unless otherwise specifically set forth in the Order Confirmation or in a separate written agreement signed by CCC, invoices are due and payable on “net 30” terms. While User may exercise the rights licensed immediately upon issuance of the Order Confirmation, the license is automatically revoked and is null and void, as if it had never been issued, if complete payment for the license is

not received on a timely basis either from User directly or through a payment agent, such as a credit card company. 3.3 Unless otherwise provided in the Order Confirmation, any grant of rights to User (i) is “one-time” (including the editions and product family specified in the license), (ii) is non-exclusive and non-transferable and (iii) is subject to any and all limitations and restrictions (such as, but not limited to, limitations on duration of use or circulation) included in the Order Confirmation or invoice and/or in these terms and conditions. Upon completion of the licensed use, User shall either secure a new permission for further use of the Work(s) or immediately cease any new use of the Work(s) and shall render inaccessible (such as by deleting or by removing or severing links or other locators) any further copies of the Work (except for copies printed on paper in accordance with this license and still in User's stock at the end of such period). 3.4 In the event that the material for which a republication license is sought includes third party materials (such as photographs, illustrations, graphs, inserts and similar materials) which are identified in such material as having been used by permission, User is responsible for identifying, and seeking separate licenses (under this Service or otherwise) for, any of such third party materials; without a separate license, such third party materials may not be used. 3.5 Use of proper copyright notice for a Work is required as a condition of any license granted under the Service. Unless otherwise provided in the Order Confirmation, a proper copyright notice will read substantially as follows: “Republished with permission of [Rightsholder’s name], from [Work's title, author, volume, edition number and year of copyright]; permission conveyed through Copyright Clearance Center, Inc. ” Such notice must be provided in a reasonably legible font size and must be placed either immediately adjacent to the Work as used (for example, as part of a by-line or footnote but not as a separate electronic link) or in the place where substantially all other credits or notices for the new work 7/8/2017 Copyright Clearance Center <https://www.copyright.com/printCoiConfirmPurchase.do?operation=defaultOperation&confirmNum=11654890&showTCCitation=TRUE> 5/7 but not as a separate electronic link) or in the place where substantially all other credits or notices for the new work containing the republished Work are located. Failure to include the required notice results in loss to the Rightsholder and CCC, and the User shall be liable to pay liquidated damages for each such failure equal to twice the use fee specified in the Order Confirmation, in addition to the use fee itself and any other fees and charges specified. 3.6 User may only make alterations to the Work if and as expressly set forth in the Order Confirmation. No Work may be used in any way that is defamatory, violates the rights of third parties (including such third parties' rights of copyright, privacy, publicity, or other tangible or intangible property), or is otherwise illegal, sexually explicit or obscene. In addition, User may not conjoin a Work with any other material that may result in damage to the reputation of the Rightsholder. User agrees to inform CCC if it becomes aware of any infringement of any rights in a Work and to cooperate with any reasonable request of CCC or the Rightsholder in connection therewith. 4. Indemnity. User hereby indemnifies and agrees to defend the Rightsholder and CCC, and their respective employees and directors, against all claims,

liability, damages, costs and expenses, including legal fees and expenses, arising out of any use of a Work beyond the scope of the rights granted herein, or any use of a Work which has been altered in any unauthorized way by User, including claims of defamation or infringement of rights of copyright, publicity, privacy or other tangible or intangible property.

5. Limitation of Liability. UNDER NO CIRCUMSTANCES WILL CCC OR THE RIGHTSHOLDER BE LIABLE FOR ANY DIRECT, INDIRECT, CONSEQUENTIAL OR INCIDENTAL DAMAGES (INCLUDING WITHOUT LIMITATION DAMAGES FOR LOSS OF BUSINESS PROFITS OR INFORMATION, OR FOR BUSINESS INTERRUPTION) ARISING OUT OF THE USE OR INABILITY TO USE A WORK, EVEN IF ONE OF THEM HAS BEEN ADVISED OF THE POSSIBILITY OF SUCH DAMAGES. In any event, the total liability of the Rightsholder and CCC (including their respective employees and directors) shall not exceed the total amount actually paid by User for this license. User assumes full liability for the actions and omissions of its principals, employees, agents, affiliates, successors and assigns.

6. Limited Warranties. THE WORK(S) AND RIGHT(S) ARE PROVIDED "AS IS". CCC HAS THE RIGHT TO GRANT TO USER THE RIGHTS GRANTED IN THE ORDER CONFIRMATION DOCUMENT. CCC AND THE RIGHTSHOLDER DISCLAIM ALL OTHER WARRANTIES RELATING TO THE WORK(S) AND RIGHT(S), EITHER EXPRESS OR IMPLIED, INCLUDING WITHOUT LIMITATION IMPLIED WARRANTIES OF MERCHANTABILITY OR FITNESS FOR A PARTICULAR PURPOSE. ADDITIONAL RIGHTS MAY BE REQUIRED TO USE ILLUSTRATIONS, GRAPHS, PHOTOGRAPHS, ABSTRACTS, INSERTS OR OTHER PORTIONS OF THE WORK (AS OPPOSED TO THE ENTIRE WORK) IN A MANNER CONTEMPLATED BY USER; USER UNDERSTANDS AND AGREES THAT NEITHER CCC NOR THE RIGHTSHOLDER MAY HAVE SUCH ADDITIONAL RIGHTS TO GRANT.

7. Effect of Breach. Any failure by User to pay any amount when due, or any use by User of a Work beyond the scope of the license set forth in the Order Confirmation and/or these terms and conditions, shall be a material breach of the license created by the Order Confirmation and these terms and conditions. Any breach not cured within 30 days of written notice thereof shall result in immediate termination of such license without further notice. Any unauthorized (but licensable) use of a Work that is terminated immediately upon notice thereof may be liquidated by payment of the Rightsholder's ordinary license price therefor; any unauthorized (and unlicensable) use that is not terminated immediately for any reason (including, for example, because materials containing the Work cannot reasonably be recalled) will be subject to all remedies available at law or in equity, but in no event to a payment of less than three times the Rightsholder's ordinary license price for the most closely analogous licensable use plus Rightsholder's and/or CCC's costs and expenses incurred in collecting such payment.

8. Miscellaneous.

8.1 User acknowledges that CCC may, from time to time, make changes or additions to the Service or to these terms and conditions, and CCC reserves the right to send notice to the User by electronic mail or otherwise for the purposes of notifying User of such changes or

additions; provided that any such changes or additions shall not apply to permissions already secured and paid for. 8.2 Use of User-related information collected through the Service is governed by CCC's privacy policy, available online here: <http://www.copyright.com/content/cc3/en/tools/footer/privacypolicy.html>. 8.3 The licensing transaction described in the Order Confirmation is personal to User. Therefore, User may not assign or transfer to any other person (whether a natural person or an organization of any kind) the license created by the Order Confirmation and these terms and conditions or any rights granted hereunder; provided, however, that User may assign such license in its entirety on written notice to CCC in the event of a transfer of all or substantially all of User's rights in the new material which includes the Work(s) licensed under this Service. 8.4 No amendment or waiver of any terms is binding unless set forth in writing and signed by the parties. The Rightsholder and CCC hereby object to any terms contained in any writing prepared by the User or its principals, employees, agents or affiliates and purporting to govern or otherwise relate to the licensing transaction described in the Order Confirmation, which terms are in any way inconsistent with any terms set forth in the Order Confirmation and/or in these terms and conditions or CCC's standard operating procedures, whether such writing is prepared prior to, simultaneously with or subsequent to the Order Confirmation, and whether such writing appears on a copy of the Order Confirmation or in a separate instrument. 8.5 The licensing transaction described in the Order Confirmation document shall be governed by and construed under the law of the State of New York, USA, without regard to the principles thereof of conflicts of law. Any case, controversy, suit, action, or proceeding arising out of, in connection with, or related to such licensing transaction shall be brought, at CCC's sole discretion, in any federal or state court located in the County of New York, State of New York, USA, or in any federal or state court whose geographical jurisdiction covers the location of the Rightsholder set forth in the Order Confirmation. The parties expressly submit to the personal jurisdiction and venue of each such federal or state court. If you have any comments or questions about the Service or Copyright Clearance Center, please contact us at 978-750- 8400 or send an e-mail to info@copyright.com

Order Detail ID: 70572449 ASHRAE standard by AMERICAN SOCIETY OF HEATING, REFRIGERATING AND AIR Reproduced with permission of THE SOCIETY, in the format Republish in a thesis/dissertation via Copyright Clearance Center.

Order Detail ID: 70595954 ASHRAE standard by AMERICAN SOCIETY OF HEATING, REFRIGERATING AND AIR Reproduced with permission of THE SOCIETY, in the format Republish in a thesis/dissertation via Copyright Clearance Center.